Enhancements to Control Charts for Monitoring Process Dispersion and Location

A thesis submitted in fulfilment of the requirements for the degree of Doctor of Philosophy in Statistics
The University of Auckland, 2012

Saddam Akber Abbasi

Department of Statistics
The University of Auckland
New Zealand

Abstract

Control charts are widely used to monitor stability and performance of processes with an aim of detecting abnormal variations in process parameters. Control charts typically work in two phases: the retrospective phase (Phase I) and the monitoring phase (Phase II). Phase I involves estimating the in-control state of a process by using a historical dataset, whereas, in Phase II the focus mainly lies in the quick detection of process parameters from their in-control values.

Chapter 2 of this thesis investigates a wide range of Shewhart type dispersion control charts in Phase II for normal and a variety of non-normal parent distributions. These charts are based on the sample range, the sample standard deviation, the inter-quartile range, Downton's estimator, the average absolute deviation from median, the median absolute deviation, Sn and Qn estimates. The Phase I analysis of these charts together with the charts based on the pooled sample standard deviation and the distribution-free scale rank statistic is investigated in Chapter 3. The performance of a variety of Phase II EWMA dispersion charts is evaluated and compared in Chapter 4, using different run length characteristics (the average run length, the median run length and the standard deviation of the run length distribution). The overall effectiveness of these EWMA charts is examined using the extra quadratic loss and the relative ARL measures.

Chapter 5 investigates the effect of two component measurement error (model) on the performance of the EWMA location chart, for the monitoring of analytical measurements. The two component model proposed by Rocke and Lorenzato (1995) combines both additive and multiplicative errors in analytical measurements in a single model. It is shown that the two component measurement error can seriously effect the detection ability of the EWMA location chart and this effect can be reduced by the use of multiple measurements at each sample point. A cost function approach is used to determine appropriate choices of the sample size and the number of multiple measurements per sample to maximize the detection ability of the EWMA chart in presence of two component measurement error. Chapter 6 proposes two run rule schemes for the CUSUM dispersion chart. The run length characteristics of the proposed schemes are evaluated using the Markov chain approach and compared with the simple dispersion CUSUM and the relevant EWMA dispersion charts for individual observations. Finally, Chapter 7 proposes a nonparametric progressive mean control chart for the quick detection of out-of-control signals in the process target or location.

This thesis, in general, will help quality practitioners to choose efficient control charts for the monitoring of process dispersion and location.

Acknowledgments

All praise is to Almighty Allah, creator of the heavens and the earths and Lord of lords, it is by His blessing, who gave me potential and ability to complete this dissertation. All of my respect goes to Holy Prophet Muhammad (peace be upon him), who emphasized the significance of knowledge and research. The Prophet Muhammad (peace be upon him) said:

> *If anyone travels on a road in search of knowledge, Allah (God) will cause him to travel on one of the roads of Paradise. The angels will lower their wings in their great pleasure with one who seeks knowledge. The inhabitants of the heavens and the Earth and (even) the fish in the deep waters will ask forgiveness for the learned man. The superiority of the learned over the devout is like that of the moon, on the night when it is full, over the rest of the stars.* (Sunan of Abu-Dawood, Hadith 1631)

I would like to say special thanks to my supervisor Dr. Arden Miller, who has given me all the support, guidance and advice to carry out this research. I am very grateful to him for having trust in my abilities. Dr. Miller gave me the maximum freedom to attempt whatever I desired in the research. Dr. Miller was easily accessible in his office to discuss any research related issues.

The discussions with him will guide me throughout my future career.

I am also thankful to Dr. Chris Triggs, Dr. Alan Lee and Dr. James Curran for being on the advisory panel. I appreciate the teaching capabilities of Dr. Ross Ihaka and Dr. Yong Wang that really helped me in solving complex statistical issues.

I offer tribute to Dr. Muhammad Riaz, Assistant Professor, Mathematics and Statistics department, King Fahd University of Petroleum and Minerals, KSA, for his help right throughout the PhD degree. He is a great person and I always learned a lot from him thorough fruitful discussions. I am sincerely thankful to him for working hard on my professional and personal development.

I am also thankful to Education *NZ* for supporting my PhD research through New Zealand International Doctoral Research Scholarship (NZIDRS). Without their support, it would have been very hard for me to concentrate on PhD research. Thanks to The University of Auckland, for providing funds at the later stage of PhD and all the other facilities that were under my use throughout. Thanks are also extended to all the admin staff at the Department of Statistics particularly Nancy Wong, Aileene Koh and Alexandra Miliotis.

I would like to thank both the examiners for their positive comments that helped a lot in improving the contents of the thesis and in exploring new ideas in Statistical Process Control.

I salute my father for his love and ambitions for me. Although he is no more in this world but I still remember the days when he used to play with me. He was a great father and a great person. He really did his best in providing me with quality education.

I would like to pay tributes and thanks to my mother, Jamila Akhtar Abbasi, for her support and love, unending and countless prayers that really helped me to out of difficult situations in life. I don't have words to express my feelings for her. I better simply say, YOU ARE THE BEST. Bundles of thanks goes to my sisters (Saima Abbasi, Asima Abbasi, Kousar Ahsan and Munazza Arslan), my brothers (Ahsan Abbasi, Sajjad Abbasi, Siddique Abbasi, Arslan Abbasi and Zafar Iqbal) and my cousins (Surmad Iqbal, Wajahat Iqbal, Saroash Iqbal and Adnan) for their continuous support, love and encouragement.

During my PhD I really missed the love of my nephews and nieces. They are always a great source of pleasure for me. Love you all kids.

I am also grateful to all my teachers and friends at the Quaid-i-Azam University, Islamabad, for enlightening my statistical know-how during M.Sc Statistics program, particularly Dr. Javid Shabbir, Dr. Muhammad Aslam, Dr. Zahid Asghar, Dr. Zawar, Mrs. Maryam Asim, Shabbir Ahmad, Nasir Abbas, Hafiz Zafar Nazir, Amir Saghir and Muhammad Ali Shah.

Last but not the least, I would also like to say thanks to all my friends from Pakistan and The University of Auckland for their prayers, cooperation and assistance in all respects, particularly Majid Ali, Faiz Rasool, Husnain Shah, Shakeel Ahmad, Sher Khan, Adeel Ali, Usman Butt, Shehzad Akhtar, Ameer Hassan, Waqar Qureshi, Monis Kazmi, Amtiaz Nadeem, Saghir Ahmad, Khurram Jamil and Shahid Kaleem ullah Niazi . Sorry if I missed someone.

Contents

List of Figures

List of Tables

Chapter 1

Introduction

Statistical process control (SPC) is a collection of tools that helps in improving the quality of products by reducing dispersion in the process. The seven basic tools of SPC tool kit, often referred to as the "magnificent seven", include histogram, Pareto chart, scatter plot, control chart, check sheet, cause-and-effect diagram and defect concentration diagram (Montgomery (2009)). Moreover Hare (1993) introduced seven new tools that include affinity diagram, interrelationship diagram, tree diagram, prioritization matrix, matrix diagram, process decision program chart and activity network diagram. A major objective of implementing these tools is to differentiate between the two main types of variations: common cause variation and assignable cause variation.

Common cause variation is an inherent part of any process and is due to some random or chance causes. This can also be referred as the "natural variation" or the "background noise". In the presence of common cause variation, the process remains stable as expected and results in the random distribution of output around the average value. Assignable cause variation, on the other hand, is a result of certain factors that can not be treated as a part of chance causes, such as improperly adjusted or controlled machines, operator errors or raw material (Montgomery (2009)). Assignable cause variations can have a significant impact on the performance of a process and it is extremely necessary to detect the sources of these assignable causes as soon as possible for the implementation of corrective actions at an early stage. The control chart is a well known tool used for this purpose.

A process is said to be in a state of statistical control if only common causes are at work. If there are some assignable causes present, the process is declared to be out-of-control.

1.1 Control Charts

Control charts, introduced by Walter A Shewhart in 1920's, act as the most important and widely used process monitoring tool in Statistical Process Control (SPC). The basic purpose of implementing control chart procedures is to detect abnormal variations in the process (location & scale) parameters. Although first proposed for the manufacturing industry, control charts have now been applied in a wide variety of disciplines, such as in nuclear engineering (Hwang et al. (2008)), health care (Woodall (2006)), education (Wang and Liang (2008)) and analytical laboratories (Abbasi (2010), Masson (2007)). Montgomery (2009) reported the following main reasons for control charts popularity in such a wide range of disciplines:

- Control charts are a proven technique for improving productivity
- Control charts are effective in defect prevention
- Control charts prevent unnecessary process adjustments
- Control charts provide diagnostic information
- Control charts provide information about process capability

The monitoring of quality characteristics help in improving the quality of products. Quality characteristics can be measured on a quantitative scale (such as pressure, weight, diameter etc) or a qualitative scale (such as conforming/ non-conforming units etc). The charts used for the monitoring of these characteristics are well known as the variable and attribute control charts, respectively. This thesis will focus on the variable control charts. For quantitative characteristics, it is useful to monitor both the location and the dispersion of the concerned variable.

For the application of control charts, samples are usually collected from a process in the form of rational subgroups. The concept of rational subgroups was introduced by Shewhart, which means that, in the presence of assignable causes, "the chance for differences between subgroups will be maximized while the chance for differences within subgroups will be minimized" (Montgomery (2009)). The design of a typical control chart is based on plotting some summary statistic (such as the subgroup mean $\overline{X}$), computed from these rational subgroups, against time or sample number. The chart further contains three horizontal lines, namely the upper control limit (UCL), the center line (CL) and the lower control limit (LCL). CL is mostly set at the target or average of all the plotted data points, while the control limits are generally plotted at a distance of 3σ from the CL. These control limits help to determine the state of the process; the process is said to be in control if all the sample points should appear as random scatter around the target value within the control limits. Otherwise, if one or more points lie outside the control limits or if the plotted points show some pattern (such as a trend, shift etc), the process is said to be out-of-control.

1.1.1 Control Chart Phases

There are typically two phases in implementing a control chart: retrospective phase (Phase I) and monitoring phase (Phase II). Phase I is more of an exploratory analysis on a set of observations assumed to come from an in-control process (often referred as the historical data set). From an in-control process, we mean a process that is stable and predictable. The goal of Phase I is to screen out any inconsistent observations/samples from the historical data set and then compute control limits for real time Phase II process monitoring. In Phase II, the focus is more on the quick detection of departures of the process parameters from their in-control values (Woodall (2000)). The performance of the control chart in Phase II largely depends on the parameter estimates and the control limits computed as a result of Phase I analysis. It is not necessary to use the same control chart for both phases. One needs to search for a control chart that performs efficiently for a particular phase.

The cleaning of the historical dataset is very important because, in most real life processes, contaminations do occur and the presumed data set is not purely represented as coming from an in-control process. Different ways for screening of out-of-control samples from the historical data set have been proposed in the literature. The most common procedure is to set the trial limits based on an initial set of observations. If one or more points of the plotted sample statistic (such as $\overline{X}$) lie outside the trial limits, there is a need to remove these samples after searching for an assignable cause. Sometimes it is difficult to find assignable causes for the out-of-control points, but it is usually recommended to remove these points from the initial data set and to recompute the unknown parameters and limits based on the remaining samples. This procedure continues until all the observations lie inside the trial limits.

Vining (2009) recommended setting the initial trial limits based on a set of observations (e.g. 20 subgroups of size 5). Preliminary limits are then computed after the removal of out-of-control samples lying outside the trial limits. His procedure then uses these preliminary limits for the monitoring of the next 20 samples, investigates any out-of-control samples, and updates the estimates and limits using these 20 new samples. He recommended to continue this process for 80-100 presumed in-control subgroups. The resulting estimates and control limits are then used for Phase II monitoring.

Shiau and Sun (2010) proposed to remove only one extreme out-of-control point at a time, lying outside the trial limits. The limits are computed again after the removal of this extreme point and the procedure continues until all points lie inside the limits. They showed that this strategy maintains the same out-of-control detection ability of charts but with an added advantage of a reduced false alarm rate.

In Phase I, the probability to signal is mostly used as a measure to evaluate the performance of a control chart. As all the sample points are plotted against the same set of control limits, so the signaling events are not independent. Hence the control limits should be computed for a fixed overall false alarm rate instead of fixing the false alarm rate for individual points. In Phase II, the probability to signal for a single point or some characteristic of the run length distribution is mostly used as a performance measure, where run length is defined as the number of samples until an out-of-control signal is detected by a control chart.

The paper by Woodall (2000) (with discussions) gives an excellent description regarding Phase I and Phase II control charts. For details one may also see the studies by Jensen et al. (2006), Vining (2009) and Chakraborti et al. (2009).

1.1.2 Control Chart Types

Control charts are divided in to three main types: the Shewhart chart, the CUSUM chart and the EWMA chart. Shewhart charts can be put in the list of memoryless control charts, whereas CUSUM and EWMA charts as the memory control charts.

Let X represents a quality characteristic of interest distributed with mean μ and variance σ^2. Further, let $X_1, X_2, \ldots, X_n$ represent a sample of size n from this distribution.

1.1.2.1 Shewhart Control Charts

The control charts based on the original structure of Walter A. Shewhart are well known as the Shewhart control charts. The introduction of control charts began a new era of improving the quality of products by the use of simple statistical methods. Although there exist other types of control charts, Shewhart charts are the most widely used due to the combination of simplicity and effectiveness. Process location is mostly monitored by the $\bar{X}$ chart whereas process scale or dispersion by the R or S charts.

The control limits for a Shewhart type (location) control chart, for the parameter known case, are given as:

$$UCL = \mu + L\sigma/\sqrt{n}, \qquad CL = \mu, \qquad LCL = \mu - L\sigma\sqrt{n} \tag{1.1}$$

where L is the control chart multiplier, usually set at 3. In most real life situations, parameters are unknown and need to be estimated from an historical data set. μ is mostly estimated by the average of subgroup means (i.e. $\overline{\overline{X}}$) whereas σ by the average of sample ranges or sample standard deviations (i.e. $\overline{S}$ or $\overline{R}$). The estimated control limits (when σ is estimated by $\overline{R}$) are hence given as:

$$UCL = \overline{\overline{X}} + L\frac{\overline{R}}{d_2\sqrt{n}}, \qquad CL = \overline{\overline{X}}, \qquad LCL = \overline{\overline{X}} - L\frac{\overline{R}}{d_2\sqrt{n}} \tag{1.2}$$

Similarly the design of the dispersion R chart is based on the following set of limits:

$$UCL = \overline{R} + L\frac{d_3\overline{R}}{d_2}, \qquad CL = \overline{R}, \qquad LCL = \overline{R} - L\frac{d_3\overline{R}}{d_2} \tag{1.3}$$

where d_2 and d_3 are the control chart constants dependent on sample size n. These are defined as the mean and the standard deviation of the distribution of relative range ($W = R/\sigma$), i.e. $d_2 = E(W)$ and $d_3 = \sigma_W$ (provided in most SPC books for normally distributed quality characteristic, see – Montgomery (2009) or Ryan (2000)).

The Shewhart charts trigger an out-of-control signal for any point of the plotted statistic (e.g. $\overline{X}$ or R) lying outside the control limits.

Shewhart charts are only based on the current sample information. Due to this, they are effective for the detection of large process shifts but are well known to be inefficient for the detection of small shifts in process parameters. The detection ability of the Shewhart charts can be increased by the application of some other signaling rules that use an additional set of limits called the warning limits – for details see Section 1.2.

1.1.2.2 Cumulative Sum (CUSUM) Control Charts

To increase the ability of control charts for the detection of small persistent process shifts, Page (1954) proposed Cumulative sum (CUSUM) control charts. The CUSUM control chart uses information of both the current as well as the past sample/samples. This makes the CUSUM charts effective for detecting small shifts in process parameters. CUSUM charts can be represented in two ways: i) V-mask CUSUM and ii) tabular CUSUM.

The V-mask CUSUM procedure was proposed by Barnard (1959) and is based on superimposing a V-mask on the plot of cumulative sums. The origin of the V-mask is always positioned at the recent cumulative sum point and the previous cumulative sums are examined to determine the state of the process. If all the previous points lie inside the two arms of the V-mask, the process is declared to be in-control. If any of the points lie outside the arms, the process is declared to be out-of-control. The V-mask procedure has been mentioned as laborious and confusing by many researchers and its use has been mostly criticized (for details – see Ryan (2000); Montgomery (2009)).

The tabular CUSUM procedure, however, is more popular and easy to follow. For ease we will refer to the tabular CUSUM as simply the CUSUM chart for the rest of the study.

For a tabular CUSUM chart, the deviations from the target value of the parameter are accumulated in the upward and downward directions separately, using two different statistics: one for the upward shift (e.g. C^+) and the other for the downward shift (e.g. C^-). For monitoring process location, C^+ and C^- can be defined as:

$$\begin{aligned} C_t^+ &= max[0, (X_t - k) + C_{t-1}^+] \\ C_t^- &= max[0, (-X_t - k) + C_{t-1}^-] \end{aligned} \tag{1.4}$$

where k is known as the reference/allowance/slack value and it is often chosen to be about half of the shift (in standard units) we want to detect quickly. The statistics C^+ and C^- (known as the upper and lower CUSUMs) are initially set to zero (i.e. $C_0^+ = C_0^- = 0$). The values of these two statistics are calculated for each sample and are plotted against time on a chart which has control limits superimposed. The CUSUM control chart indicates an out-of-control signal when any of the two statistics plot beyond a prefixed control limit (h) (for details see Alwan (2000), Ryan (2000) and Montgomery

(2009)). The choice of h and k depends on achieving a desired in-control performance of the CUSUM chart. The V-mask CUSUM becomes equivalent to the tabular CUSUM at some specific choices of the design parameters (Montgomery (2009)).

Since the introduction of CUSUM charts by Page (1954), many researchers have examined these charts from different perspectives - see for example Brook and Evans (1972), North (1982), Reynolds and Arnold (1990), Hawkins (1981), Hawkins (1993), H and M. (1985), Jones et al. (2004) and Chatterjee and Qiu (2009). CUSUM charts are widely used for the efficient monitoring of internal quality control parameters and their use in analytical laboratories has been emphasized by many researchers, including Funk et al. (1995), Mullins (2003) and Hibbert (2007). As compared to Shewhart or EWMA chart (described below), "the CUSUM chart seems more suitable to the needs of control in laboratory" (Kateman and Buydens (1993)). CUSUM charts are effective even with rational subgroups of size one, which makes them an attractive option for many applications in chemical and process industries (see Montgomery (2009)). The book by Hawkins and Olwell (1998) includes a comprehensive description of the construction of CUSUM charts.

1.1.2.3 Exponentially Weighted Moving Average (EWMA) Control Charts

Exponentially weighted moving average (EWMA) is the third main type of control chart, proposed by Roberts (1959). The EWMA chart is based on using the entire sequence of sample information. The chart uses a varying weight scheme, assigning highest weight to the most recent observation and the weights decrease exponentially for less recent observations. For a random observation X at time t, the EWMA statistic W_t is defined as:

$$W_t = \lambda X_t + (1 - \lambda) W_{t-1} \tag{1.5}$$

where λ $(0 \leq \lambda \leq 1)$ is the weight assigned to the current sample observation and W_0 is usually set at a target value (μ or $\overline{\overline{X}}$). The design of the EWMA location chart (under parameter known case) is based on the following set of limits.

$$\begin{aligned} UCL =& \mu + L\frac{\sigma}{\sqrt{n}}\sqrt{\frac{\lambda}{2-\lambda}\left[1-(1-\lambda)^{2t}\right]} \\ CL =& \mu \\ LCL =& \mu - L\frac{\sigma}{\sqrt{n}}\sqrt{\frac{\lambda}{2-\lambda}\left[1-(1-\lambda)^{2t}\right]} \end{aligned} \tag{1.6}$$

The above control limits for the EWMA chart are known as the exact or the time varying limits (as they depend on time t). As $t \to \infty$ (i.e. for a process to be running for a long time), the time varying limits reduce to the asymptotic limits, as given below:

$$\begin{aligned} UCL =& \mu + L\frac{\sigma}{\sqrt{n}}\sqrt{\frac{\lambda}{2-\lambda}} \\ CL =& \mu \\ LCL =& \mu - L\frac{\sigma}{\sqrt{n}}\sqrt{\frac{\lambda}{2-\lambda}} \end{aligned} \tag{1.7}$$

For the purpose of ease in computation, asymptotic limits are mostly used for the EWMA charts but the use of these limits makes the EWMA chart insensitive to start up quality problems.

Selection of λ allows the practitioners to adjust the EWMA chart to a specific purpose. If small shifts in the process parameters are of major concern, it is better to use small values of λ. For the detection of large shifts, large values of λ are mostly recommended. It is to be noted that the Shewhart chart becomes a special case of the EWMA chart at $\lambda = 1$. An advantage of using the EWMA charts with small value of λ is to make it robust to the normality assumption, as investigated by several authors including Borror et al. (1999) and Maravelakis et al. (2005). This robustness is mostly limited to location charts and EWMA dispersion charts have been shown in literature to be affected by non-normality (see Abbasi and Miller (2011c)).

The sensitivity of EWMA charts can be increased by the use of fast initial response feature as studied by Lucas and Saccucci (1990), Rhoads et al. (1996) and Steiner (1999) for EWMA location charts. Recently Abbasi and Miller (2011b) also investigated the effect of time varying and fast initial response features on the performance of EWMA dispersion charts.

1.2 Literature Review

Control charts were introduced by Walter, A. Shewhart in 1924 during his work in Bell Labs. At the start, Shewhart proposed $\overline{X}, R$ and S charts (known as the variable control charts) for the monitoring of quantitative quality characteristics and p, np, c and u charts (known as the attribute control charts) for the monitoring of qualitative characteristics. Although these charts are widely used, they are only based on current sample information, which makes them insensitive to small shifts in process parameters. Memory control charts, in the form of the CUSUM chart and the EWMA chart, proposed by Page (1954) and Roberts (1959) respectively, help in quick detection of small shifts in process parameters. The theory, design, implementation and application of these charts have been extended in many different directions. A brief literature review concerning the control chart issues investigated in this thesis is described below.

Effect of Parameter Estimation and Norn-Normality: Most SPC charts are based on the assumption of known parameters, but for the monitoring of real life processes these parameters are usually estimated from sample data in Phase I. For quantitative characteristics, the location and dispersion parameters are of major concern. Process location (μ) is mostly estimated by the overall sample mean ($\overline{\overline{X}}$), whereas process dispersion (σ) by the average sample range ($\overline{R}$) or the average sample standard deviation ($\overline{S}$). Control charts based on these standard estimates can perform efficiently under the (ideal) assumption of normality for the quality characteristic of interest but are well known to be inefficient when this assumption is violated.

The estimation of σ is well known to be affected more than the estimation of μ under the violation of the normality assumption (cf. Burr (1967); Braun and Park (2008)). Keeping this in mind, researchers have investigated different estimates of σ for the purpose of achieving efficient and resistant charting – see Rocke (1989), Cryer and Ryan (1990), Rocke (1992), Cruthis and Rigdon (1992), Derman and Ross (1995), Pappanastos and Adams (1996), Tatum (1997), Chen (1998), Abu-Shawiesh (2008), Riaz (2008); Riaz and Saghir (2009), Mukherjee and Chakraborti (2012) and references therein. Recently, Wu et al. (2002) examined the effects of different estimators of σ on the performance of the Shewhart $\overline{X}$ chart when measurements are taken from contaminated normal distributions. Braun and Park (2008) investigated the effects of different σ estimators on the performance of the EWMA location chart for individual measurements from contaminated normal and t distributions. Schoonhoven et al. (2008) and Schoonhoven and Does (2010) use different estimates of σ to examine their effects on the performance of $\overline{X}$ chart under the existence and the violation of normality assumption. Schoonhoven et al. (2011) and Schoonhoven and Does (2012) investigated the effect of estimating σ in Phase I on control chart's performance in Phase II for monitoring process dispersion. Jones-Farmer and Champ (2010) proposed a distribution-free structure for monitoring dispersion and compared the performance of this proposal with R and S charts.

Most of the research is focused on investigating the dispersion charts for normal or contaminated normal distributions. Little work has been done to investigate the performance of a wide range of Phase I and Phase II dispersions charts for processes following non-normal distributions. Many quality characteristics such as capacitance, insulation resistance, surface finish, roundness, mold dimension, customer waiting time and the impurity levels in semi conductor process chemicals follow non-normal distributions (cf. Bissell (1994), Alwan and Roberts (1995), James (1989) and Levinson and Polny (1999)). The underlying distributional environment can have a significant impact on the detection ability of control charts. This has been investigated in detail in Chapters 2-4.

The Effect of Measurement Error: For a unit in the population, the value of the concerned characteristic is sometimes contaminated with measurement errors. The presence of this contamination can seriously affect the performance of control charts. Researchers have investigated the performance of control charts considering different measurement error models. Many researchers including Bennett (1954), Abraham (1977), Kanazuka (1986), Mittag (1995) and Mittag and Stemann (1998a) examined the effects of the additive error model on the performance of control charts. The additive error model is given as:

$$Y = X + \epsilon \tag{1.8}$$

where Y represents the observed value, X the true value (distributed normally with mean μ and variance σ^2) and ϵ is the error term (distributed normally with mean 0 and variance σ_ϵ^2). Bennett (1954) examined the effect of the above error model on the performance of $\overline{X}$ chart. He concluded that if the variance due to the measurement errors is smaller than the variance due to the process, it can be overlooked. Abraham (1977) considered the same model and studied process variation in the presence of measurement errors. Kanazuka (1986) examined the effects of measurement errors on the process variance of the joint $\overline{X} - R$ chart. He remarked that the power of the chart to detect shifts diminished in the presence of measurement errors and one had to use a larger sample size to increase power. Mittag (1995) and Mittag and Stemann (1998a) examined the measurement error effects on the joint $\overline{X} - S$ chart assuming the error model given in Equation (1.8).

Linna and Woodall (2001) and Linna et al. (2001) monitored the effects of measurement errors on univariate and multivariate Shewhart type control charts respectively, using, the additive model with covariates, given as:

$$Y = A + BX + \epsilon \tag{1.9}$$

where A and B are constants. They concluded that the power of the Shewhart control chart to detect shifts in process location diminishes with an increase in the magnitude of measurement error. Maravelakis et al. (2004) and Maravelakis (2007) investigated the performance of the EWMA and CU-

SUM charts under the covariate model given in (1.9). They showed that the detection of out-of-control signals becomes difficult in the presence of measurement error. Compared to the no measurement error case, the control chart requires more samples to detect the same magnitude of shift in presence of measurement error.

Control charts are also widely used for the monitoring of analytical measurements, particularly for internal quality control undertaken by analytical laboratories. Measurement error in analytical measurements is not accurately described by the additive model (given in Equation (1.8) or (1.9)) because these measurements are mostly subject to two types of error: i) additive error that dominates for zero and near zero concentrations, ii) proportional or multiplicative error that dominates at higher concentrations (Currie (1968); Hubaux (1970); Rocke et al. (2003)). Rocke and Lorenzato (1995) proposed a two component model for analytical measurements, given as:

$$Y_t = \alpha + \beta X_t e^{\eta_t} + \epsilon_t \tag{1.10}$$

Where Y is response at concentration X observed at time t, α and β are the intercept and the slope of the linear calibration curve, random disturbances η and ϵ are distributed normally and independently with mean 0 and variances σ_η^2 and σ_ϵ^2 respectively (i.e. $\eta \sim N\left(0, \sigma_\eta^2\right)$ and $\epsilon \sim N\left(0, \sigma_\epsilon^2\right)$). Here η represents multiplicative error and ϵ represents additive error.

The literature on exploring the performance of control charts for measurement errors described by the TCME model is very limited. I am only aware of Cocchi and Scagliarini (2007) and Abbasi (2010), which investigate the performance of Shewhart and EWMA charts respectively (for details – see Chapter 5).

The use of Sensitizing/Runs Rules: For a control chart, a process is declared to be out-of-control whenever a point lies outside the control limits, which are usually set at a distance of 3σ from the centre line. To increase the sensitivity of the chart for the detection of small shifts, some supplementary rules have been proposed by researchers that use an additional set of limits called the warning limits. The Western Western-Electric (1956) contained a set of rules to declare a process to be out-of-control, if:

- Any one point falls outside the 3σ control limit or
- 2 out of the last 3 points fall outside the 2σ warning limits or
- 4 out of the last 5 points fall outside the 1σ warning limits or
- Eight consecutive points fall on one side of the centre line.

A number of studies appeared in SPC literature that not only investigated different control chart structures based on these rules but also to propose new rules to increase the detection ability of control charts.

Champ and Woodall (1987) used the Markov chain approach for providing exact results for the run length properties of Shewhart $\overline{X}$ chart supplemented with run rules. They provided a comparison of these results with ARL results of $\overline{X}$ chart and the CUSUM chart. Palm (1990) also employed the Markov chain method to provide tables for the run length percentiles of the run rules schemes for the Shewhart $\overline{X}$ chart. Walker et al. (1991) investigated the false alarm rates of the $\overline{X}$ chart based on eight different runs test. They showed that the false alarm rate is directly related with the number of runs tests applied with the $\overline{X}$ chart. Champ and Woodall (1997) investigated signal probabilities of the run rules schemes for the $\overline{X}$ chart. Klein (2000) proposed two new run rules schemes for the $\overline{X}$ chart suggesting a process to be out-of-control for any 2 out of 2 or 2 out of 3 successive points plotting outside the adjusted control limits. The comparison of his proposed schemes with the usual $\overline{X}$ chart showed superiority for the detection of small shifts. Shmueli and Cohen (2003) provided exact expressions for the run rules schemes used for the $\overline{X}$ chart. Khoo (2003) presented plots to determine the control limits of different run rules schemes for the Shewhart chart to fix the average run length at a particular level. Zhang and Wu (2005) presented some interesting features concerning different run rules schemes. Khoo (2006) proposed improvements over the run rules schemes introduced by Klein (2000). Lim and Cho (2009) investigated the economic statistical properties of the $\overline{X}$ chart supplemented with both 1 out of 1 and m out of m rules (m out of m rules indicate a process to be out-of-control if all the recent m values lie outside the warning limits). They also used cost function to study the sensitivity of the design parameters of different run rules schemes.

Some researchers also investigated the effect of run rules on the performance of Shewhart type variability control charts. Acosta-Mejia and Pignatiello (2008), Acosta-Mejia and Pignatiello (2009) and Antzoulakos and Rakitzis (2010) analyzed the performance of Shewhart type variability R and S charts supplemented with some r out of m and m out of m rules. They showed that the R and S charts supplemented with run rules outperformed the simple R and S charts for the detection of shifts in the process dispersion.

The literature on the use of these rules with CUSUM and EWMA control structures is very limited. Westgard et al. (1977) studied some control rules for combined Shewhart-CUSUM structures and demonstrated the superiority of their approach to the Shewhart chart. Recently Riaz et al. (2011) and Abbas et al. (2011) have extended the run rules approach to the CUSUM and EWMA type charts for the monitoring of the process location parameter.

Nonparametric Structures: Most of the Statistical Process Control (SPC) charts are based on the assumption that the parametric distribution of the quality characteristic of interest is normal. The statistical properties of these charts may not remain valid for processes following non-normal (heavy tailed symmetric or skewed) distributions. When the distributional assumption is invalid, the use of parametric control charts for the monitoring of process parameters can give unfavorable results in the form of low detection ability and high false alarm rates. Many researchers including Noble (1951), Bakir and Reynolds (1979), Gunter (1989) and Chakraborti et al. (2001) recommend that distribution-free/nonparametric charts should be developed for the purpose of process monitoring. A brief literature review regarding the development of nonparametric charts is as follows:

Bakir and Reynolds (1979) proposed CUSUM location charts using the Wilcoxon sign-rank statistic. Park and Reynolds (1987) proposed distribution free Shewhart and CUSUM type control charts for the monitoring of process location using the linear placement statistic. Alloway and Raghavachari (1991) and Pappanastos and Adams (1996) investigated Shewhart type control charts for process median based on the Hodges-Lehman estimator, while the proposal of McDonald (1990) is based on sequential ranks. Amin and Searcy (1991) proposed a non parametric EWMA control chart based on the Wilcoxon signed-rank statistic. They investigated the proposed chart for normal, non-normal and autocorrelated processes and further provided a comparison with the performance of the usual EWMA control chart. Amin and Widmaier (1999) proposed Shewhart type nonparametric control charts with variable sampling intervals using the sign test statistic for the monitoring of process location and variability. A review of nonparametric control charts until 2001 can be seen in Chakraborti et al. (2001).

Bakir (2006) proposed three distribution-free location charts based on the sign rank statistic. His procedure estimates the process location from an in-control reference sample. The comparison with parametric structures showed the superiority of these charts for (heavy tailed symmetric) double exponential and Cauchy distributions. Das and Bhattacharya (2008) proposed a nonparametric control chart for monitoring process dispersion based on the two sample rank-sum test. The comparison with the Shewhart S chart revealed that his variability structure is robust for the in-control case but out-of-control performance is relatively poor. Balakrishnana et al. (2009) proposed a nonparametric chart using the Wilcoxon type rank sum statistic and showed the superiority of this proposal in terms of in-control robustness. Chakraborti and Eryilmaz (2007) proposed nonparametric Shewhart structures using the Wilcoxon-signed rank statistic and further provided a comparison of their proposals with the $\overline{X}$ chart. Chakraborti et al. (2009) made use of the precedence statistic for the design of nonparametric charts and also investigated the signaling ability of charts based on runs rules. Khilare and Shirke (2010) proposed a synthetic Shewhart type location control chart by combing the sign chart and the conforming run length chart. The synthetic chart showed better performance for various symmetric distributions than the $\overline{X}$ chart and the location chart simply based on sign statistic.

Li et al. (2010) proposed nonparametric CUSUM and EWMA charts based on Wilcoxon rank sum test. Their proposed charts showed superiority over other location charts when the assumption of normality is violated. They also investigated the effect of reference sample size and the number of subgroups on the detection ability of control charts. Li and Wang (2010) proposed nonparametric EWMA and nonparametric CUSUM charts based on the Man-Whitney statistics; Zou and Tsung (2011) proposed a multivariate EWMA control chart using the weighted version of sign test; while Graham et al. (2011) proposed nonparametric EWMA sign chart for monitoring process location using individual observations, Yang et al. (2011) proposed two nonparametric EWMA control charts, namely the nonparametric EWMA sign chart and the nonparametric Arcsine EWMA sign chart; and Yang and Cheng (2011) proposed a nonparametric CUSUM chart for quick detection of shifts from the process target using the sign statistic.

1.3 Thesis Contribution

This thesis investigates new control charts for the efficient monitoring of process parameters in Phase I and II. The thesis contains material that is included in the following studies (see next page).

Chapter 2

- Abbasi, S. A. and Miller, A. (2012). On proper choice of variability control chart for normal and non-normal processes, **Quality and Reliability Engineering International**, 28 (3), 279-296.
- Abbasi, S. A. and Miller, A. (2013). An Efficient Dispersion Control Chart, **IAENG Transactions on Engineering Technologies**, 2013, 2013, X, 388 p. 204 illus, Springer.
- Abbasi, S. A. and Miller, A. (2011a). D Chart: An Efficient Alternative to Monitor Process Dispersion, **Proceedings of the World Congress on Engineering and Computer Science 2011** Vol II, WCECS 2011, October 19-21, 2011, pages 933-938, San Francisco, USA.

Chapter 3

- Abbasi, S. A., Riaz, M. and Miller, A. (2012b). On proper choice of Phase I dispersion control chart, To be submitted

Chapter 4

- Abbasi, S. A. and Miller, A. (2011c). MDEWMA Chart: An efficient and robust alternative to monitor process dispersion, **Journal of Statistical Computation and Simulation**, ifirst, DOI:10.1080/00949655.2011.601416
- Abbasi, S. A. and Miller, A. (2011b). Increasing the Sensitivity of dispersion EWMA Control Charts, **Electrical Engineering and Applied Computing**, 1st Edition., VI, 739, Springer.
- Abbasi, S. A., Miller, A. and Riaz, M. (2012a). Monitoring process dispersion using EWMA control charts, To be submitted

Chapter 5

- Abbasi, S. A. (2010). On the performance of EWMA chart in presence of Two Component Measurement error, **Quality Engineering**, Vol. 22, No. 3, 199 213.

Chapter 6

- Abbasi, S. A., Riaz, M. and Miller, A. (2012a). Enhancing the performance of CUSUM scale chart, **Computers & Industrial Engineering**, 63, 400-409.

Chapter 7

- Abbasi, S. A., Miller, A. and Riaz, M.(2012b). Nonparametric Progressive Mean Control Chart for the Monitoring of Process Target, **Quality and Reliability Engineering International**, Early View, DOI: 10.1002/qre.1458
- Abbasi, S. A. (2012). Letter to the Editor: A new nonparametric EWMA sign control chart, **Expert Systems with Applications**, 39, 8503.

1.4 Outline of the Thesis

The thesis is divided in to eight chapters. The contents of Chapters 2-7 are based on different research studies, as described in Section 1.3. We recommend these chapters should be read out in individual capacity.
Chapter 2 investigates a wide range of Shewhart type dispersion charts in the monitoring phase (Phase II) under the assumption that a sufficiently large and clean historical dataset is available for the estimation of control limits in Phase I. Chapter 3 presents a comparison of a variety of dispersion charts for Phase I of SPC when only a limited number of samples are available for the estimation of parameters and control limits. Chapter 4 investigates different dispersion charts using the EWMA structure for the efficient detection of small shifts in process dispersion. These chapters provide a comparison of a range of dispersion charts considering normal and a variety of non-normal parent distributions. The performance of the EWMA location chart in the presence of two component measurement error is investigated in Chapter 5. Chapter 6 implements run rules schemes for the CUSUM dispersion chart. Chapter 7 proposes an efficient nonparametric progressive mean control chart and finally Chapter 8 presents summary of results and a discussion on future research issues. A brief description of the chapters is given below:

Chapter 2 investigates the effects of different estimators of σ on the performance of dispersion charts for Phase II quality control. The performances of some existing and some newly proposed charts have been investigated considering normal and non-normal processes. In particular, a comparison of the eight dispersion chart structures based on the sample range, the sample standard deviation, the inter-quartile range, Downton's estimator, the mean deviation, the median absolute deviation, Sn and Qn is provided. The performance of these dispersion charts is examined under normal and a wide range of non-normal distributions. This will aid quality practitioners in choosing the best dispersion control charts when the assumption of normality is questionable. This chapter is based on Abbasi and Miller (2012).

Chapter 3 investigates the effects of different estimators of σ on the performance of dispersion control charts for Phase I quality control. The performance of eleven control charting structures is evaluated and compared for normal and non-normal processes, using probability to signal as a performance measure. The control structures are based on the sample range, the sample standard deviation, the pooled sample standard deviation, the inter-quartile range, Downton's estimator, the mean deviation, the median absolute deviation, S_n, Q_n and the distribution free scale-rank statistic. This study will help quality practitioners to choose an efficient dispersion control chart for Phase I SPC. This chapter is based on Abbasi et al. (2012b).

Chapter 4 investigates the Phase II performance of EWMA dispersion charts based on different estimates of σ – as was done in Chapter 2 for Shewhart charts. The performance of all the charts is evaluated and compared using run length characteristics (the average run length, the median run length and the standard deviation of the run length distribution). The overall effectiveness of the EWMA charts have been examined using extra quadratic loss (EQL) and relative ARL (RARL) measures. This chapter is based on Abbasi and Miller (2011c), Abbasi et al. (2012a) and Abbasi and Miller (2011b).

Chapter 5 examines the effects of two component measurement error on the performance of the EWMA control chart for the monitoring of analytical measurements. The two component error model for analytical measurements, proposed by Rocke and Lorenzato (1995), combines both the additive and multiplicative errors into a single model. This model has gained immense importance in analytical chemistry and environmental settings. A cost function approach is used to determine appropriate choices of sample size and the number of multiple measurements per sample to maximize the detection ability of the EWMA chart in presence of two component measurement error. The comparison with the EWMA chart performance in the presence of one component (additive) error model is also provided. This chapter is based on Abbasi (2010).

Chapter 6 proposes the implementation of sensitizing rules in CUSUM dispersion charts to enhance their ability for the detection of smaller changes in process dispersion. The performance of the proposed schemes is evaluated using Markov Chains and compared with the simple dispersion CUSUM chart, the EWMS chart, the M-EWMS chart and the COMB chart, in terms of run length characteristics. This chapter is based on Abbasi et al. (2012a).

Chapter 7 proposes a nonparametric progressive mean control chart, namely the $NPPM$ chart, for efficient detection of disturbances in process location or target. Progressive mean (PM) is defined as the cumulative average of the sample values observed over time. The benefit of using the PM statistic is its quick convergence to the process target compared to the Shewhart, EWMA or CUSUM monitoring statistics. The proposed chart is compared with the recently proposed nonparametric EWMA and nonparametric CUSUM charts, using different run length characteristics (the average run length, the standard deviation of the run length and the percentile points of the run length distribution). This chapter is based on Abbasi et al. (2012b).

Chapter 8 presents a summary of the main findings and a discussion on future research issues.

Chapter 2

Shewhart Control Charts for Monitoring Process Dispersion in Phase II

Control charts are an important statistical process control tool, used to monitor changes in process location and dispersion. This chapter addresses issues regarding the structure of a Shewhart control chart for the efficient Phase II monitoring of process dispersion. The performance of eight control charts, based on different estimates of process standard deviation, is investigated for normal and non-normal parent distributions. Control chart constants required for setting control limits are provided for all these dispersion charts. This chapter aims at providing guidance to quality practitioners for choosing the appropriate Shewhart type Phase II dispersion control chart for normal and non-normal processes. The contents of this chapter are based on Abbasi and Miller (2012).

2.1 Introduction

Control charts are widely used to monitor stability and performance of manufacturing processes with an aim of detecting unfavorable variations in process (location and spread) parameters. Although first proposed for the manufacturing industry, control charts have now been applied in a wide variety of disciplines, such as in nuclear engineering (Hwang et al. (2008)), health care (Woodall (2006)), education (Wang and Liang (2008)), analytical laboratories (Abbasi (2010), Masson (2007)) etc. The application of control charts consists of two phases: a retrospective phase and a monitoring phase. In the retrospective phase, historical data are analyzed to estimate the in-control state of the process, while the monitoring phase focuses on the current state of the process by analyzing the current data. The goal for the monitoring phase is the quick detection of departures of the process parameters from their in-control values (Woodall (2000)).

Parameter estimation significantly affects the performance of control charts in both phases and has attracted the attention of many researchers in recent years. Some important studies in this area are Quesenberry (1993), Roes et al. (1993), Rigdon et al. (1994), Jones et al. (2001), Jensen et al. (2006) and the references therein. The choice of parameter estimator(s) is an important issue related to parameter estimation. Proper choice of estimator(s) plays a critical role in developing an efficient and robust control chart design. Samples from a process are usually taken in the form of rational subgroups of size n. When the process is absolutely stable (the process parameters do not change at all over time), then the most efficient way to estimate the process dispersion is to use an estimate based on the set of observations formed by combining the subgroups into a single group. However, if some instability exists in the process, then this procedure will tend to over-estimate the short term dispersion and a more reliable approach is to estimate the dispersion for each subgroup separately and then pool these estimates. The mean μ is generally estimated from the overall sample mean $\overline{\overline{X}}$ while process standard deviation σ can be estimated in many different ways, the most popular choices are based on sample range (R) or sample standard deviations (S). Control charts based on these standard estimates perform reasonably well under the usual assumptions that observations come from a normal distribution but are known to be inefficient when the assumption of normality is violated. Many authors have reported that the estimate of σ is more affected by non-normality than the estimate of μ (see Burr (1967), Braun and Park

(2008)) .

Researchers have investigated different estimates of σ with the aim of improving the efficiency and robustness of control charts performance (see Cryer and Ryan (1990), Cruthis and Rigdon (1992), Derman and Ross (1995) and Chen (1998)). There has been considerably more quality literature published on investigating the effect of σ estimators on the performance of location charts than on the performance of dispersion charts. Recently, Wu et al. (2002) examined the effect of different estimators of σ on the performance of the Shewhart $\overline{X}$ chart when measurements are taken from contaminated normal distributions. Braun and Park (2008) investigated the effect of different σ estimators on the performance of the EWMA location chart for individual measurements from contaminated normal and t distributions. Schoonhoven et al. (2008) and Schoonhoven and Does (2010) use different estimates of σ to examine their effect on the performance of the $\overline{X}$ chart under the existence and violation of normality assumption.

The problems in the estimation of σ due to non-normality should be expected to have a greater impact on the performance of dispersion charts than on the performance of location charts. According to Montgomery (2009) "the R chart (a dispersion chart) is more sensitive to departures from normality than the $\overline{X}$ chart (a location chart)". Jensen et al. (2006) states "the estimation effect appears to be more severe for charts monitoring changes in dispersion than for those monitoring changes in the mean" – see also Ryan (2000) and Chen (1998) for further discussion on this issue. For monitoring process dispersion, there exist some proposals which are based on robust σ estimates and have shown their superiority over the classical R or S charts under non-normality or contamination in the data (Rocke (1992); Riaz (2008), Abu-Shawiesh and Abdullah (2000)). However, the choice of the best estimator to be used for dispersion charts has not been made clear in the literature. Also, there exist some other estimators of σ which have not been properly investigated. Moreover, the performance of most of the existing dispersion charts has not been thoroughly studied for non-normal processes.

The purpose of this chapter is to evaluate and compare the performance of various dispersion charts in the monitoring phase. The performance is evaluated for processes following normal and non-normal distributions (both heavy tailed symmetric and skewed distributions are used). The rest of this chapter is organized as follows. In section 2.2, we describe different dispersion statistics that can be used to estimate σ. A general control chart structure is presented in section 2.3, which is then used to create dispersion charts based on these statistics. Methods of evaluating control chart performance and the details of the simulation study are explained in section 2.4. In section 2.5, the performance of the dispersion charts is investigated under the ideal assumption of normal observations. Section 2.6 presents a comparison of the dispersion charts when measurements come from non-normal distributions. Conclusions are made in section 2.7.

2.2 Dispersion Statistics

In this section, the dispersion statistics that are the basis for a dispersion control chart are described. Two important attributes of these dispersion statistics are their efficiency and their robustness, which are briefly discussed.

Let X be the quality variable of interest and let $X_1, X_2, \cdots, X_n$ be a random sample of size n. Further, let $X_{(i)}$ be the ith order statistic (smallest to largest), $\overline{X}$ be the sample mean, $\tilde{X}$ be the sample median and $|X|$ be the absolute value of X.

Sample Range

The sample range (R) is the most widely used dispersion statistic for control charts and is defined as

$$R = X_{(n)} - X_{(1)} \tag{2.1}$$

As R only depends on the smallest and largest observations, it is an efficient estimate of dispersion for small sample sizes but loses efficiency as the sample size increases. Montgomery (2009) recommends using the sample standard deviation instead of R for moderate to large sample sizes. It is also very sensitive to outliers and departures from normality.

Sample Standard deviation

Another commonly used dispersion statistic is the sample standard deviations (S):

$$S = \sqrt{\frac{1}{n-1}\sum_{i=1}^{n}(X_i - \bar{X})^2}. \tag{2.2}$$

For normally distributed quality characteristics, S is the most efficient estimator of dispersion. However, studies have shown that it can be sensitive to departures from normality and outliers. Dispersion control charts based on R and S (the R chart and S chart) can be found in almost all statistical process control (SPC) books – for example, see Alwan (1999) and Montgomery (2009).

Interquartile Range

The interquartile range (IQR) has been proposed as a dispersion statistic which results in control charts that are more robust to departures from normality and outliers than either the R chart or the S chart. IQR is defined as the difference between the third and first quartiles. For sample data, these quartiles can be estimated using the 75^{th} and the 25^{th} sample quantiles respectively. Several different ways of estimating these sample quantiles exist in literature. Rocke (1992) proposed the R_Q chart using $IQR = X_{(n-\lfloor n/4 \rfloor)} - X_{(\lfloor n/4 \rfloor + 1)}$, where $\lfloor x \rfloor$ represents the "floor" function and is defined as the largest integer less than or equal to x. Rocke (1992) showed that this R_Q chart is superior to the R chart for detecting changes in dispersion in the presence of outliers. Riaz (2008) pointed out the irregularities in the structure of R_Q chart due to the use of $(n - \lfloor n/4 \rfloor)$ and $(\lfloor n/4 \rfloor + 1)$ order statistics, which are integers – see Table 1 of Rocke (1992). He further proposed the Q chart using an alternative estimator of IQR, given as:

$$IQR = (Q_3 - Q_1)/1.34898 \tag{2.3}$$

where Q_1 and Q_3, respectively, represent the lower and upper sample quartiles. He further investigated the performance of R, S and Q charts for exponential and Student's t distribution.

The definition of IQR used by Riaz (2008) is more attractive and is also used in this study. The quartiles Q_1 and Q_3 have been computed using sample quantiles. Hyndman and Fan (1996) described six desirable properties of sample quantiles and presented nine different ways of defining them. Although they have shown that Type 5 (of the nine definitions presented) satisfies all the six of the desirable properties, in this study we have computed sample quantiles by `quantile` function in R statistical language (Ihaka and Gentleman (1996)) using Type 6 which satisfies five of the six desirable properties (for definitions of Type 5 & 6 – see Hyndman and Fan (1996)). The reason behind choosing Type 6, for the computation of quantiles is because this definition is also used by other commonly used statistical packages such as Minitab and SPSS. If the sample quartiles do not correspond to a particular order statistic in the sample, these are computed by linear interpolation between the two nearest order statistics.

In later sections, we will see that the dispersion chart based on IQR is superior to R and S charts for some non-normal distributions, but there are alternatives available that perform even better than the IQR chart.

Downton's Estimator

Downton (1966) proposed the following estimator of σ:

$$D = \sqrt{\pi} \sum_{i=1}^{n} \frac{(2i-n-1)X_{(i)}}{n(n-1)} \tag{2.4}$$

$$= \frac{2\sqrt{\pi}}{n(n-1)} \sum_{i=1}^{n} \left[i - \frac{1}{2}(n+1) \right] X_{(i)} \tag{2.5}$$

which is unbiased for normally distributed quality characteristics. It should be noted that the sampling distribution of D is not symmetric for small and moderate sample sizes. Abu-Shawiesh and Abdullah (2000) proposed the

S^* chart for monitoring process dispersion using Downton's estimator at the stage of the computation of control limits while using the sample standard deviation S as the monitoring statistic. They showed that, in the presence of outliers and non-normality, the S^* chart performs better than the R chart and is as efficient as the S chart.

The dispersion chart, (entirely) based on D proposed in this study, shows clear superiority over both R and S charts and over many other dispersion charts as well, especially for non-normal processes (see Section 6). Further discussion on the use of Downton's estimator in statistical quality control can be seen in Khoo (2004) and Abbasi and Miller (2011a).

Average Absolute Deviation from the Median

The next dispersion estimator we consider is average absolute deviation from the median:

$$MD = \frac{1}{n}\sum_{i=1}^{n}\left|X_i - \tilde{X}\right| \tag{2.6}$$

where $\widetilde{X}$ represents sample median. Although MD incorporates a robust estimate of location, it is still sensitive to outliers but not as sensitive as either R or S. Riaz and Saghir (2008) proposed a MD chart which showed less sensitivity to non-normality than either the R or S charts.

A closely related estimator, MDM, is based on taking absolute deviations from the sample mean $\overline{X}$. Some authors have advocated MDM estimator in place of S (Gorard (2005)) but this has not been considered in this study.

Median Absolute Deviation

The median absolute deviation (MAD)

$$MAD = 1.4826 \text{ med}\left|X_i - \tilde{X}\right| \tag{2.7}$$

has the highest possible breakdown point (50%) and is therefore a very robust estimator of σ, where the breakdown point is the proportion of data that can be given unusually high or low values without having a significant effect on the estimator. Wu et al. (2002) show that for contaminated normal data, MAD outperformed some other robust estimators. However, MAD does have two main drawbacks that were pointed out by Rousseeuw and Croux (1993): low Gaussian efficiency (36.74%) and its reliance on the distribution being symmetric. Dispersion charts based on MAD have not received much attention in the SPC literature.

S_n and Q_n

To overcome the drawbacks of MAD, Rousseeuw and Croux (1993) proposed two alternatives, S_n and Q_n, which both have breakdown points of 50% (same as MAD), but significantly higher Gaussian efficiencies. S_n, defined as

$$S_n = 1.1926 \text{ med}_i \left\{ \text{med}_j \left| X_i - X_j \right| ; i \neq j \right\}, \tag{2.8}$$

is based on the use of repeated medians: the inner median (med_j) is the $\lfloor (n/2)+1 \rfloor^{th}$ order statistic, while the outer median (med_i) is the $\lfloor (n+1)/2 \rfloor^{th}$ order statistic. Rousseeuw and Croux (1993) described these as "high" and "low" medians. Similarly, Q_n is defined as

$$Q_n = 2.2219 \left\{ \left| X_i - X_j \right| ; i < j \right\}_{(k)} \text{ where } k = \begin{pmatrix} \lfloor n/2 \rfloor + 1 \\ 2 \end{pmatrix}. \tag{2.9}$$

In simple terms, Q_n is the k^{th} order statistic of the n-choose-2 interpoint distances. Note that, unlike MD and MAD, S_n and Q_n do not incorporate an estimate of location. Both S_n and Q_n have much higher Gaussian efficiencies than MAD: 58% for S_n and 82% for Q_n. Dispersion charts based on S_n or Q_n have not been investigated in the SPC literature.

Rousseeuw and Croux (1993) suggested that MAD, S_n and Q_n are particularly useful as estimators of σ for heavy-tailed (symmetric) distributions and skewed distributions. They showed through simulations that Q_n is more efficient then either S_n or MAD.

In short, we investigated the following estimators of σ:

$$\begin{cases} S & \text{based on squared deviations from mean} \\ R, IQR, D & \text{based on order statistics} \\ MD, MAD & \text{based on absolute deviations from median} \\ S_n, Q_n & \text{based on interpoint distances} \end{cases}$$

2.3 Control Chart Structure

In this section, we present a general structure that will allow us to construct dispersion charts based on different statistics described in section 2.2. Suppose T represents a dispersion statistic computed from a subgroup of size n obtained from a process which has been scaled to estimate σ (T can be any of the above mentioned dispersion statistics). Let Z be the standardized version of the dispersion statistic T: $Z = T/\sigma$ (similar to $W = R/\sigma$, for R chart; Montgomery (2009) and $D = Q/\sigma$, for Q chart; Riaz (2008)). To develop control limits for the dispersion chart based on T, estimates of σ and σ_T are required, where σ_T represents the standard deviation of the distribution of the dispersion statistic T.

By applying expectation on Z, we get:

$$E(Z) = E(T/\sigma) = E(T)/\sigma$$

Let $E(Z) = t_2$, for a given parent distribution and particular choice of T; t_2 depends on sample size n (Mahoney (1998), Kao and Ho (2007)). $E(T)$ can be replaced with the average of sample Ts, computed from an appropriate number of random samples obtained from a process during normal operating conditions. An unbiased estimator of σ is thus defined as $\hat{\sigma} = \overline{T}/t_2$. Similarly, for an estimate of σ_T, we have $\sigma_Z = \sigma_T/\sigma$. Let $\sigma_Z = t_3$ and by substituting $\hat{\sigma}$ for σ, the estimate for σ_T is defined as $\hat{\sigma}_T = t_3\overline{T}/t_2$.

Hence, the L-sigma control limits (based on statistic T), are given as:

$$\begin{aligned} LCL &= max(0, \overline{T} - Lt_3\overline{T}/t_2) \\ CL &= \overline{T} \\ UCL &= \overline{T} + Lt_3\overline{T}/t_2 \end{aligned}$$

where L is the control chart multiple, usually set at 3 but it can be adjusted to get a specified false alarm rate for an in-control situation.

In most books on SPC, the control chart constants (t_2 and t_3) for R and S charts are provided under the assumption of normality of quality characteristics. When the assumption of normality is disturbed, the use of these constants no longer remains valid, as shown by Mahoney (1998) and Kao and Ho (2007). They considered several non-normal distributions and examined their effect on the values of t_2 and t_3 for Shewhart $\overline{X}$ and R charts. They concluded that the inappropriate use of t_2 and t_3 values increase/decrease the false alarm rate of both $\overline{X}$ and R charts. Hence, there is a need to compute these values for different choices of T by giving proper consideration to the parent distribution.

Probability limits can also be used to develop the design structure of a control chart. For a dispersion chart (based on the statistic T), these limits can be computed by using the quantile points of distribution of Z. Let α be the specified probability of making a Type-I error and Z_α the α-quantile of the distribution of Z. The probability limits for the dispersion chart, based on statistic T, are thus given as:

$$\begin{aligned} LCL &= Z_{(\alpha/2)}\overline{T}/t_2 \quad \text{with} \quad \Pr(Z \leq Z_{(\alpha/2)}) = \alpha/2 \\ UCL &= Z_{(1-\alpha/2)}\overline{T}/t_2 \quad \text{with} \quad \Pr(Z \geq Z_{(1-\alpha/2)}) = \alpha/2 \end{aligned}$$

For a particular parent distribution, the $(\alpha/2)^{th}$ and $(1-\alpha/2)^{th}$ quantile points of the distribution of Z depend on the choice of T and the subgroup size n (Sim and Wong (2003)). Similarly, the use of quantile points that have been computed under the assumption of normality is inappropriate for setting up probability limits for processes following non-normal distributions. Hence, these quantile points must also be computed by giving proper consideration to the parent distribution. In this study, we use the probability limit approach for the performance evaluation of different dispersion charts under the assumption that a large number of in-control samples are available for the estimation of σ in Phase I.

For the computation of the control chart constants (t_2 and t_3) and quantile points, we need to know the distributional results of Z for every combination of T and parent distribution, which are not well known for most of the dispersion statistics considered in section 2.2, particularly for non-normal parent distributions. However, one can estimate the characteristics of any distribution such as mean, standard deviation and cumulative probabilities through repeated generation of random samples. Hence, we use a comprehensive Monte Carlo simulation study to compute the required results. The simulation steps will be explained in the next section. For the rest of this chapter we will refer to the control charts based on R, S, IQR, D, MD, MAD, S_n and Q_n as the R chart, the S chart, the IQR chart (Q chart), the D chart, the MD chart, the MAD chart, the S_n chart and the Q_n chart, respectively.

2.4 Simulation Study

To evaluate the performance of various control chart schemes considered in section 2.3, a comprehensive Monte Carlo simulation study has been performed. A total of eight dispersion charts have been studied, based on different choices of T as described in section 2.2. A wide range of continuous distributions have been considered to investigate the performance of these charts. The density function of these continuous distributions together with parameter values used in this study and the corresponding skewness and excess kurtosis are given in Table 2.1.

Figure 2.1 shows density plots of these distributions; panel (a) presents plots for symmetric normal, logistic and Student's t distributions, while panel (b)

Table 2.1: Density functions and parameter values used for different continuous distributions

Distribution	Density Function	Parameter values	Skewness	Excess Kurtosis
Normal(μ, σ^2) $\mu \in \mathbb{R}, \sigma > 0$	$\frac{1}{\sqrt{2\pi\sigma^2}} e^{-(x-\mu)^2/2\sigma^2}$	$\mu = 0, \sigma = 1$	0	0
Logistic(μ, k) $\mu \in \mathbb{R}, k > 0$	$\frac{e^{-(x-\mu)/k}}{k\left(1+e^{-(x-\mu)/k}\right)^2}$	$\mu = 0, k = 1$	0	1.2
Student's t (t_k) $k > 0$	$\frac{\Gamma[(k+1)/2]}{\sqrt{k\pi}\Gamma(k/2)} \left(1 + \frac{x^2}{k}\right)^{-\frac{(k+1)}{2}}$	$k = 5$	0	6
Weibull(η, β) $\eta > 0, \beta > 0$	$\frac{\eta}{\beta} \left(\frac{x}{\beta}\right)^{\eta-1} e^{-(x/\beta)^\eta}$	$\eta = 1.5, \beta = 1$	1.072	1.390
Chi-square(χ^2) $k > 0$	$\frac{x^{(k/2)-1} e^{-x/2}}{2^{k/2}\Gamma(k/2)}$	$k = 5$	1.265	2.4
Gamma(η, β) $\eta > 0, \beta > 0$	$\frac{\beta^\eta}{\Gamma(\eta)} x^{\eta-1} e^{-\beta x}$	$\eta = 2, \beta = 1$	1.414	3
Exponential(λ) $\lambda > 0$	$\lambda e^{-\lambda x}$	$\lambda = 1$	2	6
Lognormal(μ, σ^2) $\mu \in \mathbb{R}, \sigma > 0$	$\frac{1}{x\sqrt{2\pi\sigma^2}} e^{-\frac{(\ln(x)-\mu)^2}{2\sigma^2}}$	$\mu = 0, \sigma = 1$	6.185	110.936

presents density plots for skewed Weibull, chi-square, Gamma, exponential and lognormal distributions.

As described in section 2.3, it is inappropriate to use the normal based coefficients and quantile points in the construction of control chart limits when the assumption of normality is violated. Hence, these are computed independently under every parent distribution: 100,000 random samples of size $n = 3, 5, 7, 10$ and 12 are simulated from every distribution and the distribution of Z is obtained for every combination of T and parent population. Control chart constants (t_2 and t_3) have been computed as the mean and the standard deviation of the empirical distribution of Z for every choice of T and are provided in Appendix Tables A.1 and A.2. Similarly, for a

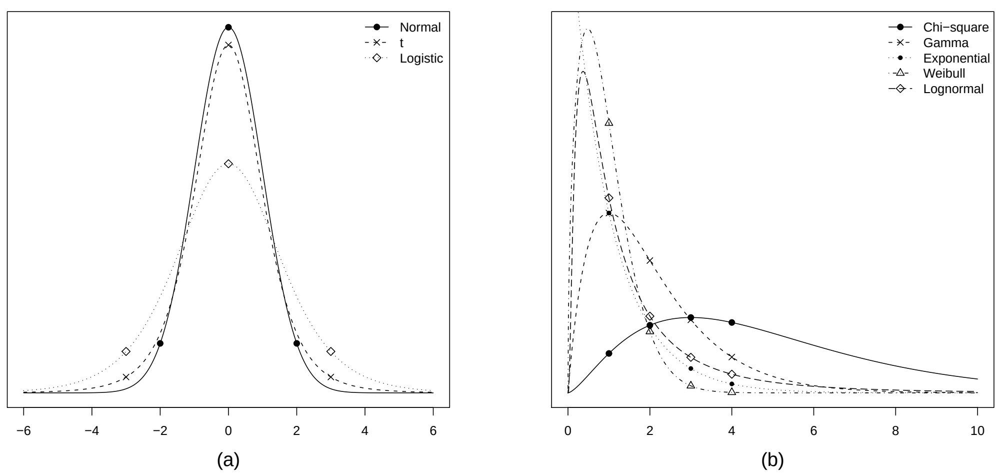

Figure 2.1: Density Curve of Distributions

specified Type-I error probability $\alpha = 0.002$, the $(\alpha/2)^{th}$ and $(1-\alpha/2)^{th}$ quantile points have been computed from the distribution of Z and are given in Appendix Tables A.3 and A.4. These quantile points help in establishing probability limits for different dispersion charts. The simulated results, as shown in Appendix Tables A.1-A.4, for the case of R and S are similar to those of exact results reported in most SPC books assuming normality of the quality characteristic (e.g. see Tables of Ryan (2000)). For the case of non-normal distributions, the results are also similar to the results reported for R chart by Mahoney (1998), Kao and Ho (2007) and Sim and Wong (2003), which confirms the validity of our simulation routines.

The power of control charts to detect shifts in process dispersion is used as a performance measure following Duncan (1951), Nelson (1985) and Riaz (2008). In our case, the process is said to be out-of-control whenever the process standard deviation σ shifts from an in control value, say σ_0 to another value say σ_1, where σ_1 is defined as $\sigma_1 = \sigma_0 + \delta\sigma_0$. We expect the false alarm rate to be close to a prespecified nominal value (α) for an in-control process($\sigma = \sigma_0$). When the process is out-of-control, the power of control charts should be high to detect any inconsistencies in the data.

Efficiency Comparison

To measure the precision of the dispersion statistics defined in section 2.2, standardized variances have been computed for each of these estimators following the recommendations of Rousseeuw and Croux (1993). For each parent distribution, 100,000 samples of size n are simulated and are used for the computation of standardized variances for each of the dispersion statistics and the results are provided in Table 2.2. Standardized variance (SV) of a dispersion statistic T is defined as

$$SV_T = \frac{n\ var(T)}{(ave(T))^2}. \tag{2.10}$$

SV gives a direct measure of the accuracy of a dispersion estimator (Bickel and Lehmann (1976)). From Table 2.2, we can observe that:

For parent normal distribution:

- For all values of n, S estimator has the smallest SV, with D and MD as close competitors.
- For small values of n, R and IQR estimators also have similar SV as S, but the difference between them increases for large values of n.
- The SV for MAD, S_n and Q_n are significantly higher than the rest of the estimators. Hence, we can expect the worst performance of dispersion charts based on these estimators for all values of n.

For parent non-normal distributions:

- For a particular choice of n, the SV for all the estimators increases with an increase in the excess kurtosis for heavy tailed symmetric distributions.
- For a particular choice of n, the SV for all the estimators increases with an increase in the skewness for skewed distributions.
- We can observe a significant change in the SV of the usual R and S estimators as parent distribution moves away from normal.

- Relatively, the D and MD estimators seem to be least affected for most of the parent non-normal distributions (except lognormal).

- For the extreme case of lognormal distribution, the Q_n estimator gets an edge over others.

In general, we can observe that:

- For $n = 3$, the MAD, S_n and Q_n estimators are having higher SV compared to other estimators for every parent environment.

- For a particular choice of parent distribution and dispersion estimator, the SV decreases with an increase in the sample size n.

Further more, Appendix Table A.5 presents results of the relative efficiency (RE) of these estimators. RE is defined as

$$RE = \frac{min(SV_T)}{SV_T} \times 100. \tag{2.11}$$

where $min(SV_T)$ represents the minimum standardized variance, taken over all choices of T. The RE will help us to identify the dispersion estimators that will perform well for specific parent distributions. Figures 2.2 and 2.3 present a graphical comparison of the relative efficiency (RE) of these estimators for heavy tailed symmetric and skewed distributions. The normal case is included in both the figures for comparison purposes. From Figures 2.2 and 2.3, we can observe that:

- For a normally distributed quality characteristic, the most efficient way to estimate σ is by using S, but it quickly loses efficiency for non-normal parent distributions.

- D and MD estimators have maintained good efficient behavior for normal parent case.

- For most of the non-normal cases, D and MD estimators have the highest relative efficiencies.

- R and S based dispersion estimators are mostly affected by departures from normality.
- MAD represents the least efficient estimator of σ for most of the distributional environments.

Table 2.2: Standardized Variance of different dispersion estimators under normal and non-normal distributions

Distribution	n	R	S	IQR	D	MD	MAD	S_n	Q_n
Normal	3	0.822	0.816	0.822	0.822	0.822	2.032	2.033	2.033
	5	0.691	0.656	0.700	0.667	0.700	1.704	1.513	1.442
	7	0.660	0.601	1.072	0.612	0.656	1.586	1.272	1.188
	10	0.674	0.573	0.986	0.584	0.640	1.370	1.132	0.903
	12	0.683	0.558	1.066	0.570	0.626	1.368	1.089	0.869
Logistic	3	1.006	1.002	1.006	1.006	1.006	2.277	2.277	2.277
	5	0.914	0.860	0.853	0.849	0.853	1.859	1.686	1.619
	7	0.945	0.831	1.234	0.807	0.812	1.743	1.452	1.365
	10	1.019	0.817	1.114	0.776	0.786	1.510	1.270	1.086
	12	1.078	0.806	1.196	0.761	0.768	1.492	1.230	1.036
Student's t	3	1.222	1.235	1.222	1.222	1.222	2.412	2.412	2.412
	5	1.200	1.147	1.030	1.069	1.030	1.940	1.780	1.718
	7	1.295	1.150	1.315	1.016	0.967	1.794	1.530	1.446
	10	1.478	1.164	1.163	0.980	0.925	1.529	1.314	1.153
	12	1.610	1.185	1.255	0.974	0.915	1.531	1.286	1.114
Weibull	3	1.035	1.052	1.035	1.035	1.035	2.217	2.217	2.217
	5	0.908	0.907	0.884	0.862	0.884	1.864	1.678	1.604
	7	0.910	0.875	1.283	0.808	0.838	1.749	1.465	1.311
	10	0.964	0.861	1.169	0.776	0.815	1.501	1.339	1.016
	12	1.003	0.855	1.260	0.762	0.799	1.505	1.308	0.971
Chi-square	3	1.146	1.169	1.146	1.146	1.146	2.316	2.316	2.316
	5	1.051	1.052	0.986	0.978	0.985	1.925	1.744	1.663
	7	1.080	1.038	1.405	0.930	0.940	1.804	1.522	1.377
	10	1.173	1.038	1.271	0.897	0.910	1.581	1.397	1.090
	12	1.237	1.039	1.367	0.883	0.897	1.560	1.361	1.028
Gamma	3	1.235	1.267	1.235	1.235	1.235	2.410	2.410	2.410
	5	1.148	1.159	1.069	1.066	1.069	2.018	1.836	1.760
	7	1.191	1.147	1.488	1.014	1.017	1.907	1.632	1.460
	10	1.298	1.150	1.337	0.972	0.976	1.639	1.493	1.150
	12	1.373	1.155	1.438	0.964	0.966	1.639	1.465	1.097
Exponential	3	1.682	1.742	1.682	1.682	1.682	2.984	2.985	2.985
	5	1.641	1.670	1.479	1.504	1.480	2.608	2.442	2.360
	7	1.742	1.687	1.966	1.447	1.412	2.466	2.244	2.020
	10	1.923	1.719	1.793	1.409	1.371	2.172	2.135	1.694
	12	2.039	1.727	1.910	1.385	1.341	2.159	2.107	1.628
Lognormal	3	4.119	4.397	4.119	4.119	4.119	4.279	4.277	4.278
	5	4.425	4.650	3.453	3.799	3.454	3.399	3.218	3.164
	7	5.233	5.239	3.444	3.846	3.362	3.136	2.889	2.687
	10	6.224	5.774	2.940	3.793	3.212	2.714	2.741	2.339
	12	7.128	6.322	3.072	3.891	3.257	2.676	2.666	2.196

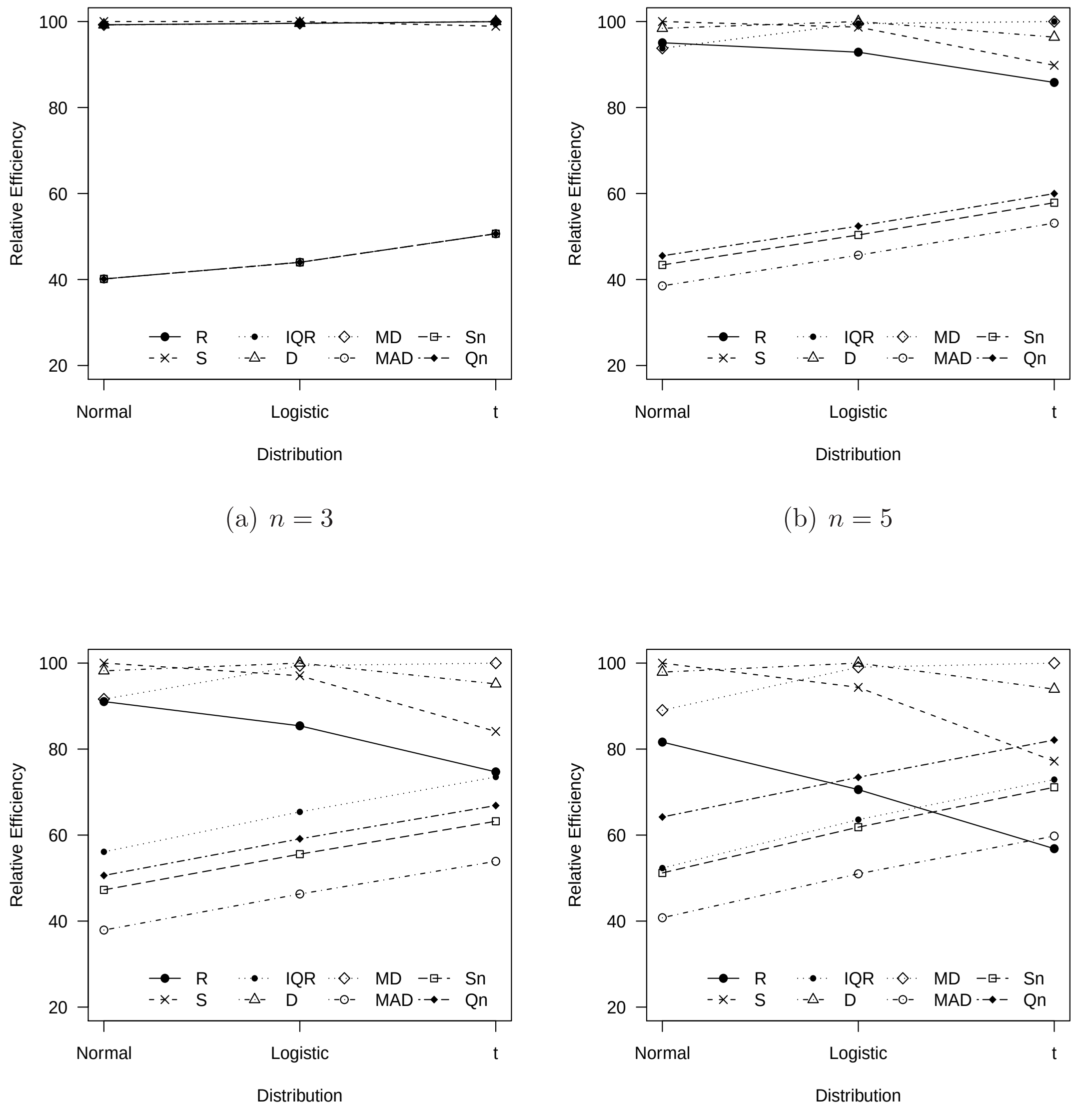

(a) $n = 3$

(b) $n = 5$

(c) $n = 7$

(d) $n = 12$

Figure 2.2: Relative efficiency of different dispersion estimators for symmetric distributions

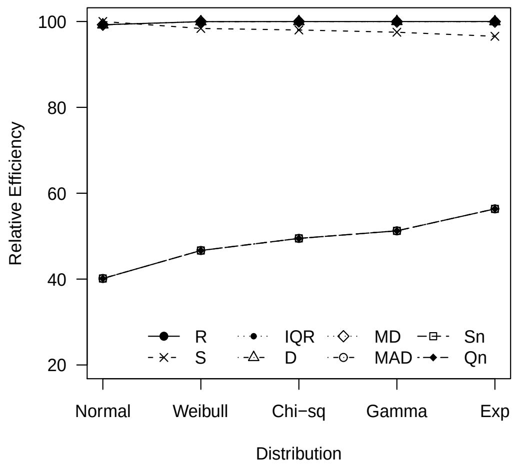

(a) $n = 3$

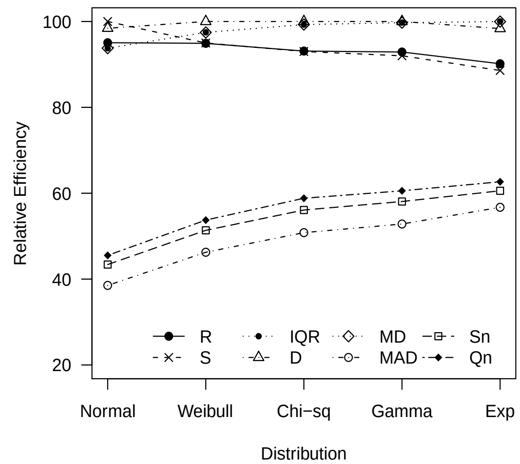

(b) $n = 5$

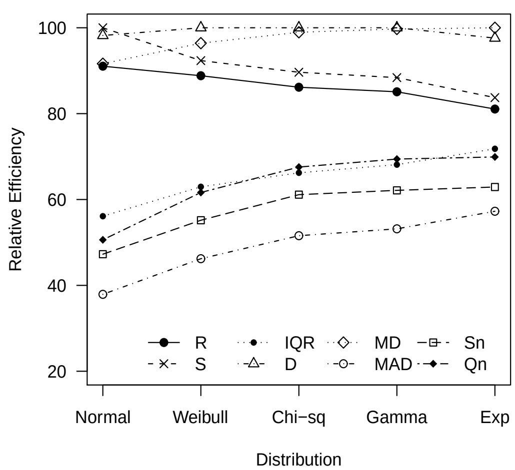

(c) $n = 7$

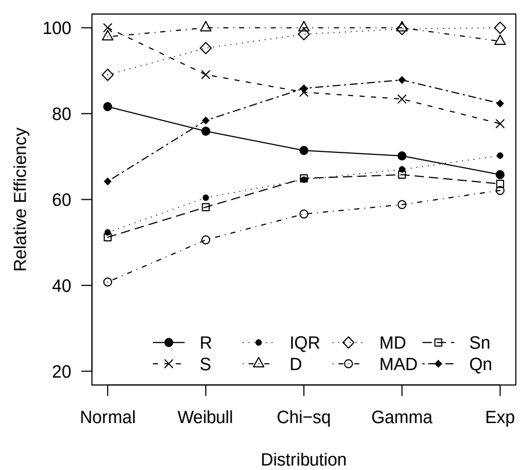

(d) $n = 12$

Figure 2.3: Relative efficiency of different dispersion estimators for skewed distributions

2.5 The Case of the Normal Distribution

First, we consider the case when the quality characteristic can safely be assumed to come from a normal distribution. Using control chart constants and quantile points from Appendix Tables A.1-A.4, for the case of normal distribution, probability limits have been determined for every control chart considered in section 2.3. The power of all the control charts is computed considering shifts of different magnitudes in process dispersion. To save space and aid in visual clarity, power curves have been constructed instead of presenting the results in tabular form. In each plot, the shift in σ, measured as a multiple δ of the in-control standard deviation, is plotted on the horizontal axis while the power of the different dispersion charts is plotted on the vertical axis.

The power curves of the different dispersion charts for normally distributed quality characteristics for $n = 3, 5, 7$ and 12 are shown in Figure 2.4. One sample of results has been presented in Table 2.3, which shows the power of different charts to detect shifts in process standard deviation at different magnitudes for the case of normal distribution when $n = 10$. Power curves and sample results reported in Table 2.3 provide useful information about the detection ability of various control charts. For example, we can see that the S chart has a 90% chance to detect a 1.579σ shift in process standard deviation (highest power among all charts) while MAD chart has only 55.8% chance to detect a shift of this magnitude (lowest power among all charts) when $n = 10$.

As expected, for a zero sigma shift in process standard deviation, the false alarm rate is very close to 0.002 for all choices of T and for every sample size, representing the case for an in control process. The power of all the charts has increased with an increase in n and the magnitude of shift. For sample size $n = 3$ and 5, it seems hard to differentiate between the power curves of the S chart and other charts, except for the MAD, S_n and Q_n charts. The performance of these charts is extremely poor for $n = 3$ and 5. In relative terms, we can see that the power of R and IQR charts decreases as sample size increases, while the power of S_n and Q_n charts increases with an increase in n. The D chart appears to behave similarly to the S chart, which has the highest power for all the cases. The MD chart also performed reasonably well, although it is slightly less efficient than the S and D charts but better than all the others. Hence, from power curves in Figure 2.4, we can conclude that under the ideal assumption of normality:

- the S chart has the best performance,
- the D chart can be treated as a strong competitor to the S chart,
- the MD chart is slightly less efficient than the S and D charts but better than other charts,
- the relative power of the R and IQR charts decreases with an increase in n, and
- the MAD chart shows the worst performance due to low Gaussian efficiency of MAD.

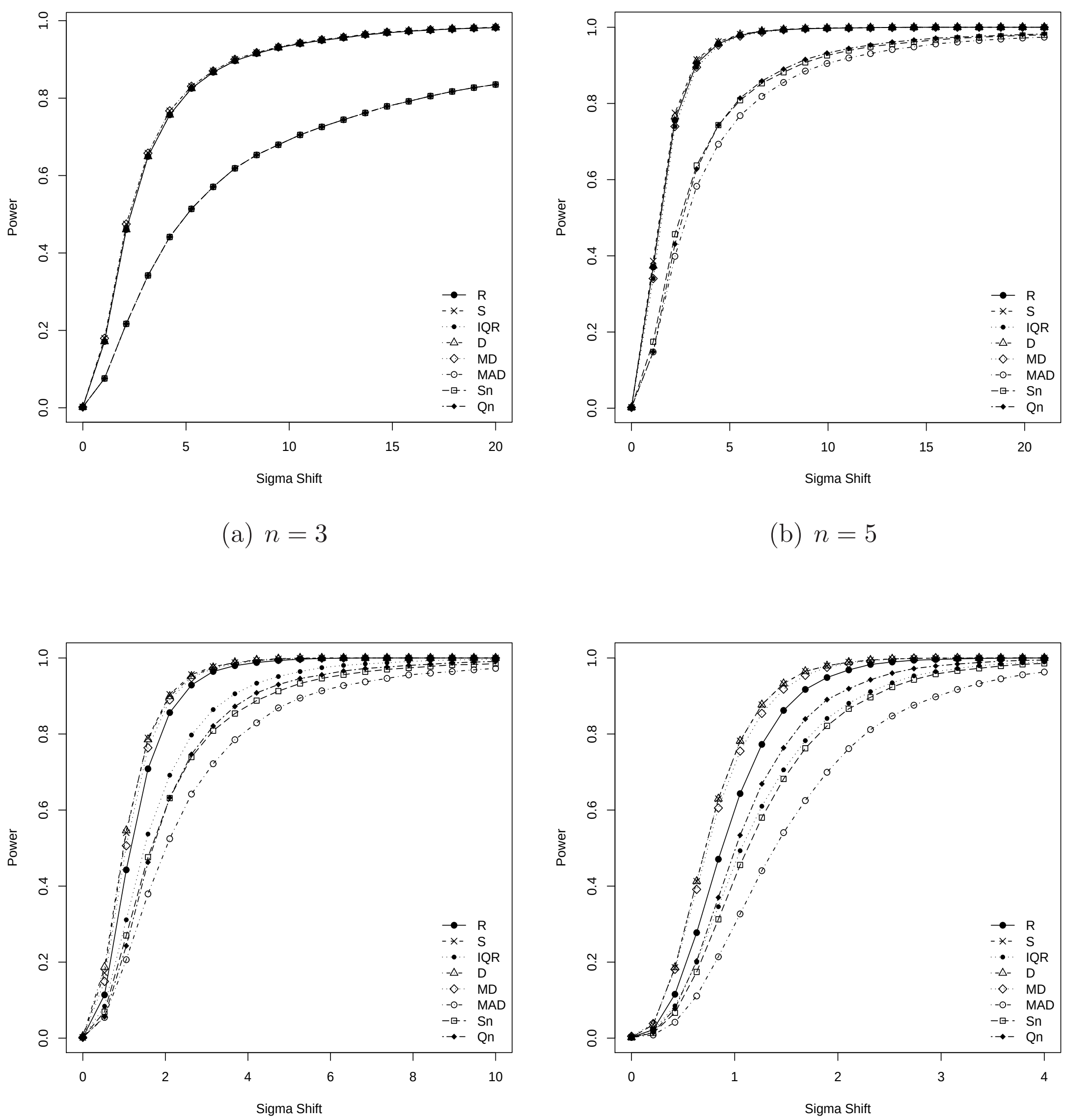

(a) $n = 3$ (b) $n = 5$

(c) $n = 7$ (d) $n = 12$

Figure 2.4: Power curves of different dispersion charts for $n = 3, 5, 7$ and 12 under normal distribution (with $\mu = 0, \sigma = 1$) when $\alpha = 0.002$

Table 2.3: Power of different dispersion charts for normally distributed quality characteristic when $n = 10$ and $\alpha = 0.002$

δ	R	S	IQR	D	MD	MAD	S_n	Q_n
0.000	0.0020	0.0020	0.0020	0.0020	0.0020	0.0020	0.0020	0.0020
0.316	0.0478	0.0573	0.0328	0.0568	0.0464	0.0274	0.0279	0.0397
0.632	0.2340	0.2916	0.1544	0.2890	0.2435	0.1193	0.1368	0.1861
0.947	0.4982	0.5923	0.3394	0.5870	0.5144	0.2682	0.3116	0.4035
1.263	0.7080	0.7880	0.5325	0.7810	0.7292	0.4177	0.4864	0.5977
1.579	0.8404	0.8998	0.6837	0.8918	0.8581	0.5579	0.6317	0.7374
1.895	0.9171	0.9558	0.7842	0.9473	0.9246	0.6649	0.7384	0.8295
2.211	0.9571	0.9839	0.8572	0.9751	0.9629	0.7513	0.8138	0.8920
2.526	0.9769	0.9892	0.9038	0.9886	0.9818	0.8092	0.8661	0.9306
2.842	0.9888	0.9955	0.9335	0.9949	0.9905	0.8560	0.9067	0.9568
3.158	0.9938	0.9982	0.9561	0.9976	0.9958	0.8893	0.9333	0.9695
3.474	0.9972	0.9996	0.9710	0.9990	0.9981	0.9132	0.9517	0.9800
3.789	0.9984	1.0000	0.9807	0.9999	0.9994	0.9336	0.9650	0.9869
4.105	0.9996	1.0000	0.9877	1.0000	1.0000	0.9504	0.9750	0.9901
4.421	1.0000	1.0000	0.9909	1.0000	1.0000	0.9627	0.9816	0.9933
4.737	1.0000	1.0000	0.9938	1.0000	1.0000	0.9714	0.9851	0.9952
5.053	1.0000	1.0000	0.9957	1.0000	1.0000	0.9763	0.9889	0.9966
5.368	1.0000	1.0000	0.9965	1.0000	1.0000	0.9807	0.9911	0.9973
5.684	1.0000	1.0000	0.9978	1.0000	1.0000	0.9848	0.9935	0.9980
6.000	1.0000	1.0000	0.9986	1.0000	1.0000	0.9875	0.9945	0.9988

2.6 The Case of Non-Normal Distributions

In the previous section, the performance of control charts was evaluated under the ideal assumption of normality. This assumption is widely used in statistics and almost all SPC charts are based on it. However, in practice, data from many real world processes follow non-normal distributions: Bissell (1994) points out that quality characteristics such as capacitance, insulation resistance and surface finish do not follow a normal distribution; James (1989) reported that characteristics such as roundness, mold dimensions and customer waiting times follow non-normal distributions; Levinson and Polny (1999) indicate that impurity levels in semiconductor process chemicals follow a gamma distribution; and in nuclear reactions, the interval between beta particle emissions follows an exponential distribution (Miller and Miller (1995)). In these situations (and many others), it is inappropriate to use the control charts based on the assumption of normality and hence there is a need to study the performance of various dispersion charts for non-normal distributions. Hence, in this section, the performance of the dispersion charts is investigated for a wide variety of non-normal distributions. For the case of heavy-tailed symmetric distributions, we have considered logistic and Student's t distributions. To cover skewed distributions, we have used the Weibull, gamma, chi-square, exponential and lognormal distributions. The performance of each dispersion chart is evaluated for every distribution to give us a clear picture of overall performance. The control chart constants and quantile points required for setting up the probability limits for non-normal processes have been computed in a similar manner to the normal distribution and are reported in Appendix Tables A.1-A.4.

2.6.1 The performance of control charts for heavy tailed symmetric distributions

The power curves for all of the dispersion charts for the symmetric logistic and Student's t distributions (the constants and quantile points for these charts are given in Appendix Tables A.1 - A.4) are shown in Figures 2.5 and

2.6 for $n = 3, 5, 7$ and 12. For the logistic distribution, the D and MD charts have shown better overall performance than the other charts. The S chart, although less efficient than the D and MD charts, has higher power than the rest of the charts. The R and IQR charts show good performance for small sample sizes ($n = 3$ and 5) but, as the sample size increases, the detection ability of both of these charts reduces significantly relative to other charts. The Q_n chart performs better for large sample sizes, while the MAD chart has the worst overall performance.

For the Student's t distribution, we see that most of the charts have shown better performance than the classical R and S charts. The MD chart shows the best overall performance. The power of the IQR chart again starts to decrease relative to other charts with an increase in n. There seems to be a significant gain in the powers of S_n and Q_n charts as the sample size increases. The D chart has shown better performance than the S_n and Q_n charts for large shifts in σ, while for the detection of small shifts, S_n and Q_n charts are performing better than the D chart. In short, we can say that for logistic processes:

- the performance of the D and MD charts is almost the same and is better than for all of the other charts,
- the S chart also seems to perform reasonably well,
- most control charts perform better than the R chart for $n > 5$, and
- the performance of the MAD chart is the worst among all the charts.

Similarly, for t-distributed quality characteristics:

- the MD chart is the most efficient,
- the Q_n and D charts are close competitors to the MD chart, and
- all of the other charts have higher discriminatory powers than the R and S charts, particularly for moderate to large sample sizes.

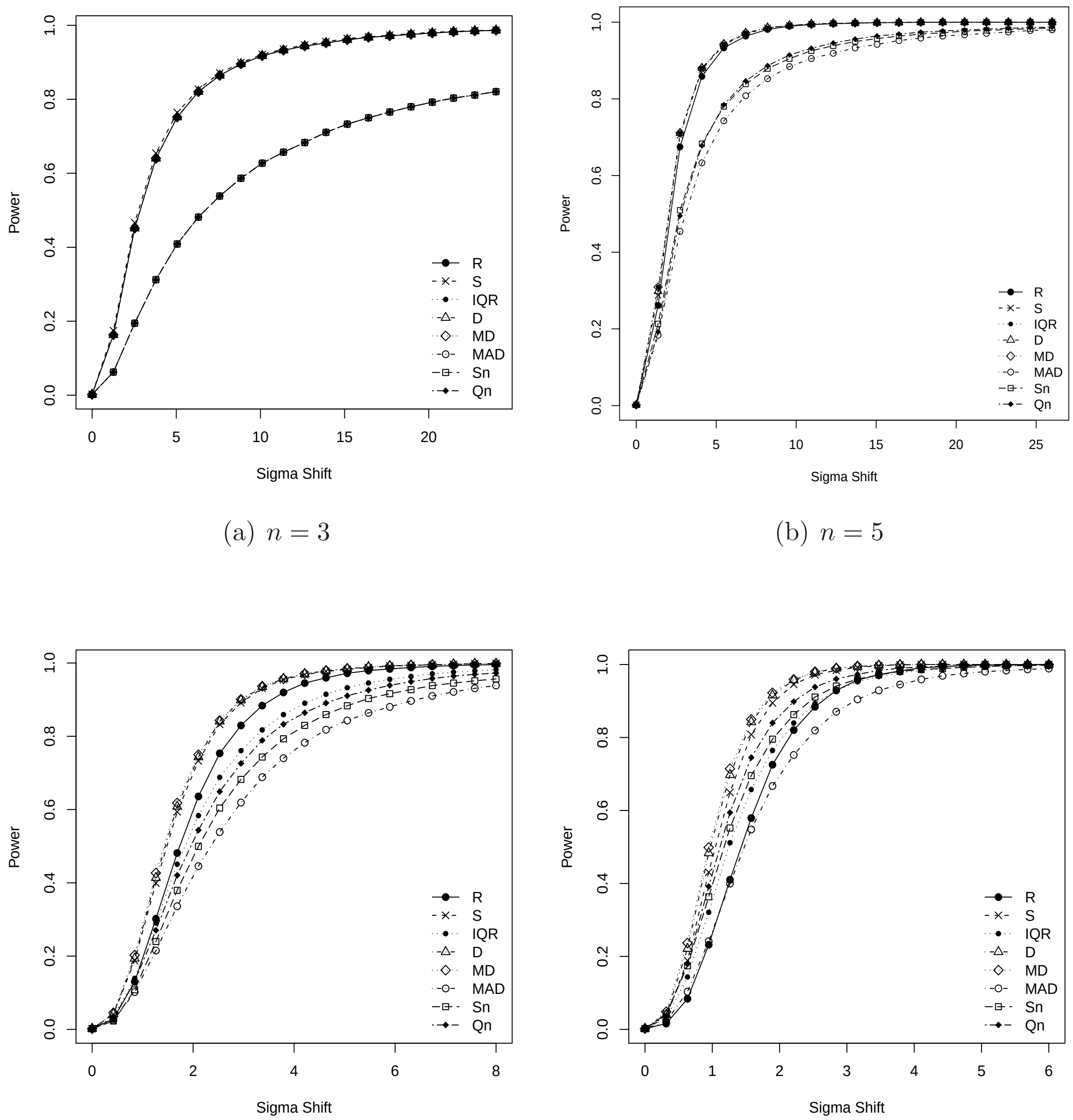

(a) $n = 3$ (b) $n = 5$

(c) $n = 7$ (d) $n = 12$

Figure 2.5: Power curves of different dispersion charts for $n = 3, 5, 7$ and 12 under logistic distribution (with $\mu = 0, k = 1$) when $\alpha = 0.002$

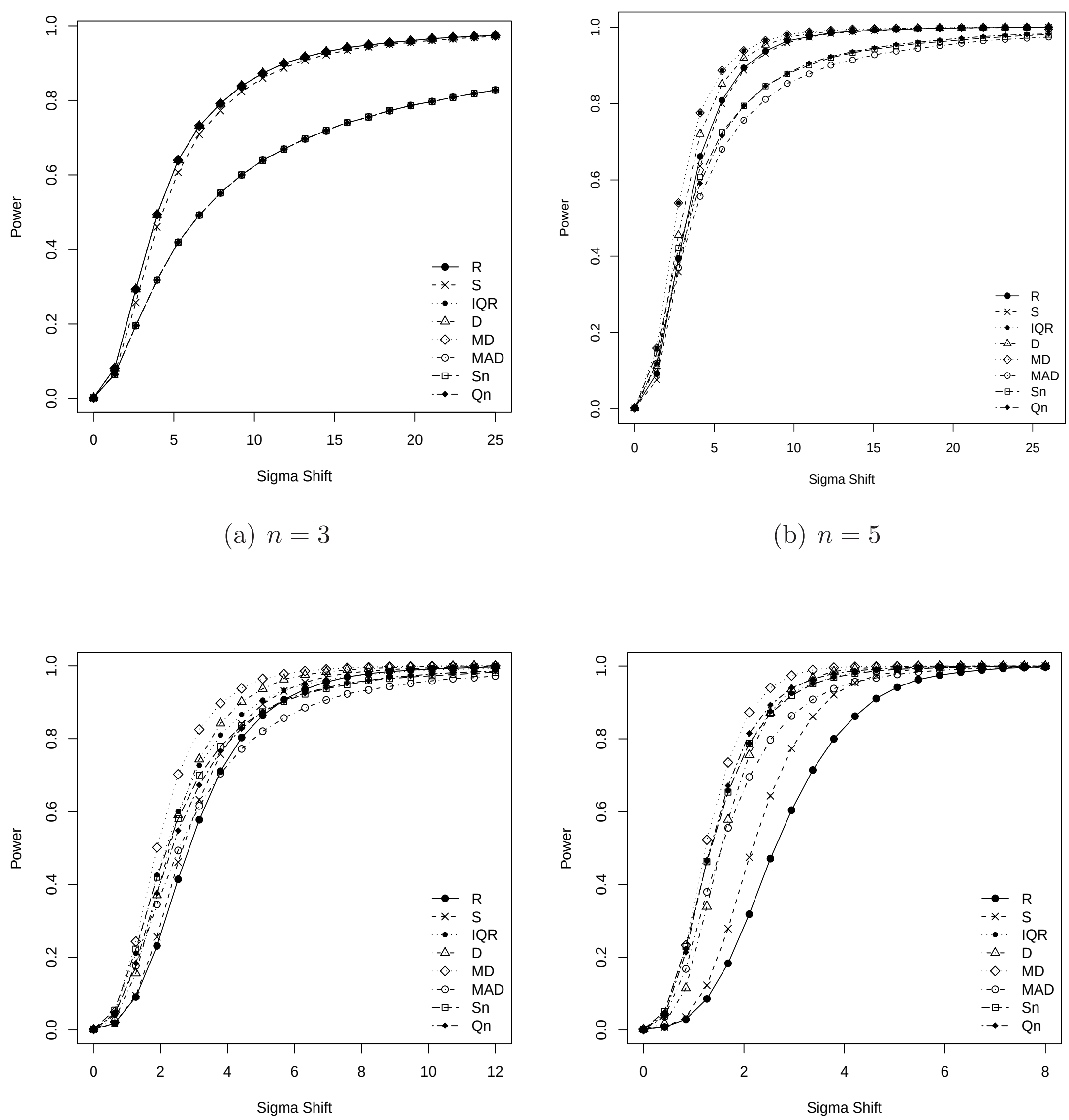

(a) $n = 3$ (b) $n = 5$

(c) $n = 7$ (d) $n = 12$

Figure 2.6: Power curves of different dispersion charts for $n = 3, 5, 7$ and 12 under t distribution (with $k = 5$) when $\alpha = 0.002$

2.6.2 The performance of control charts for skewed distributions

In this section, we evaluate the performance of various dispersion schemes when the monitoring data is generated from skewed distributions. Figure 2.7 presents the power curves of the dispersion charts when the quality characteristic is assumed to follow a Weibull distribution. We can observe that the D chart has shown the best overall performance with slightly higher power than the MD chart. The S_n, Q_n and MAD charts still perform very poorly for $n = 3$ and 5, but a significant gain in the power of the Q_n chart is seen as n increases. The power of the S chart is affected but not as much as that of the R and IQR charts, which are extremely affected for $n > 5$. Figures 2.8 and 2.9 present power curves of dispersion schemes when the distribution of the quality characteristic is assumed to be chi-square or gamma. The power curves of the D and MD charts are always higher than those for all of the other charts, indicating these charts have better detection ability. The IQR chart has again performed well for small sample sizes, while, for large n, the Q_n chart appears to be a better choice after the D and MD charts. The S_n chart shows its superiority over the S chart under the gamma distribution, while, for the chi-square distribution, the S chart appears to perform better than the S_n chart. The R chart is extremely affected by skewed distributions and has the lowest discriminatory power than most of the charts.

Figure 2.10 presents the power curves when the monitoring data are generated from the exponential distribution. The best detection ability is shown by the MD chart followed by the D chart. The power of the R and S charts is extremely affected and a significant gain in the power of the Q_n chart can be observed for large sample sizes. The power curves presented in Figure 2.11 for the lognormal distribution present a different picture. The Q_n, MAD and S_n charts have outperformed the other control charts in this case. This is due to the fact that the lognormal distribution with $\mu = 0$ and $\sigma = 1$ is extremely skewed and its excess kurtosis is also very high. Hence, the charts based on dispersion estimators with high breakdown point are performing better than the rest. The Q_n chart has the highest power among all control charts. The R and S charts have been again extremely affected, presenting the worst performance for every sample size. The IQR chart also appears to be better than the D and MD charts in this case. In short, we can say that when data follow a skewed distribution (other than the lognormal):

- the D and MD charts are superior than the other charts,
- the Q_n chart is a close competitor to the D and MD charts for large sample sizes,
- the IQR chart has reasonable performance for small sample sizes, and
- the performance of R and S charts is greatly affected.

For the case of lognormal distribution:

- the Q_n chart has the best performance,
- the S_n and MAD charts are close competitors to the Q_n chart,
- the D and MD charts are less efficient then the IQR chart, and
- the R and S charts have the lowest discriminatory power compared to rest of the charts.

Comparing the power curves in Figure 2.4 for the case of a normally distributed quality characteristic to the power curves in Figures 2.5-2.11, when the distribution of a quality characteristic is assumed to be heavy tailed symmetric or skewed, we can clearly observe that the power of most of the control charts decreases with an increase in the value of skewness and excess kurtosis. This reduction in the power is more significant for control charts based on R, S and IQR estimators compared to the control charts based on other estimators. The D and MD charts are least affected for most of the non-normal cases. These results are also in close agreement with the findings of Figures 2.2 and 2.3, which present relative efficiencies of different dispersion estimators.

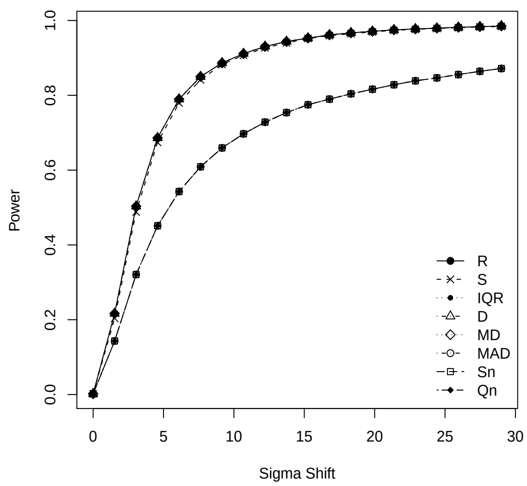

(a) $n = 3$

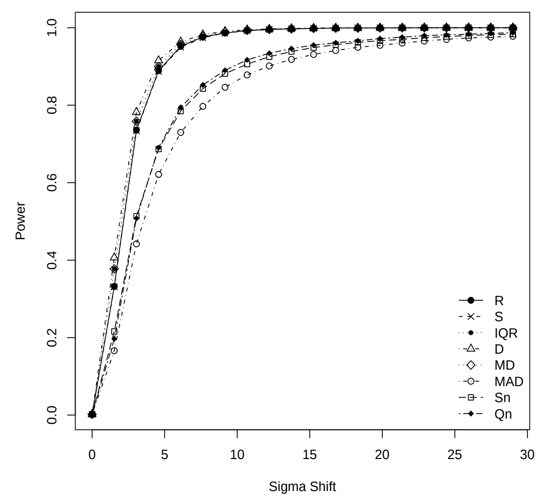

(b) $n = 5$

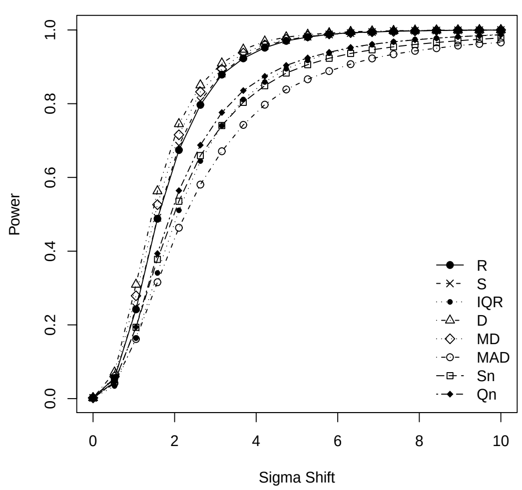

(c) $n = 7$

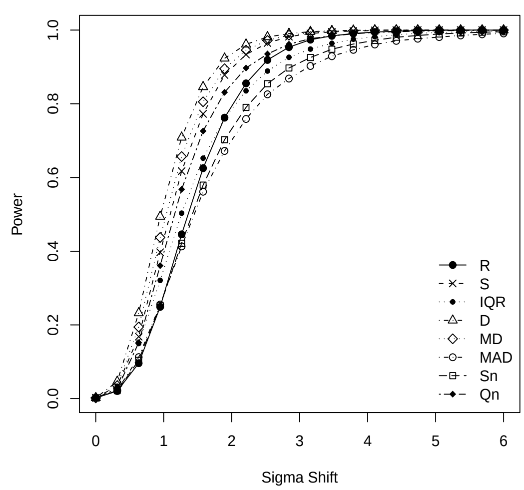

(d) $n = 12$

Figure 2.7: Power curves of different dispersion charts for $n = 3, 5, 7$ and 12 under Weibull distribution (with $\eta = 1.5, \beta = 1$) when $\alpha = 0.002$

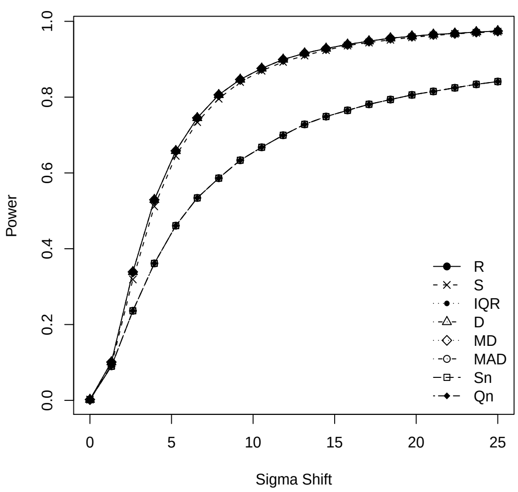

(a) $n = 3$

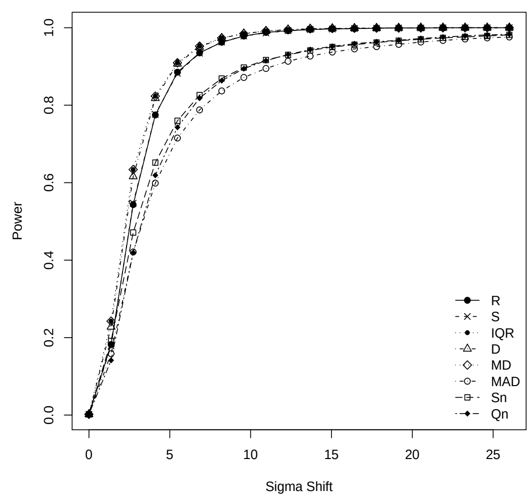

(b) $n = 5$

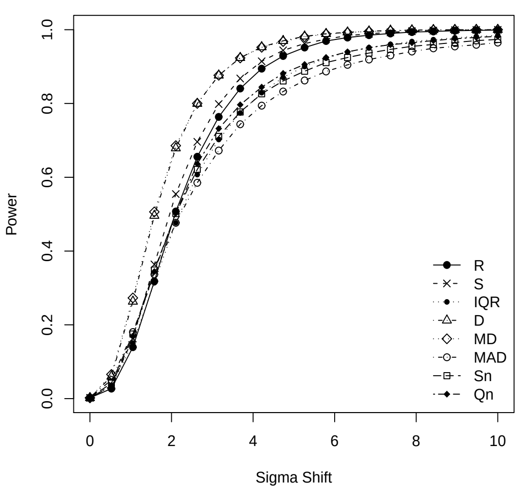

(c) $n = 7$

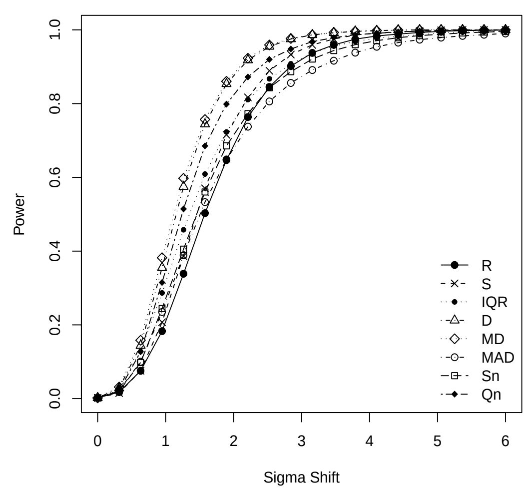

(d) $n = 12$

Figure 2.8: Power curves of different dispersion charts for $n = 3, 5, 7$ and 12 under chi-square distribution (with $k = 5$) when $\alpha = 0.002$

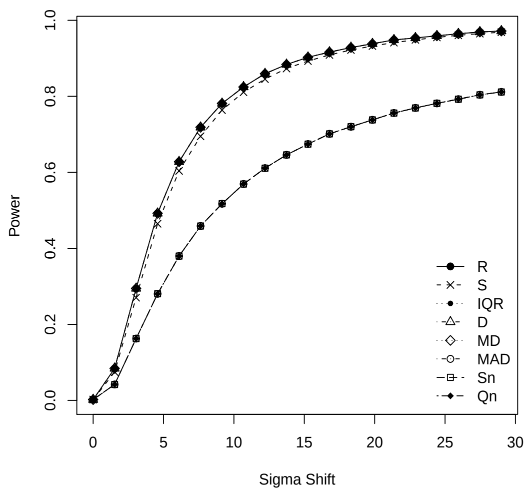

(a) $n = 3$

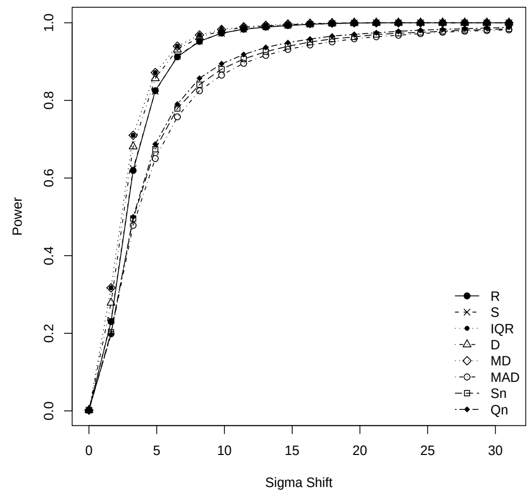

(b) $n = 5$

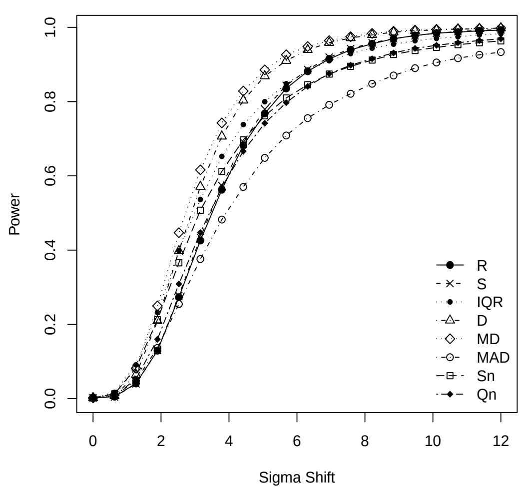

(c) $n = 7$

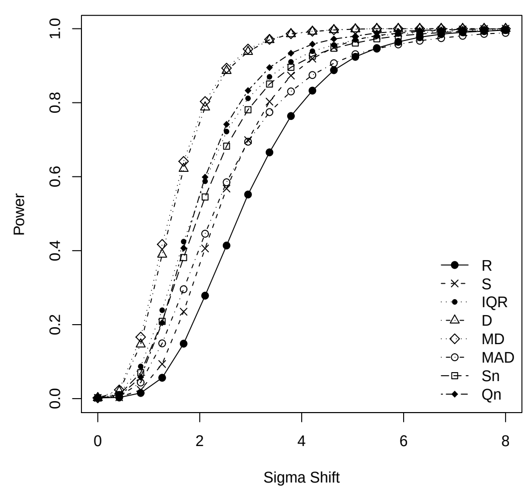

(d) $n = 12$

Figure 2.9: Power curves of different dispersion charts for $n = 3, 5, 7$ and 12 under gamma distribution (with $\eta = 2.0, \beta = 1$) when $\alpha = 0.002$

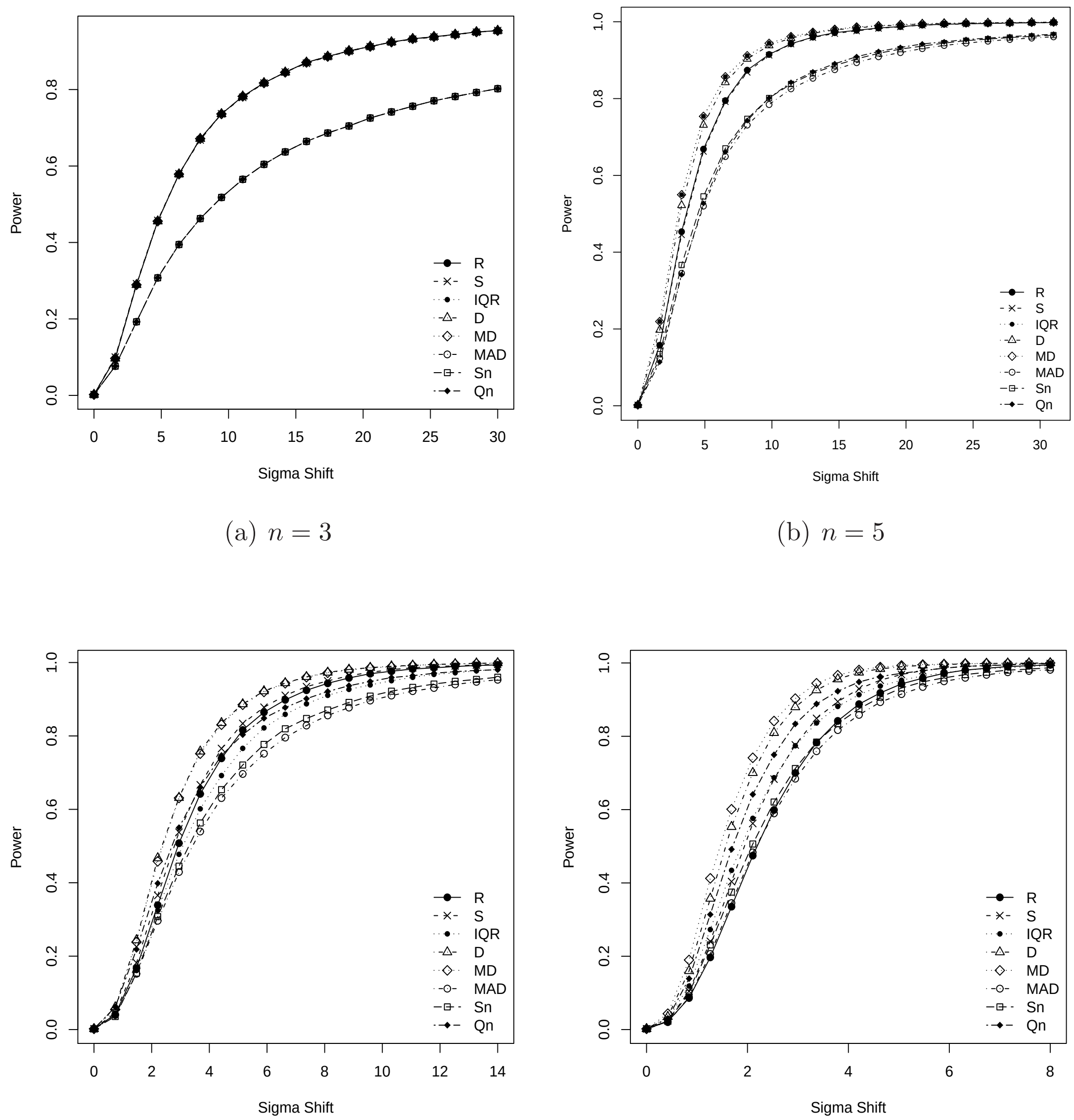

(a) $n = 3$

(b) $n = 5$

(c) $n = 7$

(d) $n = 12$

Figure 2.10: Power curves of different dispersion charts for $n = 3, 5, 7$ and 12 under exponential distribution (with $\lambda = 1$) when $\alpha = 0.002$

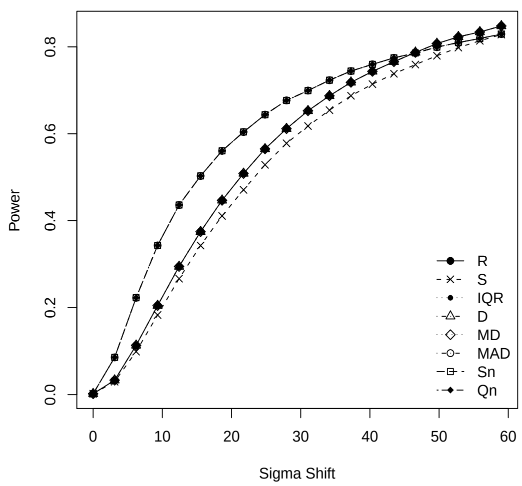

(a) $n = 3$

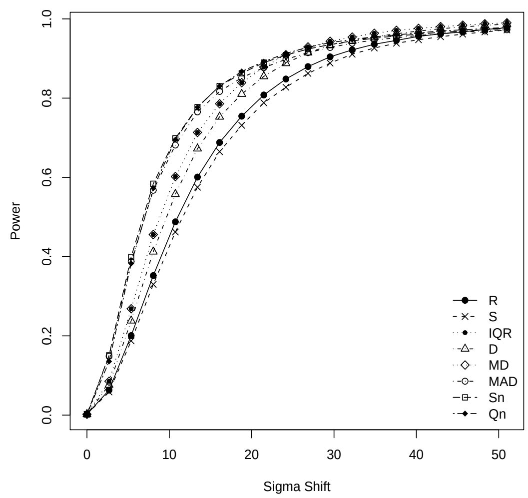

(b) $n = 5$

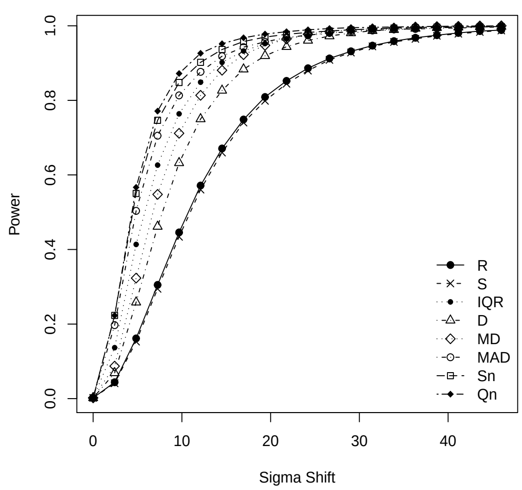

(c) $n = 7$

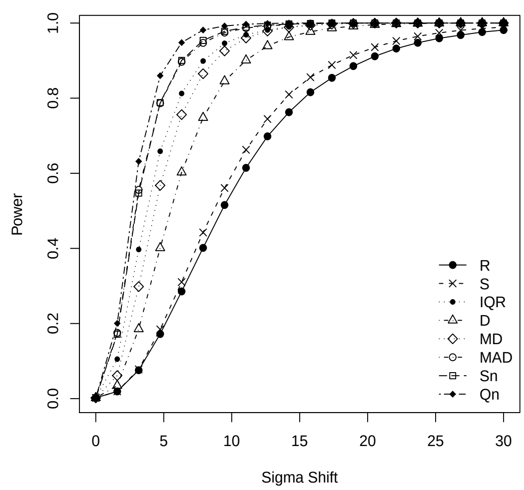

(d) $n = 12$

Figure 2.11: Power curves of different dispersion charts for $n = 3, 5, 7$ and 12 under lognormal distribution (with $\mu = 0, \sigma = 1$)when $\alpha = 0.002$

2.7 Conclusions

In this study, we investigated the performance of various dispersion charts for normal and different non-normal processes. There is always one chart which performs best for a particular case. For normally distributed quality characteristics, the S chart is superior to the rest of control charts. We have shown that the performance of the D chart is similar to that of the S chart. The R and IQR charts have shown reasonable performance for small sample sizes, but a significant decrease in the relative power of these charts has been observed for larger sample sizes. For the case of heavy-tailed symmetric distributions, D and MD charts performed better than the other charts. The Q_n chart is also performing reasonably well. The relative power of the R and S charts decreased significantly with an increase in the value of excess kurtosis. For the case of skewed distributions, the D and MD charts again showed better overall performance compared to the rest of the dispersion charts, except for the lognormal distribution where the Q_n chart has shown its superiority. The IQR chart has shown reasonable performance for small sample sizes. The performance of R and S charts is extremely affected for the distributions with high skewness. We also observed that, compared to the normal case, relatively larger sample size is required to detect a particular amount of shift under the non-normal parent environments.

We have shown that the power of a dispersion chart is strongly related to the efficiency of the dispersion estimator used in its construction, under a particular distributional environment. If one needs to select a chart for the monitoring of dispersion in Phase II, it is recommended to check its relative efficiency as compared to the other available estimators.

Chapter 3

Shewhart Control Charts for Monitoring Process Dispersion in Phase I

Control charts are usually implemented in two phases: the retrospective phase (Phase I) and the monitoring phase (Phase II). The performance of any control chart structure depends on the preciseness of the control limits obtained from Phase I analysis. In SPC, the performance of Phase I dispersion charts has mostly been investigated for normal or contaminated normal distributions of the quality characteristic of interest. Little work has been done to investigate the performance of a wide range of Phase I dispersion charts for processes following non-normal distributions. The current study deals with the proper choice of a control chart for the evaluation of process dispersion in Phase I. We have analyzed the performance of a wide range of dispersion control charts, including two distribution-free structures. The performance of the control charts is evaluated in terms of probability to signal, under normal and non-normal process setups. These results will be useful for quality control practitioners in their decision making. This chapter is based on Abbasi et al. (2012b).

3.1 Introduction

We perform retrospective analysis during Phase I in order to get a controlled structure for the prospective analysis. In the retrospective phase, historical data are analyzed to estimate the in-control state of the process, whereas the prospective phase involves assessing the current state of the process by analyzing the current data. In Phase I, we expect that if there are some inconsistencies in the initial set of samples, there should be high chances for their detection during retrospective analysis. The goal for the monitoring phase (Phase II) is the quick detection of departures of the process parameters from their in-control values. The focus of this study is Phase I analysis, particularly with reference to the monitoring of the dispersion parameter. For a good discussion on Phase I and Phase II control charts, one may see the studies by Jensen et al. (2006), Vining (2009) and Chakraborti et al. (2009).

The performance of any Phase II control chart depends on the preciseness of the control limits obtained from the Phase I analysis. In SPC applications, process (location and dispersion) parameters are usually unknown and need to be estimated from the historical dataset. If the historical dataset is known to consist entirely of observations from the in-control process then the Phase I procedure would simply involve using the most efficient estimator (for a particular parent distribution) for the estimation of unknown parameters and control limits (for Phase II monitoring). However, mostly the historical dataset is contaminated with some unusual samples/observations, that affect the estimation process and also the detection ability of control charts. The focus of this study is on monitoring process dispersion so we are mostly concerned with the estimation of σ. The usual estimates of σ are based on sample range R or sample standard deviation S. Both these estimators perform well under the ideal assumption of normality but are well known to be inefficient when the assumption of normality is violated.

Following Shewhart's pioneering proposals of R and S charts, many researchers have developed different control charts having resistant design structures, e.g. see – Rocke (1989, 1992), Pappanastos and Adams (1996), Tatum

(1997), Abu-Shawiesh (2008), Riaz (2008); Riaz and Saghir (2009), Mukherjee and Chakraborti (2012) and the references therein. In recent years, the estimation effects of σ have been investigated by different researchers. Wu et al. (2002) examined the effects of different estimators of σ on the performance of the Shewhart $\overline{X}$ chart when measurements are taken from contaminated normal distributions. Braun and Park (2008) investigated the effect of different σ estimators on the performance of the EWMA location chart for individual measurements from contaminated normal and t distributions. Schoonhoven et al. (2008) and Schoonhoven and Does (2010) used different estimates of σ to examine their effect on the performance of $\overline{X}$ chart under the existence and the violation of the normality assumption. Schoonhoven et al. (2011) and Schoonhoven and Does (2012) investigated the effect of estimating σ in Phase I on control chart's performance in Phase II for monitoring process dispersion. Jones-Farmer and Champ (2010) proposed a distribution-free structure for monitoring dispersion and compared the performance of his proposal with R and S charts.

No study, as yet, has investigated a wide range of dispersion charts in Phase I for processes following non-normal parent distributions. Many quality characteristics such as capacitance, insulation resistance, surface finish, roundness, mold dimension, customer waiting time and the impurity levels in semi conductor process chemicals follow non-normal distributions (cf. Bissell (1994), James (1989) and Levinson and Polny (1999)). The underlying distributional environment can have a significant impact on the detection ability of control charts. As reported by Woodall (2000), "*As one works in Phase I to remove assignable causes and to achieve process stability, the form of the hypothesized underlying distribution becomes more important in determining control limits and in assessing process capability. To interpret a chart in Phase I, practitioners need to be aware that the probability to signals can vary considerably depending on the shape of the underlying distribution for a stable process*". This is the focus of the current study. We will study how the probability to signal of dispersion charts varies for different parent distributions of the quality characteristic of interest in Phase I.

The purpose of this study is to evaluate and compare the performance of various dispersion charts during Phase I for normal and non-normal parent environments, using probability to signal as a performance measure. For representing non-normal cases, we have considered both heavy-tailed symmetric (logistic & Student's t) and skewed (Gamma & exponential) distributions. The dispersion control charts investigated in this study are based on the sample range, the sample standard deviation, the pooled sample standard deviation (Vardeman (1999)), the interquartile range, Downton estimator, the average absolute deviation from median, the median absolute deviation, S_n statistic, Q_n statistic and the distribution-free scale rank statistic (Jones-Farmer and Champ (2010)).

The organization of the rest of this chapter is: Section 3.2 presents different dispersion estimators and their corresponding control chart structures; Section 3.3 describes steps taken for the performance evaluations of these dispersion charts in Phase I; Section 3.4 offers the discussion of the results and gives comparisons of different charting structures; Section 3.5 includes illustrative examples with real data application; and Section 3.6 summarizes and concludes the findings of the study along with the recommendations for some future research in this direction.

3.2 Monitoring of Process Dispersion Parameter

The monitoring of a process dispersion parameter is carried out using dispersion control charts. A dispersion control chart that can perform better under the existence and violation of ideal assumptions is of more practical value. In this section, we describe different ways of estimating the process standard deviation σ in Phase I and further provide control chart structures based on these σ estimators.

Dispersion Estimators

Suppose the historical dataset comprises of m subgroups of size n. Let

X_{ij}, $i = 1, 2, \cdots, m$ and $j = 1, 2, \cdots, n$ denote the observations of this historical dataset from a process distributed with mean μ and standard deviation σ. Further let $\bar{X}_i$ be the sample mean, $\tilde{X}_i$ be the sample median and $|X_i|$ be the absolute value of X for the i^{th} sample. Below we define different ways of estimating σ in Phase I. Most of these estimators have been investigated in Chapter 2 for Phase II monitoring of process dispersion.

Sample Range: $R_i = X_{i(n)} - X_{i(1)}$, where $X_{i(1)}$ and $X_{i(n)}$ represents the extreme observations in the i^{th} sample. An unbiased estimator of σ based on R is given as: $\hat{\sigma}_R = \overline{R}/d_{2_R}(n)$, where $\overline{R} = \frac{1}{m}\sum_{i=1}^{m} R_i$

Sample Standard deviation: $S_i = \sqrt{\frac{1}{n-1}\sum_{j=1}^{n}(X_{ij} - \bar{X}_i)^2}$. An unbiased estimator of σ based on S is given as: $\hat{\sigma}_S = \overline{S}/d_{2_S}(n)$.

In most SC books, $d_{2_R}(n)$ and $d_{2_S}(n)$ are given as d_2 and c_4, but we are using these notations in this chapter for consistency.

Pooled standard deviation: Vardeman (1999) considered different forms of combining sample ranges and sample standard deviations to estimate σ. He recommended that the most efficient estimate of σ is a biased estimate based on the pooled sample standard deviation given as: $\hat{\sigma}_{S_p} = d_{2_S}(v+1)S_p$, where $S_p = \sqrt{\frac{1}{m}\sum_{i=1}^{m} S_i^2}$ and $v = m(n-1)$

Interquartile Range: $IQR_i = (Q_{i(3)} - Q_{i(1)})/1.34898$, where $Q_{i(1)}$ and $Q_{i(3)}$ respectively represents the lower and the upper quartiles of the i^{th} sample. These quartiles have been computed using Type 6 of the `quantile` function in R statistical language (Ihaka and Gentleman (1996)). The reason behind choosing Type 6 for the computation of quantiles is because this definition is also used by other commonly used statistical packages such as Minitab and SPSS.
An unbiased estimator of σ based on Q is given as: $\hat{\sigma}_Q = \overline{IQR}/d_{2_Q}(n)$.

Downton's Estimator: $D_i = \frac{2\sqrt{\pi}}{n(n-1)}\sum_{j=1}^{n}\left[j - \frac{1}{2}(n+1)\right]X_{i(j)}$. An unbiased estimator of σ based on D is given as: $\hat{\sigma}_D = \overline{D}/d_{2_D}(n)$. For normally distributed quality characteristic, D is an unbiased estimate of σ (i.e. $d_{2_D}(n) = 1$). Two other estimators, namely the probability weighted moments (S_{pw}) and the Gini's estimator (G), are equivalent to the Downton's estimator (D), where S_{pw} and G are defined as: $S_{pw,i} = \frac{\sqrt{\pi}}{n^2}\sum_{j=1}^{n}(2j-n-1)X_{i(j)}$ and $G_i = \frac{\sqrt{\pi}}{2}\left(4\frac{1}{n-1}\sum_{j=1}^{n}\frac{2j-n-1}{2n}X_{i(j)}\right)$. The exact relationship among these three estimators is given by: $D = G = \frac{n}{n-1}S_{pw}$ (cf. Schoonhoven et al. (2011)).

In this study we are only using D estimator for comparison purposes. For the other two estimators (i.e. S_{pw} and G), we can expect a similar behavior.

Average Absolute Deviation from Median: $MD_i = \frac{1}{n}\sum_{j=1}^{n}\left|X_j - \tilde{X}_i\right|$, An unbiased estimator of σ based on MD is given as: $\hat{\sigma}_{MD} = \overline{MD}/d_{2_{MD}}(n)$. Studies have pointed out the efficient behaviour of MD estimator for non-normal processes (cf. Abbasi and Miller (2012), Abbasi and Miller (2011c)).

Median absolute deviation: $MAD_i = 1.4826 \text{ med}\left|X_j - \tilde{X}_i\right|$ An unbiased estimator of σ based on MAD is given as: $\hat{\sigma}_{MAD} = \overline{MAD}/d_{2_{MAD}}(n)$. With a breakdown point of 50%, the MAD estimator can be considered as a very robust estimator to contaminations in the data. However, MAD does have two main drawbacks that were pointed out by Rousseeuw and Croux (1993): low Gaussian efficiency (36.74%) and its reliance on the distribution being symmetric.

S_n **estimate:** $S_{n,i} = 1.1926 \text{ med}_j \left\{\text{med}_l \left|X_{ij} - X_{il}\right|; j \neq l\right\}$. The inner median ($\text{med}_l$) is the $\lfloor(n/2)+1\rfloor^{th}$ order statistic while the outer median (med_j) is the $\lfloor(n+1)/2\rfloor^{th}$ order statistic. Rousseeuw and Croux (1993) described these as "high" and "low" medians. An unbiased estimator of σ based on S_n is given as: $\hat{\sigma}_{S_n} = \overline{S_n}/d_{2_{S_n}}(n)$.

Q_n **estimate:** $Q_{n,i} = 2.2219\left\{\left|X_{ij} - X_{il}\right|; j < l\right\}_{(k)}$ where $k = \binom{\lfloor n/2\rfloor + 1}{2}$. In simple terms, Q_n is the k^{th} order statistic of the n-choose-2 interpoint

distances. An unbiased estimator of σ based on Q_n is given as: $\hat{\sigma}_{Q_n} = \overline{Q_n}/d_{2_{Q_n}}(n)$.
Unlike MD and MAD, S_n and Q_n do not incorporate an estimate of location. Moreover, both S_n and Q_n have much higher Gaussian efficiencies than MAD: 58% for S_n and 82% for Q_n.

Scale-rank statistic: Jones-Farmer and Champ (2010) proposed a distribution free structure for estimating process dispersion based on ranks. Let P_{ij} represent the absolute deviations of X_{ij} taken from the overall median (M), i.e. $P_{ij} = |X_{ij} - M|$. Let C_{ij} be the rank of P_{ij} in the pooled sample of size $n * m$. Jones-Farmer and Champ (2010) considered 4 different transformations of the ranks C_{ij} and showed that their proposed T_2 chart based on the squared ranks (C_{ij}^2) had the best overall performance. Hence, in this study we are only using T_2 chart for comparison purposes. For T_2 chart, the scale-rank statistic is defined as $\overline{T}_{2,i} = (1/n)\sum_{j=1}^{n} C_{ij}^2$ (cf. Jones-Farmer and Champ (2010)).

We will refer to the dispersion charts based on R, S, S_p, IQR, D, MD, MAD, S_n, Q_n and $\overline{T}_2$ as the R chart, the S chart, the S_p chart, the Q chart, the D chart, the MD chart, the MAD chart, the S_n chart, the Q_n chart and the T_2 chart for the rest of this study. These charts are based on plotting their respective monitoring statistics against the following set of control limits:

R **Chart:** $\max\left[0, \overline{R}\left(1 \pm L\frac{d_{3_R}(n)}{d_{2_R}(n)}\right)\right]$

S **Chart:** $\max\left[0, \overline{S}\left(1 \pm L\frac{d_{3_S}(n)}{d_{2_S}(n)}\right)\right]$

S_p **Chart:** $\max\left[0, d_{2_S}(v+1)S_p\left(d_{2_S}(n) \pm L d_{3_S}(n)\right)\right]$

Q **Chart:** $\max\left[0, \overline{IQR}\left(1 \pm L\frac{d_{3_Q}(n)}{d_{2_Q}(n)}\right)\right]$

D **Chart:** $\max\left[0, \overline{D}\left(1 \pm L\frac{d_{3_D}(n)}{d_{2_D}(n)}\right)\right]$

MD **Chart:** $\max\left[0, \overline{MD}\left(1 \pm L\frac{d_{3_{MD}}(n)}{d_{2_{MD}}(n)}\right)\right]$

MAD **Chart:** $\max\left[0, \overline{MAD}\left(1 \pm L\frac{d_{3_{MAD}}(n)}{d_{2_{MAD}}(n)}\right)\right]$

S_n **Chart:** $\max\left[0, \overline{S_n}\left(1 \pm L\frac{d_{3_{S_n}}(n)}{d_{2_{S_n}}(n)}\right)\right]$

Q_n **Chart:** $\max\left[0, \overline{Q_n}\left(1 \pm L\frac{d_{3_{Q_n}}(n)}{d_{2_{Q_n}}(n)}\right)\right]$

T_2 **Chart:** $\overline{\overline{T_2}} \pm L\left(S_{pr}/c_{4,v}\right)/\sqrt{n}$

where $\overline{\overline{T_2}}$ and S_{pr} represent the overall mean and the pooled standard deviation based on the squared ranks C_{ij}^2. For a particular parent distribution, the control chart constants $d_{2_R}(n), d_{3_R}(n), d_{2_Q}(n), d_{3_Q}(n)$ etc., depend on sample size (n) and are available in Appendix Tables A.1 and A.2 for a variety of continuous distributions.

Modified Scale-Rank (V_2) Chart: In T_2 charting structure of Jones-Farmer and Champ (2010)), the control limits are computed by estimating the location and the dispersion of the squared ranks (C_{ij}^2) by $\overline{\overline{T_2}}$ and S_{pr} respectively. These estimates can be seriously affected in the presence of contaminations in the Phase I dataset. To overcome this deficiency of the T_2 chart, we proposed a modified charting structure, namely the V_2 chart. The V_2 chart is based on plotting the squared scale-rank statistic $(\overline{T}_{2,i})$ against the following set of control limits.

$$UCL = \tilde{\overline{T_2}} + L\overline{D}_{T_2}/\sqrt{n}, \qquad CL = \tilde{\overline{T_2}} \qquad \text{and} \qquad LCL = \tilde{\overline{T_2}} - L\overline{D}_{T_2}/\sqrt{n}$$

where $\tilde{\overline{T_2}}$ represents the median of sample $\overline{T}_{2,i}$ and $\overline{D}_{T_2}$ represents the Downton's estimator based estimate of the variation in the $\overline{T}_{2,i}$. The use of $\tilde{\overline{T_2}}$ and $\overline{D}_{T_2}$ in the V_2 charting structure helps significantly in better detection of inconsistent samples in the Phase I dataset – see Section 3.5.

3.3 Performance Evaluation of Charts in Phase I

The performances of all the charts discussed in Section 3.2 are evaluated using the signal probability as the performance measure for normal and non-normal parent environments. The density functions of the continuous distributions together with parameter values used in this study, the skewness and the excess kurtosis are provided in Table 3.1.

Table 3.1: Density functions and parameter values used for different continuous distributions

Distribution	Density Function	Parameter values	Skewness	Excess Kurtosis
Normal$(\mu,\ \sigma^2)$ $\mu \in \mathbb{R}, \sigma > 0$	$\frac{1}{\sqrt{2\pi\sigma^2}} e^{-(x-\mu)^2/2\sigma^2}$	$\mu = 0, \sigma = 1$	0	0
Logistic$(\mu,\ k)$ $\mu \in \mathbb{R}, k > 0$	$\frac{e^{-(x-\mu)/k}}{k\left(1+e^{-(x-\mu)/k}\right)^2}$	$\mu = 0, k = 1$	0	1.2
Student's t (t_k) $k > 0$	$\frac{\Gamma[(k+1)/2]}{\sqrt{k\pi}\Gamma(k/2)} \left(1 + \frac{x^2}{k}\right)^{-\frac{(k+1)}{2}}$	$k = 5$	0	6
Gamma$(\alpha,\ \beta)$ $\alpha > 0, \beta > 0$	$\frac{\beta^\alpha}{\Gamma(\alpha)} x^{\alpha-1} e^{-\beta x}$	$\alpha = 2, \beta = 1$	1.414	3
Exponential(λ) $\lambda > 0$	$\lambda e^{-\lambda x}$	$\lambda = 1$	2	6

For the application of control charts, samples are usually collected from a process in the form of rational subgroups. The concept of rational subgroups was introduced by Shewhart and it means that, in the presence of assignable causes, "the chance for differences between subgroups will be maximized while the chance for differences within subgroups will be minimized" (Montgomery (2009)). We have considered $m = 30$ subgroups, each of size $n = 5$ & 9 from different probability models; m_0 of these subgroups are assumed to be stable and the remaining m_1 have inconsistencies in the form of shifted samples. The goal of Phase I analysis is the quick detection of these inconsistent samples. The stable (in-control) samples are supposed to be distributed with the parameter settings specified in Table 1 for different normal and non-normal distributions. Without loss of generality, the observations from different probability models are rescaled to have the in-control mean and standard deviation as $\mu_0 = 0$ and $\sigma_0 = 1$, while the contaminated samples correspond to rescaled observations with shifted standard deviation as $\sigma_1 = \lambda\sigma_0$ (here the value of λ will indicate the intensity of inconsistency).

The control limits multipliers L are appropriately chosen for all the charts so that false alarm probability (FAP) may be achieved for the prefixed α, assuming the Phase I data set consists of m in-control samples with no contamination. It is to be mentioned that we have chosen α^* as the probability of signal on a single sample and worked out the overall FAP (α) for the m samples using the relationship $\alpha = 1 - (1 - \alpha^*)^m$ (cf. Jones-Farmer and Champ (2010), Shiau and Sun (2010)). After setting the limits of a specific control chart, we use its respective sample statistic (like R_i, S_i, $\overline{T}_{2,i}$ etc.) as monitoring statistic to detect any out-of-control signals. This procedure is repeated 10,000 times and the values of L using $m = 30$ and $n = 5$ & 9 are chosen to fix the FAP, $\alpha = 0.01$ for all the charts, as provided in Table 3.2.

We have investigated the signaling probabilities for $m_1 = 3, 6, 9$ & 12, i.e. when 3, 6, 9 or 12 samples out of 30 are considered to be contaminated with shift λ. To save space, the resulting signaling probabilities for varying values of λ are presented graphically for only $m_1 = 6$ & 12 in the form of power curves. These curves are provided in Figure 3.1 for normal distribution, Figure 3.2 for logistic distribution, Figure 3.3 for t distribution, Figure 3.4 for Gamma distribution and Figure 3.5 for exponential distribution for all the eleven charts investigated in this study. For other combinations of n, m, m_1 and α, one may obtain similar outcomes at varying values of λ for different choices of parent distributions.

Table 3.2: Control chart multiplier L to fix FAP, $\alpha = 0.01$ for all the charts

Distribution	n	R	S	S_p	IQR	D	MD	MAD	Sn	Q_n	T_2	V_2
Normal	5	3.983	3.875	3.744	4.018	3.917	4.025	4.514	4.309	4.545	3.645	3.893
	9	3.967	3.739	3.662	3.983	3.787	3.841	4.125	3.908	4.069	3.585	3.788
Logistic	5	4.793	4.712	4.489	4.501	4.584	4.503	4.856	4.818	4.885	3.661	3.904
	9	4.793	4.578	4.417	4.283	4.296	4.179	4.538	4.283	4.427	3.606	3.782
Student's t	5	6.893	6.957	6.111	5.795	6.341	5.792	5.218	5.091	5.329	3.633	3.904
	9	7.218	7.339	6.569	4.568	5.991	5.349	4.672	4.569	4.737	3.606	3.782
Gamma	5	5.309	5.349	4.895	4.901	4.975	4.921	5.258	4.979	5.392	3.685	3.992
	9	5.141	5.029	4.772	4.664	4.532	4.461	4.681	4.635	4.519	3.608	3.792
Exponential	5	5.579	5.632	5.072	5.091	5.272	5.119	5.656	5.587	5.771	3.654	3.904
	9	5.559	5.397	4.994	4.897	4.793	4.714	5.167	5.088	5.026	3.534	3.734

3.4 Discussion and Comparative Analysis

In this section, we provide a comparison of all the dispersion charts described in Section 3.2. For a fixed FAP (α), the chart that has the highest probability to signal out-of-control samples will be considered as better than others. We can expect signaling probabilities of the charts to change for different parent environments (Woodall (2000)). The goal is to identify charts that perform well for particular parent environments and further to find out a chart that performs better for most of the situations (if not all).

The specific findings for each of the parent environments considered in this study are given below.

Normal Distribution: In the normally distributed process environment, we have observed that MAD, S_n and Q_n charts have the worst performance. The structures of the S, D and MD charts have exhibited the best performance for smaller choices of m_1 which deteriorates with an increase in the value of m_1. For the larger values of m_1 the proposed scale-rank V_2 charting structure has the highest signaling probability to detect out-of-control subgroups. The relative performance of the S_p chart has shown an inverse relation with m_1 and λ. The detection ability of the T_2 chart is lower than the S, D, MD and R charts. R and IQR charts perform well for $n = 5$ but loses relative efficiency for $n = 9$. In general, the detection ability of all the charting structures increases with an increase in the values of n and λ (cf. Figure 3.1).

Logistic Distribution: In the logistic distribution we have noticed that detection abilities of all the charting structures, except T_2 and V_2, are seriously affected (relative to the normal case) due to an increase in the value of excess kurtosis (cf. Figures 3.1 & 3.2). The V_2 chart is performing significantly better than the T_2 chart as m_1 increases. The MAD, S_p, S_n and Q_n charts have shown poor performance (like in the normal case) and the widely used R and S charts are also seriously affected. The best performance has been shown by the V_2 chart, followed by the D & MD charts for $m_1 = 6$ and

T_2 chart for $m_1 = 12$.

Student's *t* Distribution: For the case of t distributed process scenario, the V_2 chart has shown the best performance for all the cases, followed by the T_2 chart. Apart from these two, the design structures of all the charts are significantly affected (relative to the normal case), particularly for smaller choices of n and larger values of m_1. Although less efficient than V_2 and T_2 charts, the MAD, S_n and Q_n charts have shown better detection ability compared to R, S, D and S_p charts. The worst performance has been shown by the S_p chart, with R/S charts as close competitors. The effect on the probability to signal for the case of t distribution is even more severe than for the case of logistic distribution (cf. Figures 3.2 & 3.3) due to the increase in the excess kurtosis.

Gamma Distribution: For the gamma distributed process setup, the V_2 chart again showed the best performance followed by the T_2 chart, irrespective of the choices of n and m_1. The worst performance is shown by the S_p chart as in the other distributional environments. In general the R, S, MAD, S_n and Q_n charts have shown poor detection abilities because of increase in the excess kurtosis along with the skewed behavior of parent distribution. The larger choices of n and the smaller values of m_1 have provided a reasonable safeguard against serious deterioration of signaling probabilities for these charting structures (cf. Figure 3.4).

Exponential Distribution: In an exponentially distributed process situation, the relative superiority orders of different charting structures under investigation stay in close agreement, in general, with the orders observed under Gamma distribution, i.e. V_2 and T_2 charts are performing significantly better than the rest of charts. The higher intensity of skewness and excess kurtosis (cf. Table 3.1) for exponential model presses the curves even lower than those of the gamma distributed process characteristic. (cf. Figure 3.4 & 3.5).

In a nutshell, we observed that the V_2 chart outperforms all the competing charts in normal and non-normal setups (in general), for the detection of out-of-control samples in the historical dataset. S, D and MD charts offer superior performances for the normal parent distribution when m_1 is small. The T_2 charting structure appears as a second best choice for non-normal distributions. On the inferior side, the S_p chart gives the worst performance under non-normal processes while the MAD chart under normally distributed situation. The signalling ability of all the charts (except V_2 and T_2) is significantly affected with increase in the skewness and excess kurtosis for non-normal parent environments compared to the normal case.

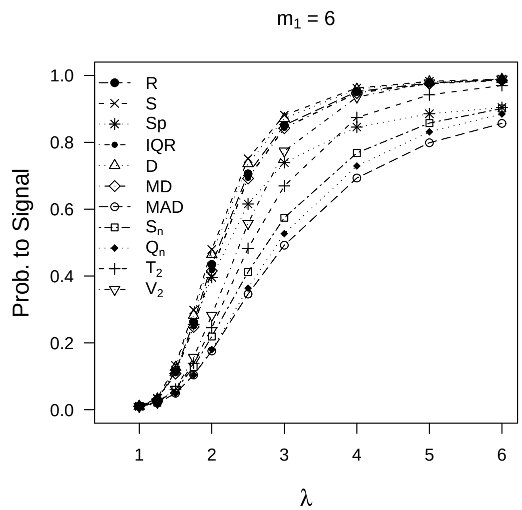

(a) $n = 5$

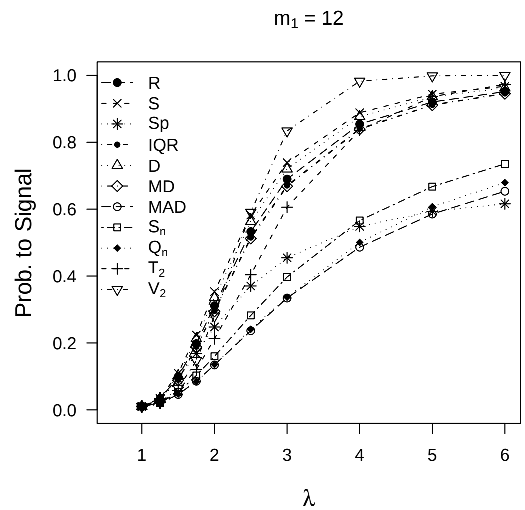

(b) $n = 5$

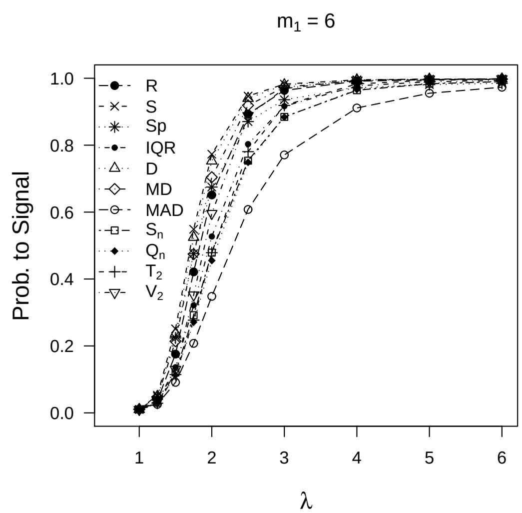

(c) $n = 9$

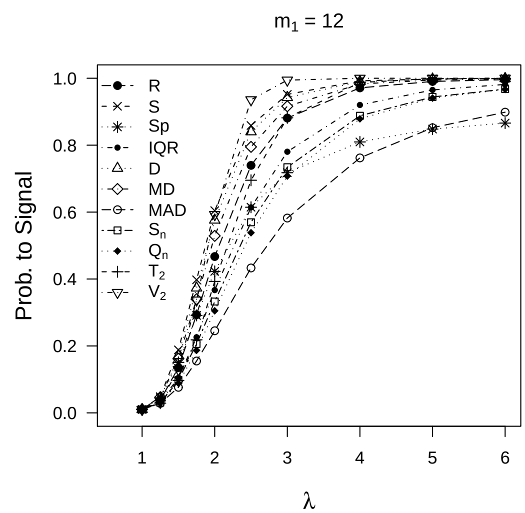

(d) $n = 9$

Figure 3.1: Probability to signal of all the charts under Normal distribution for $\alpha = 0.01$ when $m = 30, m_1 = 6$ & 12 and $n = 5$ and 9

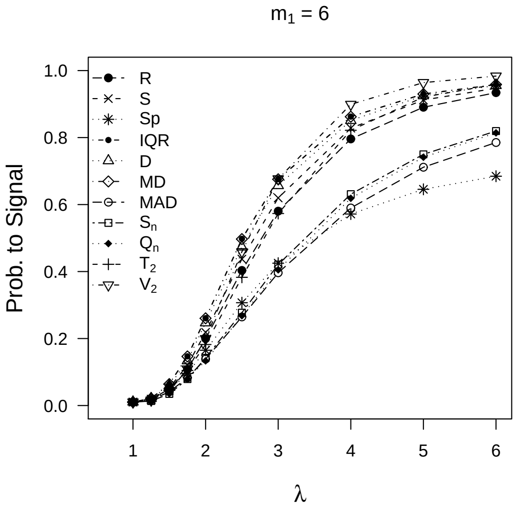

(a) $n = 5$

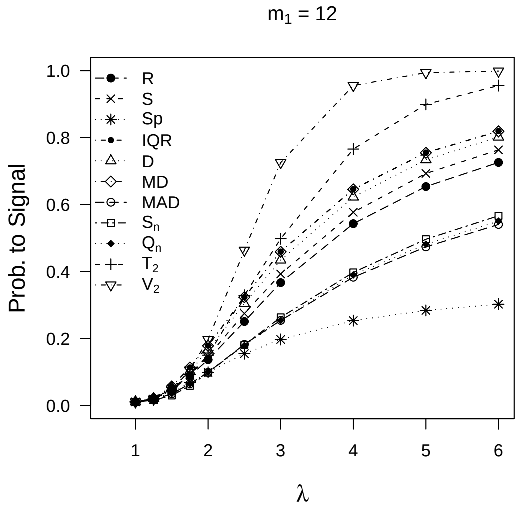

(b) $n = 5$

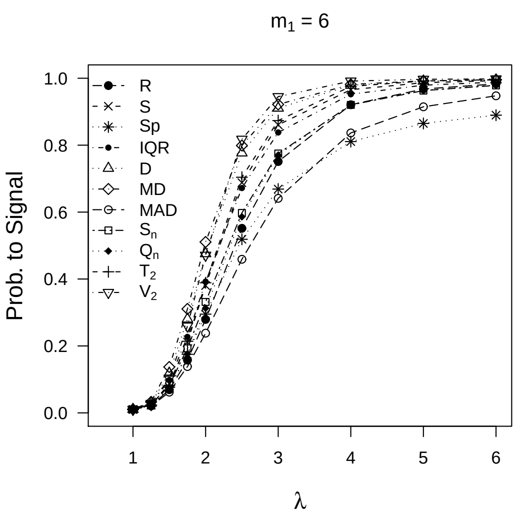

(c) $n = 9$

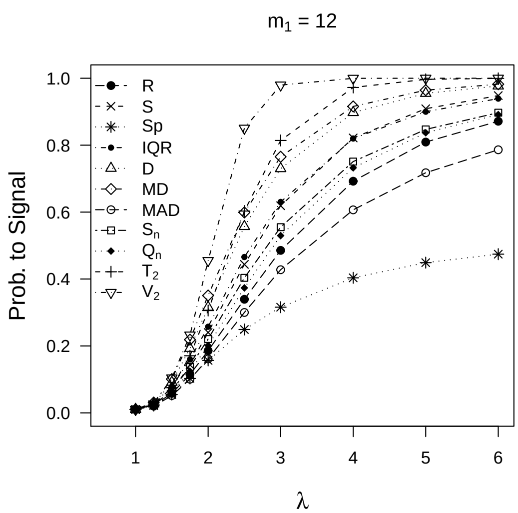

(d) $n = 9$

Figure 3.2: Probability to signal of all the charts under Logistic distribution for $\alpha = 0.01$ when $m = 30, m_1 = 6$ & 12 and $n = 5$ and 9

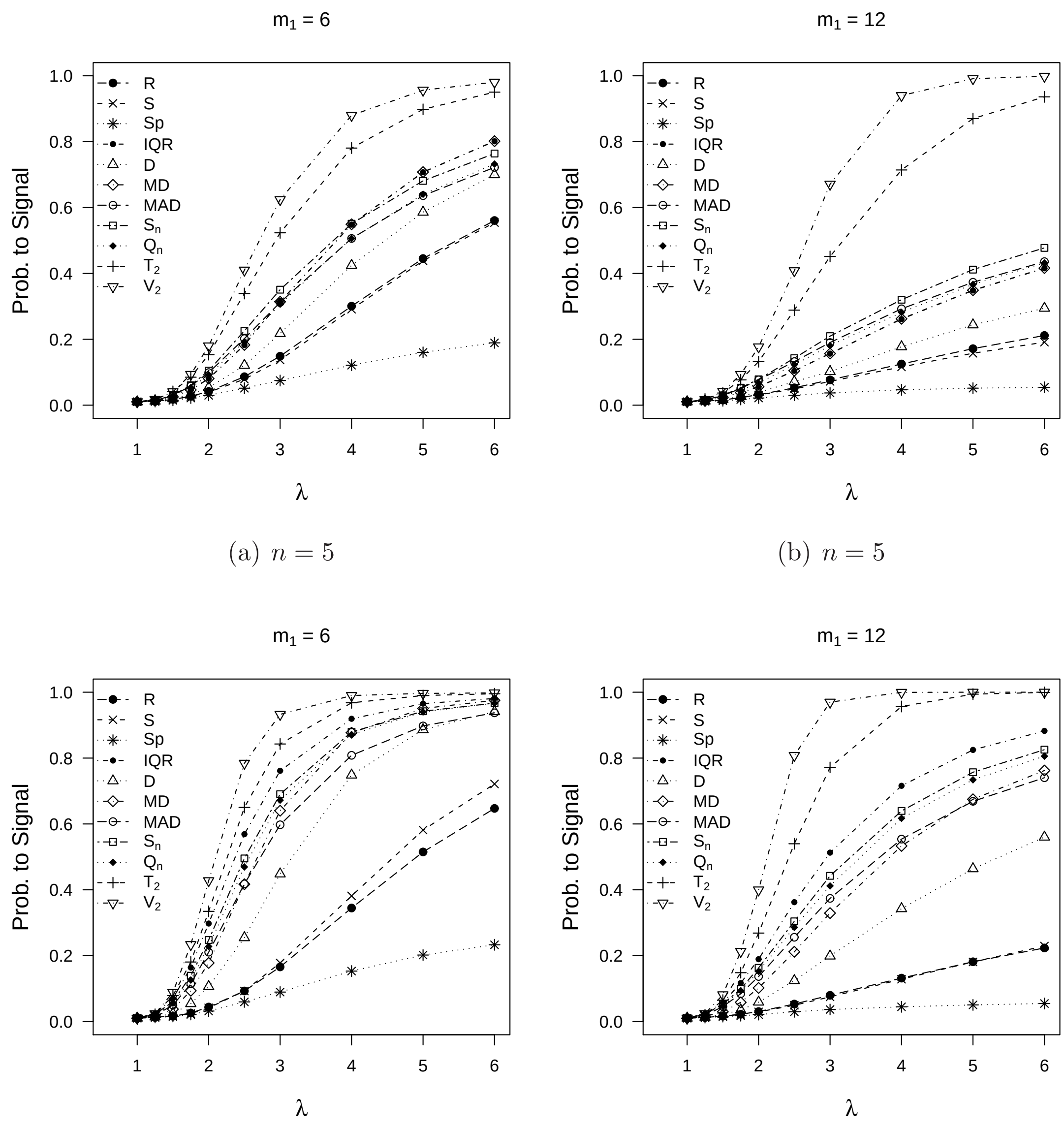

(a) $n = 5$ (b) $n = 5$

(c) $n = 9$ (d) $n = 9$

Figure 3.3: Probability to signal of all the charts under t distribution for $\alpha = 0.01$ when $m = 30, m_1 = 6$ & 12 and $n = 5$ and 9

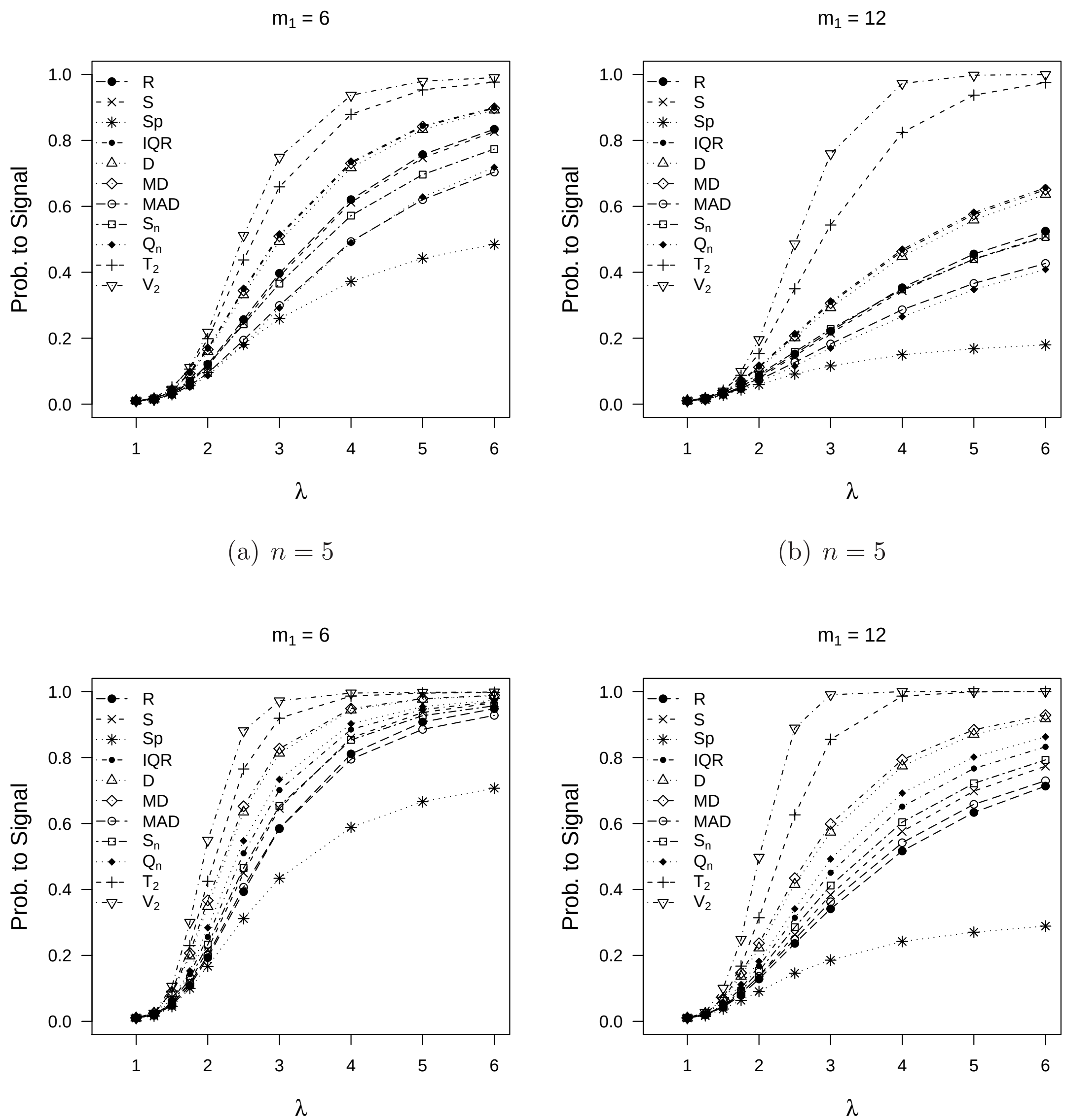

(a) $n = 5$

(b) $n = 5$

(c) $n = 9$

(d) $n = 9$

Figure 3.4: Probability to signal of all the charts under Gamma distribution for $\alpha = 0.01$ when $m = 30, m_1 = 6$ & 12 and $n = 5$ and 9

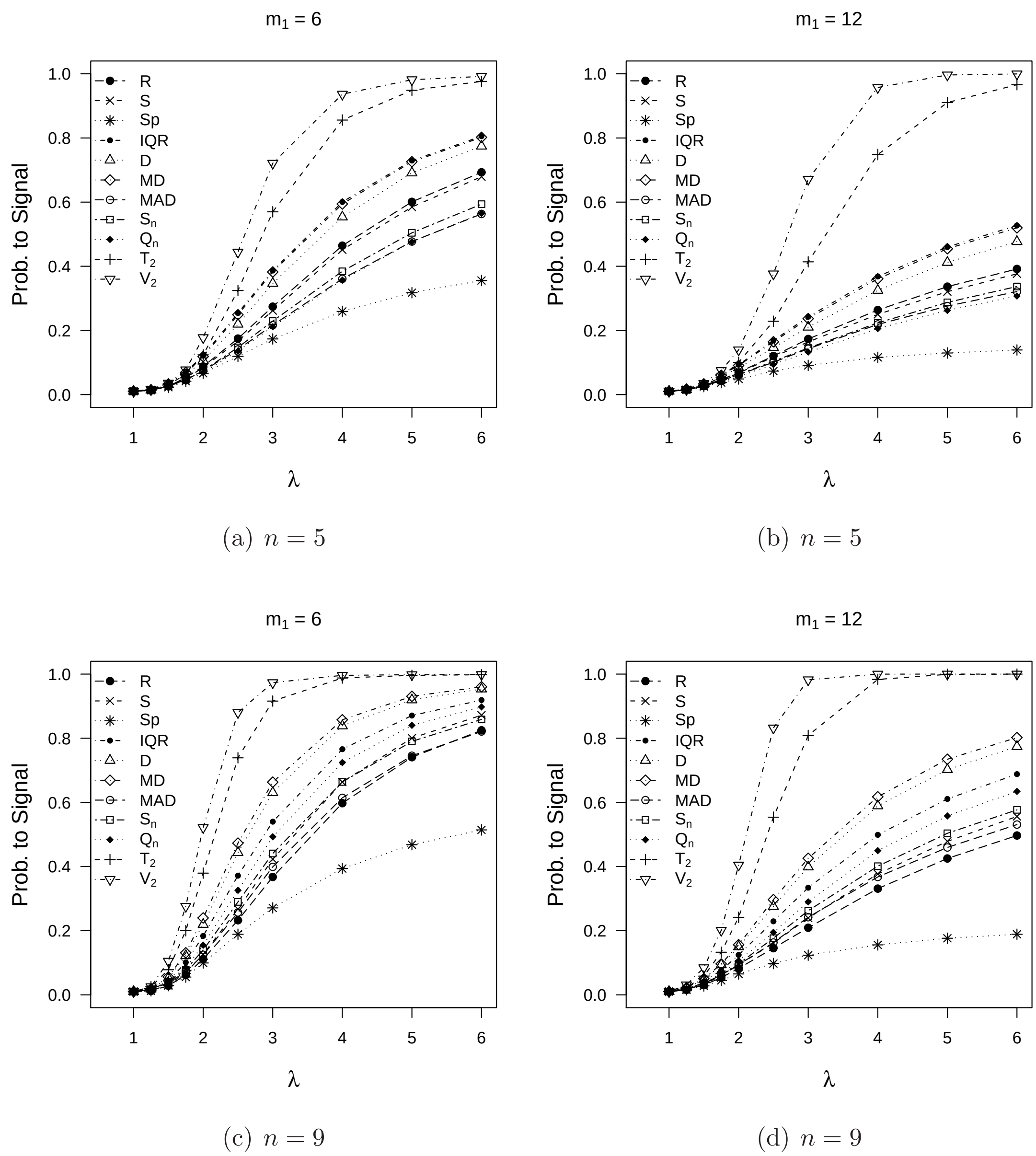

Figure 3.5: Probability to signal of all the charts under Exponential distribution for $\alpha = 0.01$ when $m = 30, m_1 = 6$ & 12 and $n = 5$ and 9

3.5 Illustrative Examples

To illustrate the application of the charts under discussion in this study (particularly V_2 versus T_2 charting structures) for Phase I analysis, we provide here a numerical example using a real dataset given by Jones-Farmer and Champ (2010). The data consist of patients waiting time (in minutes) for a colonoscopy procedure. We have provided plots for the V_2 and T_2 charts in the said numerical example. The other charting structures may be worked out on similar lines.

In order to highlight the ability of the two charting structures for efficient detection of changes in process dispersion parameter in Phase I, we have introduced contaminations in the original data in two forms: using i) $m_1 = 6$ with $\lambda = 3$ and ii) $m_1 = 12$ with $\lambda = 4$, i.e. the last 6 or 12 samples of the original data have been multiplied with λ to represent contaminated samples. The resulting data sets are used to carry out computations for the V_2 and T_2 charting structures for a fixed FAP, $\alpha = 0.01$. The graphical displays of both the control charts for cases (i) and (ii) are provided in Figures 3.6 and 3.7 respectively. The sample numbers are shown on the horizontal axis while the sample statistic $\overline{T}_{2,i}$ is plotted on the vertical axis in these figures. LCL, CL and UCL of the V_2 and T_2 charts are represented by the dashed (- - -) and dotted (...) horizontal lines respectively

It is evident from Figures 3.6 and 3.7 that the T_2 charting structure of Jones-Farmer and Champ (2010) detects out-of-control signals at five sample points, while the V_2 chart detects all the six problem points for the case when m_1=6 and $\lambda = 3$ (cf. Figures 3.6). For case (ii), when m_1=12 and $\lambda = 4$, the V_2 chart has signaled ten out-of-control points while the T_2 chart has indicated eight such points (cf. Figures 3.7). Moreover, we can see from Figure 3.7 that the T_2 chart is giving 6 extra false signals compared to the V_2 chart. It shows that the proposed V_2 charting structure not only detects more out-of-control samples but has an added advantage of producing significantly less false signals. The superiority of the design structure of the V_2 chart keeps improving, relative to the T_2 chart, with increasing values of m_1 and λ. Note that the V_2 chart also plots $\overline{T}_{2,i}$ as the monitoring statistic but with a modified set of control limits. The similar superior detection ability may also be expected for the V_2 chart relative to the other charting structures covered in this study, based on the findings of Section 3.4.

3.6 Conclusions

This study has investigated the choice of an appropriate control charting structure for efficient monitoring of process dispersion parameter during Phase I. We have analyzed the performance of eleven dispersion charts, including two distribution-free structures, based on ranks. The performance of control charts is evaluated in terms of probability to signal, under different distributional setups covering normal, logistic, t, gamma and exponential models. The comparative analysis under different process setups has advocated that the worst performance is exhibited by S_p chart under non-normal processes and MAD chart under the normal environment. The inferior performance of the S_p chart is due to the fact of having contaminations in the Phase I samples as for this situation a better way of estimating σ is to estimate the variability for each subgroup separately and then pool these estimates (cf. Abbasi and Miller (2012)).

The newly suggested V_2 charting structure offers the best ability in most of the practical situations. The T_2 structure has attractive detection abilities in non-normal environments, while in normal setup it becomes relatively less efficient. The structures of S, D and MD charts appear as efficient choices in normally distributed case when m_1 is smaller, while for larger values of m_1 the V_2 chart gets an edge. The design structures of D, IQR, MD and Q_n charts have also shown reasonable performance for skewed distributions, especially when m_1 is large.

To sum up, the V_2 charting structure has shown the best ability for the detection of out-of-control subgroups in Phase I under different normal and non-normal processes considered in this study. It may be used as a powerful tool by quality control practitioners and researchers for efficient monitoring and decision making in their practice.

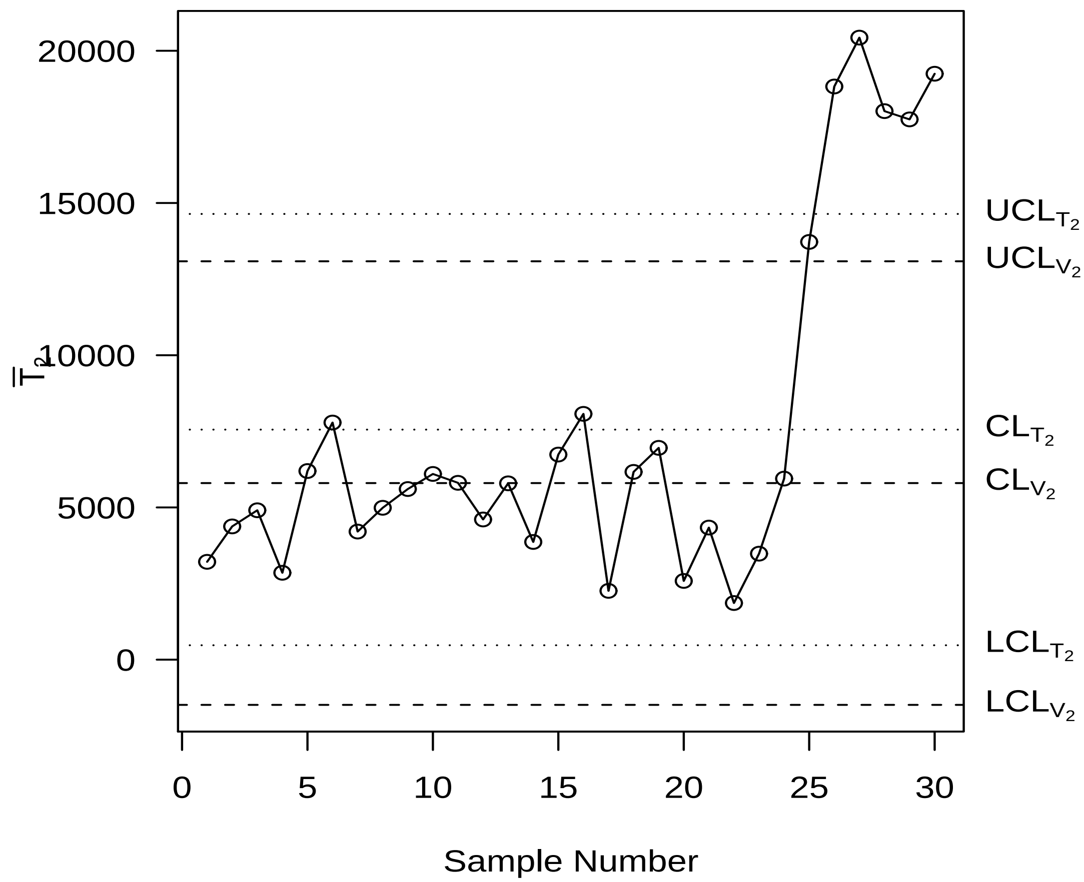

Figure 3.6: T_2 and V_2 charts for $m_1 = 6$ and $\lambda = 3$

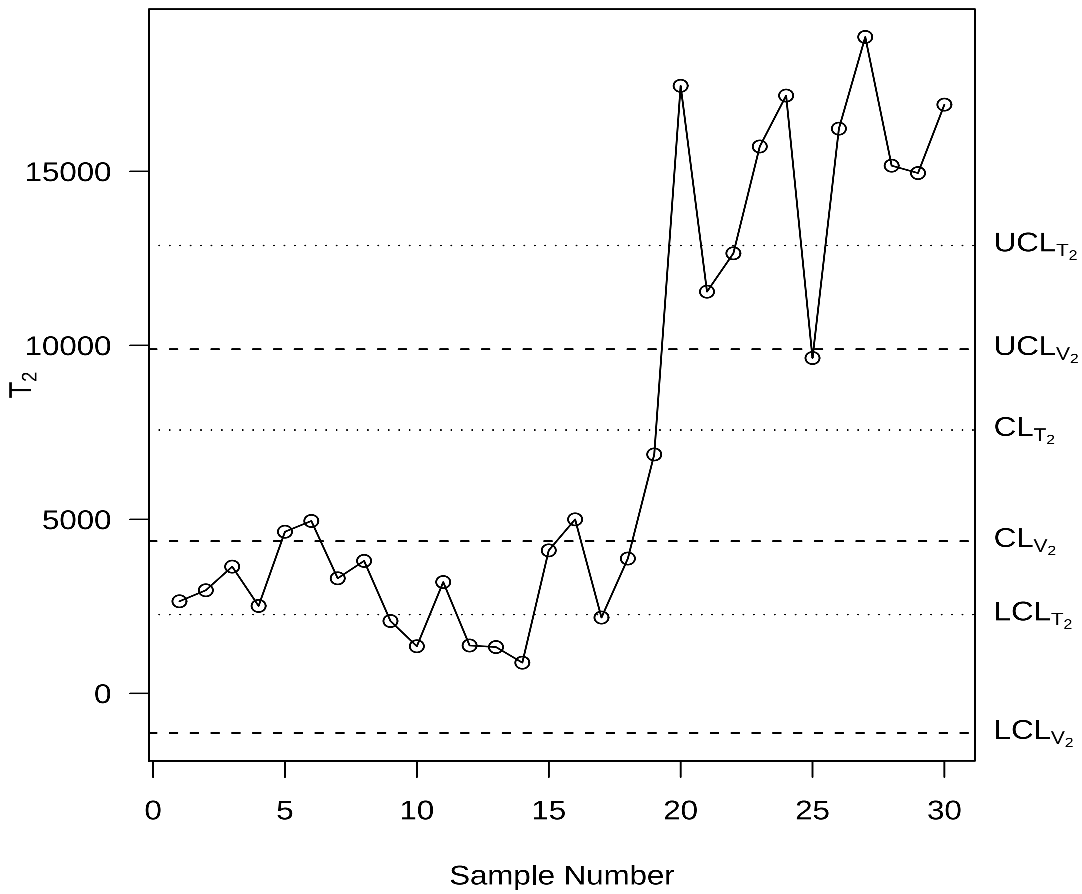

Figure 3.7: T_2 and V_2 charts for $m_1 = 12$ and $\lambda = 4$

Chapter 4

EWMA Dispersion Control Charts

EWMA dispersion charts are used for the quick detection of small and moderate shifts in process dispersion or variability. Most of the EWMA dispersion charts that have been proposed are based on the assumption that the parent distribution of the quality characteristic is normal, which is not always the case. In this chapter we develop new EWMA charts based on a wide range of dispersion estimates for processes following normal and non-normal parent distributions. The performance of all the charts is evaluated and compared using run length characteristics (the average run length (ARL), the median run length (MDRL) and the standard deviation of the run length distribution (SDRL)). Extra Quadratic Loss (EQL) and Relative Average Run Length (RARL) measures are also used to examine the overall effectiveness of the EWMA dispersion charts. This chapter is based on Abbasi and Miller (2011c), Abbasi et al. (2012a) and Abbasi and Miller (2011b).

4.1 Introduction

Shewhart type dispersion charts, as discussed in Chapters 2 and 3, are most effective when large shifts in the process parameters are of concern. For the efficient detection of small or moderate shifts in the process parameters, the use of an EWMA chart is usually recommended. Monitoring process dispersion using an EWMA chart has attracted the attention of different researchers – some important contributions are Wortham and Ringer (1971); Ng and Case (1989); Domangue and Patch (1991); Crowder and Hamilton (1992); MacGregor and Harris (1993); Stoumbos and Reynolds (2000); Chen et al. (2001) and Shu and Jiang (2008).

Most of the proposed EWMA dispersion charts are based on the assumption of normality of the quality characteristic, which is not always the case. In fact, many real life processes do follow non-normal distributions (cf. Bissell (1994), James (1989) and Levinson and Polny (1999)). It has been observed in Chapter 2 that a Shewhart type dispersion chart that is superior for the normal environment may not remain the same for non-normal parent distributions. This can also be expected for the EWMA dispersion charts. Maravelakis et al. (2005) showed that the run length behaviour of the EWMA dispersion charts can be seriously affected when the assumption of normality is violated. Hence, there is a need to investigate a wide range of EWMA dispersion charts for normal and non-normal parent distributions, to identify a chart (or a set of charts), that performs well for both the cases or at least under a particular distributional environment.

The purpose of this chapter is to develop new EWMA dispersion charts that can be used for the efficient detection of shifts in process dispersion, considering normal and non-normal parent distributions. We considered the Student's t and Gamma distributions for representing the non-normal cases: the Student's t is a heavy tailed distribution and the Gamma is a skewed distribution. EWMA dispersion charts investigated in this chapter are based on sample range (R), sample standard deviation (S), inter quartile range (IQR), average absolute deviation from median (MD), median absolute deviation (MAD), S_n and Q_n estimates. These dispersion statistics have been studied in Chapter 2 for the Shewhart charts.

The rest of this chapter is organized as follows: Section 4.2 briefly describes different dispersion estimates that form the basis of the EWMA dispersion charts; the design structure of these charts is developed in Section 4.3; a discussion of the performance measures used to evaluate control charts and a description of the simulation study is given in Section 4.4; the results of the study are then used to compare all the dispersion charts under normal and non-normal parent environments in Section 4.5; and finally, the chapter ends with conclusions in Section 4.6.

4.2 Dispersion Estimates

Let X be the quality variable of interest and let $X_1, X_2, \cdots, X_n$ be a random sample of size n from a distribution with mean μ and standard deviation σ. Further let $X_{(i)}$ be the ith order statistic (smallest to largest), $\bar{X}$ be the sample mean, $\tilde{X}$ be the sample median and $|X|$ be the absolute value of X. The definitions of different dispersion estimates are given as:

Sample Range: $R = X_{(n)} - X_{(1)}$

Sample Standard deviation: $S = \sqrt{\frac{1}{n-1}\sum_{i=1}^{n}(X_i - \bar{X})^2}$

Interquartile range: $IQR = (Q_3 - Q_1)/1.34898$

Downton's Estimate: $D = \frac{2\sqrt{\pi}}{n(n-1)}\sum_{i=1}^{n}\left[i - \frac{1}{2}(n+1)\right]X_{(i)}$

Average Absolute Deviation from Median: $MD = \frac{1}{n}\sum_{i=1}^{n}\left|X_i - \tilde{X}\right|$

Median Absolute Deviation: $MAD = 1.4826\ \text{med}\left|X_i - \tilde{X}\right|$

S_n **estimate:** $S_n = 1.1926\ \text{med}_i\ \{\text{med}_j\ |X_i - X_j|\,; i \neq j\}$

Q_n **estimate:** $Q_n = 2.2219\,\{|X_i - X_j|\,; i < j\}_{(k)}$ where $k = \begin{pmatrix} \lfloor n/2 \rfloor + 1 \\ 2 \end{pmatrix}$

The details regarding these dispersion estimates can be seen in Chapter 2 (Section 2.2). All these estimates will be used to develop EWMA dispersion charts.

4.3 Design of the EWMA dispersion charts

In this section, a general design structure is developed for the EWMA dispersion charts. Let T define a dispersion statistic and T_t $(t = 1, 2, \cdots)$ be the sequence of the observed values for T computed from the subgroup of n observations, taken at time t. Note that T can be any of the dispersion estimates described in Section 4.2. As we are only interested in monitoring changes in process standard deviation, we assume that the process mean is stable at a fixed level. Let the EWMA statistic W_t, for the dispersion estimate E, be defined as

$$W_t = \lambda T_t + (1 - \lambda) W_{t-1} \tag{4.1}$$

where λ is the smoothing parameter lying between 0 and 1. By continuous substitution of W_{t-i}, the EWMA statistic W_t can be written as (see Roberts (1959) and Montgomery (2009))

$$W_t = \lambda \sum_{i=0}^{t-1} (1 - \lambda)^i T_{t-i} + (1 - \lambda)^t W_0; \qquad W_0 = \overline{T} \tag{4.2}$$

As t gets larger, we have

$$\hat{\sigma}_{W_t} \approx \hat{\sigma}_{T_t} \sqrt{\frac{\lambda}{2 - \lambda}} \tag{4.3}$$

It can be easily shown that (cf. Montgomery (2009), Riaz (2008))

$$\hat{\sigma}_T = t_3 \overline{T} / t_2 \tag{4.4}$$

where t_2 and t_3 are the control chart coefficients based on sample statistic T. These are defined as the mean and the standard deviation of the distribution of relative dispersion $(Z = T/\sigma)$, i.e. $t_2 = \mathrm{E}(Z)$ and $t_3 = \sigma_Z$. For a particular parent distribution, these coefficients depend on the sample size (n) (see Mahoney (1998), Kao and Ho (2007), Montgomery (2009)). The constant t_2 is required to obtain an unbiased estimate of σ using the dispersion statistic T.

From Equations (4.3) and (4.4) we have

$$\hat{\sigma}_{W_t} \approx \frac{t_3\overline{T}}{t_2}\sqrt{\frac{\lambda}{2-\lambda}} \tag{4.5}$$

The upper control limit (UCL) of the EWMA chart based on the dispersion statistic E is thus defined as

$$UCL = \overline{T} + L\frac{t_3\overline{T}}{t_2}\sqrt{\frac{\lambda}{2-\lambda}} \tag{4.6}$$

where L is the control chart multiplier. L is usually set at 3 but can be adjusted to set the false alarm rate to a specified value. The major concern of this study is to detect the upward shifts in process dispersion, hence we are only considering a one-sided UCL. For a two-sided chart, the control chart multiplier L needs to be adjusted accordingly.

After setting the UCL for the EWMA dispersion chart, the EWMA statistic given in Equation (4.1) is plotted against time. For an in-control process all of the W_t values should lie below the UCL, whereas an out-of-control process is signaled by one or more of the W_t values exceeding the UCL. It is desirable that an out-of-control situation is detected as early as possible so that corrective actions can be implemented. For the choice of T as $R, S, IQR, D, MD, MAD, Sn$ and Qn, we will refer to the EWMA charts as the R_E chart (Ng and Case (1989)), the S_E chart, the Q_E chart, the D_E chart, the MD_E chart (Abbasi and Miller (2011c)), the MAD_E chart, the SN_E chart and the QN_E charts for the rest of this chapter.

4.4 Performance Evaluation

To evaluate the performance of control charts, the average run length (ARL), the mean of the run length distribution, is the most important and widely used measure. The performance can be evaluated by two ARL values:

- ARL_0: the average number of samples until an out-of-control signal is detected by a control chart when the process standard deviation is in-control.

- ARL_1: the average number of samples until an out-of-control signal is detected by a control chart when the process standard deviation is shifted to an out-of-control value.

Large values of ARL_0 and small values of ARL_1 are preferable for any control chart setting. In this study, a Monte Carlo simulation approach with 10,000 iterations is used to approximate the run length distribution of the EWMA dispersion charts, following the methods of Maravelakis et al. (2005), Neubauer (1997), Zhang and Chen (2004), Abbasi (2010) and Abbasi and Miller (2011c). Note that Kim (2005) and Schaffer and Kim (2007) indicate that 5000 replications are sufficient to estimate the ARL to an acceptable level of precision in many control chart settings. Due to the skewed nature of the run length distribution, the sole use of ARL measure in interpreting a chart's performance is criticized by some authors including, Barnard (1959), Gan (1993, 1994) and Woodall (1983). It is usually recommended to report median run length (MDRL) and the standard deviation of the RL distribution (SDRL) (cf. Gan (1993), Maravelakis et al. (2005)). Similarly to the ARL, low values for MDRL and SDRL are also desirable.

The goal of this study is to propose efficient EWMA dispersion charts for Phase II of SPC. Hence, we assume that a sufficiently large and clean historical data set is available which represents the state of an in-control process. From this historical data set, control limits are computed for all the dispersion charts using their respective control chart constants (t_2 and t_3). The control chart multipliers L are chosen to fix the in-control ARL (ARL_0) at the desired level for all the charts. In each simulation run, samples of a particular size (n) are generated and the dispersion statistic T are computed to be used as the monitoring statistic. The run length (RL) is defined as the number of samples until the plotting statistic exceeds the upper control limit. The run length was simulated 10,000 times and the average, the median and the standard deviation of the RL distribution (ARL, MDRL and SDRL) were computed.

The performance of all the charts is evaluated and compared under the usual normality assumption and for cases where this is violated. For the non-normal cases, we used the Student's t distribution to investigate a heavy-tailed symmetric distribution and a Gamma distribution to investigate a skewed distribution. The density functions of these distributions are given below.

Normal(μ, σ^2), $\mu \in \mathbb{R}, \sigma > 0$

$$f(x|\mu, \sigma^2) = \frac{1}{\sqrt{2\pi\sigma^2}} e^{-(x-\mu)^2/2\sigma^2}, \quad -\infty < x < \infty$$

Student's t (t_k), $\quad k > 0$

$$f(x|k) = \frac{\Gamma[(k+1)/2]}{\sqrt{k\pi}\Gamma(k/2)} \left(1 + \frac{x^2}{k}\right)^{-(k+1)/2}, \quad -\infty < x < \infty$$

Gamma(α, β), $\quad \alpha > 0, \beta > 0$

$$f(x|\alpha, \beta) = \frac{\beta^\alpha}{\Gamma(\alpha)} x^{\alpha-1} e^{-\beta x}, \quad x > 0$$

In our simulation study, we used Normal distribution with $\mu = 0$ and $\sigma^2 = 1$, Student's t distribution with $k = 5$ and Gamma distribution with $\alpha = 2$ and $\beta = 1$.

The run length results are reported for subgroups of sizes $n = 5$ & 10 and $\lambda = 0.05, 0.25, 0.50$ & 0.75. The ARL, SDRL and MDRL for one of the charts (i.e. the MD_E chart) are provided in Tables 4.1-4.3 for normal, Student's t and Gamma distributed quality characteristic respectively. The results for the remaining seven charts are reported in Appendix Tables B.1 - B.21. The relative standard errors of the results reported in these tables are found to be around 1.5%, as checked by repeating the simulations. This is quite acceptable in control chart studies - for details see Kim (2005) and Schaffer and Kim (2007).

In these tables, δ represents the multiplicative change in the process standard deviation relative to the in-control scenario: that is $\delta = 1$ represents the in-control situation where the standard deviation is σ and $\delta = 1.5$ represents an out-of-control scenario where the process standard deviation is $1.5 \times \sigma$. For each scenario, the control chart multiplier L was chosen to give an in-control average run length of 200 (i.e. $\text{ARL}_0 = 200$) for all the charts – these values are reported in Table 4.4. Control chart coefficients (t_2 and t_3), used for setting control limits for all the dispersion charts, are provided in Appendix Tables A.1 and A.2, for some representative values of n considering normal and a range of non-normal distributions.

Run length characteristics evaluate the detection ability of a chart for a specific shift value. To evaluate the overall effectiveness of a control chart over an entire shift range, the measures such as Extra Quadratic Loss (EQL) and Relative ARL (RARL) can be used. EQL and RARL are described below:

Extra Quadratic Loss (EQL)

EQL is defined as the weighted average ARL over the entire shift domain ($\delta_{min} < \delta < \delta_{max}$) using the square of shift (δ^2) as the weight. Mathematically EQL is given as:

$$\text{EQL} = \frac{1}{\delta_{max} - \delta_{min}} \int_{\delta_{min}}^{\delta_{max}} \delta^2 \text{ARL}(\delta)\, d\delta \tag{4.7}$$

where $\text{ARL}(\delta)$ is the ARL of a particular chart at shift δ. The above expression of EQL is based on the assumption that the process shift δ has a uniform distribution over the interval $[\delta_{min}, \delta_{max}]$. Thus, the density function is $\frac{1}{\delta_{max} - \delta_{min}}$ over this interval. The uniform distribution for δ is assumed by many researchers including Domangue and Patch (1991), Reynolds Jr. and Stoumbos (2004b) and Wu et al. (2009).

Ou et al. (2012) also investigated the effect of non-uniform distributions for δ on the EQL values. They showed that the distribution of δ has a limited influence on the relative performance of control charts based on EQL. They mentioned that if a chart is performing better in terms of EQL compared to the other chart under a uniform distribution for δ, it also has better performance under different non-uniform distributions for δ.

Many researchers used EQL as a criterion to measure the overall performance of a control chart (Reynolds Jr. and Stoumbos (2004a); Zhang and Tian (2005); Ou et al. (2012)). The smaller value of EQL indicates a better overall performance of a chart compared to other competitive charts.

Relative ARL (RARL)

RARL is another measure that can be used to evaluate the overall effectiveness of a control structure. RARL calculates the average of the ratios between the ARL of a particular chart (ARL(δ)) with the ARL of the benchmark chart ($\text{ARL}_{benchmark}(\delta)$). Mathematically, RARL is defined as:

$$\text{RARL} = \frac{1}{\delta_{max} - \delta_{min}} \int_{\delta_{min}}^{\delta_{max}} \frac{\text{ARL}(\delta)}{\text{ARL}_{benchmark}(\delta)} \, d\delta \tag{4.8}$$

The benchmark can be selected as a chart with lowest EQL. This will produce RARL = 1 for the benchmark chart and RARL > 1 for the other charts. The distance between the RARL of different charts and the benchmark chart (RARL - 1) shows the extent of inferior performance of a chart as compared to the benchmark chart.

The expressions of EQL and RARL are evaluated using numerical integration method and the results are reported in Tables 4.5 and 4.6 respectively, for all the EWMA dispersion charts considering normal, t and Gamma parent distributions using $\delta_{min} = 1.1$ and $\delta_{max} = 4.0$.

Table 4.1: RL characteristics of the MD_E chart for normally distributed quality characteristic when $\text{ARL}_0 = 200$

		n							
		5				10			
		λ				λ			
δ		0.05	0.25	0.50	0.75	0.05	0.25	0.50	0.75
1.00	ARL	201.02	200.35	200.41	201.06	199.75	199.59	200.70	201.74
	MDRL	140.00	140.00	140.00	140.00	138.00	137.00	138.00	141.00
	SDRL	197.69	200.73	200.87	198.67	194.08	193.33	196.40	203.47
1.10	ARL	34.31	43.36	53.04	61.00	21.41	27.45	36.13	44.69
	MDRL	27.00	31.00	37.00	44.00	17.00	20.00	25.00	31.00
	SDRL	26.96	40.69	51.80	58.59	15.13	25.18	34.65	43.32
1.20	ARL	15.89	17.63	21.94	25.80	9.89	10.20	12.45	15.83
	MDRL	13.00	13.00	16.00	18.00	9.00	8.00	9.00	11.00
	SDRL	10.40	15.01	20.39	25.38	5.39	7.85	11.14	15.29
1.30	ARL	10.13	10.10	11.66	13.61	6.40	5.77	6.37	7.73
	MDRL	9.00	8.00	9.00	10.00	6.00	5.00	5.00	6.00
	SDRL	5.73	7.73	10.34	12.86	3.02	3.75	5.07	6.81
1.40	ARL	7.44	6.73	7.38	8.60	4.79	3.99	4.17	4.67
	MDRL	7.00	5.00	6.00	6.00	4.00	3.00	3.00	3.00
	SDRL	3.86	4.77	6.15	7.71	2.00	2.35	2.99	3.93
1.50	ARL	5.95	5.12	5.32	5.99	3.85	3.11	3.02	3.23
	MDRL	5.00	4.00	4.00	4.00	4.00	3.00	3.00	2.00
	SDRL	2.95	3.38	4.14	5.21	1.53	1.68	1.99	2.49
1.60	ARL	5.00	4.16	4.11	4.50	3.29	2.57	2.45	2.49
	MDRL	5.00	4.00	3.00	3.00	3.00	2.00	2.00	2.00
	SDRL	2.38	2.59	3.07	3.79	1.25	1.29	1.50	1.74
1.80	ARL	3.76	3.00	2.86	3.00	2.55	1.94	1.78	1.77
	MDRL	3.00	3.00	2.00	2.00	2.00	2.00	2.00	1.00
	SDRL	1.68	1.74	1.93	2.31	0.91	0.90	0.95	1.06
2.00	ARL	3.09	2.43	2.25	2.25	2.12	1.61	1.46	1.43
	MDRL	3.00	2.00	2.00	2.00	2.00	2.00	1.00	1.00
	SDRL	1.33	1.32	1.41	1.56	0.75	0.70	0.69	0.72
2.50	ARL	2.21	1.71	1.59	1.55	1.54	1.22	1.14	1.12
	MDRL	2.00	2.00	1.00	1.00	2.00	1.00	1.00	1.00
	SDRL	0.93	0.84	0.84	0.87	0.57	0.44	0.37	0.34
3.00	ARL	1.77	1.41	1.32	1.29	1.26	1.07	1.04	1.04
	MDRL	2.00	1.00	1.00	1.00	1.00	1.00	1.00	1.00
	SDRL	0.74	0.63	0.59	0.58	0.45	0.27	0.21	0.20
3.50	ARL	1.52	1.24	1.19	1.17	1.12	1.03	1.02	1.01
	MDRL	1.00	1.00	1.00	1.00	1.00	1.00	1.00	1.00
	SDRL	0.63	0.48	0.44	0.43	0.33	0.17	0.13	0.12
4.00	ARL	1.36	1.17	1.12	1.10	1.06	1.01	1.00	1.01
	MDRL	1.00	1.00	1.00	1.00	1.00	1.00	1.00	1.00
	SDRL	0.53	0.41	0.35	0.32	0.23	0.10	0.06	0.07

Table 4.2: RL characteristics of the MD_E chart for t-distributed quality characteristic when $\text{ARL}_0 = 200$

		n							
		5				10			
		λ				λ			
δ		0.05	0.25	0.50	0.75	0.05	0.25	0.50	0.75
1.00	ARL	199.11	201.02	200.91	200.97	201.02	200.11	199.49	200.20
	MDRL	137.00	141.00	140.00	140.00	142.00	143.00	142.00	142.00
	SDRL	196.07	203.37	201.00	202.69	199.06	199.43	201.79	200.98
1.10	ARL	43.51	67.08	86.02	100.17	28.33	42.79	58.56	72.34
	MDRL	33.00	48.00	60.00	69.00	22.00	31.00	40.00	51.00
	SDRL	36.35	64.39	84.88	100.43	21.58	40.09	57.23	71.04
1.20	ARL	20.52	30.58	41.99	53.70	12.92	16.08	23.14	31.68
	MDRL	17.00	22.00	30.00	37.00	11.00	12.00	16.00	22.00
	SDRL	14.75	27.84	40.99	53.17	7.71	13.22	22.00	31.15
1.30	ARL	12.86	16.68	24.12	32.11	8.20	8.81	11.77	15.81
	MDRL	11.00	13.00	17.00	22.00	7.00	7.00	9.00	11.00
	SDRL	7.95	14.35	22.79	31.55	4.15	6.42	10.26	14.90
1.40	ARL	9.46	11.04	15.04	20.69	6.09	5.86	7.26	9.57
	MDRL	8.00	9.00	11.00	15.00	6.00	5.00	6.00	7.00
	SDRL	5.40	8.79	13.72	19.92	2.83	3.84	5.84	8.62
1.50	ARL	7.45	7.92	10.45	13.82	4.87	4.36	4.90	6.27
	MDRL	7.00	6.00	8.00	10.00	5.00	4.00	4.00	5.00
	SDRL	4.03	5.76	9.14	13.00	2.07	2.56	3.74	5.46
1.60	ARL	6.17	6.24	7.85	10.27	4.07	3.52	3.79	4.50
	MDRL	6.00	5.00	6.00	7.00	4.00	3.00	3.00	3.00
	SDRL	3.08	4.33	6.50	9.54	1.67	1.95	2.58	3.66
1.80	ARL	4.65	4.35	4.87	6.17	3.14	2.58	2.54	2.83
	MDRL	4.00	4.00	4.00	5.00	3.00	2.00	2.00	2.00
	SDRL	2.20	2.72	3.78	5.47	1.19	1.28	1.55	2.06
2.00	ARL	3.75	3.35	3.55	4.25	2.57	2.08	1.98	2.08
	MDRL	3.00	3.00	3.00	3.00	2.00	2.00	2.00	2.00
	SDRL	1.72	1.95	2.55	3.49	0.95	0.96	1.07	1.33
2.50	ARL	2.66	2.26	2.23	2.37	1.86	1.48	1.38	1.37
	MDRL	2.00	2.00	2.00	2.00	2.00	1.00	1.00	1.00
	SDRL	1.14	1.17	1.37	1.67	0.68	0.61	0.61	0.66
3.00	ARL	2.12	1.77	1.70	1.76	1.50	1.23	1.16	1.14
	MDRL	2.00	2.00	1.00	1.00	1.00	1.00	1.00	1.00
	SDRL	0.90	0.86	0.92	1.07	0.56	0.44	0.39	0.38
3.50	ARL	1.80	1.53	1.46	1.46	1.29	1.11	1.07	1.06
	MDRL	2.00	1.00	1.00	1.00	1.00	1.00	1.00	1.00
	SDRL	0.76	0.69	0.71	0.76	0.47	0.32	0.27	0.25
4.00	ARL	1.59	1.37	1.30	1.30	1.16	1.05	1.03	1.03
	MDRL	2.00	1.00	1.00	1.00	1.00	1.00	1.00	1.00
	SDRL	0.67	0.58	0.56	0.59	0.36	0.22	0.17	0.16

Table 4.3: RL characteristics of the MD_E chart for Gamma distributed quality characteristic when $\text{ARL}_0 = 200$

		n							
		5				10			
		λ				λ			
δ		0.05	0.25	0.50	0.75	0.05	0.25	0.50	0.75
1.00	ARL	200.01	199.49	200.07	199.18	199.07	200.66	209.84	200.90
	MDRL	138.00	138.00	139.00	138.00	138.00	141.00	142.00	142.00
	SDRL	206.32	198.47	198.72	200.72	196.97	199.04	199.28	196.90
1.10	ARL	44.74	60.11	75.64	83.75	28.58	39.87	52.13	62.90
	MDRL	34.00	43.00	53.00	59.00	23.00	29.00	36.00	44.00
	SDRL	38.41	57.29	73.91	81.90	21.33	37.43	51.21	62.02
1.20	ARL	20.67	27.40	36.08	43.11	13.04	15.27	20.56	26.42
	MDRL	17.00	20.00	25.00	30.00	11.00	12.00	15.00	19.00
	SDRL	14.77	24.88	34.86	42.16	7.79	12.41	19.19	25.33
1.30	ARL	13.16	15.62	20.25	24.85	8.42	8.50	10.46	13.59
	MDRL	11.00	12.00	14.00	18.00	8.00	7.00	8.00	10.00
	SDRL	8.41	13.15	19.10	24.15	4.37	6.18	9.10	12.83
1.40	ARL	9.55	10.17	13.01	15.97	6.19	5.68	6.68	8.19
	MDRL	8.00	8.00	10.00	11.00	6.00	5.00	5.00	6.00
	SDRL	5.55	7.93	11.78	15.25	2.93	3.72	5.46	7.42
1.50	ARL	7.58	7.55	9.05	11.31	4.93	4.31	4.76	5.64
	MDRL	7.00	6.00	7.00	8.00	5.00	4.00	4.00	4.00
	SDRL	4.17	5.62	7.84	10.40	2.18	2.56	3.58	4.85
1.60	ARL	6.26	5.96	6.90	8.34	4.15	3.51	3.63	4.17
	MDRL	6.00	5.00	5.00	6.00	4.00	3.00	3.00	3.00
	SDRL	3.25	4.18	5.70	7.55	1.73	1.96	2.51	3.36
1.80	ARL	4.77	4.21	4.59	5.20	3.20	2.56	2.50	2.63
	MDRL	4.00	4.00	4.00	4.00	3.00	2.00	2.00	2.00
	SDRL	2.36	2.66	3.53	4.49	1.27	1.30	1.53	1.87
2.00	ARL	3.84	3.35	3.43	3.81	2.63	2.09	1.97	2.02
	MDRL	4.00	3.00	3.00	3.00	2.00	2.00	2.00	2.00
	SDRL	1.82	2.04	2.44	3.05	1.00	1.00	1.10	1.31
2.50	ARL	2.73	2.23	2.19	2.27	1.88	1.49	1.38	1.36
	MDRL	3.00	2.00	2.00	2.00	2.00	1.00	1.00	1.00
	SDRL	1.21	1.20	1.35	1.60	0.71	0.64	0.61	0.64
3.00	ARL	2.17	1.78	1.71	1.73	1.53	1.23	1.17	1.16
	MDRL	2.00	2.00	1.00	1.00	1.00	1.00	1.00	1.00
	SDRL	0.93	0.90	0.93	1.04	0.58	0.46	0.41	0.40
3.50	ARL	1.84	1.53	1.46	1.45	1.32	1.12	1.08	1.07
	MDRL	2.00	1.00	1.00	1.00	1.00	1.00	1.00	1.00
	SDRL	0.79	0.71	0.72	0.75	0.49	0.33	0.28	0.26
4.00	ARL	1.62	1.37	1.31	1.29	1.19	1.06	1.04	1.03
	MDRL	2.00	1.00	1.00	1.00	1.00	1.00	1.00	1.00
	SDRL	0.69	0.59	0.57	0.58	0.40	0.25	0.20	0.18

Table 4.4: Control chart coefficients L to fix the $\mathrm{ARL}_0 = 200$ for the EWMA dispersion charts

Distribution	n	λ	R_E	S_E	Q_E	D_E	MD_E	MAD_E	SN_E	QN_E
Normal	5	0.05	1.869	1.867	1.852	1.819	1.883	1.887	1.888	1.874
		0.25	2.588	2.566	2.606	2.585	2.609	2.735	2.688	2.711
		0.50	2.823	2.782	2.830	2.795	2.829	3.063	2.942	3.025
		0.75	2.925	2.865	2.949	2.895	2.931	3.215	3.057	3.173
	10	0.05	1.835	1.823	1.843	1.801	1.805	1.851	1.826	1.797
		0.25	2.562	2.508	2.581	2.502	2.513	2.607	2.582	2.519
		0.50	2.792	2.686	2.813	2.689	2.740	2.861	2.845	2.731
		0.75	2.893	2.765	2.923	2.771	2.836	2.979	2.953	2.826
Student's t	5	0.05	1.892	1.891	1.879	1.885	1.883	1.937	1.891	1.916
		0.25	2.981	2.984	2.866	2.921	2.892	2.902	2.834	2.894
		0.50	3.527	3.545	3.361	3.425	3.329	3.336	3.255	3.317
		0.75	3.849	3.851	3.567	3.682	3.581	3.546	3.443	3.554
	10	0.05	1.921	1.884	1.851	1.862	1.889	1.884	1.882	1.882
		0.25	3.041	2.989	2.686	2.811	2.758	2.719	2.696	2.693
		0.50	3.627	3.538	3.025	3.252	3.117	3.019	3.015	3.023
		0.75	3.946	3.829	3.171	3.492	3.302	3.190	3.164	3.165
Gamma	5	0.05	1.883	1.896	1.864	1.915	1.879	1.881	1.923	1.891
		0.25	2.867	2.895	2.801	2.827	2.784	2.863	2.853	2.878
		0.50	3.327	3.351	3.181	3.232	3.172	3.299	3.261	3.320
		0.75	3.545	3.578	3.375	3.421	3.355	3.531	3.461	3.539
	10	0.05	1.898	1.890	1.912	1.875	1.879	1.871	1.882	1.861
		0.25	2.851	2.802	2.762	2.703	2.695	2.708	2.759	2.682
		0.50	3.293	3.198	3.097	3.012	2.991	3.041	3.106	2.997
		0.75	3.518	3.401	3.261	3.179	3.140	3.209	3.299	3.162

Table 4.5: Extra Quadratic Loss (EQL) for different EWMA dispersion charts for Normal, Student's t and Gamma distributed quality characteristic ($\delta_{min} = 1.1$, $\delta_{max} = 4.0$)

		n							
		5				10			
		λ				λ			
Distribution	Chart	0.05	0.25	0.50	0.75	0.05	0.25	0.50	0.75
Normal	R_E	16.19	13.75	13.67	14.31	11.71	10.28	10.35	10.81
	S_E	15.73	13.31	13.21	13.70	10.94	9.63	9.59	9.92
	Q_E	16.17	13.93	13.81	14.68	13.78	11.91	11.91	12.49
	D_E	15.65	13.52	13.33	13.89	10.94	9.72	9.65	10.03
	MD_E	16.27	13.88	13.88	14.41	11.40	10.02	10.06	10.50
	MAD_E	25.05	22.49	22.94	24.28	15.97	13.77	13.85	14.65
	SN_E	23.54	20.61	20.55	21.52	14.50	12.56	12.77	13.41
	QN_E	22.94	20.48	21.09	22.40	13.14	11.42	11.36	11.82
Student's t	R_E	21.37	21.44	25.13	29.86	17.23	17.06	20.19	24.03
	S_E	20.86	21.04	24.94	29.52	15.18	14.88	17.47	20.71
	Q_E	19.72	18.73	21.17	23.74	14.93	13.25	13.84	14.89
	D_E	20.15	19.69	22.42	25.88	13.92	12.79	14.11	16.10
	MD_E	19.71	18.97	20.87	24.05	13.64	12.28	12.92	14.27
	MAD_E	27.30	25.79	27.91	30.39	17.11	15.19	15.48	16.71
	SN_E	25.75	24.18	26.04	28.03	15.93	13.96	14.46	15.56
	QN_E	25.62	24.37	26.31	29.34	14.96	13.15	13.68	14.69
Gamma	R_E	20.87	19.77	21.85	24.24	16.03	14.74	16.07	17.98
	S_E	20.99	20.07	22.12	24.62	15.08	13.64	14.58	16.18
	Q_E	19.96	18.46	19.57	21.50	16.27	14.33	15.01	16.26
	D_E	20.19	18.48	19.91	21.76	13.87	12.26	12.63	13.70
	MD_E	20.14	18.43	19.63	21.37	13.90	12.19	12.55	13.47
	MAD_E	27.46	26.29	28.26	30.81	17.59	15.64	16.17	17.47
	SN_E	26.42	24.56	26.29	28.54	16.89	15.20	16.00	17.59
	QN_E	25.61	24.60	26.75	29.49	14.92	13.13	13.62	14.74

Table 4.6: Relative ARL (RARL) for different EWMA dispersion charts for Normal, Student's t and Gamma distributed quality characteristic ($\delta_{min} = 1.1$, $\delta_{max} = 4.0$)

		n							
		5				10			
		λ				λ			
Distribution	Chart	0.05	0.25	0.50	0.75	0.05	0.25	0.50	0.75
Normal	R_E	1.03	1.03	1.03	1.04	1.07	1.07	1.08	1.09
	S_E	1.01	1.00	1.00	1.00	1.00	1.00	1.00	1.00
	Q_E	1.03	1.04	1.04	1.07	1.27	1.26	1.27	1.28
	D_E	1.00	1.01	1.01	1.01	1.00	1.01	1.01	1.01
	MD_E	1.04	1.04	1.05	1.05	1.04	1.04	1.05	1.06
	MAD_E	1.61	1.71	1.78	1.83	1.47	1.47	1.49	1.53
	SN_E	1.51	1.56	1.58	1.61	1.33	1.33	1.36	1.38
	QN_E	1.47	1.55	1.62	1.66	1.21	1.20	1.20	1.21
Student's t	R_E	1.08	1.14	1.20	1.26	1.26	1.38	1.55	1.69
	S_E	1.06	1.11	1.17	1.23	1.11	1.19	1.31	1.40
	Q_E	1.00	1.00	1.01	1.00	1.09	1.09	1.08	1.07
	D_E	1.02	1.05	1.07	1.08	1.02	1.04	1.08	1.10
	MD_E	1.00	1.01	1.00	1.01	1.00	1.00	1.00	1.00
	MAD_E	1.39	1.40	1.39	1.36	1.26	1.24	1.23	1.22
	SN_E	1.31	1.31	1.29	1.24	1.17	1.14	1.14	1.12
	QN_E	1.30	1.32	1.30	1.29	1.10	1.08	1.07	1.05
Gamma	R_E	1.05	1.07	1.11	1.13	1.16	1.21	1.27	1.32
	S_E	1.05	1.09	1.12	1.15	1.09	1.12	1.15	1.18
	Q_E	1.00	1.00	1.00	1.00	1.17	1.18	1.20	1.21
	D_E	1.01	1.00	1.02	1.01	1.00	1.00	1.00	1.01
	MD_E	1.01	1.00	1.00	1.00	1.00	1.00	1.00	1.00
	MAD_E	1.38	1.44	1.47	1.48	1.27	1.29	1.30	1.32
	SN_E	1.33	1.34	1.37	1.36	1.22	1.25	1.28	1.31
	QN_E	1.29	1.34	1.38	1.40	1.08	1.08	1.08	1.09

4.5 Comparison of Control Charts Performance

In this section, the performance of the all the EWMA dispersion charts is compared for processes following normal or non-normal parent distributions using ARL, EQL and RARL measures. The MDRL and SDRL measures are closely related to the ARL, as can be seen from the results in Table 4.1-4.3 and Appendix Tables B.1-B.21. The recommendations based on ARL are also valid when using MDRL and SDRL as performance measures.

To make comparisons easy, ARL curves for all the charts have been plotted for various combinations of n, λ and δ in Figures 4.1-4.6. In each plot, the multiplicative shift δ is plotted on the horizontal axis while the corresponding value of Log (ARL_1) for the different charts is plotted on the vertical axis. The log scale is used for better visual comparison. These charts have all been designed to have $\text{ARL}_0 = 200$ so that the values of ARL_1 can be compared directly - the lower the better. These plots are presented in Figures 4.1-4.2 for normal distribution, Figures 4.3-4.4 for t distribution and Figures 4.5-4.6 for Gamma distribution using $n = 5$ & 10 respectively. The purpose is to identify a control structure that performs better for both normal and non-normal parent distributions.

Normal Distribution: Comparing the run length performance of different dispersion charts for normally distributed quality characteristic, we observed that the best performance is shown by the S_E chart because the ARL curves for the S_E chart are lower than other competing charts for every combination of n, λ and δ. The S_E chart also has the lowest EQL value (see Table 4.5) and has been used as a benchmark chart, hence attaining RARL = 1 for almost all the cases (see Table 4.6). When n is small (i.e. $n = 5$), there is a very little difference between the S_E chart and the R_E, D_E, MD_E and Q_E charts in terms of ARL_1 and EQL. For $n = 10$, the D_E and MD_E charts have RARL values that are approximately 1 while the R_E and Q_E charts start to lose efficiency (e.g. for Q_E chart, the RARL increases from 1.04 (for $n = 5$) to 1.26 (for $n = 10$) when $\lambda = 0.25$). The ARL curves and the EQL values for MAD_E, SN_E and QN_E charts are always higher than the other charts, indicating the worst performance and low detection ability of these charts. The detection ability (in terms of ARL) of all the charts increases with an increase in the sample size (i.e. as we move from $n = 5$ to $n = 10$, the ARL_1 and EQL decreases for all the charts considering every choice of λ). The relative performance of the QN_E chart gets better with an increase in the sample size, whereas for R_E and Q_E charts, this phenomenon is opposite. From EQL tables, we can also observe that all the charts have better overall performance for either $\lambda = 0.25$ or $\lambda = 0.50$.

Student's t Distribution: For t-distributed quality characteristic, we observed that (in general) the MD_E chart is performing better than the rest of the charts because the ARL curves and the EQL values of the MD_E chart are lower than that for the other charts for almost all combinations of n, λ and δ. The Q_E chart is almost as efficient as the MD_E chart for $n = 5$. When $n = 10$, the D_E chart has the closest RARL to that of the MD_E chart for $\lambda \leq 0.50$ while for $\lambda = 0.75$, the QN_E chart is slightly efficient than the D_E chart. R_E and S_E charts are extremely affected for all combinations of n and λ but these charts are performing better than the MAD_E, SN_E and QN_E charts for $n = 5$ while for $n = 10$ this phenomenon is opposite. For a fixed value of n and λ, the ARL_1 and EQL of all the charts increases when the parent distribution is t, compared to the ARL_1 and EQL for the normal case. From the EQL table, we can also observe that all the dispersion charts are having better overall performance for either $\lambda = 0.05$ or $\lambda = 0.25$ when $n = 5$ while for $n = 10$, the overall performance of these dispersion charts is better for $\lambda = 0.25$.

Gamma Distribution: We observed that, for the skewed Gamma case, the performance of the D_E, MD_E and Q_E charts is almost similar and better than the other charts when n is small. As n increases, the ARL_1 and EQL of the Q_E chart increases, whereas the performance of the QN_E chart starts getting better. The difference between the D_E and MD_E charts, compared to the other charts, increases with an increase in λ. The performance of the S_E chart is better than the MAD_E and SN_E charts for $n = 5$ and 10 while the QN_E chart is performing better than the S_E chart for $n = 10$. The MAD_E chart has shown the worst performance like in the normal case. Compared to the normal case, the ARL_1 and the EQL for all the charts increases for the parent Gamma distribution. From the EQL table, we can observe that all the charts are having better overall performance for $\lambda = 0.25$

Run length distribution curves

To get more insight into the run length distributions of all the EWMA dispersion charts, Figure 4.7 presents the run length distribution curves (RLCs) of these charts, considering $n = 10$, $\lambda = 0.25$ and $\delta = 1.2$ for normal and non-normal cases. These charts give the probability of detecting an out-of-control situation within a given run length. A higher RLC indicates the superiority of a chart in terms of the quick detection of changes in the process parameters. We observed that the RLCs of the S_E, D_E and MD_E charts are higher than those of the other charts under normality. The Q_E and MD_E charts perform better for the t distribution, whereas for Gamma distribution, the MD_E and D_E charts are clearly superior than the rest of the charts, as the RLCs of these charts are higher than those of the other charts, particularly at shorter run lengths. The RLCs for the MAD_E chart are the lowest for the normal environment while, for other cases, the R_E chart seems to be the worst choice.

In short, we observed that the MD_E chart is performing better for non-normal cases and its performance for normal case is not bad either. D_E chart can be another good choice. We noticed that these superiority orders depend on the relative efficiency (Eq. 2.11) of a dispersion estimate, under a particular distributional environment.

Next, we explore some other characteristics of these EWMA dispersion charts, such as the comparison with their respective Shewhart structures and the effect of sample size. To save space, the results will be provided for only the MD_E chart. Similar results have been observed for the other EWMA dispersion charts.

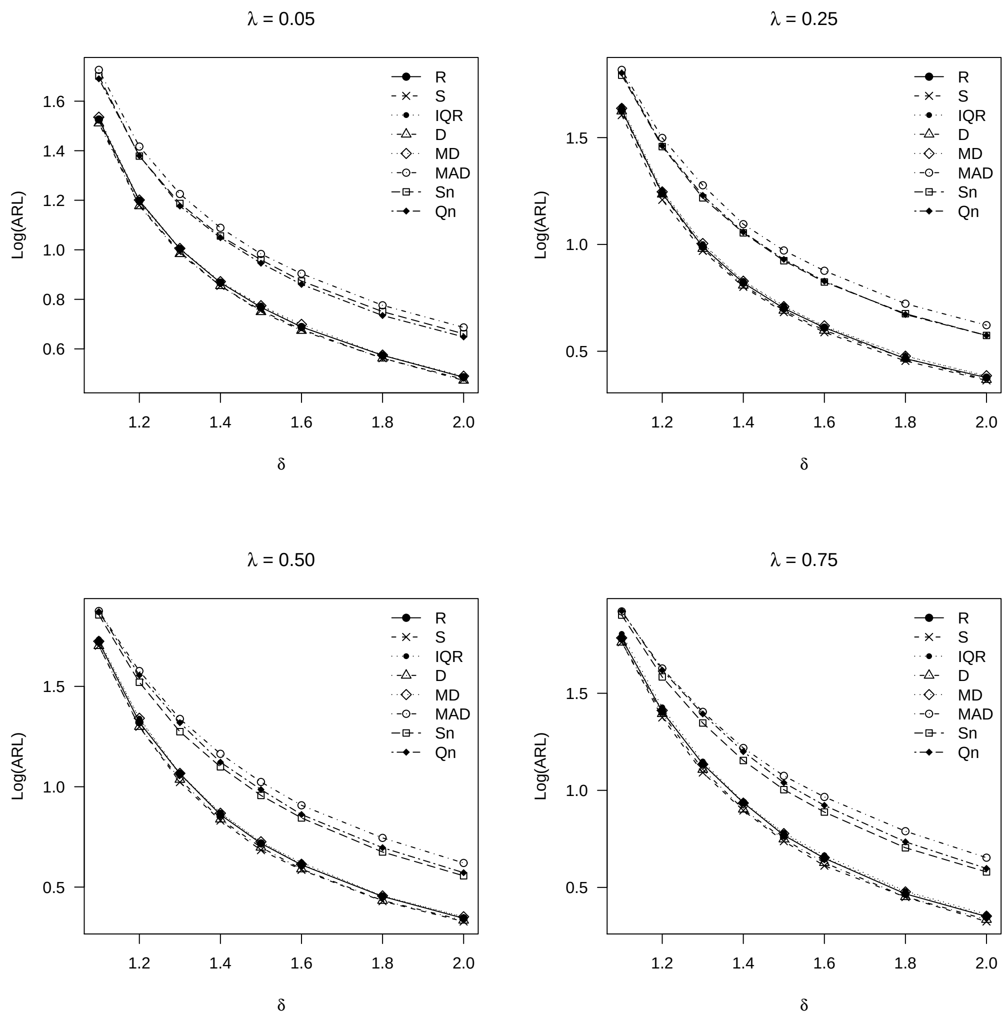

Figure 4.1: ARL comparison of dispersion EWMA control charts for Normally distributed quality characteristic when $n = 5$ and $\mathrm{ARL}_0 = 200$

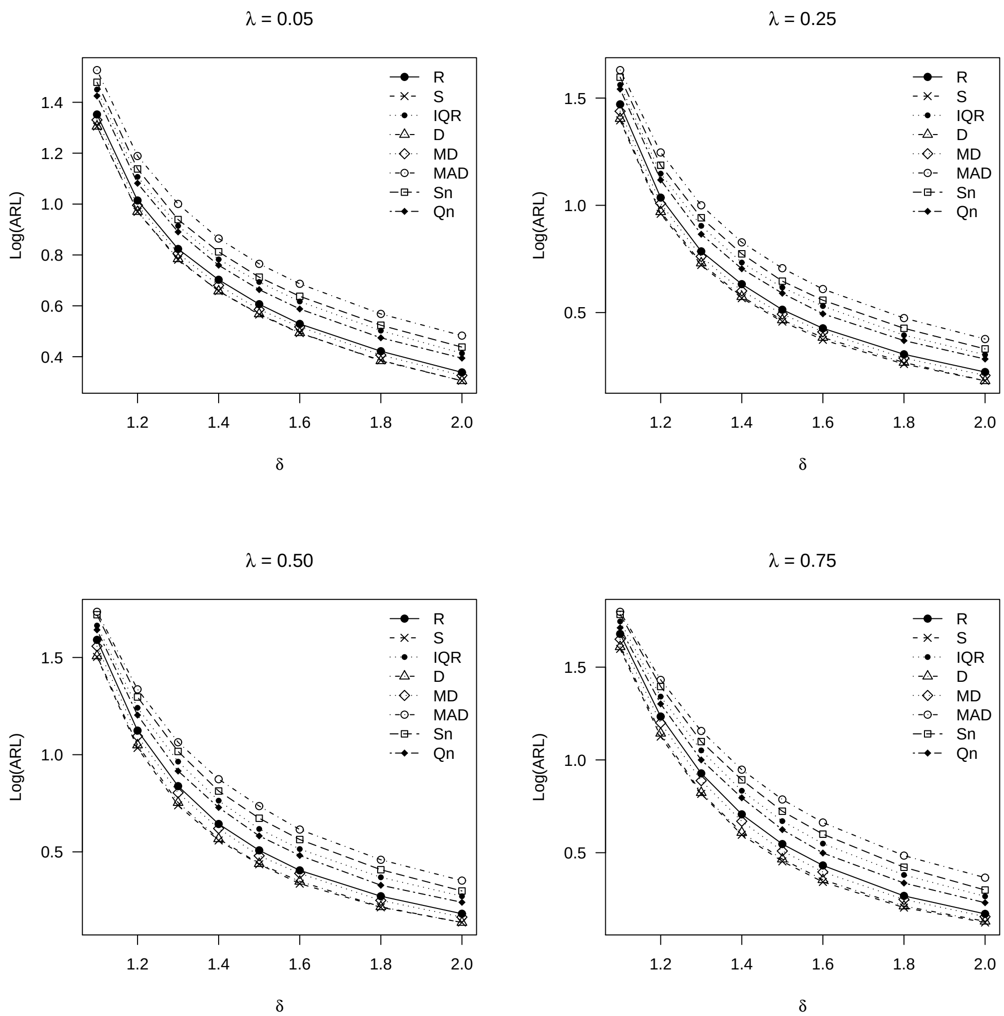

Figure 4.2: ARL comparison of dispersion EWMA control charts for Normally distributed quality characteristic when $n = 10$ and $\text{ARL}_0 = 200$

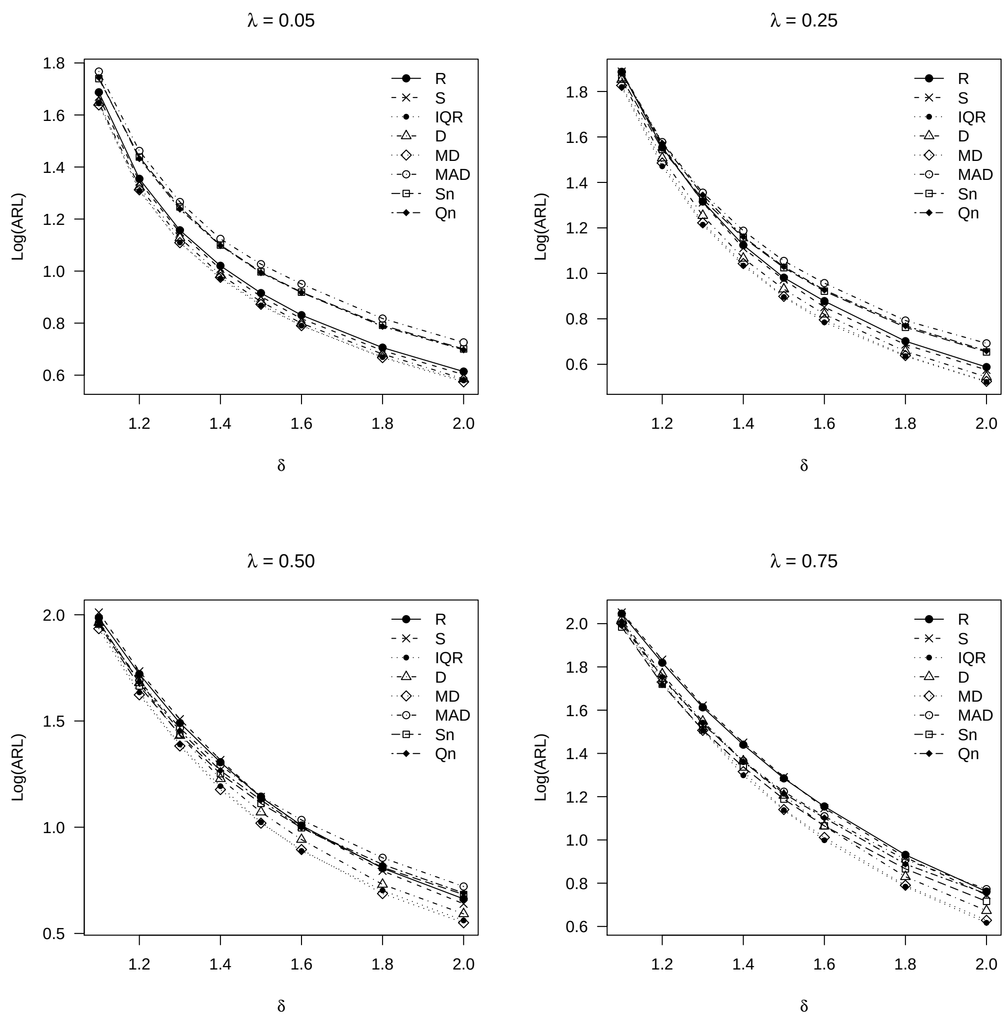

Figure 4.3: ARL comparison of dispersion EWMA control charts for t distributed quality characteristic when $n = 5$ and $\mathrm{ARL}_0 = 200$

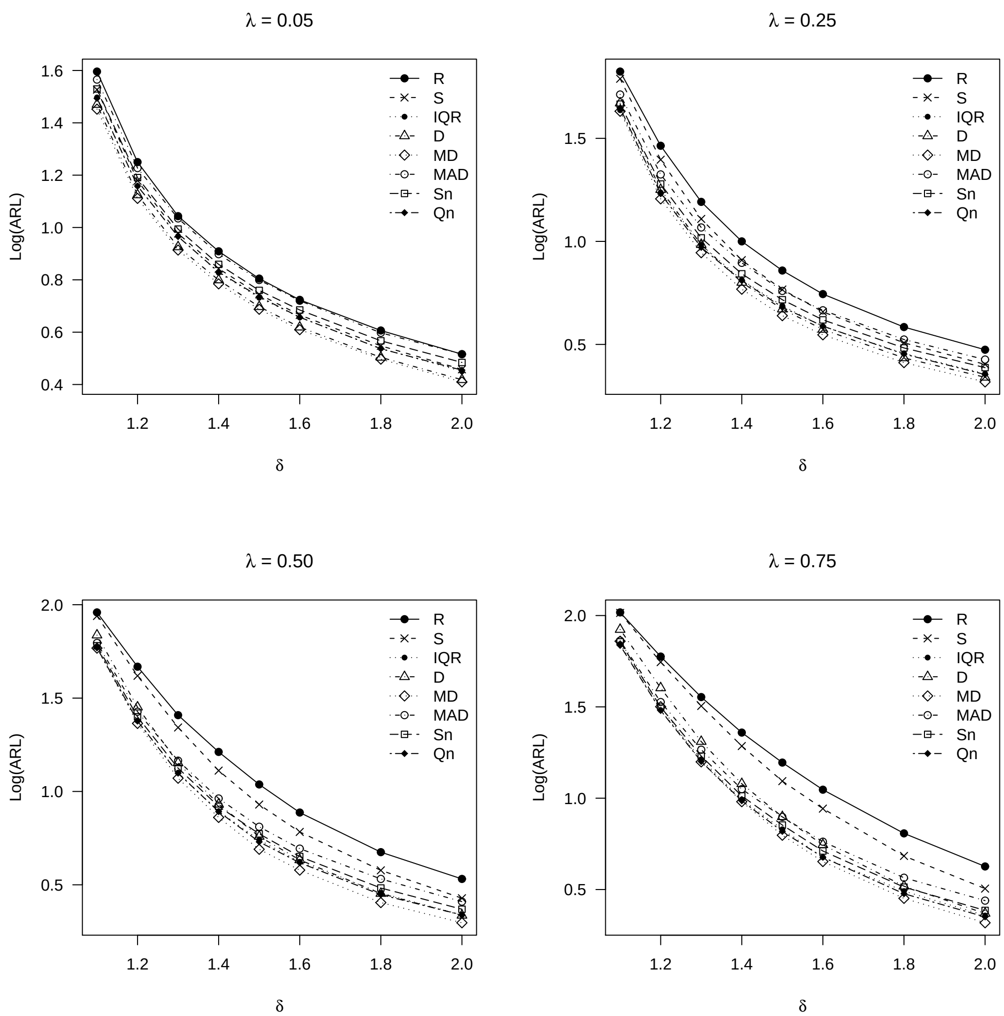

Figure 4.4: ARL comparison of dispersion EWMA control charts for t distributed quality characteristic when $n = 10$ and $\text{ARL}_0 = 200$

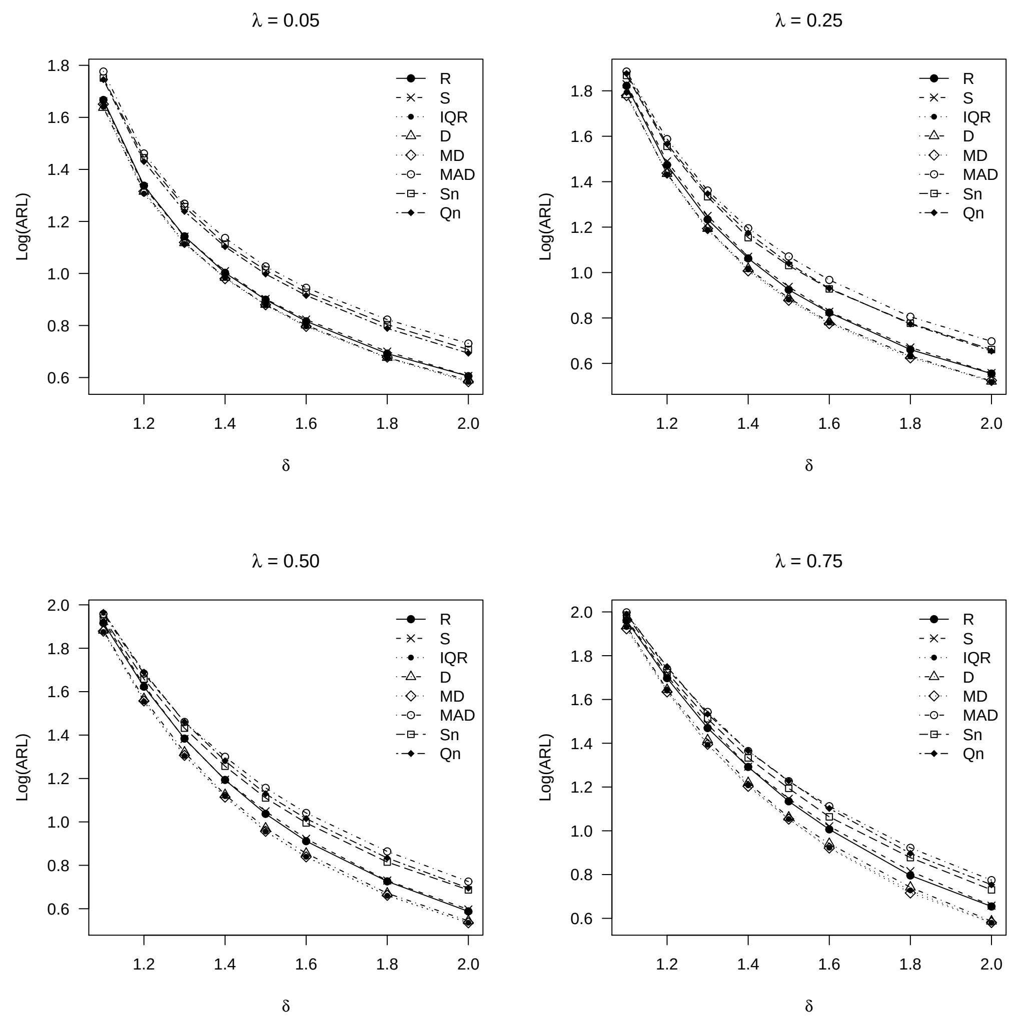

Figure 4.5: ARL comparison of dispersion EWMA control charts for Gamma distributed quality characteristic when $n = 5$ and $\mathrm{ARL}_0 = 200$

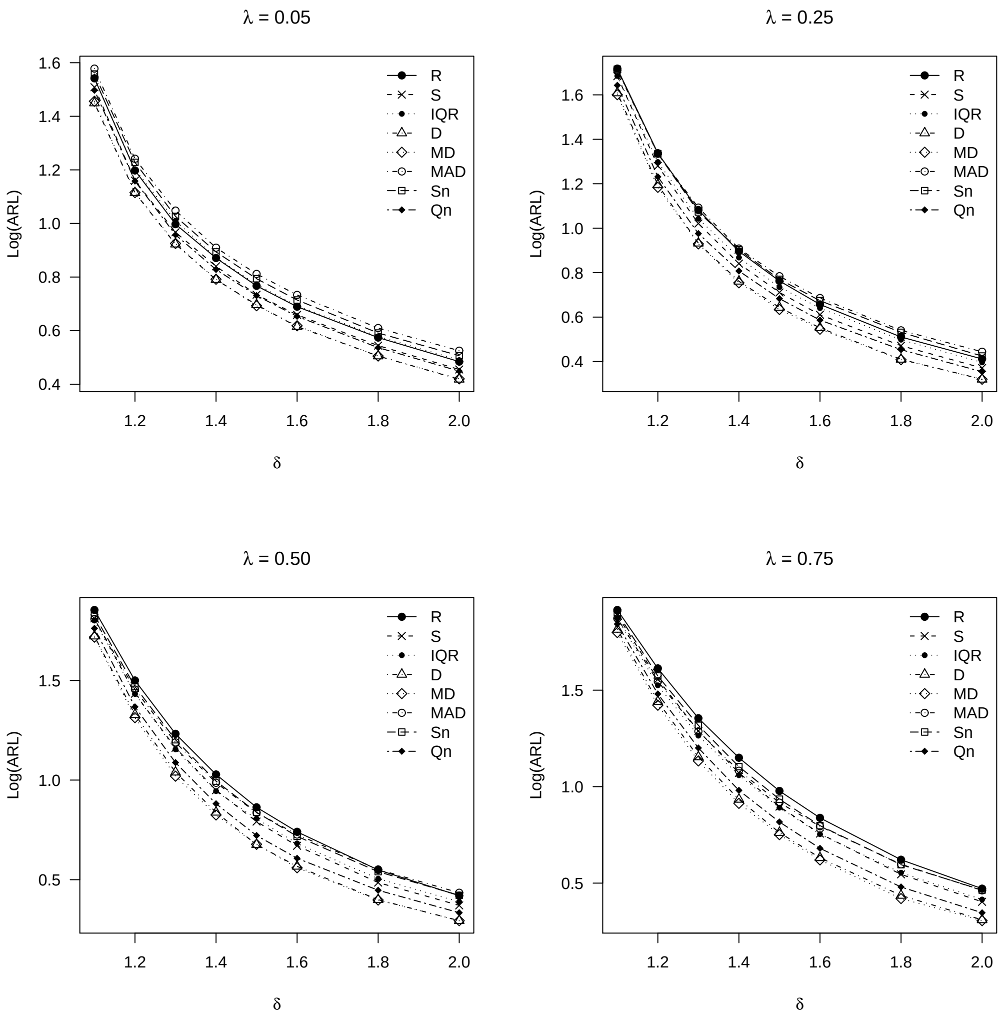

Figure 4.6: ARL comparison of dispersion EWMA control charts for Gamma distributed quality characteristic when $n = 10$ and $\text{ARL}_0 = 200$

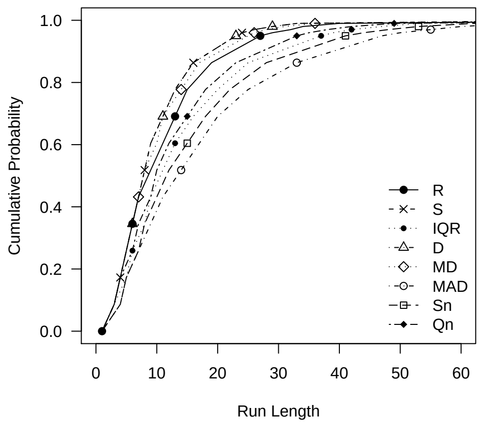

(a) Normal distribution

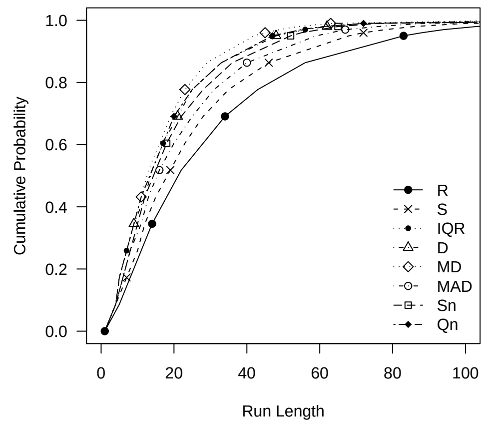

(b) t distribution

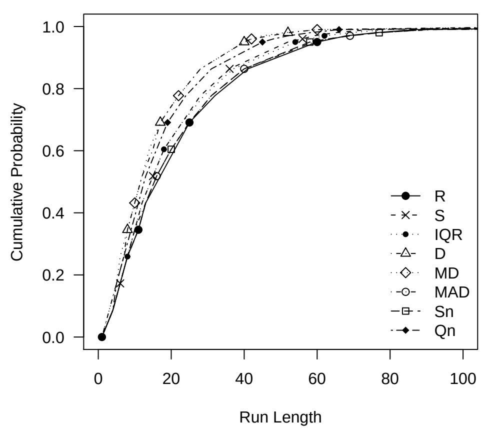

(c) Gamma distribution

Figure 4.7: Run length curves (RLCs) for dispersion EWMA control charts for Normal, t and Gamma distributed quality characteristic when $n = 10, \lambda = 0.25, \delta = 1.2$ and $\text{ARL}_0 = 200$

4.5.1 Comparison with Shewhart dispersion charts

In this section, we compared the ARL performance of the MD_E chart with its respective Shewhart MD chart structure studied in Chapter 2. Note that the MD chart of Riaz and Saghir (2009) becomes a special case of the MD_E chart at $\lambda = 1$. The run length characteristics of the MD chart are also computed using similar simulation routines and the results are provided in Table 4.7 for normal, t and Gamma distributions considering $n = 5$ & 10.

Comparing the results for the MD_E chart (in Tables 4.1 - 4.3) with the MD chart (in Table 4.7), we observed that, for all values of $\lambda < 1$ used in this study, the ARL_1 for the MD_E chart is much better than that for the MD chart, particularly for small and moderate changes in σ. As expected for large changes in σ, the performance of the Shewhart type MD chart is slightly better than that of the MD_E chart. Figure 4.8 presents the ARL comparison of the MD chart with MD_E chart when $\lambda = 0.05$ and 0.25 using $n = 10$. The ARL curves for the MD_E chart are clearly lower than for the MD chart when δ is low for all the cases. Overall, the performance of the MD_E chart with $\lambda = 0.25$ seems to be best for all the values of δ. Similar behaviours can also be observed for other charts investigated in this study.

4.5.2 Effect of sample size

In this section we discuss the effect of sample size on the performance of the MD_E chart. The performance is evaluated considering observations from the normal and the two non-normal parent distributions for $n = 3, 5, 7, 10, 12$ and 15. The results have been reported in Table 4.8 for the case when $\lambda = 0.25$ and $\text{ARL}_0 = 200$.

We can observe from the results in Table 4.8 that, for a specified in-control ARL ($\text{ARL}_0 = 200$), the detection ability of the MD_E chart improves with an increase in the sample size. In all the cases, we can see that the out-of-control RL characteristics of the MD_E chart decreases with an increase in the value of n at a particular value of δ. For example, under normally distributed quality characteristics, the ARL_1 decreases from 26.62 for $n = 3$ to 7.37 for

$n = 15$ when $\delta = 1.2$. This means that for the detection of a 1.2σ shift in process variability, the MD_E chart requires, on average, 19 less observations when the sample size increases from $n = 3$ to $n = 15$. For a particular value of λ, the choice of sample size depends upon the magnitude of shift (δ) to be detected quickly. For efficient detection of small shifts, large samples are required but for the detection of large shifts, even small samples can serve the purpose. We also observed that when the assumption of normality is violated, larger samples are required to detect a particular magnitude of shift. For all the other EWMA dispersion charts, we can expect similar improvements in run length performance with increase in the sample size.

4.6 Conclusions

In this chapter we investigated a set of EWMA charts for monitoring process dispersions. These EWMA charts are based on a wide range of dispersion estimates as discussed in Section 4.2. We observed that, under the ideal assumption of normality, the best performance is shown by the S_E chart, followed by D_E and MD_E charts. For non-normal Student's t and Gamma distributions, the best performance has been generally shown by the MD_E chart. The comparison with respective Shewhart dispersion charts revealed the superiority of EWMA charts, particularly for low values of shift (δ) in the process standard deviation. Although run length characteristics are only provided for normal, t and Gamma parent distributions, one can generalize the relative performance of these charts for other distributional environments, based on the findings in Chapter 2.

The EWMA dispersion charts, investigated in this study, are all based on the asymptotic control limits (given in Equation (4.6)). The sensitivity of these charts can be increased by using the exact time varying limits and the Fast Initial Response (FIR) feature, as examined in Abbasi and Miller (2011b, chap. 35).

Table 4.7: RL characteristics of the MD chart for normal, Student's t and Gamma distributed quality characteristic when $\text{ARL}_0 = 200$

		n					
		5			10		
δ		Normal	t	Gamma	Normal	t	Gamma
1.00	ARL	199.02	201.210	200.70	201.50	201.930	199.86
	MDRL	134.00	139.00	138.00	139.00	140.00	138.00
	SDRL	198.80	199.72	203.56	198.99	200.63	200.56
1.10	ARL	66.84	108.18	92.57	53.02	86.17	72.72
	MDRL	46.00	75.00	64.00	37.00	60.00	51.00
	SDRL	66.71	107.81	92.02	53.18	86.06	71.70
1.20	ARL	30.69	63.79	49.90	20.46	40.18	32.88
	MDRL	21.00	44.00	35.00	15.00	28.00	23.00
	SDRL	30.13	63.47	49.54	19.60	39.14	32.53
1.30	ARL	16.66	38.67	29.56	9.74	21.45	17.33
	MDRL	12.00	27.00	20.00	7.00	15.00	12.00
	SDRL	16.31	38.19	29.24	9.20	20.75	16.68
1.40	ARL	10.12	25.38	19.35	5.75	12.86	10.30
	MDRL	7.00	18.00	14.00	4.00	9.00	7.00
	SDRL	9.55	24.70	18.68	5.25	12.45	9.70
1.50	ARL	6.98	17.46	13.55	3.74	8.23	6.92
	MDRL	5.00	12.00	9.00	3.00	6.00	5.00
	SDRL	6.41	16.97	13.05	3.17	7.61	6.36
1.60	ARL	5.16	12.66	10.06	2.79	5.73	5.03
	MDRL	4.00	9.00	7.00	2.00	4.00	4.00
	SDRL	4.56	12.02	9.60	2.27	5.20	4.54
1.80	ARL	3.29	7.54	6.14	1.83	3.34	3.04
	MDRL	2.00	5.00	4.00	1.00	2.00	2.00
	SDRL	2.68	6.99	5.61	1.24	2.79	2.47
2.00	ARL	2.46	5.06	4.40	1.46	2.30	2.19
	MDRL	2.00	4.00	3.00	1.00	2.00	2.00
	SDRL	1.91	4.51	3.85	0.80	1.75	1.62
2.50	ARL	1.58	2.66	2.48	1.11	1.37	1.39
	MDRL	1.00	2.00	2.00	1.00	1.00	1.00
	SDRL	0.95	2.09	1.86	0.35	0.71	0.74
3.00	ARL	1.29	1.86	1.79	1.04	1.14	1.15
	MDRL	1.00	1.00	1.00	1.00	1.00	1.00
	SDRL	0.61	1.25	1.22	0.20	0.41	0.42
3.50	ARL	1.17	1.49	1.47	1.01	1.06	1.07
	MDRL	1.00	1.00	1.00	1.00	1.00	1.00
	SDRL	0.44	0.85	0.81	0.12	0.26	0.26
4.00	ARL	1.10	1.31	1.31	1.00	1.03	1.03
	MDRL	1.00	1.00	1.00	1.00	1.00	1.00
	SDRL	0.34	0.64	0.63	0.07	0.16	0.18

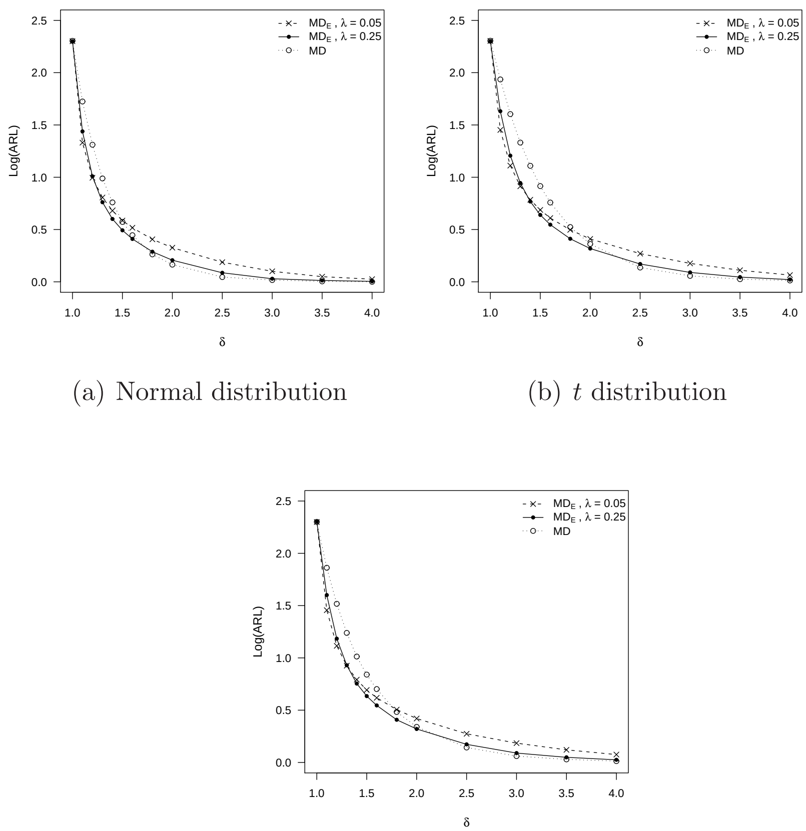

(a) Normal distribution

(b) t distribution

(c) Gamma distribution

Figure 4.8: ARL comparison of the MD chart with MD_E chart when $\lambda = 0.05$ and 0.25 for $n = 10$ and $\text{ARL}_0 = 200$

Table 4.8: Run length characteristics of MD_E chart for Normal , Student's t and Gamma distributed quality characteristic when $\lambda = 0.25$ and $\text{ARL}_0 = 200$

		n					
δ		3	5	7	10	12	15
				Normal			
1.00	ARL	199.23	200.35	200.49	199.59	199.92	199.61
	MDRL	138.00	140.00	140.00	137.00	138.00	136.00
	SDRL	199.07	200.73	197.57	193.33	198.83	199.46
1.20	ARL	26.62	17.63	13.37	10.20	8.77	7.37
	MDRL	19.00	13.00	10.00	8.00	7.00	6.00
	SDRL	24.37	15.01	10.89	7.85	6.40	5.13
1.40	ARL	6.24	6.73	3.22	3.99	2.32	3.03
	MDRL	5.00	5.00	3.00	3.00	2.00	3.00
	SDRL	4.52	4.77	1.78	2.35	1.10	1.52
1.60	ARL	3.52	4.16	1.94	2.57	1.46	2.01
	MDRL	3.00	4.00	2.00	2.00	1.00	2.00
	SDRL	2.28	2.59	0.94	1.29	0.60	0.88
				Student's t			
1.00	ARL	201.84	201.02	200.39	200.11	199.58	199.01
	MDRL	143.00	141.00	140.00	143.00	140.00	136.00
	SDRL	199.32	203.37	199.98	199.43	198.74	198.59
1.20	ARL	46.50	30.58	22.11	16.08	13.60	11.22
	MDRL	33.00	22.00	16.00	12.00	10.00	9.00
	SDRL	44.18	27.84	19.69	13.22	11.02	8.65
1.40	ARL	18.67	11.04	8.00	5.86	4.95	4.20
	MDRL	14.00	9.00	6.00	5.00	4.00	4.00
	SDRL	16.19	8.79	5.74	3.84	3.03	2.35
1.60	ARL	10.40	6.24	4.61	3.52	3.06	2.67
	MDRL	8.00	5.00	4.00	3.00	3.00	2.00
	SDRL	8.33	4.33	2.82	1.95	1.57	1.27
				Gamma			
1.00	ARL	200.50	199.49	202.62	200.66	200.88	199.82
	MDRL	142.00	138.00	144.00	141.00	142.00	140.00
	SDRL	199.52	198.47	198.07	199.04	198.60	196.83
1.20	ARL	41.07	27.40	20.32	15.27	13.11	10.93
	MDRL	29.50	20.00	15.00	12.00	10.00	9.00
	SDRL	38.71	24.88	17.72	12.41	10.45	8.50
1.40	ARL	16.87	10.17	7.60	5.68	4.96	4.23
	MDRL	12.00	8.00	6.00	5.00	4.00	4.00
	SDRL	14.68	7.93	5.51	3.72	3.05	2.46
1.60	ARL	9.76	5.96	4.58	3.51	3.05	2.67
	MDRL	8.00	5.00	4.00	3.00	3.00	2.00
	SDRL	7.80	4.18	2.92	1.96	1.62	1.32

Chapter 5

On the Performance of EWMA Location Chart in Presence of Two Component Measurement Error

Control charts are increasingly adopted by laboratories for affective monitoring of analytical processes particularly in the internal quality control phase. Analytical responses from a laboratory measurement system are plotted on a chart versus time or sample number to ensure the stability of a control material. In practice, the measurements from these processes are mostly subject to two types of errors: i) additive error and ii) multiplicative or proportional error. These errors can have a serious impact on the detection ability of control charts. The additive and multiplicative errors have been combined in a single model, namely the two component measurement error model, proposed by Rocke and Lorenzato (1995). In this chapter, we investigate the performance of the EWMA control chart in the presence of two component measurement error due to its importance in analytical chemistry and environmental settings. The comparison with the EWMA chart performance in the presence of one component (additive) error model is also provided. This chapter is based on Abbasi (2010).

5.1 Introduction

Analytical Quality Assurance (AQA) programs are increasingly adopted by laboratories to ensure the quality of analytical measurements. According to Taverniers et al. (2004), AQA is a set of procedures that a laboratory must undertake to ensure that its measurement procedures are of a high standard. It should include method validation, estimation of measurement uncertainty, effective internal quality control procedures, participation in proficiency testing schemes and accreditation to an international standard (e.g. ISO/IEC 17025). The objective of these AQA programs is to ensure that laboratories work efficiently and effectively. 'Method validation is an important requirement in the practice of chemical analysis' and forms the first level of the AQA system. Any newly developed method should be validated 'to verify that its performance parameters are adequate for use for a particular analytical problem' (EURACHEM-GUIDE (1998)). After method validation, level II of the AQA system consists of a series of procedures that need to be taken to ensure the verified analytical process is available for routine analysis. Internal quality control (IQC) procedures are usually applied to continuously monitor analytical results obtained daily in laboratories. As defined in "Harmonized Guidelines for Internal Quality Control in Analytical Chemistry Laboratories" prepared by Thompson and Wood (1995), "IQC is a set of procedures undertaken by laboratory staff for the continuous monitoring of operation and the results of the measurements in order to decide whether results are reliable enough to be released". The guide further states that the interpretation of IQC analyses results depend largely on statistical process control concepts and that the control chart acts as the most important tool for effective monitoring of IQC results. The use of control charts in analytical laboratories has also been recommended by Bartram and Ballance (1996), CITAC/EURACHEM-GUIDE (2002) and Bonet-Domingo et al. (2006). Details regarding different levels of AQA programs, together with the use of specific control charts can be found in Funk et al. (1995) and Garfield (1984). Detailed description of the design, use and interpretation of control charts, with examples from analytical chemistry, can be found in numerous text-books regarding quality assurance in analytical chemistry laboratories: for example see Funk et al. (1995, chap. 2), Crosby et al. (1995, chap. 5), Mullins (2003, chap. 2) and Hibbert (2007, chap. 4). Control charts have also been included as part of several ISO standards (ISO8258 (1991); ISO7870 (1993); ISO7873 (1993); ISO7966 (1993)).

Control charts are useful for the rapid recognition of unusual variations in analytical results. Shewhart type control charts are the most widely used (as can be seen in most of the above references). Due to the memoryless nature of these control charts, they do not perform well for the detection of small and moderate process shifts, which are usually of a major concern in analytical processes. So, analysts need to be aware of more efficient control procedures such as cumulative sum (CUSUM) or exponentially weighted moving average (EWMA) control charts. Recently, Carson and Yeh (2008) emphasized the use of EWMA charts for the monitoring of an analytical process by analyzing real data sets concerning the quality control of total organic carbon in water. The EWMA charts make use of information in historical observations as well as in the current observations by adopting a varying weight scheme, assigning highest weight to the most recent observations and having the weights decrease exponentially for less recent observations. This helps in earlier detection of small shifts in process (location and scale) parameters (for details, see Montgomery (2009)).

The presence of measurement error can seriously affect the performance of any analytical process and also affects the detection ability of control charts. Many researchers have investigated the effect of measurement error on the performance of control charts: see Mittag and Stemann (1998b); Linna and Woodall (2001); Linna et al. (2001); Maravelakis et al. (2004); Cocchi and Scagliarini (2007) and Maravelakis (2007). It has been observed that for analytical methods, measurement error can often be composed of two components: additive error, which is dominant at low concentrations, and multiplicative error, which is dominant at high concentrations. Due to this, estimation of the overall precision of the analytical method becomes difficult, especially in the area where transition occurs between near-zero and higher concentration levels. The additive model works well for only low concentration levels, whereas the multiplicative model for only higher concentrations. The two component model proposed by Rocke and Lorenzato (1995) resolves these problems by combining both additive and proportional errors in a single model. Thus, a single model can be used to adequately describe the measurement error over the entire range of observations for an analytical process. The two component model is:

$$Y_t = \alpha + \beta X_t e^{\eta_t} + \epsilon_t \tag{5.1}$$

Where X represents true concentration of an analyte at time t and Y is the measured response which is related to X by the calibration curve with intercept α and slope β. Let $X \sim N(\mu, \sigma^2)$ and random disturbances η and ϵ are distributed normally and independently with mean 0 and variances σ_η^2 and σ_ϵ^2 respectively (i.e. $\eta \sim N\left(0, \sigma_\eta^2\right)$ and $\epsilon \sim N(0, \sigma_\epsilon^2)$). Here η represents multiplicative error and ϵ represents additive error. For this model, observations at higher concentration are approximately lognormally distributed and observations at low concentration are approximately normally distributed. This agrees with the findings of Gibbons and Bhaumik (2001) and Aryal et al. (2009).

Studies have demonstrated the importance and applicability of the above model in analytical chemistry and environmental settings (see Zorn et al. (1999); Rocke et al. (2003)). Rocke and Durbin (2001) have shown that measurement error in gene expression microarray data can be appropriately expressed by the two component model. In addition, the generalization of the two component model for multiple laboratories has been presented by Gibbons and Bhaumik (2001). A significant literature is also available concerning the estimation of the two component model parameters $(\alpha, \beta, \sigma_\epsilon, \sigma_\eta)$. Rocke and Lorenzato (1995) used the method of maximum likelihood to estimate these parameters. Gibbons et al. (1997) suggested estimating model parameters using the weighted least squares (WLS) method, but it has been pointed out by Rocke et al. (2003) that WLS method is often very unstable and can lead to non convergence or impossible estimates. Jones (2004) considered a Bayesian framework and adopted Markov chain Monte Carlo techniques for estimating the parameters. For the purpose of this study, the parameters of the two component model are assumed to be known.

The purpose of this chapter is to investigate the performance of the EWMA chart in the presence of two component measurement error. The performance is evaluated for both the individual and the multiple measurement cases. The rest of this chapter is organized as follows: The next section describes the general structure of the EWMA control charts for monitoring process location parameter and also establishes the EWMA control chart structure in the presence of two component measurement error. The different characteristics of the run length distribution, such as the average run length (ARL), the median run length (MDRL) and the standard deviation of the run length (SDRL) are then presented for the proposed scheme. To reduce the effect of measurement error, the design structure for the case of multiple measurements at each sample point has been developed and the run length results are provided in Section 5.4. Comparison of the two component error model is then made with one component error model, as was discussed by Maravelakis et al. (2004). The effect of two component error model is investigated in Section 6.6 and finally we give concluding remarks.

5.2 EWMA Chart in Presence of Two Component Measurement Error

Since the introduction of EWMA charts by Roberts (1959), many researchers have examined these charts from different perspectives – see for example Lucas and Saccucci (1990), Montgomery et al. (1995), Steiner (1999), Chan and Zhang (2000), Maravelakis et al. (2004), Carson and Yeh (2008), Shu and Jiang (2008) and references therein. The basic structure of EWMA charts can be seen in Chapter 1. In brief, suppose in the measurement error free case we have a variable Z which is related to X as $Z_t = \alpha + \beta X_t$. If we assume that $X \sim N(\mu, \sigma^2)$, it follows that $Z \sim N(\alpha + \beta\mu, \beta^2\sigma^2)$. Suppose we have observed values of Z that consist of subgroups of size n taken at period $t = 1, 2, 3, \ldots$. The EWMA statistic S_t is defined as: $S_t = \lambda\overline{Z}_t + (1-\lambda) S_{t-1}$, where λ (lying between 0 and 1) is the weight assigned to each observation and $\overline{Z}_t$ is the average of the sample observations at time t. The control limits are thus defined as:

$$UCL = \alpha + \beta\mu + L\frac{\sigma_z}{\sqrt{n}}\sqrt{\left(\frac{\lambda}{2-\lambda}\right)\left[1-(1-\lambda)^{2t}\right]}$$

$$LCL = \alpha + \beta\mu - L\frac{\sigma_z}{\sqrt{n}}\sqrt{\left(\frac{\lambda}{2-\lambda}\right)\left[1-(1-\lambda)^{2t}\right]} \tag{5.2}$$

where UCL and LCL respectively represents upper and lower control limits for EWMA statistic S_t, and $\sigma_z = \beta\sigma$. For the case of the two component error model, the EWMA statistic based on Equation (5.1) is defined as:

$$Q_{tc,t} = \lambda\overline{Y}_t + (1-\lambda)\,Q_{tc,t-1}, \quad Q_{tc,0} = \mu_Y = \alpha + \beta\mu\sqrt{e^{\sigma_\eta^2}} \tag{5.3}$$

To establish the control limits based on the above EWMA statistic, we need to find its mean and variance. By continuous substitution of $Q_{tc,t-i}, i = 1, 2, \ldots, t$; the EWMA statistic $Q_{tc,t}$ can be written as (see Roberts (1959) and Montgomery (2009)):

$$Q_{tc,t} = \lambda\sum_{i=0}^{t-1}(1-\lambda)^i\overline{Y}_{t-i} + (1-\lambda)^t Q_{tc,0} \tag{5.4}$$

For independent random observations from a stable process, $E(\overline{Y}_t) = E(\overline{Y}_{t-i}) = \mu_Y$ and $var(\overline{Y}_t) = var(\overline{Y}_{t-i}) = \sigma_Y^2/n$. Hence, by taking expectation on both sides of Equation (5.4), we obtain

$$\begin{aligned}
E(Q_{tc,t}) &= \lambda \sum_{i=0}^{t-1} (1-\lambda)^i E(\overline{Y}_{t-i}) + (1-\lambda)^t E(Q_{tc,0}) && (5.5)\\
&= (\alpha + \beta\mu\sqrt{e^{\sigma_\eta^2}}) \left(\lambda \sum_{i=0}^{t-1} (1-\lambda)^i + (1-\lambda)^t \right)\\
&= (\alpha + \beta\mu\sqrt{e^{\sigma_\eta^2}}) \left(\lambda \left[\frac{1-(1-\lambda)^t}{1-(1-\lambda)} \right] + (1-\lambda)^t \right)\\
&= \alpha + \beta\mu\sqrt{e^{\sigma_\eta^2}}.
\end{aligned}$$

Similarly, taking the variance on both sides of Equation (5.4), we obtain

$$\begin{aligned}
Var(Q_{tc,t}) &= \lambda^2 \sum_{i=0}^{t-1} (1-\lambda)^{2i} Var(\overline{Y}_{t-i}) + (1-\lambda)^{2t} Var(Q_{tc,0}) && (5.6)\\
&= \frac{\sigma_y^2}{n} \left(\lambda^2 \left[\frac{1-(1-\lambda)^{2t}}{1-(1-\lambda)^2} \right] \right)\\
&= \frac{\sigma_y^2}{n} \left(\left(\frac{\lambda}{2-\lambda} \right) \left[1-(1-\lambda)^{2t} \right] \right)
\end{aligned}$$

Hence, the proposed control limits are defined as:

$$UCL_{tc} = \alpha + \beta\mu\sqrt{e^{\sigma_\eta^2}} + L\frac{\sigma_y}{\sqrt{n}} \sqrt{\left(\frac{\lambda}{2-\lambda} \right) \left[1-(1-\lambda)^{2t} \right]}$$

$$LCL_{tc} = \alpha + \beta\mu\sqrt{e^{\sigma_\eta^2}} - L\frac{\sigma_y}{\sqrt{n}} \sqrt{\left(\frac{\lambda}{2-\lambda} \right) \left[1-(1-\lambda)^{2t} \right]} \qquad (5.7)$$

where σ_y is given as (see Rocke and Lorenzato (1995) and Cocchi and Scagliarini (2007)):

$$\sigma_y = \sqrt{\beta^2(\sigma^2 e^{\sigma_\eta^2} + \mu^2(e^{\sigma_\eta^2}(e^{\sigma_\eta^2}-1)) + \sigma^2(e^{\sigma_\eta^2}(e^{\sigma_\eta^2}-1))) + \sigma_\epsilon^2}. \qquad (5.8)$$

The above control limits are known as exact or time varying control limits but, as t gets larger, the factor $(1-(1-\lambda)^{2t})$ quickly converges to unity so we can use the asymptotic control limits, which are given as:

$$UCL_{tc} = \alpha + \beta\mu\sqrt{e^{\sigma_\eta^2}} + L\frac{\sigma_y}{\sqrt{n}}\sqrt{\left(\frac{\lambda}{2-\lambda}\right)}$$

$$LCL_{tc} = \alpha + \beta\mu\sqrt{e^{\sigma_\eta^2}} - L\frac{\sigma_y}{\sqrt{n}}\sqrt{\left(\frac{\lambda}{2-\lambda}\right)}. \tag{5.9}$$

For the rest of this study, asymptotic control limits given in Equation (5.9) are used instead of time varying limits given in Equation (5.7). For numerical computations on the proposed charts, we assume that the parameters are fixed and their values have been taken from the toluene example reported by Rocke and Lorenzato (1995), i.e. $\alpha = 11.51, \beta = 1.524, \sigma_\eta = 0.1032$ and $\sigma_\epsilon = 5.698$. The two component error model has approximately constant coefficient of variation (CV) for high concentrations and constant standard deviation for low concentrations. To cover the entire range of possibilities, concentration mean level μ from 5 picogram to 15 nanograms and CV values from 0.01 to 0.5 are used in this study, following Rocke and Lorenzato (1995) and Cocchi and Scagliarini (2007). Relative standard deviation or coefficient of variation (CV) is a dimensionless measure and is defined as the ratio of process standard deviation (σ) to the mean (μ). It is expressed as

$$CV = \frac{\sigma}{\mu} \tag{5.10}$$

The CV value is an important measure of the precision of an analytical system and helps in assessing the importance of the likely analytical error in relation to the magnitude of the quantity being measured (Mullins (2003)).

Suppose in the error free case, the shift δ in the process location parameter is defined as $\delta = (\mu_1 - \mu_0)/\sigma$, where μ_0 and μ_1 respectively denote in-control and out of control mean levels for the random variable X. In the two component error case, the corresponding shift in the random variable Y, given as δ_{tc}, is defined as (see Linna and Woodall (2001); Linna et al. (2001) and Cocchi and Scagliarini (2007)):

$$\begin{aligned}
\delta_{tc} &= \frac{E(Y_t|\mu=\mu_1)-E(Y_t|\mu=\mu_0)}{\sigma_y} \qquad (5.11)\\
&= \frac{\alpha+\beta\mu_1\sqrt{e^{\sigma_\eta^2}}-\alpha+\beta\mu_0\sqrt{e^{\sigma_\eta^2}}}{\sqrt{\beta^2(\sigma^2 e^{\sigma_\eta^2}+\mu^2(e^{\sigma_\eta^2}(e^{\sigma_\eta^2}-1))+\sigma^2(e^{\sigma_\eta^2}(e^{\sigma_\eta^2}-1)))+\sigma_\epsilon^2}}\\
&= \frac{\delta}{\sqrt{1+\frac{\mu^2}{\sigma^2}(e^{\sigma_\eta^2}-1)+(e^{\sigma_\eta^2}-1)+\frac{\sigma_\epsilon^2}{\beta^2\sigma^2 e^{\sigma_\eta^2}}}}\\
&= \frac{\delta}{\sqrt{CV^{-2}(e^{\sigma_\eta^2}-1)+e^{\sigma_\eta^2}+\frac{\sigma_\epsilon^2}{\beta^2\sigma^2 e^{\sigma_\eta^2}}}}
\end{aligned}$$

The term in the denominator is always greater than one and hence makes the magnitude of shift δ_{tc} smaller than δ. To illustrate this effect, Figure 5.1 presents curves for δ_{tc}/δ versus CV at different levels of mean concentration (μ).

It is clearly seen from Figure 5.1 that the magnitude of shift δ is greatly affected by two component measurement error for small values of μ and CV. As μ and CV increase, δ_{tc}/δ approaches 1.

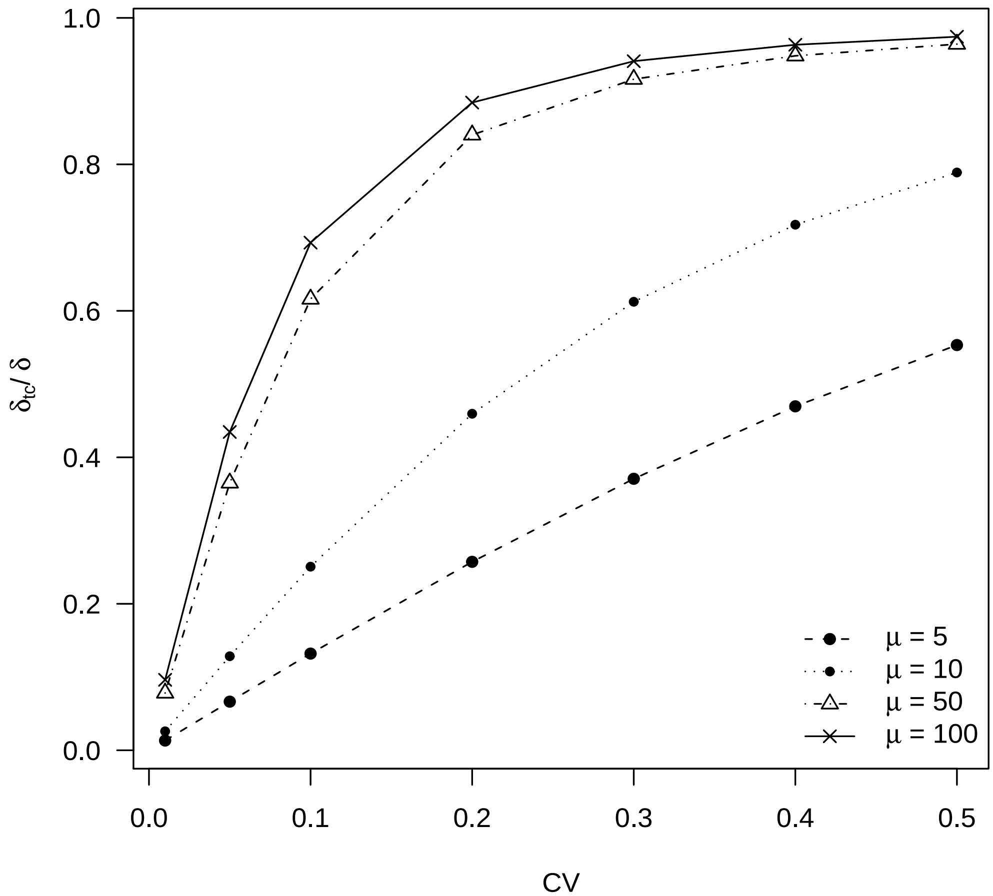

Figure 5.1: Decrease in the magnitude of shift due to two component measurement error.

5.3 Control Chart Performance

In this section, we evaluate the performance of EWMA chart in the presence of the two component measurement error using the average run length (ARL), the standard deviation of the run length distribution (SDRL) and the median of the run length distribution (MDRL). Tables 5.1-5.3 give a summary of the run length distribution of the EWMA chart in the presence of two component error using the control limits given in Equation (5.9). For efficient detection of small to moderate process shifts, we use $\lambda = 0.25$ and $L = 2.898$, following the recommendations of Maravelakis et al. (2004). These choices of L and λ give an in-control ARL (ARL_0) of 370 for no-measurement error case. For representing the out of control situations, shifts ($\delta = 0.5, 1.0$ and 1.5) have been introduced in the mean in standard deviation units.

The results in the Tables 5.1-5.3 indicate that, in the presence of two component measurement error, the EWMA control chart is slower in detecting the shift, especially for smaller values of μ and CV, see for example $\text{ARL}_1 = 368.99$ when $CV = 0.01$ and $\mu = 5$ for $\delta = 0.5$, which is very close to $\text{ARL}_0 = 370$. The reason for this is that the magnitude of shift reduces from 0.5 to 0.0067 (from Equation 5.11), which is almost similar to zero sigma shift in the mean. So, the performance of EWMA chart is greatly affected for the case of small CV and low concentration level of the analyte. The performance of the control chart improves as μ and CV increases. In the extreme case, when we have $CV = 0.5$ and $\mu = 15000$, $\text{ARL}_1 = 8.74$, which is reasonably low and indicates that for high CV and large concentration levels, two component error does not greatly affect the control chart performance. This is because, in this case, $\delta_{tc} = 0.4871$ for $\delta = 0.50$ (from Equation 5.11). Hence the magnitude of shift is not much affected and nor is the chart's performance. Similarly, we can see that, the MDRL and SDRL performances of the EWMA chart are also significantly affected for smaller values of μ and CV.

Table 5.4 gives run length characteristics of the EWMA chart in the presence of two component measurement error for the detection of negative shifts in μ. The results are presented for the case when $\delta = -1.0$ at different

Table 5.1: ARL, MDRL and SDRL of the EWMA Chart in presence of two component measurement error for $\delta = 0.5$ when $ARL_0 = 370$

	μ	CV 0.01	0.05	0.1	0.2	0.3	0.4	0.5
ARL	5	368.18	324.76	230.73	108.71	57.58	36.70	26.23
MDRL		264.00	225.00	161.00	78.00	42.00	27.00	20.00
SDRL		365.02	318.46	227.47	102.39	52.90	32.59	21.60
ARL	10	361.11	233.18	112.78	37.76	21.59	15.56	12.92
MDRL		252.00	163.00	80.00	27.00	16.00	12.00	10.00
SDRL		361.29	228.40	109.36	33.79	17.29	11.85	9.24
ARL	50	287.17	56.19	20.42	11.45	9.77	9.15	9.00
MDRL		200.00	41.00	16.00	9.00	8.00	8.00	8.00
SDRL		279.89	51.93	16.31	7.94	6.39	5.92	5.65
ARL	100	262.46	43.53	17.31	10.66	9.41	9.02	8.86
MDRL		183.00	31.00	13.00	9.00	8.00	8.00	7.00
SDRL		258.42	40.01	13.44	7.20	6.08	5.71	5.51
ARL	1000	249.43	39.75	16.57	10.31	9.38	8.97	8.76
MDRL		173.00	29.00	13.00	8.00	8.00	7.00	7.00
SDRL		247.10	35.11	12.75	6.81	5.93	5.63	5.46
ARL	10000	251.21	40.50	16.38	10.29	9.42	8.94	8.81
MDRL		175.00	30.00	13.00	8.00	8.00	8.00	7.00
SDRL		246.50	36.16	12.69	6.92	5.97	5.52	5.55
ARL	15000	247.46	39.56	16.47	10.34	9.28	8.95	8.67
MDRL		174.00	29.00	13.00	9.00	8.00	7.00	7.00
SDRL		244.15	35.33	12.78	6.80	5.94	5.59	5.43

Table 5.2: ARL, MDRL and SDRL of the EWMA Chart in presence of two component measurement error for $\delta = 1.0$ when $ARL_0 = 370$

		CV						
	μ	0.01	0.05	0.1	0.2	0.3	0.4	0.5
ARL	5	360.99	235.27	106.86	30.95	14.48	9.38	7.00
MDRL		253.00	164.00	75.00	23.00	11.00	8.00	6.00
SDRL		359.69	232.66	102.65	26.23	10.67	5.92	3.97
ARL	10	335.07	108.86	31.87	9.67	6.00	4.68	4.11
MDRL		237.00	77.00	23.00	8.00	5.00	4.00	4.00
SDRL		330.49	104.15	27.70	6.38	3.18	2.19	1.75
ARL	50	182.91	14.49	5.91	3.78	3.35	3.22	3.15
MDRL		126.00	11.00	5.00	3.00	3.00	3.00	3.00
SDRL		179.26	10.79	3.17	1.58	1.30	1.21	1.14
ARL	100	150.82	11.70	5.20	3.61	3.30	3.17	3.13
MDRL		106.00	9.00	5.00	3.00	3.00	3.00	3.00
SDRL		148.03	8.10	2.62	1.45	1.25	1.19	1.16
ARL	1000	141.36	10.60	4.95	3.53	3.26	3.17	3.13
MDRL		98.00	9.00	4.00	3.00	3.00	3.00	3.00
SDRL		139.12	7.21	2.44	1.42	1.26	1.17	1.16
ARL	10000	140.18	10.61	4.94	3.54	3.27	3.17	3.13
MDRL		101.00	9.00	4.00	3.00	3.00	3.00	3.00
SDRL		136.16	7.24	2.44	1.41	1.25	1.19	1.17
ARL	15000	141.49	10.52	4.94	3.52	3.27	3.17	3.12
MDRL		99.00	9.00	4.00	3.00	3.00	3.00	3.00
SDRL		136.27	7.18	2.39	1.41	1.25	1.18	1.16

Table 5.3: ARL, MDRL and SDRL of the EWMA Chart in presence of two component measurement error for $\delta = 1.5$ when $ARL_0 = 370$

		CV						
	μ	0.01	0.05	0.1	0.2	0.3	0.4	0.5
ARL	5	353.74	157.79	52.06	13.49	6.96	4.80	3.83
MDRL		245.00	111.00	38.00	11.00	6.00	4.00	4.00
SDRL		349.48	154.35	47.17	9.69	3.87	2.25	1.61
ARL	10	310.16	53.64	14.14	4.98	3.36	2.78	2.50
MDRL		219.00	39.00	11.00	4.00	3.00	3.00	2.00
SDRL		307.32	48.91	10.21	2.39	1.29	0.95	0.79
ARL	50	114.87	7.09	3.32	2.33	2.15	2.06	2.03
MDRL		81.00	6.00	3.00	2.00	2.00	2.00	2.00
SDRL		109.31	4.12	1.30	0.72	0.63	0.59	0.58
ARL	100	89.25	5.83	3.01	2.25	2.10	2.05	2.02
MDRL		63.00	5.00	3.00	2.00	2.00	2.00	2.00
SDRL		85.30	3.19	1.13	0.68	0.61	0.58	0.57
ARL	1000	80.99	5.45	2.90	2.22	2.09	2.03	2.02
MDRL		57.00	5.00	3.00	2.00	2.00	2.00	2.00
SDRL		77.55	2.87	1.06	0.68	0.60	0.58	0.57
ARL	10000	81.28	5.39	2.89	2.22	2.09	2.03	2.02
MDRL		58.00	5.00	3.00	2.00	2.00	2.00	2.00
SDRL		77.80	2.80	1.06	0.67	0.62	0.59	0.57
ARL	15000	82.00	5.40	2.92	2.21	2.08	2.04	2.01
MDRL		58.00	5.00	3.00	2.00	2.00	2.00	2.00
SDRL		76.80	2.77	1.05	0.66	0.61	0.58	0.57

Table 5.4: ARL, MDRL and SDRL of the EWMA Chart in presence of two component measurement error for $\delta = -1.0$ when $ARL_0 = 370$

		CV						
	μ	0.01	0.05	0.1	0.2	0.3	0.4	0.5
ARL	5	368.18	233.36	108.97	31.38	14.90	9.33	7.04
MDRL		257.00	162.00	76.50	23.00	12.00	8.00	6.00
SDRL		361.94	228.16	105.68	27.23	11.16	5.95	3.96
ARL	10	348.26	113.26	32.88	9.76	5.93	4.71	4.11
MDRL		241.00	80.00	24.00	8.00	5.00	4.00	4.00
SDRL		347.57	109.96	28.46	6.23	3.07	2.18	1.75
ARL	50	226.39	15.66	5.95	3.75	3.33	3.20	3.14
MDRL		157.00	12.00	5.00	3.00	3.00	3.00	3.00
SDRL		223.13	11.49	3.02	1.48	1.22	1.15	1.13
ARL	100	203.69	12.06	5.17	3.54	3.26	3.17	3.13
MDRL		141.00	10.00	5.00	3.00	3.00	3.00	3.00
SDRL		199.62	8.25	2.43	1.34	1.21	1.15	1.12
ARL	1000	194.43	11.06	4.94	3.48	3.26	3.15	3.10
MDRL		135.00	9.00	4.00	3.00	3.00	3.00	3.00
SDRL		188.66	7.31	2.26	1.31	1.18	1.11	1.09
ARL	10000	190.48	10.99	4.92	3.49	3.25	3.13	3.12
MDRL		134.00	9.00	4.00	3.00	3.00	3.00	3.00
SDRL		184.75	7.27	2.21	1.32	1.16	1.12	1.10
ARL	15000	193.48	11.10	4.95	3.53	3.24	3.15	3.12
MDRL		136.00	9.00	4.00	3.00	3.00	3.00	3.00
SDRL		187.30	7.45	2.27	1.35	1.18	1.13	1.10

levels of μ and CV. Comparing results in Tables 5.2 and 5.4 for positive and negative shifts indicate the asymmetric detection behaviour of the EWMA chart in the presence of two component measurement error, particularly at lower values of CV. When CV is small, the EWMA chart performs better for the detection of positive shifts compared to the negative shifts of the same magnitude. As CV increases, the difference between the run length characteristics for the detection of positive and negative shifts are almost negligible.

5.4 Effect of Multiple Measurements

To reduce the effect of measurement error on the performance of the proposed chart, the method suggested by Linna and Woodall (2001), and also implemented by Maravelakis et al. (2004), is used by taking multiple measurements at each sample point for all n observations. Suppose at each sample point we take k measurements for n observations. The EWMA statistic is thus defined as:

$$Q_{tck,t} = \lambda \overline{\overline{Y}}_t + (1 - \lambda)\, Q_{tck,t-1} \tag{5.12}$$

where $\overline{\overline{Y}}_t$ is the average of n observations collected at time t (each observation comprising of k measurements). Similar to the computation of Equations (6.5) and (6.6), the mean and variance of the EWMA statistic (in Equation (5.12)) are given as

$$E(Q_{tck,k}) = \alpha + \beta\mu\sqrt{e^{\sigma_\eta^2}} \tag{5.13}$$

and

$$Var(Q_{t^{tck}}) = \frac{\sigma_{y_{(k)}}}{n}\left(\left(\frac{\lambda}{2-\lambda}\right)\left[1-(1-\lambda)^{2t}\right]\right) \tag{5.14}$$

respectively.

Hence, for the case of k measurements, asymptotic control limits are defined as:

$$UCL_{tck} = \alpha + \beta\mu\sqrt{e^{\sigma_\eta^2}} + L\frac{\sigma_{y_{(k)}}}{\sqrt{n}}\sqrt{\left(\frac{\lambda}{2-\lambda}\right)}$$

and

$$LCL_{tck} = \alpha + \beta\mu\sqrt{e^{\sigma_\eta^2}} - L\frac{\sigma_{y_{(k)}}}{\sqrt{n}}\sqrt{\left(\frac{\lambda}{2-\lambda}\right)}. \tag{5.15}$$

where $\sigma_{y_{(k)}}$ is given as (see Rocke and Lorenzato (1995) and Cocchi and Scagliarini (2007)):

$$\sigma_{y_{(k)}} = \sqrt{\beta^2\sigma^2 e^{\sigma_\eta^2} + \frac{1}{k}(\beta^2\mu^2(e^{\sigma_\eta^2}(e^{\sigma_\eta^2}-1))) + \frac{1}{k}(\beta^2\sigma^2(e^{\sigma_\eta^2}(e^{\sigma_\eta^2}-1))) + \frac{1}{k}\sigma_\epsilon^2}. \tag{5.16}$$

The effect of measurement error is inversely proportional to the number measurements taken at each sample point t (i.e. the performance of the control chart improves as we increase k). The choice of k depends on the cost associated with taking extra measurements and the level of precision required. Similarly to the expression of δ_{tc} given in Equation (5.11), the shift (δ_{tck}) in the process mean level using k measurements is defined as:

$$\delta_{tck} = \frac{\delta}{\sqrt{1 + \frac{\mu^2}{k\sigma^2}(e^{\sigma_\eta^2}-1) + \frac{1}{k}(e^{\sigma_\eta^2}-1) + \frac{\sigma_\eta^2}{k\beta^2\sigma^2 e^{\sigma_\eta^2}}}}. \tag{5.17}$$

For this study, we used $k = 5$ to represent the case of multiple measurements. Figure 5.2 presents curves for δ_{tck}/δ versus CV at different levels of μ. Comparing Figures 5.1 and 5.2, the benefit of using multiple measurements ($k = 5$) at each sample point is shown and this benefit keeps on increasing as we increase k. It is observed that, compared to δ_{tc}/δ, δ_{tck}/δ converges quickly to 1. To examine the effect of k measurements on the run length distribution of the EWMA chart, Table 5.5 gives ARL, MDRL and SDRL of the EWMA chart in the presence of two component error using $k = 5$ measurements at each sample point t for the EWMA statistic in Equation (5.12) using control limits in Equation (5.15). The aim of using k measurements is to reduce the out of control ARL while maintaining the same in-control ARL (i.e. $\text{ARL}_0 = 370$). The run length characteristics are only provided for $\delta = 1.0$, but we observed similar behaviour for other values of δ.

By using multiple measurements, the ability of the control chart to detect shifts has improved significantly. It is clear from the results in Tables 5.2 and

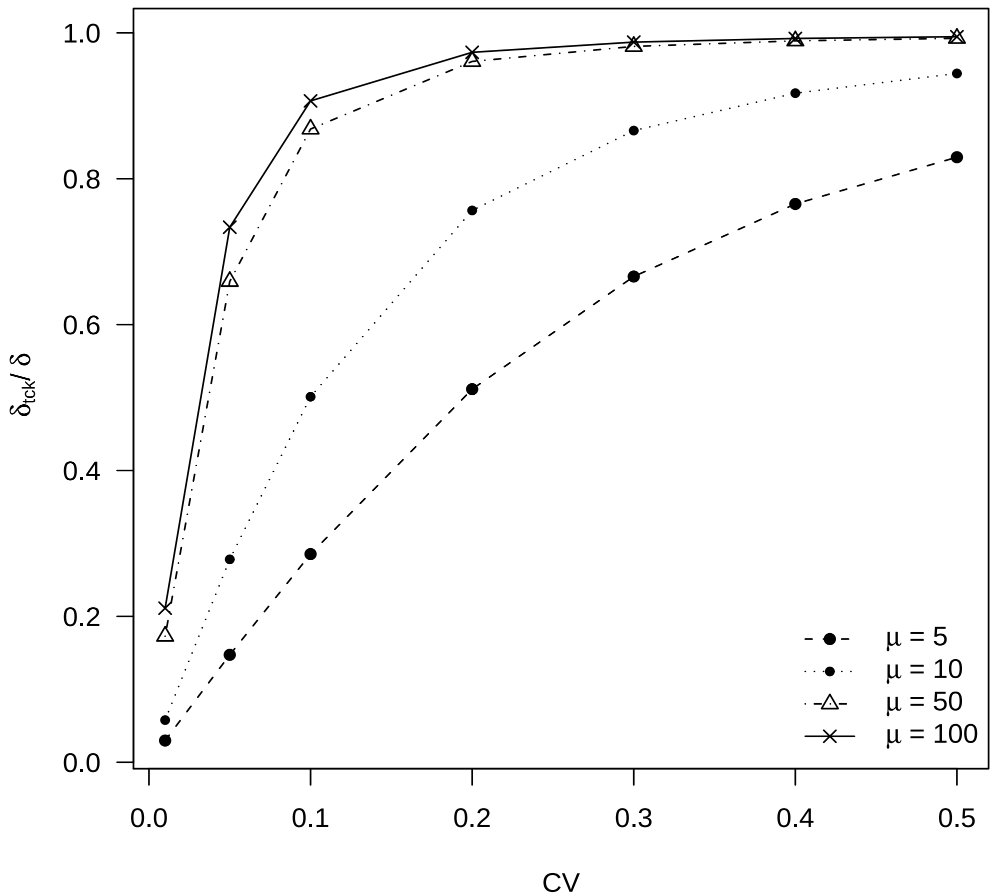

Figure 5.2: Decrease in the magnitude of shift due to two component measurement error using $k = 5$ measurements.

Table 5.5: ARL, MDRL and SDRL of EWMA Chart in presence of two component measurement error using $k = 5$ measurements for $\delta = 1.0$ when $\text{ARL}_o = 370$

		CV						
	μ	0.01	0.05	0.1	0.2	0.3	0.4	0.5
ARL	5	353.18	102.88	27.44	8.50	5.36	4.36	3.89
MDRL		250.00	72.00	21.00	7.00	5.00	4.00	4.00
SDRL		347.64	99.61	23.16	5.30	2.61	1.92	1.61
ARL	10	324.38	31.82	9.15	4.49	3.71	3.42	3.27
MDRL		224.00	24.00	8.00	4.00	3.00	3.00	3.00
SDRL		319.81	27.33	5.72	1.99	1.48	1.30	1.21
ARL	50	152.60	6.10	3.85	3.25	3.16	3.11	3.08
MDRL		106.00	5.00	4.00	3.00	3.00	3.00	3.00
SDRL		150.08	3.23	1.59	1.21	1.15	1.12	1.10
ARL	100	125.54	5.49	3.68	3.24	3.12	3.09	3.10
MDRL		91.00	5.00	3.00	3.00	3.00	3.00	3.00
SDRL		120.69	2.77	1.49	1.21	1.15	1.10	1.12
ARL	1000	116.25	5.22	3.61	3.22	3.12	3.09	3.07
MDRL		83.00	5.00	3.00	3.00	3.00	3.00	3.00
SDRL		110.87	2.59	1.43	1.20	1.12	1.11	1.09
ARL	10000	114.20	5.21	3.64	3.23	3.14	3.10	3.07
MDRL		80.00	5.00	3.00	3.00	3.00	3.00	3.00
SDRL		110.85	2.55	1.48	1.19	1.12	1.11	1.12
ARL	15000	114.70	5.23	3.64	3.21	3.14	3.12	3.09
MDRL		82.00	5.00	3.00	3.00	3.00	3.00	3.00
SDRL		110.18	2.54	1.47	1.19	1.14	1.12	1.10

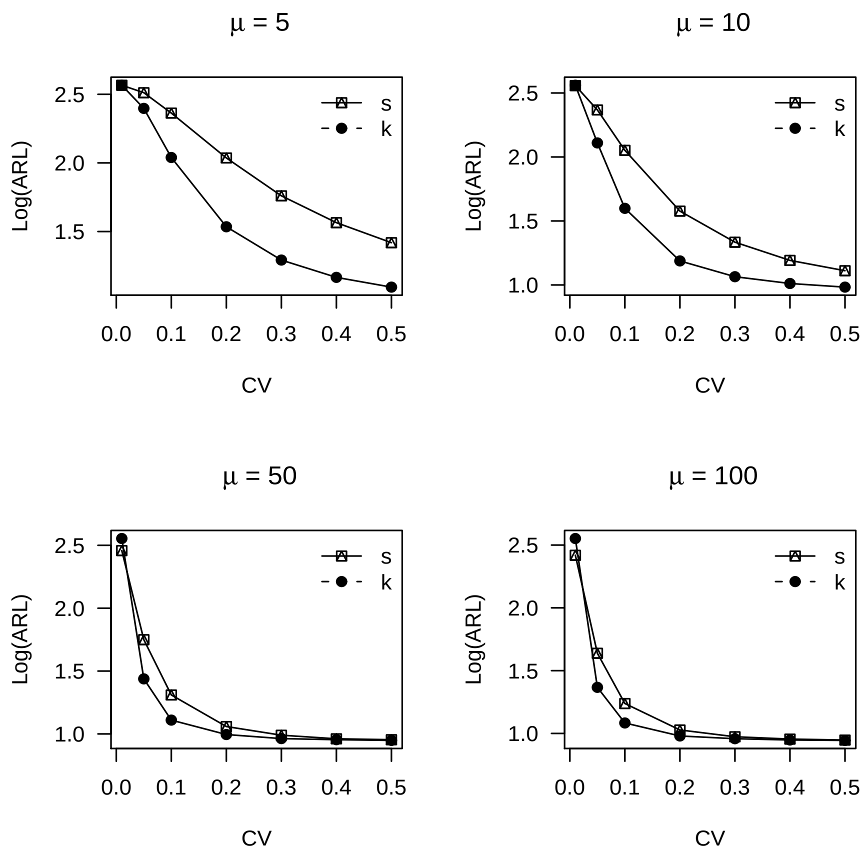

Figure 5.3: ARL performance of EWMA chart in presence of two component measurement error using single and $k = 5$ measurements for $\delta = 0.5$.

5.5 that, in comparison to individual measurement chart, the performance of the k measurements chart is far better. The out of control ARL, MDRL and SDRL have been reduced significantly for all combinations of μ and CV. Figures 5.3-5.5 clearly show the reduction in ARL of the k measurement charts compared to the individual charts for $\delta = 0.5, 1.0$ & 1.5 for several values of μ and CV.

In Figures 5.3-5.5, s and k respectively represent ARL performance for single and k measurement cases. The comparisons revealed that, regardless of the values of μ and CV, the ARL curves for the k measurement EWMA chart

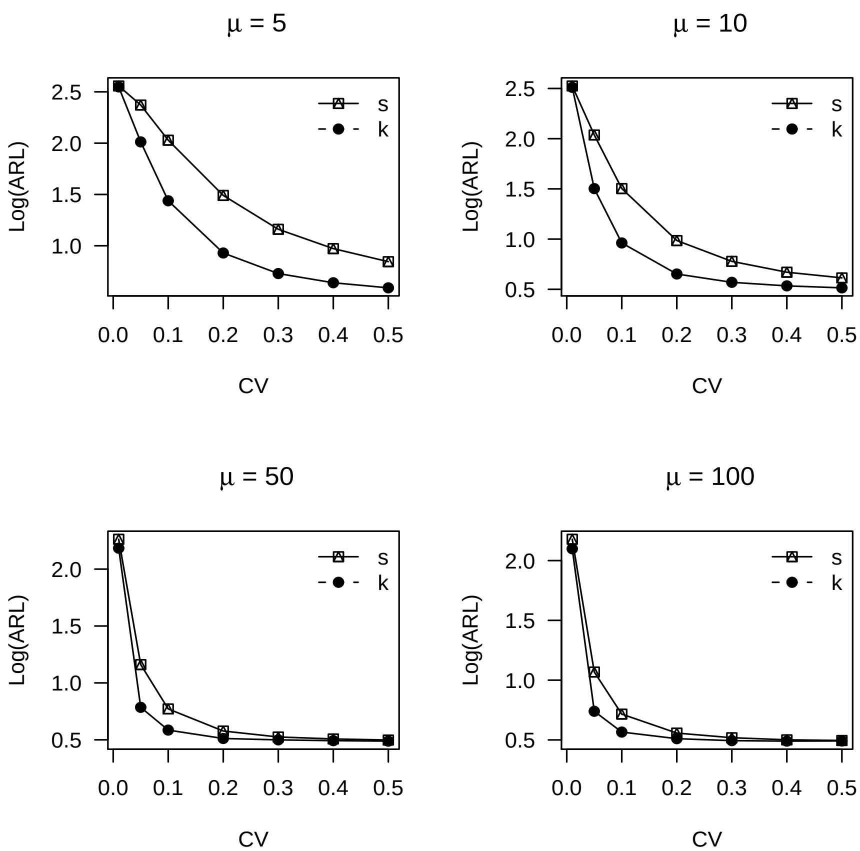

Figure 5.4: ARL performance of EWMA chart in presence of two component measurement error using single and $k = 5$ measurements for $\delta = 1.0$.

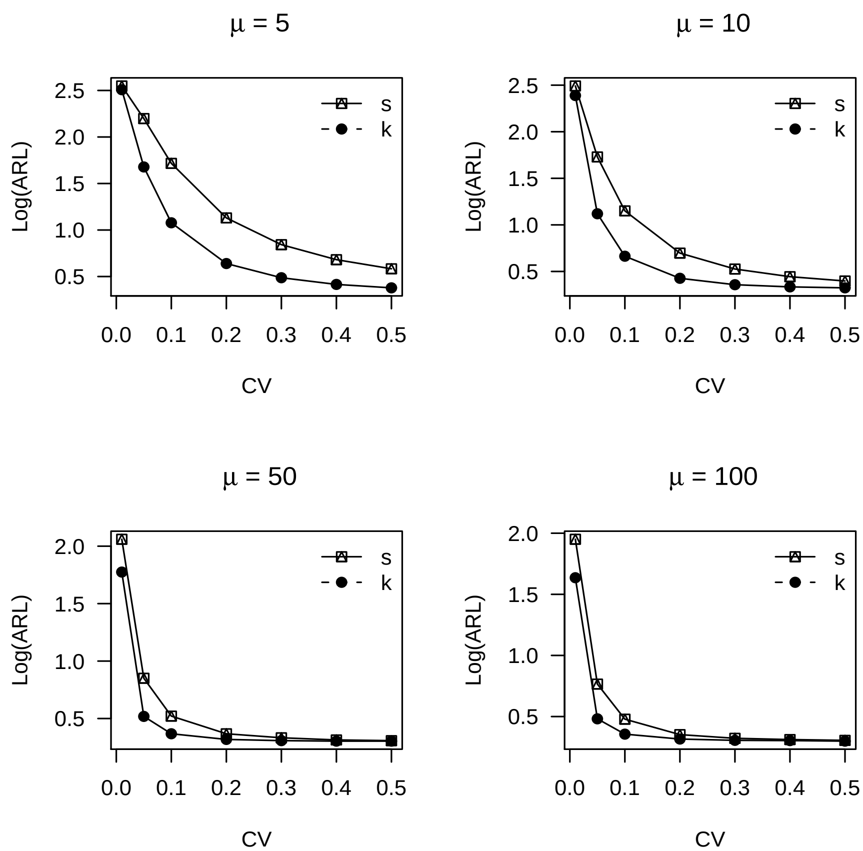

Figure 5.5: ARL performance of EWMA chart in presence of two component measurement error using single and $k = 5$ measurements for $\delta = 1.5$

are always lower compared to the individual measurement EWMA chart, indicating better out of control run length performance. The difference is greater for low CV and reduces as CV increases. Similar patterns are also observed for ARL, MDRL and SDRL using other δ values.

As was described earlier, improvement in EWMA chart performance is expected with an increase in the number of multiple measurements. To to get a better insight, Table 5.6 gives run length characteristics of the EWMA chart using different values of k ranging from 1 to 50 considering $\delta = 1.0$ and $CV = 0.05$ at different concentration levels. Significant reduction in out of control ARL, MDRL and SDRL can be observed from Table 5.6 with an increase in the number of multiple measurements. Note that we have considered an extremely affected case ($CV = 0.05$ and $\delta = 1.0$), we can conclude even better performance for the other cases.

We have seen that increasing k helps in improving the detection ability of the EWMA chart in the presence of two component measurement error. Similarly increasing n, will help in the early detection of out-of-control signals. The detection ability of the chart can be maximized by minimizing $\sigma_{y_{(k)}}/\sqrt{n}$ for appropriate values of n and k using constraint optimization technique. For this purpose, we define a cost function following Linna and Woodall (2001):

$$C_T = c_n n + c_k n(k-1) \tag{5.18}$$

where C_T represents the cost per subgroup, c_n is the cost of a unit of sample size n and c_k is the cost of taking extra measurements on the same unit. Table 5.7 presents the choice of n and k for varying levels of μ and CV by minimizing $\sigma_{y_{(k)}}/\sqrt{n}$ with respect to the above cost function. We used $C_T = 10$, $c_n = 1$ and varied the values of relative cost c_k/c_n from 0.40 to 0.01.

From Table 5.7, we can observe that for the case when $\mu = 5$ and $CV = 0.05$, the process variance σ^2 is far less than the two component measurement error variances σ_η^2 and σ_ϵ^2. Hence, we require large number of measurements to reduce the effect of these measurement errors. As we move to the case of $\mu = 1000$ and $CV = 0.4$, the process variance σ^2 is a lot bigger than the two component measurement error variances σ_η^2 and σ_ϵ^2. Hence for quick detection of shifts, increasing sample size n is more beneficial than taking extra measurements at each unit. Similar pairs of n and k can be obtained for other combinations of μ, CV and two component model parameters $(\alpha, \beta, \sigma_\eta$ and $\sigma_\epsilon)$.

Table 5.6: ARL, MDRL and SDRL of EWMA Chart in presence of two component error for multiple measurements using different values of k for $\delta = 1.0, CV = 0.05$ when $\text{ARL}_0 = 370$

		k						
	μ	1	5	10	15	20	30	50
ARL	5	235.27	102.88	58.73	40.81	31.89	21.92	14.17
MDRL		164.00	72.00	42.00	30.00	24.00	17.00	11.00
SDRL		232.66	99.61	53.91	36.44	27.51	17.74	10.25
ARL	10	108.86	31.82	17.51	12.44	10.14	7.90	6.18
MDRL		77.00	24.00	13.00	10.00	8.00	7.00	5.00
SDRL		104.15	27.33	13.59	8.65	6.73	4.70	3.27
ARL	50	14.49	6.10	4.87	4.41	4.20	3.97	3.78
MDRL		11.00	5.00	4.00	4.00	4.00	4.00	3.00
SDRL		10.79	3.23	2.28	1.95	1.84	1.64	1.53
ARL	100	11.70	5.49	4.51	4.20	4.00	3.85	3.69
MDRL		9.00	5.00	4.00	4.00	4.00	4.00	3.00
SDRL		8.10	2.77	2.08	1.82	1.66	1.58	1.47
ARL	1000	10.60	5.22	4.39	4.07	3.95	3.80	3.65
MDRL		9.00	5.00	4.00	4.00	4.00	4.00	3.00
SDRL		7.21	2.59	1.98	1.74	1.64	1.57	1.45
ARL	10000	10.61	5.21	4.36	4.06	3.97	3.78	3.68
MDRL		9.00	5.00	4.00	4.00	4.00	3.00	3.00
SDRL		7.24	2.55	1.93	1.75	1.69	1.55	1.46
ARL	15000	10.52	5.23	4.40	4.08	3.96	3.77	3.68
MDRL		9.00	5.00	4.00	4.00	4.00	3.00	3.00
SDRL		7.18	2.54	1.95	1.75	1.66	1.53	1.47

Table 5.7: Optimum values for n and k for different combinations of μ and CV at varying values of c_k/c_n

	$\mu=5$,	$CV=0.05$	$\mu=5$,	$CV=0.4$	$\mu=100$,	$CV=0.10$	$\mu=1000$,	$CV=0.05$	$\mu=1000$,	$CV=0.4$
c_k/c_n	n	k	n	k	n	k	n	k	n	k
0.4	2	11	7	2	10	1	7	2	10	1
0.35	1	26	7	2	10	1	7	2	10	1
0.3	1	31	6	3	10	1	6	3	10	1
0.25	1	37	5	5	8	2	5	5	10	1
0.2	2	21	7	3	7	3	5	6	10	1
0.15	2	27	6	5	7	3	6	5	10	1
0.1	2	41	7	5	8	3	7	5	10	1
0.075	2	54	7	6	8	4	7	6	10	1
0.05	2	81	8	6	8	6	7	9	10	1
0.04	3	59	8	7	8	7	7	11	10	1
0.03	3	78	8	9	8	9	7	15	10	1
0.02	3	117	8	13	9	6	8	13	10	1
0.01	4	151	8	26	9	12	8	26	10	1

5.5 Comparison with One Component Error Case

In this section, we compare the effect of two component error on EWMA chart performance with the one component (additive) error case investigated by Maravelakis et al. (2004). The one component model with covariates investigated by Maravelakis et al. (2004) is given as:

$$Z_t = \alpha + \beta X_t + \epsilon \tag{5.19}$$

For the one component error case, the EWMA statistic can be defined as:

$$Q_{oc,t} = \lambda \overline{Z}_t + (1-\lambda)\, Q_{oc,t-1}, \quad Q_{oc,0} = \alpha + \beta\mu \tag{5.20}$$

and the control limits are thus provided as (see Maravelakis et al. (2004)):

$$\begin{aligned} UCL &= \alpha + \beta\mu + L\sqrt{\left(\frac{\lambda}{2-\lambda}\right)\frac{\beta^2\sigma^2 + \sigma_\epsilon^2}{n}} \\ LCL &= \alpha + \beta\mu - L\sqrt{\left(\frac{\lambda}{2-\lambda}\right)\frac{\beta^2\sigma^2 + \sigma_\epsilon^2}{n}} \end{aligned} \tag{5.21}$$

We can see that, by setting $\sigma_\eta = 0$, Equations (5.1, 5.3 and 5.9) correspond to one component error model, EWMA statistics and control limits for the single measurement chart, investigated by Maravelakis et al. (2004). For comparison purposes, run length characteristics of the Maravelakis et al. (2004) charts has also been computed using similar simulation routines by fixing the parameter values as were used earlier for the two component error case. The results have been reported in Tables 5.8 and 5.9 for single and multiple measurement charts considering $\delta = 1.0$.

We can observe from Tables 5.2, 5.5, 5.8 and 5.9 that a two component error model has a more adverse effect on EWMA chart performance compared to a one component error case. The difference in the out of control run length characteristics for both the approaches (one and two component error cases) seems to be smaller for low concentration levels ($\mu = 5$ and 10). However, we can observe significant differences for higher concentration levels ($\mu > 10$), particularly for low values of CV. This is also consistent with the findings of Rocke and Lorenzato (1995), as additive error only has a significant effect at low concentrations and this effect reduces with an increase in concentration level. The comparison has been presented for $\delta = 1.0$, but similar patterns have been observed for other δ values as well. Note also that for the results of two component error case we set $\sigma_\eta = 0.1032$, we can expect a greater difference in the out of control run length characteristics of the two approaches with an increase in the value of σ_η.

Table 5.8: ARL, MDRL and SDRL of EWMA Chart in presence of one component measurement error for $\delta = 1.0$ when $\text{ARL}_0 = 370$

		CV						
	μ	0.01	0.05	0.1	0.2	0.3	0.4	0.5
ARL	5	360.98	231.35	106.18	30.73	14.40	9.36	7.01
MDRL		252.00	160.00	76.00	23.00	11.00	8.00	6.00
SDRL		359.86	227.80	101.56	26.16	10.56	6.09	3.97
ARL	10	335.51	107.20	30.59	9.23	5.76	4.56	4.01
MDRL		237.00	76.00	23.00	8.00	5.00	4.00	4.00
SDRL		329.11	101.42	25.62	5.76	2.95	2.06	1.64
ARL	50	103.58	6.97	4.05	3.25	3.13	3.09	3.06
MDRL		73.00	6.00	4.00	3.00	3.00	3.00	3.00
SDRL		99.91	3.84	1.70	1.19	1.11	1.12	1.11
ARL	100	30.98	4.01	3.27	3.07	3.04	3.04	3.01
MDRL		23.00	4.00	3.00	3.00	3.00	3.00	3.00
SDRL		26.38	1.68	1.22	1.09	1.09	1.06	1.08
ARL	1000	3.27	3.04	3.01	3.01	3.02	3.01	2.99
MDRL		3.00	3.00	3.00	3.00	3.00	3.00	3.00
SDRL		1.20	1.10	1.07	1.06	1.06	1.06	1.06
ARL	10000	3.01	3.01	3.01	3.02	3.02	3.02	3.01
MDRL		3.00	3.00	3.00	3.00	3.00	3.00	3.00
SDRL		1.08	1.06	1.09	1.07	1.07	1.07	1.07
ARL	15000	3.00	3.02	3.03	2.99	3.00	3.01	3.01
MDRL		3.00	3.00	3.00	3.00	3.00	3.00	3.00
SDRL		1.06	1.07	1.07	1.06	1.05	1.06	1.04

Table 5.9: ARL, MDRL and SDRL of EWMA Chart in presence of one component measurement error using $k = 5$ measurements for $\delta = 1.0$ when $\text{ARL}_0 = 370$

		CV						
	μ	0.01	0.05	0.1	0.2	0.3	0.4	0.5
ARL	5	330.60	88.45	24.65	7.99	5.22	4.26	3.81
MDRL		230.00	63.00	19.00	7.00	5.00	4.00	3.00
SDRL		331.88	83.36	20.33	4.77	2.57	1.82	1.56
ARL	10	249.78	24.64	8.00	4.23	3.59	3.33	3.22
MDRL		174.00	19.00	7.00	4.00	3.00	3.00	3.00
SDRL		244.73	20.64	4.81	1.84	1.43	1.26	1.18
ARL	50	24.50	3.81	3.20	3.06	3.06	3.04	3.01
MDRL		18.00	4.00	3.00	3.00	3.00	3.00	3.00
SDRL		20.12	1.55	1.16	1.11	1.08	1.06	1.06
ARL	100	8.00	3.24	3.05	3.03	3.02	3.00	3.01
MDRL		7.00	3.00	3.00	3.00	3.00	3.00	3.00
SDRL		4.80	1.20	1.09	1.08	1.07	1.06	1.06
ARL	1000	3.07	3.01	3.04	3.01	3.01	3.03	3.00
MDRL		3.00	3.00	3.00	3.00	3.00	3.00	3.00
SDRL		1.09	1.07	1.08	1.04	1.05	1.08	1.06
ARL	10000	3.01	3.04	3.01	3.02	3.02	3.04	3.02
MDRL		3.00	3.00	3.00	3.00	3.00	3.00	3.00
SDRL		1.06	1.08	1.05	1.07	1.06	1.08	1.07
ARL	15000	3.01	2.99	3.03	3.00	3.02	3.02	3.01
MDRL		3.00	3.00	3.00	3.00	3.00	3.00	3.00
SDRL		1.07	1.04	1.08	1.06	1.07	1.07	1.07

5.6 Effect of Two Component Model Parameters

In the previous sections, run length properties of the EWMA chart in the presence of two component measurement error are evaluated for fixed values of two component model parameters, i.e. we used $\alpha = 11.51, \beta = 1.524, \sigma_\eta = 0.1032$ and $\sigma_\epsilon = 5.698$. In this section, we will see how the change in these parameters affects the run length performance of the EWMA chart.

Effect of α:

We noticed that changing α does not effect the run length performance of the EWMA chart.

Effect of β:

Table 5.10 presents run length characteristics for the case when all the parameters remain fixed, except β. We used $\alpha = 11.51, \sigma_\eta = 0.1032$ and $\sigma_\epsilon = 5.698$ and varied the values of β from 1 to 7. The run length characteristics are evaluated at different levels of μ considering $\delta = 0.5$ and $CV = 0.1$. We can observe from the results in Table 5.10 that the detection ability of the chart improves with an increase in the value of β, particularly at small concentration levels ($\mu \leq 100$).

Effect of σ_η:

Table 5.11 presents run length characteristics for the case when all the parameters remain fixed, except σ_η. We used $\alpha = 11.51, \beta = 1$ and $\sigma_\epsilon = 2$ and varied the values of σ_η from 0.01 to 0.15. The run length characteristics are evaluated at different levels of μ considering $\delta = 0.5$ and $CV = 0.1$. We can observe from the results in Table 5.11 that the detection ability of the chart diminishes with an increase in the value of σ_η, particularly at high concentration levels. This is expected, as the multiplicative error (η) is known to dominate at higher concentration levels (Currie (1968); Hubaux (1970); Rocke et al. (2003)).

Effect of σ_ϵ:

Table 5.12 presents run length characteristics for the case when all the parameters remain fixed, except σ_ϵ. We used $\alpha = 11.51, \beta = 1$ and $\sigma_\eta = 0.1032$ and varied the values of σ_ϵ from 0.5 to 6. The run length characteristics are evaluated at different levels of μ considering $\delta = 0.5$ and $CV = 0.1$. We can observe from the results in Table 5.12 that the detection ability of the chart diminishes with an increase in the value of σ_ϵ, particularly at low concentration levels ($\mu \leq 100$). This is expected, as the additive error (ϵ) is known to dominate at lower (near zero) concentration levels (Currie (1968); Hubaux (1970); Rocke et al. (2003)).

Table 5.10: ARL, MDRL and SDRL of EWMA Chart in presence of two component measurement error for $\delta = 0.5$ at different levels of β and μ when $\alpha = 11.51, \sigma_\eta = 0.1032, \sigma_\epsilon = 5.698, CV = 0.1$ and $\text{ARL}_0 = 370$

		β						
	μ	1	2	3	4	5	6	7
ARL	5	299.58	184.01	114.84	77.90	56.52	45.23	36.97
MDRL		207.00	129.00	82.00	55.00	41.00	33.00	27.00
SDRL		297.85	180.58	108.53	73.71	52.06	41.07	32.74
ARL	10	184.82	77.21	44.59	32.27	26.39	23.37	21.44
MDRL		131.00	55.00	32.00	24.00	20.00	17.00	16.00
SDRL		181.66	72.06	40.54	28.15	22.35	19.65	17.47
ARL	50	26.49	18.67	17.52	16.81	16.65	16.38	16.35
MDRL		20.00	14.00	14.00	13.00	13.00	13.00	13.00
SDRL		22.70	14.86	13.63	12.94	12.93	12.62	12.73
ARL	100	18.91	17.06	16.66	16.50	16.34	16.36	16.39
MDRL		14.00	13.00	13.00	13.00	13.00	13.00	13.00
SDRL		15.12	13.34	12.73	12.64	12.68	12.68	12.65
ARL	1000	16.61	16.10	16.65	16.39	16.24	16.08	16.41
MDRL		13.00	13.00	13.00	13.00	13.00	12.00	13.00
SDRL		13.00	12.26	12.86	12.54	12.52	12.32	12.57
ARL	10000	16.43	16.31	16.48	16.33	16.40	16.50	16.46
MDRL		13.00	13.00	13.00	13.00	13.00	13.00	13.00
SDRL		12.90	12.64	12.83	12.63	12.53	12.93	12.97
ARL	15000	16.48	16.60	16.38	16.37	16.51	16.39	16.17
MDRL		13.00	13.00	13.00	13.00	13.00	13.00	13.00
SDRL		12.55	12.88	12.68	12.61	12.93	12.65	12.33

Table 5.11: ARL, MDRL and SDRL of EWMA Chart in presence of two component measurement error for $\delta = 0.5$ at different levels of σ_η and μ when $\alpha = 11.51, \beta = 1.0, \sigma_\epsilon = 2, CV = 0.1$ and $\text{ARL}_0 = 370$

		σ_η						
	μ	0.01	0.015	0.025	0.05	0.075	0.1	0.15
ARL	5	121.21	121.30	122.03	119.63	121.36	122.06	125.94
MDRL		86.00	84.00	86.00	86.00	86.00	86.00	89.00
SDRL		115.63	117.34	118.13	113.21	115.24	116.04	121.09
ARL	10	41.09	41.63	41.69	42.78	44.40	47.44	53.82
MDRL		30.00	31.00	31.00	31.00	32.00	34.00	39.00
SDRL		36.98	36.59	37.23	37.90	39.33	43.13	49.91
ARL	50	9.62	9.74	10.06	11.51	13.88	17.15	25.64
MDRL		8.00	8.00	8.00	9.00	11.00	13.00	19.00
SDRL		6.25	6.23	6.58	8.00	10.00	13.42	21.68
ARL	100	8.80	8.84	9.05	10.52	12.78	15.97	24.92
MDRL		7.00	7.00	8.00	9.00	10.00	13.00	18.00
SDRL		5.48	5.51	5.66	7.09	9.11	12.22	21.20
ARL	1000	8.43	8.64	8.82	10.30	12.59	15.76	24.67
MDRL		7.00	7.00	7.00	8.00	10.00	12.00	18.00
SDRL		5.17	5.36	5.47	6.91	8.86	12.16	20.92
ARL	10000	8.46	8.47	8.90	10.27	12.64	15.75	25.08
MDRL		7.00	7.00	7.00	9.00	10.00	12.00	19.00
SDRL		5.21	5.22	5.63	6.83	9.13	11.99	21.10
ARL	15000	8.39	8.49	8.87	10.09	12.61	15.70	24.93
MDRL		7.00	7.00	7.00	8.00	10.00	12.00	19.00
SDRL		5.04	5.19	5.53	6.70	8.98	12.22	21.05

Table 5.12: ARL, MDRL and SDRL of EWMA Chart in presence of two component measurement error for $\delta = 0.5$ at different levels of σ_ϵ and μ when $\alpha = 11.51, \beta = 1.0, \sigma_\eta = 0.1032, CV = 0.1$ and $\text{ARL}_0 = 370$

		σ_ϵ						
	μ	0.5	1	2	3	4	5	6
ARL	5	24.17	48.09	122.97	195.78	241.81	279.86	301.49
MDRL		18.00	35.00	86.00	137.00	168.00	194.00	214.00
SDRL		20.19	44.11	120.41	190.30	234.97	277.20	296.19
ARL	10	18.11	23.99	47.43	84.03	122.14	158.78	196.15
MDRL		14.00	18.00	34.00	59.00	86.00	112.00	138.00
SDRL		14.38	20.24	43.12	79.21	118.13	153.34	193.27
ARL	50	16.44	16.63	17.50	19.15	21.22	24.14	27.34
MDRL		13.00	13.00	14.00	15.00	16.00	18.00	21.00
SDRL		12.71	12.71	13.72	15.54	17.10	19.92	23.16
ARL	100	16.53	16.42	16.81	17.02	17.69	18.11	19.22
MDRL		13.00	13.00	13.00	13.00	14.00	14.00	15.00
SDRL		12.68	12.43	13.09	12.86	14.05	14.17	15.34
ARL	1000	16.44	16.27	16.42	16.36	16.46	16.48	16.42
MDRL		13.00	13.00	13.00	13.00	13.00	13.00	13.00
SDRL		12.64	12.47	12.49	12.61	12.67	12.53	12.56
ARL	10000	16.14	16.58	16.28	16.26	16.39	16.43	16.43
MDRL		13.00	13.00	13.00	13.00	13.00	13.00	13.00
SDRL		12.42	12.66	12.63	12.69	12.63	12.74	12.77
ARL	15000	16.43	16.56	16.64	16.29	16.39	16.37	16.54
MDRL		13.00	13.00	13.00	13.00	13.00	13.00	13.00
SDRL		12.57	12.88	13.08	12.70	12.53	12.65	12.85

5.7 Conclusions

This chapter examined the performance of the EWMA location chart in the presence of two component error. In the presence of measurement error, the exact performance of EWMA chart may be significantly different from that of expected performance. The run length characteristics show that EWMA chart performance is extremely affected for small CV and low concentration levels of an analyte. For high CV and large concentration levels, the EWMA chart has performed reasonably well. It has been shown that two component measurement error effect can be reduced by using multiple measurements at each sample point. The two component error model has shown a more adverse effect on EWMA chart performance compared to the one component error case, particularly for higher concentration levels ($\mu > 10$) and low values of CV. The results presented in this study are based on the assumption that two component model parameters $(\alpha, \beta, \sigma_\epsilon, \sigma_\eta)$ are known. The estimation of these parameters will also have an effect on control chart performance.

Chapter 6

Enhancing the Performance of CUSUM Dispersion Chart

Researchers have implemented different run rules to increase the sensitivity of Shewhart, CUSUM and EWMA control charts for the detection of small shifts in process location. However, for the monitoring of process dispersion, the use of such rules has been limited to Shewhart charts. This study proposes the implementation of sensitizing rules in CUSUM dispersion charts to enhance their ability to detect smaller changes in process dispersion. The performance of the proposed schemes is evaluated and compared with the simple dispersion CUSUM scheme, the EWMS chart, the M-EWMS chart and the COMB chart, in terms of run length characteristics such as average run length (ARL) and standard deviation of the run length distribution (SDRL). Control chart coefficients to set the ARL at the desired level are also provided. Two numerical examples are given to illustrate the application of the proposed schemes on practical data sets. This chapter is based on Abbasi et al. (2012a).

6.1 Introduction

For a control chart, a process is declared to be out-of-control whenever a point lies outside the control limits, which are usually set at a distance of three sigma from the centre line. To increase the sensitivity of the chart for the detection of small shifts, some additional rules have been proposed by researchers that use an additional set of limits called the warning limits. These warning limits are usually set at a distance of one or two sigma from the centre line - e.g. see Klein (2000), Khoo (2004), Koutras et al. (2007) and Antzoulakos and Rakitzis (2008). Some suggested additional rules are: (a) two out of three consecutive points outside the two sigma warning limits but still inside the control limits; (b) four out of five consecutive points beyond the one sigma warning limits; (c) a run of eight consecutive points on one side of the center line; (d) six points in a row steadily increasing or decreasing; (e) fourteen points in a row alternating up and down. The application of sensitizing rules causes an increase in false alarm rates, which can be compensated for by making appropriate adjustments to the control limits. Although these rules add complexity in the control chart design but can be very useful for the quick detection of small shifts in process parameters.

The application of the sensitizing rules was confined mainly to Shewhart type control charts for a long time and the literature on the use of these rules with CUSUM and EWMA control structures is very limited. Westgard et al. (1977) studied some control rules using combined Shewhart-CUSUM structures and demonstrated the superiority of their approach to the Shewhart chart but ignored any comparison with the CUSUM chart. Also, their control rules considered only one point at a time for testing an out-of-control situation. The false alarm rates of their control rules were not fixed at a pre-specified level, which makes the comparison among different control rules/schemes difficult. Recently, Riaz et al. (2011) and Abbas et al. (2011) have extended this approach to CUSUM and EWMA type charts for monitoring the location parameter. Some researchers also investigated the effects of run rules on the performance of Shewhart type dispersion control charts. Acosta-Mejia and Pignatiello (2008) and Acosta-Mejia and Pignatiello (2009) analyzed the performance of Shewhart type dispersion R and S charts supplemented with some m out of m rules (m out of m rules indicate a process to be out-of-control if all the recent m values lie outside the warning limits). They investigated the performance of both the charts using the m out of m

rule alone and charts that combine 1 out of 1 and m out of m rules. They recommended the use of classical charts that combined the 1 out of 1 and the m out of m rules using $m = 9$ or 10. Antzoulakos and Rakitzis (2010) investigated the performance of Shewhart S chart supplemented with r out of m rules. They showed that the S chart using the r out of m rule outperformed the simple S chart and recommended the use of a one-sided S chart with a 2 out of 5 rule for efficient detection of shifts in process dispersion. This study introduces the use of these sensitizing rules for the CUSUM dispersion chart to enhance its ability to detect small changes in process dispersion. Particularly, we will implement some of the r out of m run rule schemes with the CUSUM chart for dispersion parameter following the work of Klein (2000), Khoo (2004) and Antzoulakos and Rakitzis (2008), Riaz et al. (2011) and Abbas et al. (2011) and will compare their performance with the simple dispersion CUSUM scheme in terms of different run length characteristics. This chapter will propose the sensitizing rules based design structure of CUSUM chart for the monitoring of dispersion parameter.

6.2 Proposal for the CUSUM dispersion control chart

Since the introduction of CUSUM charts by Page (1954), many researchers have examined these charts from different perspectives - see for example Brook and Evans (1972), North (1982), Reynolds and Arnold (1990), Hawkins (1981), Hawkins (1993), Jones et al. (2004) and Chatterjee and Qiu (2009). CUSUM charts are widely used for the efficient monitoring of internal quality control parameters and their use in analytical laboratories has been emphasized by many researchers, including Funk et al. (1995), Mullins (2003) and Hibbert (2007). Kateman and Buydens (1993) mentioned "The CUSUM technique is a somewhat simplified variant of sequential analysis. Therefore the CUSUM chart seems more suitable to the needs of control in laboratory". CUSUM charts are effective even with rational subgroups of size one, which makes them an attractive option for many applications in chemical and process industries (see Montgomery (2009)). The book by Hawkins and Olwell (1998) includes a comprehensive description of the construction of CUSUM charts. For a CUSUM chart, the deviations from the target value of the parameter are accumulated in the upward and downward directions separately, using two different statistics: one for the upward shift and the other for the downward shift. The values of these two statistics are calculated for each sample and are plotted against time on a chart which has control limits superimposed. The CUSUM control chart indicates an out-of-control signal when any point falls beyond the control limits (for details see Alwan (2000), Ryan (2000) and Montgomery (2009)).

Hawkins (1981) adapted the CUSUM chart to monitor process dispersion and later (Hawkins (1993)) suggested joint monitoring of location and dispersion parameters using CUSUM charts. For a normally distributed process characteristic of interest X having mean or process target value μ_0 and known standard deviation σ_0 , Hawkins (1981, 1993) used the standardized quantity $V_t = (\sqrt{|Y_t|} - 0.822)/0.349$ to monitor dispersion of individual observations, where $Y_t = (X_t - \mu_0)/\sigma_0$. The idea was to create a statistic which would have an approximately standard normal distribution when the process was in-control (assuming a normal parent distribution) and would be sensitive to changes in process variation. The V_t statistic accomplishes this and has the desirable property of having an approximate normal distribution when X_t comes from a heavy tailed distribution such as Student's t or Laplace distribution – for details see Hawkins (1981) and Montgomery (2009). The CUSUM dispersion procedure proposed by Hawkins (1981) works by accumulating the upward and downward deviations of Y in the form of two statistics S^+ and S^-:

$$\begin{aligned} S_t^+ &= max[0, V_t - k - S_{t-1}^+] \\ S_t^- &= max[0, -V_t - k + S_{t-1}^-] \end{aligned} \tag{6.1}$$

where k is known as the reference/allowance/slack value and is often chosen to be about half of the shift (in standard units) we want to detect quickly.

The statistics S^+ and S^- (known as the upper and the lower CUSUM) are initially set to zero (i.e. $S_0^+ = S_0^- = 0$). The values of S^+ and S^- are calculated for each sample and plotted against time. The process is said to be out-of-control for any S^+ or S^- exceeds the control (action) limit (h). For more details, see Hawkins (1981, 1993) and Montgomery (2009). We will refer to the CUSUM control chart structure given in (6.1) as the simple dispersion CUSUM control scheme.

The control structure given in (6.1) can also be used to monitor process location but Hawkins (1981, 1993) and Yeh et al. (2005) suggested using V_t for the monitoring of process dispersion due to the sensitive behavior of this statistic for the detection of disturbances in process dispersion parameter. Hawkins (1993) suggested plotting both the location CUSUM and the scale CUSUM on the same graph. Out-of-control signals from both the CUSUMs indicate a shift in process location, but a signal from only the scale CUSUM indicates a shift in the standard deviation. The purpose of this study is to investigate the affect of run rules on the run length behavior of the CUSUM dispersion chart. Hence, we are only considering shifts in process dispersion of the observed quality characteristics of interest X. The process is assumed to be in-control for $X \sim N(\mu_0, \sigma_0)$ and out-of-control when $X \sim N(\mu_0, \lambda\sigma_0)$, where $\lambda \neq 1$ represents a shift in the in-control process standard deviation (σ_0). Without loss of generality we considered $\mu_0 = 0$ and $\sigma_0 = 1$ to represent the state of an in-control process.

In the simple dispersion CUSUM scheme, a process is declared to be out-of-control when any point falls outside the control limits. This simple rule does not indicate an out-of-control signal if there is a non-random pattern in the data such as consecutive points that fall close to the control limits or that fall in particular zones, which results in a loss of efficiency, particularly for smaller shifts (cf. Klein (2000)). The sensitivity of the simple dispersion CUSUM scheme (6.1) can be increased by implementing sensitizing rules which can indicate that a process is out-of-control, even when all values of S^+ and S^- lie within the control limits. These rules can be found in Alwan (2000), Klein (2000), Khoo (2004), Antzoulakos and Rakitzis (2008) and Montgomery (2009). We propose two new schemes for the CUSUM dispersion control chart which utilize sensitizing rules. Both these schemes use a warning limit (w) and an action limit (h), defined as:

- Action Limit (h): A threshold level for the value of the CUSUM charting statistic beyond which we declare the process as out-of-control.
- Warning Limit (w): A level for the value of the CUSUM charting statistic beyond which (but not crossing h) some pattern of consecutive points indicate an out-of-control situation.

Using these definitions, we propose the following two schemes for the CUSUM dispersion chart:

Scheme I: A process is said to be out-of-control if one of the following conditions is satisfied:

- Any point of either S^+ or S^- falls outside h.
- Any two consecutive points of either S^+ or S^- fall between w and h.

Scheme II: A process is said to be out of control if one of the following conditions is satisfied:

- Any point of either S^+ or S^- falls outside h.
- Two out of three consecutive points of either S^+ or S^- fall between w and h,

for S^+ and S^- as defined in (6.1), and h and w are chosen to give the desired ARL_0.

6.3 Performance Evaluation

To evaluate the performance of control charts, the average run length (ARL), the mean of the run length distribution, is the most important and widely used measure. The performance can be evaluated by two ARL values:

- ARL_0: the average number of samples until an out-of-control signal is detected by a control chart when the process standard deviation is in-control.

- ARL_1: the average number of samples until an out-of-control signal is detected by a control chart when the process standard deviation is shifted to an out-of-control value.

Large values of ARL_0 and small values of ARL_1 are preferable for any control chart setting. Different methods of computing the ARL of CUSUM charts have been proposed in the literature: Brook and Evans (1972) used a Markov-chain approach, Lucas and Crosier (1982) adopted an integral equation approach, and Siegmund (1985) proposed a method based on solving ARL equations. Monte Carlo simulation methods have also been adopted by different researchers, including Hawkins (1981), Li and Wang (2010) and Riaz et al. (2011). In this study, the Markov chain approach is used to approximate the run length of the proposed CUSUM schemes.

The Markov chain approach for the CUSUM chart has been firstly proposed by Ewan and Kemp (1960) for the basic 1 out of 1 decision rule. This approach is further used by many researchers including Brook and Evans (1972), Bohm and Hackl (1996) and Chang and Wu (2011). The use of Markov chains for the CUSUM control charts, supplemented with different run rules, is a bit complicated since the history of the CUSUM statistics must be kept. Fu et al. (2003) worked on this problem and proposed a Markov chain approach for computing the run length distribution of different control charting mechanisms (including the CUSUM charts) with simple or compound rules. In this study, we use Fu et al. (2003)'s approach with necessary adjustments to approximate the run length distribution of the proposed CUSUM schemes. The details regarding the Markov chain representation, used to obtain the run length characteristics of the proposed CUSUM schemes, can be seen in Appendix C (or Abbasi et al. (2012a)).

The design of the CUSUM charts supplemented with run rules Schemes I and II depends on the parameters k, w and h. Once k is selected, we can choose w and h for a desired in-control ARL_0. For a given ARL_0, the choice of k minimizes the ARL_1 of the CUSUM charts for detecting a shift of size λ (Montgomery (2009)). The most widely used values of k are 0.25 and 0.5, which have also been used in this study. These choices of k help in efficient detection of smaller shifts in process dispersion. To get a better insight of the performance of the proposed schemes, the standard deviation of the run length distribution is also provided as well as the ARL. These run length measures will help in studying the behavior of the run length distribution.

A summary of the run length characteristics of the proposed CUSUM schemes (i.e. Scheme I, Scheme II) and the simple dispersion CUSUM scheme is provided in Tables 6.1-6.3. In these tables, ARL denotes the average run length and SDRL denotes the standard deviation of the run length distribution. In each table, $\lambda = 1$ indicates that process dispersion parameter is in-control, while $\lambda > 1$ refers to the out-of-control situation. For a fixed ARL_0, the control scheme which minimizes the ARL_1 for a particular magnitude of shift will be regarded as better than others.

For the two proposed schemes the values of h and w depend on the selected values of k and ARL_0. However, fixing k and ARL_0 does not uniquely determine the values of h and w. In fact, for fixed k and ARL_0 there are many possible combinations of h and w which correspond to different relative weights put on the two ways of detecting out-of-control situations - see Tables 6.1-6.2. At one extreme, setting $h = w$ corresponds to the simple dispersion CUSUM chart with no additional sensitizing rule, whereas at the other extreme, setting $h = \infty$ results in a chart where the out-of-control situation is only identified by the sensitizing rules. For our proposed run rules schemes, we have observed that for a fixed value of k and ARL_0, the ARL_1 reduces as the value of h increases and w decreases, particularly for small and moderate values of λ. The choice of infinity for h is the most attractive choice in terms of ease and optimizing the ARL_1.

Table 6.1: RL characteristics of the proposed dispersion CUSUM scheme I

h	w	RL Properties	λ 1.00	1.25	1.50	1.75	2.00	2.50	3.00	4.00
						$k = 0.25, \text{ARL}_0 = 120$				
6.642	4.89	ARL	121.18	34.12	17.22	12.05	9.47	7.06	5.85	4.69
		SDRL	110.78	27.03	11.46	7.43	5.53	3.91	3.17	2.57
8.864	4.337	ARL	120.76	29.61	15.81	11.17	8.94	6.87	5.88	4.85
		SDRL	110.89	24.03	10.92	6.87	5.23	3.73	3.06	2.51
∞	4.198	ARL	120.81	28.30	15.34	10.85	8.83	6.74	5.78	4.81
		SDRL	115.19	22.70	10.65	6.66	5.22	3.69	3.05	2.48
						$k = 0.25, \text{ARL}_0 = 200$				
7.511	5.818	ARL	201.46	43.66	20.54	13.87	10.88	7.90	6.53	5.15
		SDRL	182.59	33.78	13.70	8.24	6.04	4.18	3.43	2.73
8.895	5.387	ARL	201.82	39.92	19.24	13.30	10.42	7.78	6.56	5.29
		SDRL	184.60	31.90	12.66	7.90	5.80	4.02	3.33	2.64
∞	5.098	ARL	202.42	36.92	18.46	12.67	9.95	7.58	6.43	5.28
		SDRL	188.46	29.19	12.31	7.72	5.54	3.98	3.28	2.64
						$k = 0.50, \text{ARL}_0 = 120$				
4.108	2.748	ARL	119.57	30.52	13.71	8.28	6.00	3.75	2.85	1.84
		SDRL	115.55	26.72	10.57	5.66	3.67	1.81	1.22	0.51
4.848	2.585	ARL	119.70	28.79	13.01	8.07	5.97	3.89	2.93	2.01
		SDRL	116.67	24.99	9.92	5.32	3.55	1.83	1.10	0.49
∞	2.449	ARL	119.96	26.08	12.26	7.91	5.78	3.85	3.05	2.25
		SDRL	116.92	22.52	9.40	5.21	3.35	1.73	1.04	0.43
						$k = 0.50, \text{ARL}_0 = 200$				
4.927	3.151	ARL	201.28	40.26	17.48	10.76	8.06	5.49	4.34	3.24
		SDRL	193.33	35.27	13.83	7.44	5.28	3.18	2.38	1.65
5.527	3.018	ARL	200.3	37.63	16.56	10.57	7.91	5.56	4.41	3.33
		SDRL	189.26	33.21	12.96	7.51	5.07	3.16	2.35	1.59
∞	2.937	ARL	200.11	36.55	16.29	10.43	7.85	5.52	4.53	3.55
		SDRL	192.71	32.46	12.87	7.39	4.98	3.09	2.32	1.59

Table 6.2: RL characteristics of the proposed dispersion CUSUM scheme II

		RL	λ							
h	w	Properties	1.00	1.25	1.50	1.75	2.00	2.50	3.00	4.00
						$k = 0.25, \mathrm{ARL}_0 = 120$				
6.312	5.109	ARL	120.23	35.57	16.69	11.10	8.53	6.05	4.86	3.64
		SDRL	118.19	28.28	11.04	6.47	4.59	2.94	2.24	1.58
6.646	4.926	ARL	119.58	33.88	16.34	10.97	8.48	6.06	4.89	3.71
		SDRL	116.05	26.82	10.74	6.36	4.51	2.89	2.19	1.57
∞	4.242	ARL	120.08	27.58	14.06	9.78	7.72	5.68	4.77	3.82
		SDRL	117.78	21.76	9.29	5.70	4.08	2.62	2.03	1.46
						$k = 0.25, \mathrm{ARL}_0 = 200$				
7.194	6.112	ARL	199.92	44.57	20.28	12.92	9.87	6.86	5.49	4.09
		SDRL	193.56	35.22	13.16	7.27	5.11	3.21	2.43	1.72
7.443	5.926	ARL	199.59	43.43	19.78	12.94	9.83	6.90	5.50	4.13
		SDRL	189.54	34.37	12.79	7.31	5.06	3.19	2.39	1.70
∞	5.138	ARL	200.34	35.76	17.27	11.40	8.87	6.53	5.36	4.23
		SDRL	192.32	28.27	11.31	6.46	4.55	2.95	2.22	1.56
						$k = 0.50, \mathrm{ARL}_0 = 120$				
3.786	3.013	ARL	120.25	32.62	14.65	9.10	6.62	4.43	3.38	2.46
		SDRL	114.06	28.90	11.84	6.57	4.40	2.65	1.85	1.23
4.385	2.726	ARL	120.33	30.12	13.81	8.92	6.68	4.54	3.60	2.61
		SDRL	116.78	26.46	10.76	6.28	4.28	2.51	1.83	1.21
∞	2.503	ARL	119.81	26.89	13.11	8.51	6.40	4.54	3.74	2.96
		SDRL	116.80	23.56	10.18	5.86	3.92	2.33	1.78	1.08
						$k = 0.50, \mathrm{ARL}_0 = 200$				
4.996	3.159	ARL	200.27	39.24	16.79	10.37	7.76	5.28	4.17	3.10
		SDRL	189.09	35.28	13.11	7.30	5.01	2.95	2.16	1.50
5.396	3.104	ARL	201.30	38.10	16.55	10.44	7.68	5.32	4.22	3.18
		SDRL	193.07	33.75	12.64	7.16	4.88	2.89	2.16	1.47
∞	2.999	ARL	200.29	36.51	15.97	10.12	7.54	5.32	4.36	3.43
		SDRL	192.37	32.59	12.55	6.93	4.75	2.86	2.12	1.46

Table 6.3: RL characteristics of the simple dispersion CUSUM chart

	RL	λ							
h	Properties	1.00	1.25	1.50	1.75	2.00	2.50	3.00	4.00
				$k = 0.25, \mathrm{ARL}_0 = 120$					
6.000	ARL	120.29	36.22	17.14	10.96	8.37	5.71	4.46	3.27
	SDRL	112.24	28.5	11.21	6.31	4.45	2.74	1.96	1.31
				$k = 0.25, \mathrm{ARL}_0 = 200$					
6.859	ARL	199.83	45.54	19.96	12.79	9.56	6.52	5.06	3.67
	SDRL	183.5	36.32	12.9	7.24	4.9	2.96	2.14	1.41
				$k = 0.50, \mathrm{ARL}_0 = 120$					
3.604	ARL	119.44	34.03	14.53	8.77	6.23	3.91	2.97	2
	SDRL	116.59	30.21	11.63	6.33	4.1	2.15	1.48	0.84
				$k = 0.50, \mathrm{ARL}_0 = 200$					
4.096	ARL	200.28	45.39	17.94	10.29	7.26	4.6	3.35	2.25
	SDRL	192.05	40.78	14.57	7.19	4.71	2.57	1.62	0.93

6.4 Comparisons

In this section, we provide comparisons of the proposed schemes with: i) the simple dispersion CUSUM scheme and ii) the EWMA dispersion charts for individual observations, investigated in Yeh et al. (2010).

6.4.1 Proposed Schemes vs. the Simple dispersion CUSUM Scheme

From the results in Tables 6.1-6.3, we can see the benefit of using the two run rules schemes, particularly for the detection of small magnitude shifts. For example, with $k = 0.50$ and $\mathrm{ARL}_0 = 200$, the ARL_1 of simple CUSUM scheme is 45.39 when $\lambda = 1.25$, while the corresponding ARL_1 for Schemes I and II are 36.55 and 36.51 with h at infinity. This indicates that CUSUM dispersion Schemes I and II require, on average, 9 fewer observations than the simple CUSUM scheme to detect a multiplicative shift of magnitude $\lambda = 1.25$ in the process standard deviation. Similarly, we observe a significant improvement in the out-of-control run length characteristics of the run rules schemes over the simple CUSUM dispersion scheme, particularly for smaller values of λ. Figures 6.1 and 6.2 represent the ARL comparison of the proposed CUSUM Schemes I and II (using $h = \infty$) with the simple CUSUM scheme when $\mathrm{ARL}_0 = 120$ and 200 for $k = 0.25$ and 0.5. In each plot, Log (ARL) is plotted against λ for better visual comparison. The results in Tables 6.1-6.2 and the ARL curves in Figures 6.1-6.2 indicate that:

- for the detection of small process shifts, the performance of the runs rules schemes are very similar to each other and significantly better than the performance of the simple dispersion CUSUM scheme

- for large shifts, the performance of the simple dispersion CUSUM scheme is slightly better than that for the runs rules schemes. Similar results can be easily obtained for other values of ARL_0.

Figure 6.3 displays the cumulative probability vs. run length curves of the three CUSUM dispersion schemes when $\mathrm{ARL}_0 = 120$ and 200 for $k = 0.5$

and $\lambda = 1.25$. For detecting this shift in the process standard deviation, the cumulative probability of detection for both of the proposed schemes is consistently above that of the simple dispersion CUSUM scheme, particularly at shorter run lengths, which indicates that there is a higher probability of detecting small shifts quickly.

The results have been provided for $\text{ARL}_0 = 120$ and 200 but similar results can be obtained for other values of ARL_0. Control chart coefficients for fixing the control limits of these three schemes to obtain a desired ARL_0 ranging from 100 to 500 have been presented. For the simple dispersion CUSUM scheme, plots of ARL_0 vs h have been provided in Figure 6.4, whereas for the two proposed run rule Schemes I and II, plots of ARL_0 vs w are provided when h is taken to be infinity (to achieve the smallest ARL_1) in Figures 6.5 and 6.6 respectively. These plots can be used to approximate the control limits for the desired ARL_0 values. For example, the first plot in Figure 6.6 shows that $w = 6.25$ approximately gives $\text{ARL}_0 = 370$ for Scheme II using $k = 0.25$.

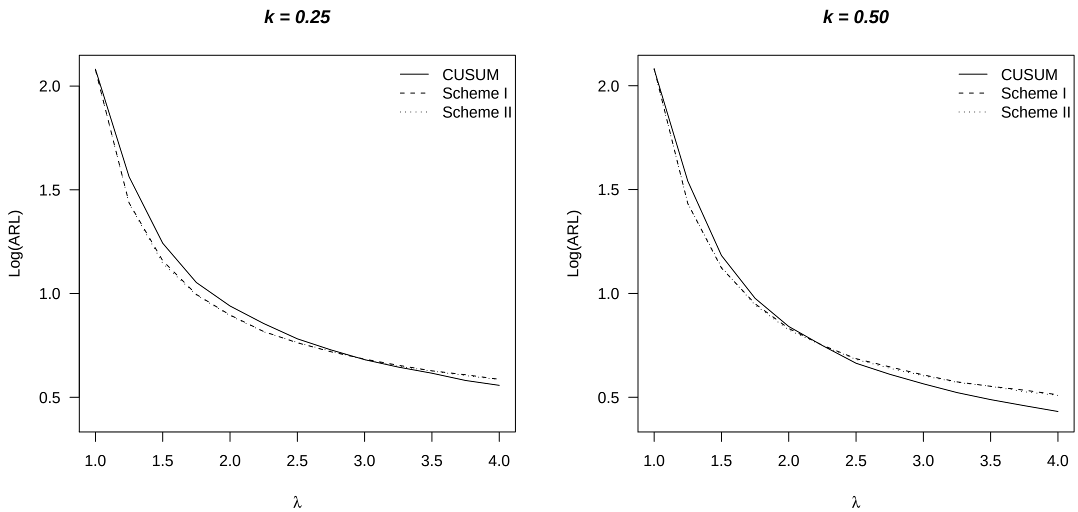

Figure 6.1: ARL comparison of the simple dispersion CUSUM scheme with CUSUM Schemes I and II (using $h = \infty$) when $\text{ARL}_0 = 120$

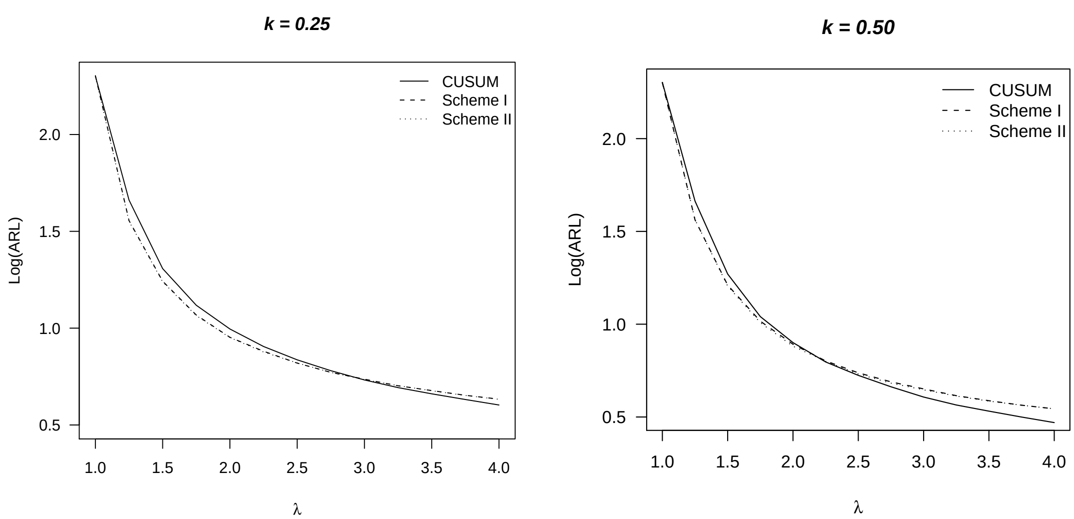

Figure 6.2: ARL comparison of the simple dispersion CUSUM scheme with CUSUM Schemes I and II (using $h = \infty$) when $\text{ARL}_0 = 200$

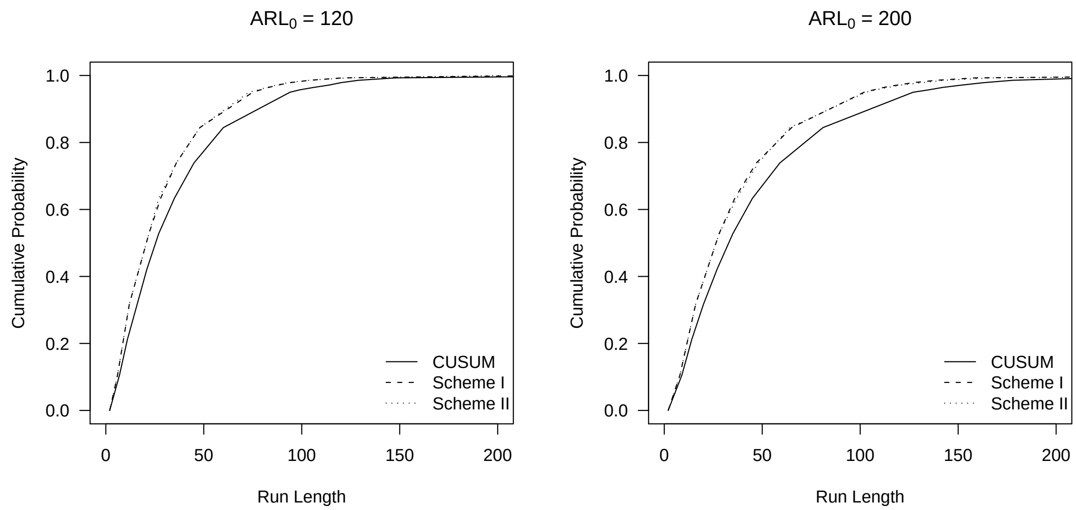

Figure 6.3: Run length curves of the simple dispersion CUSUM scheme and CUSUM Schemes I & II (using $h = \infty$) for $k = 0.5$ and $\lambda = 1.25$ when $\mathrm{ARL}_0 = 120$ and 200

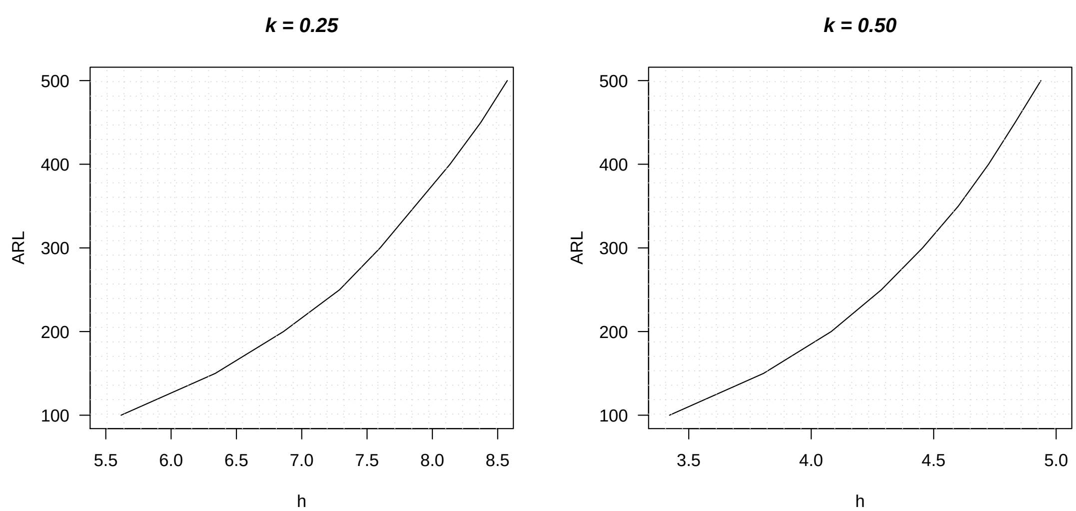

Figure 6.4: The choice of h for different ARL_0 values for the simple dispersion CUSUM scheme

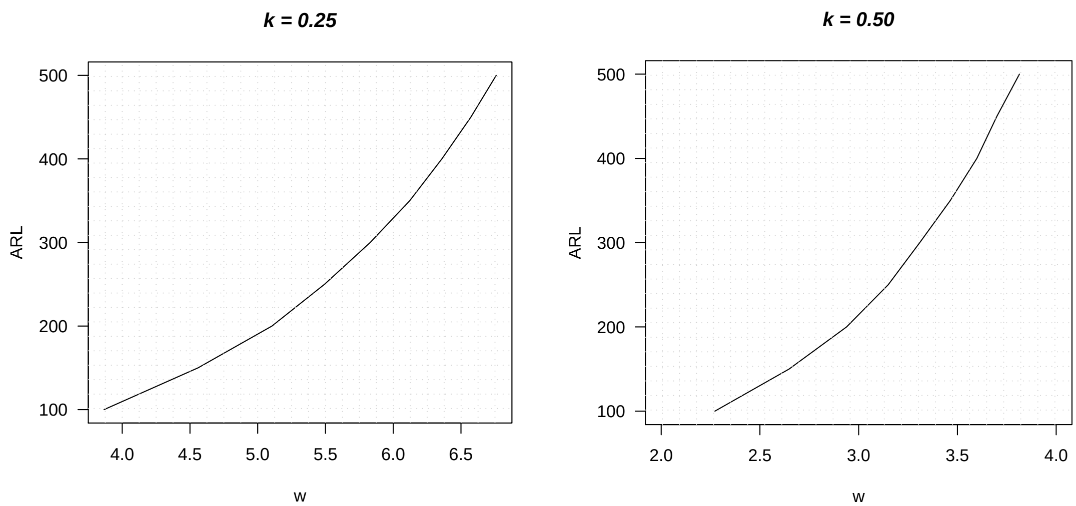

Figure 6.5: The choice of w for different ARL_0 values for the run rule dispersion CUSUM scheme I when $h = \infty$

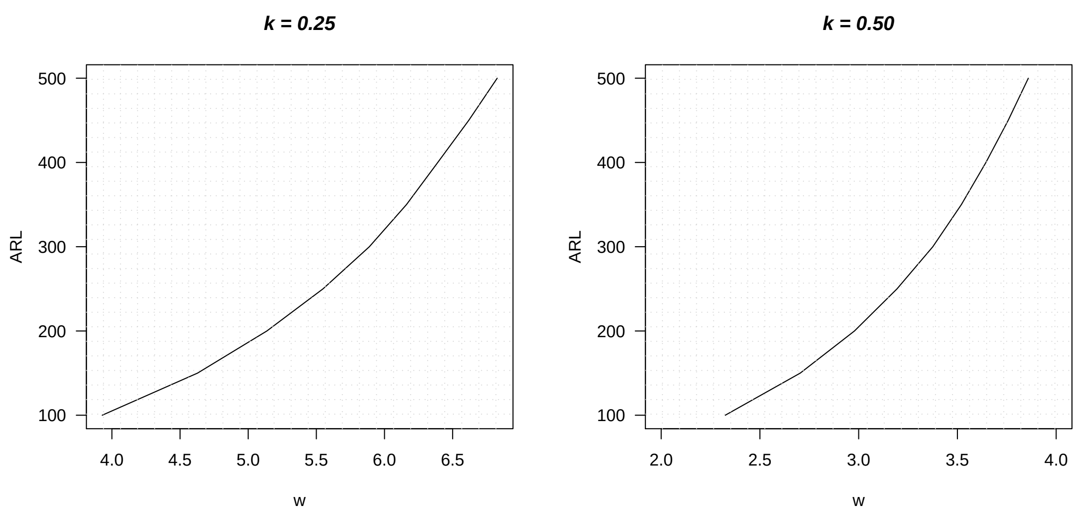

Figure 6.6: The choice of w for different ARL_0 values for the run rule dispersion CUSUM scheme II when $h = \infty$

6.4.2 Proposed Schemes vs. dispersion EWMA Charts

In this section, we compare the ARL performance of the two proposed schemes with the EWMS chart (proposed by MacGregor and Harris (1993)), the M-EWMS chart (a modified EWMS chart proposed by Huwang et al. (2009)) and the COMB chart (proposed by Yeh et al. (2010)), for the case of individual observations. The design structures of these charts are briefly described below:

The EWMS chart is based on plotting the EWMA statistic $W_t = (1-\eta)W_{t-1} + \eta(X_t - \mu_0)^2$ against the following control limits:

$$\begin{aligned} UCL &= \sigma_0^2 \chi_{1-\alpha/2} \\ LCL &= \sigma_0^2 \chi_{\alpha/2} \end{aligned} \tag{6.2}$$

where η represents the smoothing parameter.
The M-EWMS chart is based on plotting the EWMA statistic $W_t' = ln[(W_t/\sigma_0^2 - (1-\eta^t))/\eta]$ against the following set of control limits:

$$\begin{aligned} UCL &= \widehat{E}(T_t^2) + L * \sqrt{\widehat{V}ar(T_t^2)} \\ LCL &= \widehat{E}(T_t^2) + L * \sqrt{\widehat{V}ar(T_t^2)} \end{aligned} \tag{6.3}$$

where L is the control chart multiplier and W_t represents the EWMA statistic of the EWMS chart. $\widehat{E}(T_t^2)$ and $\widehat{V}ar(T_t^2)$ are defined as:

$$\begin{aligned} \widehat{E}(T_t^2) &= ln(p_k q_t) - \frac{1}{q_t} - \frac{1}{3q_t^2} + \frac{2}{15q_t^4} \\ \widehat{V}ar(T_t^2) &= \frac{2}{q_t} + \frac{2}{q_t^2} + \frac{4}{3q_t^3} - \frac{16}{15q_t^5} \end{aligned} \tag{6.4}$$

where $p_t = \sum_{i=1}^{t}(1-\eta)^{2(t-i)} / \sum_{i=1}^{t}(1-\eta)^{t-i}$ and $q_t = [\sum_{i=1}^{t}(1-\eta)^{t-i}]^2 / \sum_{i=1}^{t}(1-\eta)^{2(t-i)}$.

Yeh et al. (2010) proposed a EWMSI chart that is based on plotting the statistic $W_t'' = (1-\eta)W_{t-1}'' + \lambda\,(1/X_t - 1/\mu_0)$ against the simulated control limits.

The COMB chart is based on monitoring process dispersion by implementing the upper EWMS and the lower EWMSI charts in a single structure. The control limits are then adjusted to achieve a specified ARL_0.

Yeh et al. (2010) reported ARL results for these charts using the smoothing parameter $\eta = 0.05$, 0.1 and 0.15 for $\text{ARL}_0 = 370$. For a fair comparison, the ARL of the two proposed schemes have also been computed after fixing the $\text{ARL}_0 = 370$. Figure 6.7 presents the ARL comparison of the two proposed schemes using $k = 0.25$ and the EWMS, M-EWMS and COMB charts using $\eta = 0.1$. The ARL curves indicate that both the proposed schemes outperform the EWMS, M-EWMS and COMB charts for the detection of small process shifts. For moderate shifts in process dispersion, the performance of the COMB chart is slightly better than the rest of the control schemes.

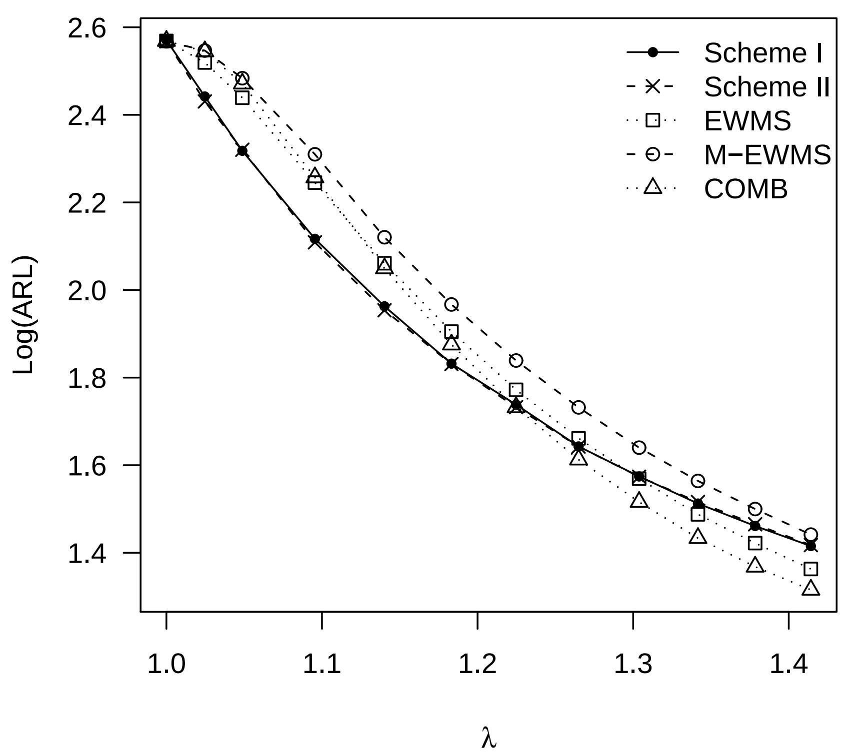

Figure 6.7: ARL comparison of the proposed schemes I and II with EWMS, M-EWMS and COMB charts when $\text{ARL}_0 = 370$

Based on our evaluation of the run length distributions, the main findings of the study are:

- the two proposals significantly improve the detection ability of the CU-

SUM chart to detect small and moderate shifts in dispersion at the cost of a very small increase in the run length for larger shifts. (cf. Tables 6.1-6.2);

- the ARL and SDRL decreases for both schemes as the value of λ increases (cf. Tables 6.1-6.2);

- the two proposed schemes have almost the same run length properties as may be seen from Tables 6.1-6.2 and Figures 6.1-6.3 and so either may be used effectively;

- for the detection of small and moderate shifts in process dispersion, $h = \infty$ performs better than all the pairs in terms of optimum ARL_1 (as may be seen from Tables 6.1-6.2). Hence, we recommend the use of $h = \infty$ (Figures 6.5 and 6.6 can be used to get the required control limits for the proposed Schemes I and II respectively);

- the proposed run rules based dispersion CUSUM schemes perform better in terms of run length efficiency compared to the simple dispersion CUSUM scheme, the EWMS chart, the M-EWMS chart and the COMB chart, particularly for the detection of small shifts in process dispersion.

6.5 Illustrative Examples

In this section, we provide illustrative examples to demonstrate the applications of the proposed procedures. For this purpose, we have generated two datasets which will be referred as Dataset 1 and Dataset 2, containing some in-control points and some out-of-control points following the work of Khoo (2004), Antzoulakos and Rakitzis (2008), Riaz et al. (2011) and Abbas et al. (2011).

Dataset 1 contains 50 observations, of which the first 20 are generated from $N(0, 1)$ referring to an in-control situation and the remaining 30 observations are generated from $N(0, 1.25)$ referring to a small shift in the process dispersion parameter (i.e. out-of-control situation). Dataset 2 contains 30

observations, of which the first 20 are generated from $N(0,1)$ referring to an in-control situation and the remaining 10 observations are generated from $N(0,2)$ referring to a moderate shift in the process dispersion parameter. The CUSUM dispersion statistics for these observations in the two datasets are calculated and the three schemes (i.e. the two proposed CUSUM dispersion Schemes I and II and the simple dispersion CUSUM scheme) are applied by fixing $\text{ARL}_0 = 120$ when $k = 0.25$. For the simple CUSUM dispersion scheme, $h = 6$ (see Table 6.3) is used as a control limit to have the desired $\text{ARL}_0 = 120$. For the proposed Scheme I, $w = 4.337$ and $h = 8.864$ (from Table 6.1) are used, whereas, for proposed Scheme II, $w = 4.926$ and $h = 6.646$ (from Table 6.2) are used for both the data sets. The graphical display of the control charts with all the three schemes applied to the Datasets 1 and 2 are given in Figures 6.8 and 6.9 respectively.
In Figures 6.8 and 6.9 the labels used for the three types of control limits are explained as:

- h: the threshold value of h for simple dispersion CUSUM scheme
- h_{S1} and w_{S1} represents the values of h and w for run rule Scheme I
- h_{S2} and w_{S2} represents the values of h and w for run rule Scheme II

In Figure 6.8, we see that out-of-control signals are received at sample points 47-49 by the simple dispersion CUSUM scheme, at sample points 34-37 and 47-50 by the proposed Scheme I, and at sample points 36, 37 and 47-50 by the proposed Scheme II. Similarly, from Figure 6.9 we can see that the simple dispersion CUSUM scheme is unable to provide any out-of-control signal, whereas out-of-control signals are received at sample points 29 and 30 by Scheme I and at sample point 30 by Scheme II. This clearly indicates that the proposed schemes are not only signaling earlier than the classical scheme but are also giving more out-of-control signals.

The outcomes of these two illustrative examples are in accordance with the findings of Section 6.4. Therefore, we recommend the application of our proposals in every type of process in general and particularly for sensitive processes (cf. Bonetti et al. (2000)) where a small change may have very serious effects.

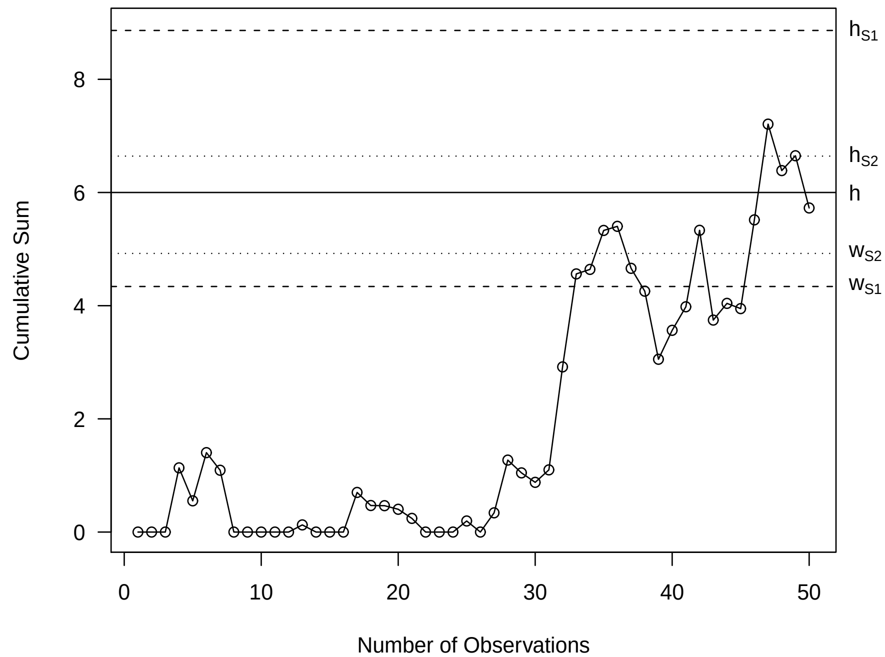

Figure 6.8: CUSUM chart for the simple dispersion CUSUM scheme and the proposed schemes I and II for dataset 1 when $k = 0.25$ and $\text{ARL}_0 = 120$

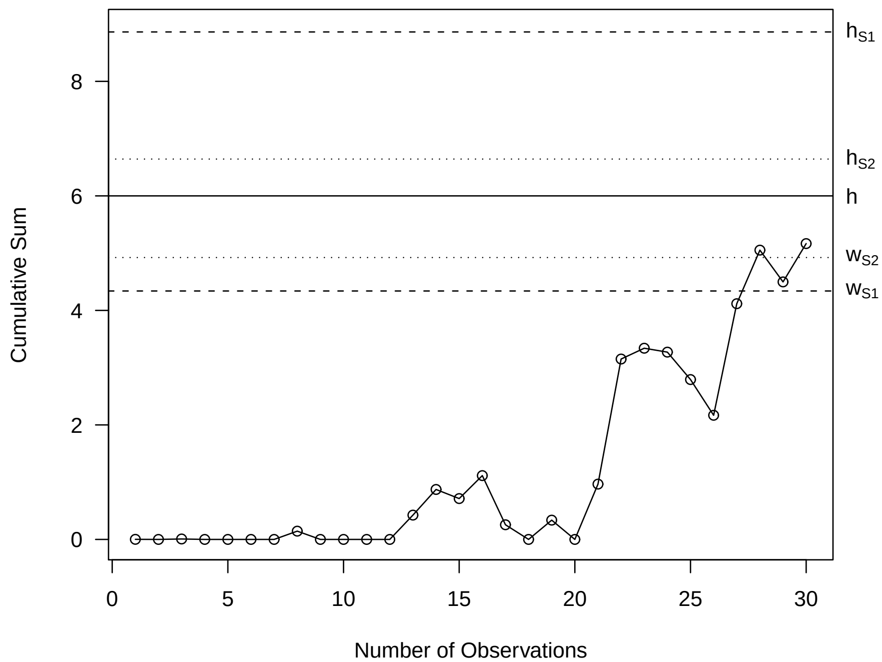

Figure 6.9: CUSUM chart for the simple dispersion CUSUM scheme and the proposed schemes I and II for dataset 2 when $k = 0.25$ and $\text{ARL}_0 = 120$

6.6 Conclusions

Every process is subject to variation. From the perspective of quality control, it is important to differentiate between the inherent variation and the unusual variation. For an efficient and smart monitoring of the process parameters, we have a variety of detection rules available but their use has been mainly limited to Shewhart type control charts for location and dispersion parameters. Recently, the use of these rules has been extended to EWMA and CUSUM structures for location parameter. In this study, we have studied their application to CUSUM charts for monitoring the dispersion parameter as well. These proposals result in better performance of a dispersion CUSUM control chart, especially for the detection of small shifts. The comparisons revealed that the proposed schemes outperformed the simple dispersion CUSUM chart in terms of ARL. Also, the implementation of the proposal is made easy by deriving the coefficients for commonly used ARL_0 values and showing its application on simulated datasets. Therefore, we recommend the use of our proposal for the efficient monitoring of process dispersion parameter.

Chapter 7

Nonparametric Progressive Mean Control Chart for Monitoring Process Location

Nonparametric control charts are widely used when the parametric distribution of the quality characteristic of interest is questionable. In this study, we proposed a nonparametric progressive mean control chart, namely the $NPPM$ chart, for efficient detection of disturbances in process location or target. The proposed chart is compared with the recently proposed nonparametric EWMA and nonparametric CUSUM charts using different run length characteristics, such as the average run length, the standard deviation of the run length and the percentile points of the run length distribution. The comparisons revealed that the proposed chart outperformed the recent nonparametric EWMA and nonparametric CUSUM charts in terms of detecting the shifts in process mean. A real life example concerning the fill heights of soft drink beverage bottles is also provided to illustrate the application of the proposed nonparametric control chart. This chapter is based on Abbasi et al. (2012b).

7.1 Introduction

Most of the Statistical Process Control (SPC) charts are based on the assumption that the parametric distribution of the quality characteristic of interest is known. In many real life situations, this assumption is not valid and hence the use of parametric control charts for the monitoring of process parameters can give unfavorable results in the form of low detection ability and high false alarm rates. In these scenarios, it may be better to use a non-parametric control chart. Research has been done in the field of nonparametric control charts by many researchers, including Das (2009), Qiu et al. (2010), Human et al. (2010), Khilare and Shirke (2010) and Pawar and Shirke (2010). Different nonparametric EWMA (NPEWMA) and nonparametric CUSUM (NPCUSUM) control charts have also been proposed recently for quick detection of small shifts in process parameters. Li and Wang (2010) proposed NPEWMA and NPCUSUM charts based on the Man-Whitney statistics, Zou and Tsung (2011) proposed a multivariate EWMA control chart using the weighted version of sign test, Graham et al. (2011) proposed a NPEWMA sign chart for monitoring process location using individual observations, Yang et al. (2011) proposed two NPEWMA control charts, namely the nonparametric EWMA sign (NPS_E) chart and the nonparametric Arcsine EWMA sign ($NPAS_E$) chart, while Yang and Cheng (2011) proposed a nonparametric CUSUM (NPS_C) chart for quick detection of shifts from the process target using the sign statistics.

In this chapter, we use the progressive mean (PM) as the process monitoring statistic instead of using a monitoring statistic based on the EWMA or the CUSUM weighting schemes. PM is defined as the cumulative average of the sample values observed over time. Suppose we are interested in monitoring a quality characteristic X, following a distribution $f(x)$. Let $X_1, X_2, \ldots, X_n$ be a sample of size n from this distribution. The progressive mean statistic is defined as:

$$PM_t = \frac{X_1 + X_2 + \cdots + X_t}{t} = \frac{\sum_{j=1}^{t} X_j}{t} \tag{7.1}$$

The benefit of using the progressive mean statistic is its quick convergence to the process target compared to the Shewhart, EWMA or CUSUM monitoring statistics. Figure 7.1 presents plots of the progressive mean, Shewhart, EWMA and CUSUM monitoring statistics for a standard normal process where the target is 0. We can clearly see the quick convergence ability of PM towards the process target, as compared to other statistics. Due to this, we expect that a control chart based on the progressive mean statistic will perform better than the Shewhart, the CUSUM and the EWMA charts.

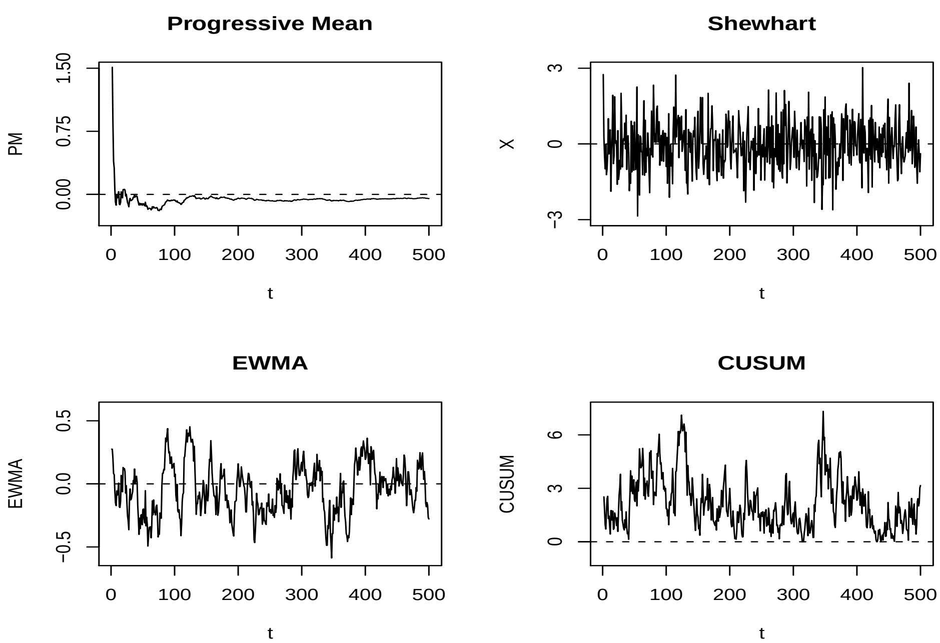

Figure 7.1: Progressive mean, Shewhart, EWMA and CUSUM monitoring statistics for a standard normal process

The rest of the study is organized as follows: Section 7.2 describes the design structure of the proposed $NPPM$ control chart; Section 7.3 evaluates the performance of the proposed chart using different run length characteristics; Section 7.4 provides the comparison of the $NPPM$ chart with recently proposed NPS_E, $NPAS_E$ and NPS_C charts; and Section 7.5 presents an example to illustrate the application of the proposed chart and finally the chapter ends with conclusions.

7.2 The Proposed Nonparametric Progressive Mean (NPPM) Chart

In this section, we describe the structure of the nonparametric progressive mean ($NPPM$) control chart, proposed for the purpose of quick detection of shifts from the process target.

Suppose $X_1 \ldots X_n$ represents a sample of size n from a process with a target (or location) at μ. Define p to be the probability of X greater than μ. i.e. $p = pr(X_i > \mu)$. For an in-control process, $p = p_0 = 0.5$ (the in-control process proportion), the process is said to be out-of-control for $p \neq p_0$. The purpose of the proposed control chart is the efficient detection of departures of p from its in-control value p_0. Yang et al. (2011) showed that $M_t = \sum_{i=1}^{n} I_i$ follows a binomial distribution with parameters n and p_0, where I_i takes value 1 for $X_i > \mu$ and 0 otherwise. The binomial distribution of M_t can be transformed into a normal random variable by the arcsine transformation (Yang et al. (2011)):

$$Z_t = sin^{-1}\sqrt{M_t/n} \sim N(\mu_Z, \sigma_Z^2) \tag{7.2}$$

where μ_Z and σ_Z are defined as:

$$\mu_Z = sin^{-1}(\sqrt{p_0}) \qquad \text{and} \qquad \sigma_Z = 1/4n \tag{7.3}$$

Instead of using the EWMA or CUSUM weighting schemes, we will use Z to produce a progressive mean statistic (PM_t) for time point t:

$$PM_t = \frac{Z_1 + Z_2 + Z_3 + \cdots + Z_t}{t} = \frac{\sum_{j=1}^{t} Z_j}{t} \tag{7.4}$$

The expected value and the variance of the PM statistic are given as:

$$E(PM_t) = \mu_Z = sin^{-1}(\sqrt{p_0}) \qquad \text{and} \qquad Var(PM_t) = \frac{\sigma_Z}{t} = \frac{1/4n}{t} \tag{7.5}$$

Using the mean and the variance of PM_t given in (5), the widely used 3-sigma limits are:

$$UCL_t = sin^{-1}(\sqrt{p_0}) + 3 * \sqrt{\frac{1/4n}{t}} \tag{7.6}$$
$$CL = sin^{-1}(\sqrt{p_0})$$
$$LCL_t = sin^{-1}(\sqrt{p_0}) - 3 * \sqrt{\frac{1/4n}{t}}$$

Similarly to the EWMA and the CUSUM schemes, the $NPPM$ chart uses both current and past information from the observed samples, which makes it effective for the detection of small shifts. A couple of problems have been identified for the above control limits: i) the use of 3 as the control chart multiplier does not guarantee a desired in-control average run length; and ii) these control limits remain too wide relative to the plotting statistics for higher values of t, leading to a small number of out-of-control signals for larger values of t. This motivates us to redefine the control limits that take care of these issues, following Abbas et al. (2011). The revised limits (that have been used for the rest of this study) are defined as:

$$UCL_t = sin^{-1}(\sqrt{p_0}) + L' * \frac{1}{f(t)}\sqrt{\frac{1/4n}{t}} \tag{7.7}$$
$$CL = sin^{-1}(\sqrt{p_0})$$
$$LCL_t = sin^{-1}(\sqrt{p_0}) - L' * \frac{1}{f(t)}\sqrt{\frac{1/4n}{t}}$$

where L' represents a control chart multiplier used to set the in-control average run length to a particular level and $f(t)$ is an arbitrary function of t. The $NPPM$ chart triggers an out-of-control signal for any PM_t lying outside the control limits at point t.

7.3 Performance Evaluation

The average run length (ARL) is the most important and widely used measure to evaluate the performance of control charts. The performance can be evaluated by two ARL values:

- ARL_0: the average number of samples until an out-of-control signal is detected by a control chart when the process is in-control
- ARL_1: the average number of samples until an out-of-control signal is detected by a control chart when the process is shifted to an out-of-control value.

Large values of ARL_0 and small values of ARL_1 are desirable for any control chart setting. In this study, a Monte Carlo simulation with 50,000 iterations is used to approximate the run length distribution of the proposed $NPPM$ chart following Lucas and Saccucci (1990), Maravelakis et al. (2005) and Abbasi (2010). Note that Kim (2005) and Schaffer and Kim (2007) indicates that 5000 replications are enough to obtain reasonable estimates of ARLs in many control chart settings. To get a better insight of the performance of the proposed charts, the standard deviation and the percentile points of the run length distribution are also provided.

The summary of the run length characteristics of the $NPPM$ chart is reported in Table 7.1, where ARL denotes the average run length and SDRL denotes the standard deviation of the run length distribution. The column corresponding to $p = 0.5$ provides the run length characteristics when the process is assumed to be in statistical control. The process is said to be out-of-control for $p \neq 0.5$. We considered different choices for $f(t)$ in our simulation study for the computation of control limits. But here the results are only provided for $f(t) = t^{0.20}$, which gives the best run length performance for the proposed $NPPM$ chart. Control chart multipliers L' are chosen to give the in-control average run length of 370 (i.e. $ARL_0 = 370$). The relative standard errors of the results reported in Tables 1 are found to be less than 1.0%, as checked by repeating the simulations. This is quite acceptable in control chart studies (for details, see Kim (2005) and Schaffer and Kim (2007)).

The simulations have been done in R and the computer programs can be obtained from the author on request. Moreover, the percentile points of the run length distribution of the proposed $NPPM$ chart are reported in Table 7.2. In Table 7.2, Q_p represents the p^{th} percentile of the run length distribution of the NPPM chart. Similarly, the run length characteristics of the proposed chart can be easily computed for other ARL_0 values. Table 7.3 presents values of control chart multipliers L' to achieve a specified ARL_0 for some representative values of n considering $p_0 = 0.5$.

The results reported in Tables 7.1 and 7.2 are for the case when the process is assumed to be out-of-control from the start (this can also be referred as the zero-state ARL). This is not always the case, hence we also investigate the steady-state behavior of the $NPPM$ chart. A monitoring statistic is said to be in steady-state if a process remains in-control for a long period (without any false signals) before the occurrence of any change in the parameters. The distribution of the detection of out-of-control sample points, after the change has occurred is known as the steady-state run length distribution and its mean as the steady-state ARL (Lucas and Saccucci (1990)). Table 7.4 presents steady-state ARL results for the proposed $NPPM$ chart, when the process is assumed to be in-control for the first t samples. The results for $t = 0$ are also included in Table 7.4 for comparison. We can observe that, as t increases, (i.e. as the in-control period before the occurrence of shift increases), the $NPPM$ chart gets slower in the detection of shifts. This is expected due to the fact that the PM statistic uses the average of all the previous PM values, hence giving a bit of extra weight to the in-control samples.

Based on our evaluation of the run length characteristics, the main findings of the study are: i) the proposed chart efficiently detects small as well as large departures from the in-control process proportion p_0; ii) the run length distribution of the proposed chart is positively skewed; iii) the ARL, the SDRL and the percentile points of the run length distribution decrease with an increase in the values of δ and n; iv) the proposed chart is equally efficient for the detection of positive and negative shifts in p_0; v) the steady-state performance of the $NPPM$ chart is less efficient compared to the zero-state performance; vi) the $NPPM$ chart uses the cumulative average of the sample values, observed over time as the monitoring statistic which can be very useful for processes that have the tendency to go out-of-control at the start of a monitoring cycle or that produce frequent out-of-control signals; and vii) the application of the proposed chart can be easily executable in this modern era of computer technology.

Table 7.1: Run length characteristics of the proposed $NPPM$ control chart when $\text{ARL}_0 = 370$

n		0.05	0.15	0.25	0.3	0.35	0.4	0.45	p 0.5	0.55	0.6	0.65	0.7	0.75	0.85	0.95
9	ARL	1.42	2.37	3.93	5.40	7.96	13.62	34.24	370.28	34.23	13.75	7.97	5.38	3.94	2.35	1.42
	SDRL	0.58	1.03	1.81	2.60	4.20	8.27	26.42	720.28	26.45	8.35	4.18	2.61	1.82	1.02	0.58
10	ARL	1.42	2.22	3.61	4.94	7.33	12.65	31.97	370.33	31.84	12.70	7.33	4.92	3.61	2.21	1.42
	SDRL	0.52	0.86	1.60	2.35	3.84	7.61	24.22	716.94	24.19	7.66	3.84	2.34	1.60	0.86	0.52
11	ARL	1.44	2.19	3.48	4.74	6.97	11.99	30.06	371.54	30.03	11.98	6.99	4.72	3.47	2.18	1.44
	SDRL	0.52	0.78	1.46	2.18	3.53	6.99	22.23	738.09	22.30	6.99	3.54	2.18	1.47	0.77	0.52
12	ARL	1.46	2.18	3.37	4.51	6.57	11.27	28.28	370.67	28.26	11.26	6.55	4.50	3.38	2.17	1.47
	SDRL	0.51	0.71	1.30	1.94	3.20	6.50	20.71	736.12	20.71	6.49	3.19	1.94	1.30	0.71	0.51
13	ARL	1.49	2.09	3.17	4.25	6.20	10.65	26.73	370.04	26.71	10.63	6.19	4.24	3.17	2.09	1.49
	SDRL	0.50	0.61	1.20	1.83	3.02	6.07	19.34	723.38	19.40	6.04	3.01	1.83	1.21	0.60	0.50
14	ARL	1.15	1.82	2.98	4.02	5.88	10.11	25.50	369.83	25.47	10.11	5.89	4.02	2.97	1.82	1.15
	SDRL	0.36	0.73	1.23	1.77	2.86	5.72	18.30	725.64	18.30	5.72	2.86	1.76	1.25	0.73	0.36
15	ARL	1.17	1.84	2.92	3.89	5.63	9.64	24.26	369.37	24.30	9.64	5.62	3.89	2.92	1.84	1.17
	SDRL	0.38	0.68	1.11	1.61	2.64	5.39	17.21	704.36	17.28	5.37	2.65	1.60	1.12	0.68	0.38
20	ARL	1.07	1.62	2.45	3.25	4.68	8.00	20.05	369.38	20.04	7.96	4.69	3.25	2.45	1.63	1.08
	SDRL	0.26	0.54	0.87	1.29	2.09	4.24	13.49	730.62	13.58	4.21	2.11	1.29	0.86	0.54	0.27
25	ARL	1.01	1.32	2.07	2.76	4.02	6.88	17.20	367.46	17.23	6.86	4.04	2.76	2.08	1.32	1.01
	SDRL	0.09	0.48	0.77	1.11	1.79	3.52	11.17	725.82	11.26	3.51	1.79	1.10	0.77	0.48	0.08

Table 7.2: Percentile points of the run length distribution for the proposed $NPPM$ control chart

n		p = 0.5	0.55	0.6	0.65	0.7	0.75	0.8	0.85	0.9	0.95
10	$Q_{0.05}$	10	6	3	2	2	1	1	1	1	1
	$Q_{0.25}$	45	14	7	5	3	3	2	2	1	1
	$Q_{0.50}$	128	26	11	7	5	3	3	2	2	1
	$Q_{0.75}$	365.75	43	17	9	6	5	3	3	2	2
	$Q_{0.95}$	1454.9	79	28	15	9	6	5	4	3	2
12	$Q_{0.05}$	11	6	4	3	2	2	1	1	1	1
	$Q_{0.25}$	48	14	7	4	3	2	2	2	1	1
	$Q_{0.50}$	137	24	10	6	4	3	3	2	2	1
	$Q_{0.75}$	387	38	15	8	6	4	3	3	2	2
	$Q_{0.95}$	1538	70	24	13	8	6	4	3	3	2
15	$Q_{0.05}$	10	5	3	2	2	1	1	1	1	1
	$Q_{0.25}$	47	11	6	4	3	2	2	1	1	1
	$Q_{0.50}$	136	20	8	5	4	3	2	2	1	1
	$Q_{0.75}$	388	31	12	7	5	3	3	2	2	1
	$Q_{0.95}$	1479.8	56	20	11	7	5	4	3	2	2
20	$Q_{0.05}$	11	5	3	2	2	1	1	1	1	1
	$Q_{0.25}$	45	10	5	3	2	2	2	1	1	1
	$Q_{0.50}$	133	17	7	4	3	2	2	2	1	1
	$Q_{0.75}$	376	26	10	6	4	3	2	2	2	1
	$Q_{0.95}$	1417.9	47	16	8	6	4	3	2	2	2

Table 7.3: Control chart multiplier L' to achieve fixed ARL_0

n	ARL_0 = 200	250	300	350	370	400	500
10	3.303	3.489	3.639	3.765	3.803	3.882	4.071
15	3.228	3.387	3.528	3.654	3.692	3.762	3.939
20	3.195	3.351	3.501	3.624	3.650	3.738	3.927
25	3.168	3.333	3.477	3.606	3.626	3.714	3.888

Table 7.4: Steady-state ARL of the proposed $NPPM$ chart

		p							
n	t	0.5	0.55	0.6	0.65	0.7	0.75	0.85	0.95
10	0	370.33	31.84	12.70	7.33	4.92	3.61	2.21	1.42
	25	378.81	37.16	17.58	11.26	8.22	6.40	4.37	3.05
	50	387.82	41.14	19.37	12.46	9.36	7.33	5.02	3.57
	100	420.91	43.22	21.39	14.27	10.46	8.18	5.70	4.10
12	0	370.67	28.26	11.26	6.55	4.50	3.38	2.17	1.47
	25	379.55	34.61	15.79	10.27	7.56	5.95	4.08	2.85
	50	393.62	36.87	17.61	11.59	8.66	6.86	4.72	3.31
	100	418.16	39.61	19.92	12.94	9.74	7.76	5.38	3.81
15	0	369.37	24.30	9.64	5.62	3.89	2.92	1.84	1.17
	25	368.66	30.19	13.96	9.12	6.73	5.34	3.70	2.62
	50	378.90	31.73	15.53	10.31	7.67	6.08	4.24	3.03
	100	404.16	35.03	17.05	11.54	8.73	6.95	4.83	3.47
20	0	369.38	20.04	7.96	4.69	3.25	2.45	1.63	1.08
	25	367.87	25.34	12.10	7.89	5.87	4.68	3.27	2.35
	50	370.54	27.60	13.50	8.93	6.77	5.40	3.78	2.72
	100	408.24	29.97	14.93	10.14	7.63	6.19	4.39	3.13

7.4 Comparisons

In this section we compare the zero-state ARL performance of the proposed $NPPM$ chart with the recent proposals of Yang et al. (2011) and Yang and Cheng (2011). Yang et al. (2011) proposed two nonparametric EWMA charts, namely the nonparametric EWMA sign (NPS_E) chart and the nonparametric arcsine EWMA sign ($NPAS_E$) chart, while Yang and Cheng (2011) proposed the nonparametric CUSUM (NP_C) chart for quick detection of departures from the in-control process proportion p_0.
The NPS_E chart is based on plotting the EWMA statistic W_t, given as:

$$W_t = \lambda M_t + (1-\lambda)W_{t-1} \tag{7.8}$$

where M_t is defined in Section 7.2. Abbasi (2012) provided the corrected limits for the NPS_E chart, given as:

$$\begin{aligned} UCL &= n/2 + K\sqrt{\frac{\lambda}{2-\lambda}(n/4)} \\ CL &= n/2 \\ LCL &= n/2 - K\sqrt{\frac{\lambda}{2-\lambda}(n/4)} \end{aligned} \tag{7.9}$$

where λ is the weight assigned to the most recent observation. The NPS_E chart gives an out-of-control signal for any W_t lying outside the above control limits.

Yang et al. (2011) also proposed the $NPAS_E$ chart by making use of the arcsine transformation defined in (7.2). The $NPAS_E$ chart is based on plotting the statistic W'_t, given as:

$$W'_t = \lambda Z_t + (1-\lambda)W'_{t-1} \tag{7.10}$$

where Z_t is defined in Section 7.2. The chart gives an out-of-control signal when W_t' goes out of the given limits:

$$\begin{aligned} UCL &= sin^{-1}(\sqrt{0.5}) + K\sqrt{\frac{\lambda}{2-\lambda}(1/4n)} \\ CL &= sin^{-1}(\sqrt{0.5}) \\ LCL &= sin^{-1}(\sqrt{0.5}) - K\sqrt{\frac{\lambda}{2-\lambda}(1/4n)} \end{aligned} \tag{7.11}$$

Moreover, a nonparametric CUSUM chart (NPS_C) has been proposed by Yang and Cheng (2011), which is based on plotting the CUSUM statistics, given as:

$$\begin{aligned} C_t^+ &= \max(0, C_{t-1}^- + M_t - (np_0 + k)) \\ C_t^- &= \min(0, C_{t-1}^+ + M_t - (np_0 - k)) \end{aligned} \tag{7.12}$$

where k is known as the reference value, defined as $k = n\frac{|p_0-p_1|}{2}$ and $C_0^+ = C_0^- = 0$. The NPS_C chart gives an out-of-control signal for any $C_0^+ \geq H$ or $C_0^- \leq -H$, where H is chosen to obtain a specified in-control average run length.

The ARL results of the NPS_E, $NPAS_E$ and NPS_C charts for some representative values of n are computed using similar simulation routines and are reported in Table 7.5. The ARL results for these charts are in close agreement with the results reported in Yang et al. (2011) and Yang and Cheng (2011) which confirms the validity of our simulation routines. The design structures of the charts compared in this study are summarized in Table 7.6.

The results in Tables 7.1 and 7.5 indicate that the out-of-control ARL (ARL$_1$) of the $NPPM$ chart is significantly lower than the ARL$_1$ of the NPS_E, $NPAS_E$ and NPS_C charts: for example, when $n = 12$ the ARL$_1$ = 28.26, 11.26, 6.55 for the proposed $NPPM$ chart for $p = 0.55, 0.6$ and 0.65, while the corresponding values of ARL$_1$ for the NPS_E chart are 44.74, 17.07, 10.29, for the $NPAS_E$ chart are 44.93, 16.91, 10.10, and for the NPS_C chart are $59.07, 18.58$, and 10.96. It indicates that the proposed $NPPM$ chart requires, on average, nearly 16, 6 and 4 fewer subgroups than the NPS_E and $NPAS_E$ charts and 31, 7 and 4 fewer subgroups than the NPS_C chart to detect these shifts in p_0.

Figure 7.2 compares the ARL of the proposed $NPPM$ chart with NPS_E, $NPAS_E$ and NPS_C charts using different values of p and n when $ARL_0 = 370$. In each plot, p is plotted on the horizontal axis, while the ARL is plotted on the vertical axis using a logarithmic scale to facilitate better visual comparison. Clearly, the ARL curves of the $NPPM$ chart are consistently lower than the ARL curves of the NPS_E, $NPAS_E$ and NPS_C charts indicating a better detection ability of the proposed chart.

To get more insight into the run length distribution of the $NPPM$, NPS_E, $NPAS_E$ and NPS_C charts, Figure 7.3 presents run length curves (RLCs) of these charts for certain values of n when $p = 0.6$. We can observe that the RLCs of the proposed $NPPM$ chart are higher than the RLCs of the other charts, indicating that the $NPPM$ chart has greater probability of detection for shorter run lengths. Note that this high probability at shorter run lengths indicates that the shifts in the process location will be detected quickly with high probability. The superiority of the proposed $NPPM$ chart over the other charts can be seen for all sample sizes.

We also observed that, even at sufficiently large values of t (say $t = 100$), the steady-state behaviour of the proposed $NPPM$ chart shows superiority over the other competing charts, particularly for the detection of small shifts in process location.

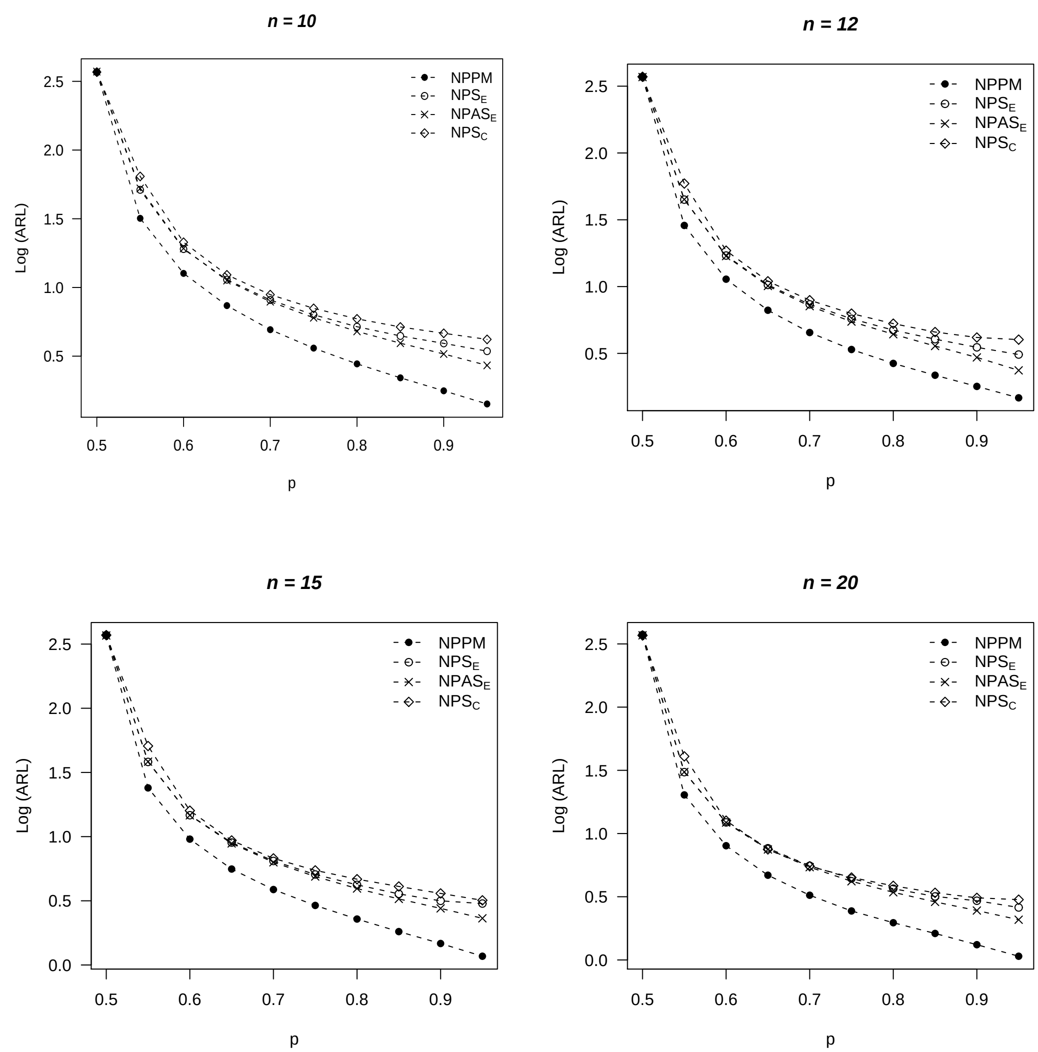

Figure 7.2: ARL comparison of the proposed $NPPM$ chart with NPS_E, $NPAS_E$ and NPS_C charts when $ARL_0 = 370$

Table 7.5: ARL of NPS_E, $NPAS_E$ and NPS_C charts when $ARL_0 =$ 370

		p														
Chart	n	0.05	0.15	0.25	0.3	0.35	0.4	0.45	0.5	0.55	0.6	0.65	0.7	0.75	0.85	0.95
NPS_E	10	3.44	4.44	6.29	8.08	11.37	19.10	51.47	369.53	51.37	19.04	11.40	8.11	6.33	4.44	3.44
	12	3.10	4.05	5.73	7.33	10.20	16.92	45.29	371.25	44.74	17.07	10.29	7.36	5.74	4.04	3.10
	15	3.01	3.59	5.07	6.48	8.99	14.64	38.12	371.55	38.19	14.68	8.99	6.46	5.07	3.58	3.01
	20	2.60	3.18	4.40	5.58	7.65	12.27	31.16	371.91	30.60	12.25	7.65	5.56	4.41	3.18	2.60
$NPAS_E$	10	2.71	3.94	6.01	7.90	11.26	19.12	52.54	372.33	52.56	19.23	11.23	7.88	6.02	3.93	2.71
	12	2.36	3.60	5.48	7.15	10.13	16.93	45.50	370.00	44.93	16.91	10.10	7.14	5.47	3.59	2.36
	15	2.31	3.27	4.92	6.32	8.88	14.62	38.84	369.02	38.37	14.65	8.85	6.31	4.89	3.27	2.31
	20	2.09	2.89	4.21	5.40	7.47	12.13	30.48	370.00	30.71	12.21	7.48	5.42	4.19	2.88	2.08
NPS_C	10	4.19	5.17	7.02	8.87	12.35	21.39	64.55	369.20	64.30	21.33	12.36	8.87	7.05	5.16	4.19
	12	4.01	4.56	6.26	7.92	10.88	18.65	58.13	372.00	59.07	18.58	10.96	7.91	6.28	4.57	4.01
	15	3.18	4.08	5.45	6.76	9.31	15.78	50.99	371.50	50.81	15.94	9.34	6.77	5.46	4.09	3.19
	20	3.00	3.41	4.47	5.49	7.51	12.69	40.71	369.23	40.77	12.65	7.49	5.51	4.49	3.40	3.00

Table 7.6: Design structures of different control charts

Control Chart	Monitoring Statistic	Control limits
$NPPM$	$PM_i = \frac{\sum_{j=1}^{t} Z_j}{t}$	$LCL = sin^{-1}(\sqrt{p_0}) - L' * \frac{1}{f(t)} * \sqrt{\frac{1/4n}{t}}$
		$UCL = sin^{-1}(\sqrt{p_0}) + L' * \frac{1}{f(t)} * \sqrt{\frac{1/4n}{t}}$
NPS_E	$W_t = \lambda M_t + (1-\lambda)W_{t-1}$	$LCL = n/2 - K\sqrt{\frac{\lambda}{2-\lambda}(n/4)}$
		$UCL = n/2 + K\sqrt{\frac{\lambda}{2-\lambda}(n/4)}$
$NPAS_E$	$W'_t = \lambda Z_t + (1-\lambda)W'_{t-1}$	$LCL = sin^{-1}(\sqrt{0.5}) - K\sqrt{\frac{\lambda}{2-\lambda}(1/4n)}$
		$UCL = sin^{-1}(\sqrt{0.5}) + K\sqrt{\frac{\lambda}{2-\lambda}(1/4n)}$
NPS_C	$C_t^+ = \max(0, C_{t-1}^- + M_t - (np_0 + k))$	H
	$C_t^- = \min(0, C_{t-1}^+ + M_t - (np_0 - k))$	

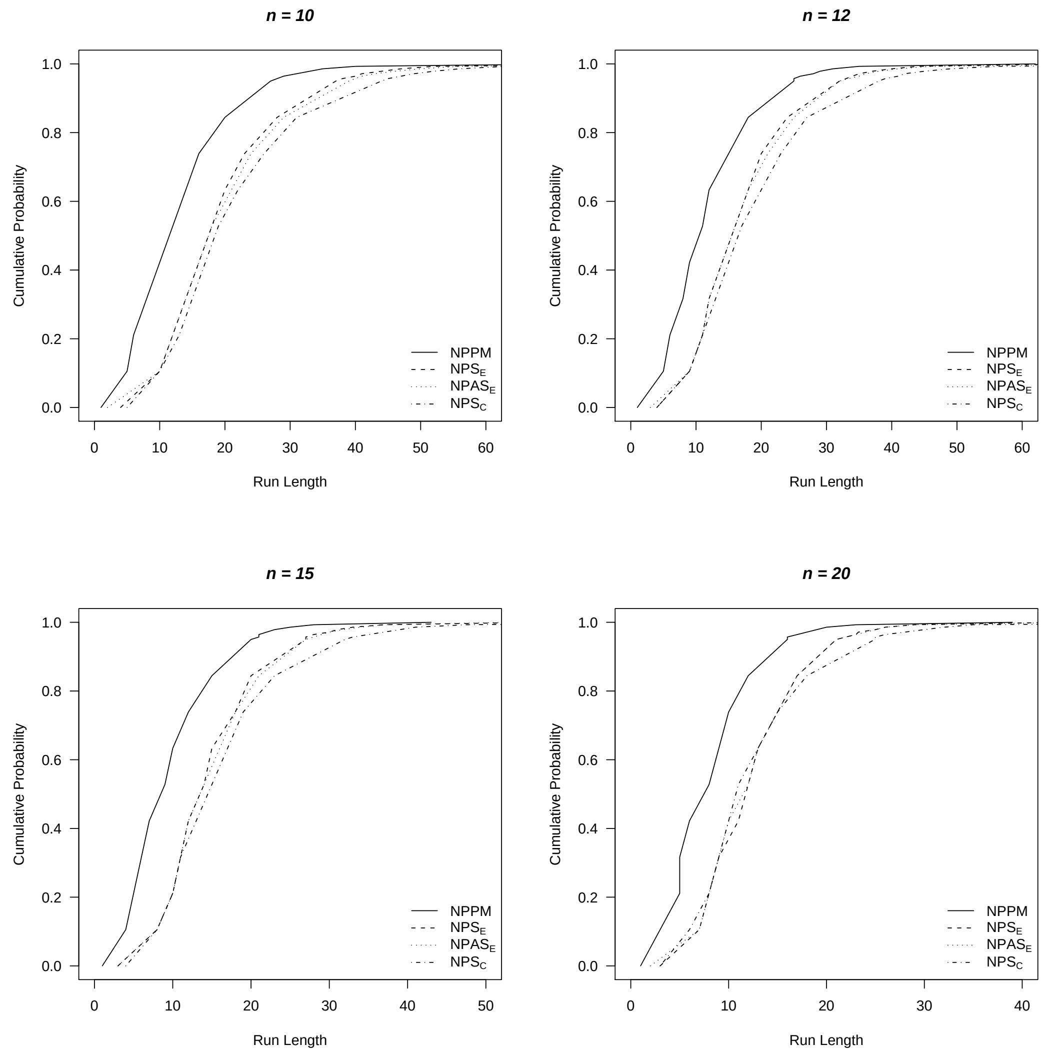

Figure 7.3: Run length curves of the $NPPM$, NPS_E, $NPAS_E$ and NPS_C charts when $ARL_0 = 370$ and $p = 0.6$

7.5 Example

To illustrate the application of the proposed $NPPM$ chart, we use the same example as used by Yang et al. (2011) and Yang and Cheng Yang and Cheng (2011) from Montgomery (2009)

> "The fill volume of soft-drink beverage bottles is an important quality characteristic. The volume is measured (approximately) by placing a gauge over the crown and comparing the height of the liquid in the neck of the bottle against a coded scale. On this scale, a reading of zero corresponds to the correct fill height. Fifteen samples of size $n = 10$ have been analyzed, and the fill heights are shown below:"

The data set with the PM, the EWMA (W_t and W_t') and the CUSUM (C_t^+ and C_t^-) statistics is given in Table 7.7. The control chart multipliers have been chosen to give the desired in-control average run length of 370 for all the charts. We use $L' = 3.803$ for the proposed $NPPM$ chart, $L = 2.49$ for NPS_E and $NPAS_E$ charts and $H = 9.98$ for the NPS_C chart. The resulting four control charts have been plotted in Figure 7.4.

The proposed $NPPM$ chart shows better detection ability as it detects the out-of-control signal at the 10th sample compared to the 13th sample for NPS_E, the 12th sample for the $NPAS_E$ chart, while the NPS_C chart is unable to detect any out-of-control signal. This simple example clearly shows the benefit of using the $NPPM$ chart as compared to its counterparts.

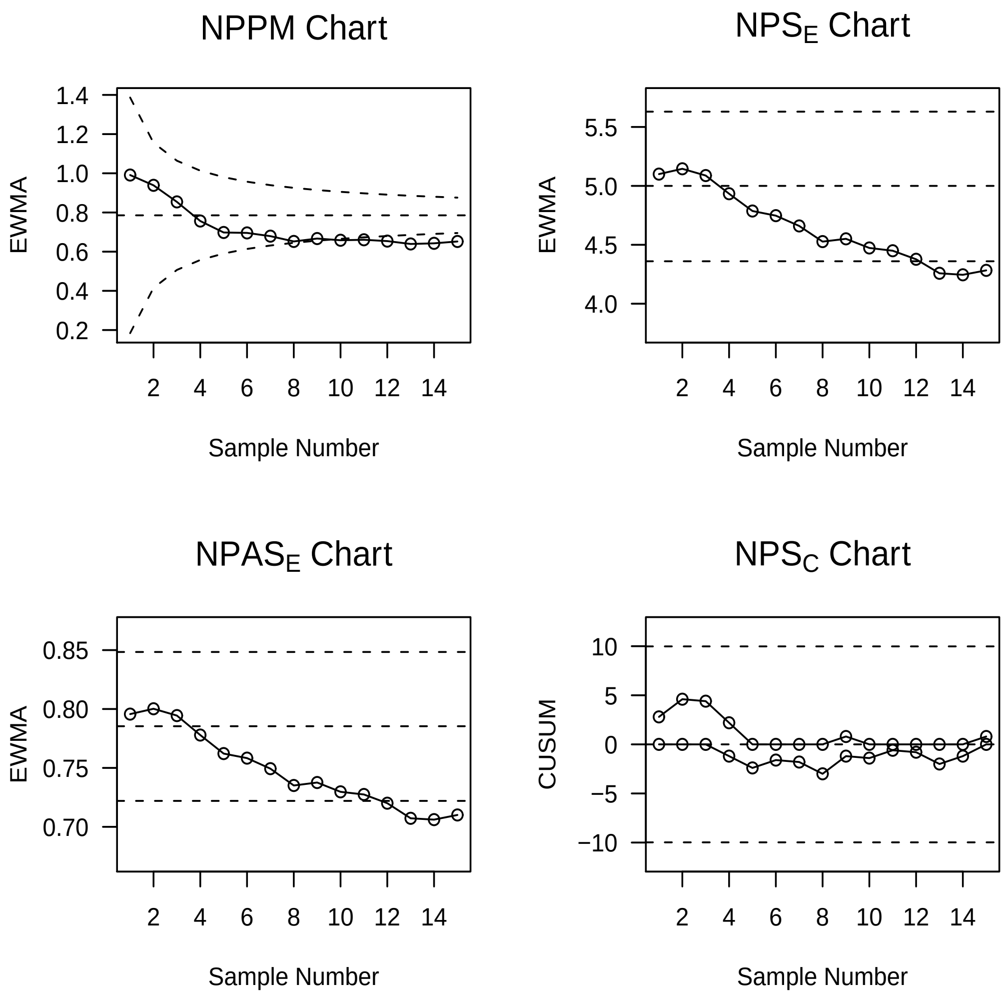

Figure 7.4: Control chart plots of $NPPM$, NPS_E, $NPAS_E$ and NPS_C charts for the given dataset

Table 7.7: Data set with Progressive mean, EWMA and CUSUM monitoring statistics

Sample	X_1	X_2	X_3	X_4	X_5	X_6	X_7	X_8	X_9	X_{10}	M	Z	PM_i	W_t	W'_t	C_t^+	C_t^-
1	2.5	0.5	2.0	-1.0	1.0	-1.0	0.5	1.5	0.5	-1.5	7	0.991	0.991	5.100	0.796	2.8	0.0
2	0.0	0.0	0.5	1.0	1.5	1.0	-1.0	1.0	1.5	-1.0	6	0.886	0.939	5.145	0.800	4.6	0.0
3	1.5	1.0	1.0	-1.0	0.0	-1.5	-1.0	-1.0	1.0	-1.0	4	0.685	0.854	5.088	0.794	4.4	0.0
4	0.0	0.5	-2.0	0.0	-1.0	1.5	-1.5	0.0	-2.0	-1.5	2	0.464	0.756	4.933	0.778	2.2	-1.2
5	0.0	0.0	0.0	-0.5	0.5	1.0	-0.5	-0.5	0.0	0.0	2	0.464	0.698	4.787	0.762	0.0	-2.4
6	1.0	-0.5	0.0	0.0	0.0	0.5	-1.0	1.0	-2.0	1.0	4	0.685	0.696	4.747	0.758	0.0	-1.6
7	1.0	-1.0	-1.0	-1.0	0.0	1.5	0.0	1.0	0.0	0.0	3	0.580	0.679	4.660	0.749	0.0	-1.8
8	0.0	-1.5	-0.5	1.5	0.0	0.0	0.0	-1.0	0.5	-0.5	2	0.464	0.652	4.527	0.735	0.0	-3.0
9	-2.0	-1.5	1.5	1.5	0.0	0.0	0.5	1.0	0.0	1.0	5	0.785	0.667	4.551	0.738	0.8	-1.2
10	-0.5	3.5	0.0	-1.0	-1.5	-1.5	-1.0	-1.0	1.0	0.5	3	0.580	**0.658**	4.473	0.730	0.0	-1.4
11	0.0	1.5	0.0	0.0	2.0	-1.5	0.5	-0.5	2.0	-1.0	4	0.685	0.661	4.449	0.727	0.0	-0.6
12	0.0	-2.0	-0.5	0.0	-0.5	2.0	1.5	0.0	0.5	-1.0	3	0.580	0.654	4.377	**0.720**	0.0	-0.8
13	-1.0	-0.5	-0.5	-1.0	0.0	0.5	0.5	-1.5	-1.0	-1.0	2	0.464	0.639	**4.258**	0.707	0.0	-2.0
14	0.5	1.0	-1.0	-0.5	-2.0	-1.0	-1.5	0.0	1.5	1.5	4	0.685	0.643	4.245	0.706	0.0	-1.2
15	1.0	0.0	1.5	1.5	1.0	-1.0	0.0	1.0	-2.0	-1.5	5	0.785	0.652	4.283	0.710	0.8	0.0

7.6 Conclusions

In this study we proposed a nonparametric progressive mean control chart, namely the $NPPM$ chart, using the progressive mean statistic. The proposed chart can be used for the efficient detection of departures from the process location or target, when the distribution of the quality characteristic of interest is uncertain. The performance of the proposed chart is compared with the recently proposed NPEWMA and NPCUSUM charts using different run length characteristics. The comparisons revealed that the proposed $NPPM$ chart has better detection ability compared to its counterparts. This study will help quality practitioners to choose an efficient nonparametric control chart for the monitoring of process location or target.

Chapter 8

Summary and Future Recommendations

8.1 Summary

Statistical process control provides tools for the monitoring of processes that help in the detection of abnormal variations in process (location and spread) parameters. This doctoral thesis deals with the variable control charts, for the monitoring of quantitative characteristics. The main findings from the conducted research are as follow:

- Chapter 2 investigated a number of Shewhart type dispersion control charts for normal and non-normal processes in the monitoring phase (Phase II). These dispersion charts are based on the sample range (R), the sample standard deviation (S), the inter-quartile range (IQR), Downton's estimator (D), the average absolute deviation (MD), the median absolute deviation (MAD), Sn and Qn estimates. Standardized variances and relative efficiencies were provided for all the estimators, considering normal and non-normal parent distributions. Logistic and Student's t distributions are used to represent the heavy-tailed symmetric distributions whereas Weibull, Gamma, Chi-square, Exponential and Lognormal distributions represented the case of skewed distributions.

The comparisons revealed that, for the case when the assumption of normality is valid, the S chart was the most efficient dispersion chart and the D and the MD charts can be considered as close competitors. For small values of sample size (n), the R and the IQR charts also performed well but lost efficiency (compared to the other charts) with increase in n. For non-normal parent distributions, the D and the MD charts showed better performance compared to the rest of the charts. The performance of the widely used R and S charts was greatly affected for most of the non-normal parent distributions. The MAD, S_n and Q_n charts were generally less efficient except for (the extremely skewed) lognormal distribution where these charts showed better detection ability, compared to the other charts. We discovered that, for a particular parent distribution, the performance of a Phase II dispersion chart is strongly related to the relative efficiency of the dispersion estimator used in its construction.

- Chapter 3 investigated a wide range of Shewhart type charts for the monitoring of process dispersion in the retrospective phase (Phase I). In addition to the dispersion estimates considered for Phase II monitoring, the pooled sample standard deviation and the distribution-free scale rank statistic (Jones-Farmer and Champ (2010)) were also examined. In SPC literature, the investigation of Phase I charts is mostly limited to normal or contaminated normal distributions. Little work has been to done to investigate a wide range of Phase I dispersion charts for processes following non-normal distributions. In this chapter, the Phase I performances of different dispersion charts for normal, heavy tailed symmetric (Logistic and Student's t) and skewed (Gamma and Exponential) distributions were evaluated. The probability of the charts to signal out-of-control samples (m_1) in the Phase I dataset was used as a performance measure. Control chart constants, required to set the control limits for the under study charts, were provided for the different parent distributions.

  The comparison among the ability of different structures for the detection of out-of-control samples revealed that, under the ideal assumption of normality, the S, D and MD charts exhibited the best performance for smaller choices of m_1 which deteriorated with an increase in the value of m_1. For larger values of m_1, the newly suggested V_2 charting structure had the highest signaling probability to detect out-of-control subgroups. The performance of most of the dispersion charts (except the distribution-free T_2 and V_2 charts) was extremely affected by an increase in the number of out-of-control samples. The detection ability of the charts was even more affected with an increase in the excess kurtosis and skewness for non-normal parent distributions. The newly suggested V_2 charting structure showed the best overall performance for both normal and non-normal parent environments.

- Chapter 4 investigated the EWMA dispersion charts for the monitoring phase (Phase II). The design structures of these charts were based on different dispersion estimates that were studied for Phase II monitoring using Shewhart charts (in Chapter 2). The performance of all the EWMA dispersion charts was evaluated using different run length characteristics such as average run length (ARL), median run length (MDRL) and standard deviation of the run length distribution (SDRL). To measure the overall effectiveness of the EWMA dispersion charts, the extra quadratic loss (EQL) and the relative ARL (RARL) criterion were examined. The results were reported for EWMA smoothing parameter $\lambda = 0.05, 0.25, 0.50$ and 0.75 considering $n = 5$ and 10.

  The comparisons revealed the superior performance of the S_E chart for normally distributed process with the D_E and the MD_E charts as close competitors. The R_E and Q_E charts also showed better performance for $n = 5$, but not as good when n was increased. For non-normal t and Gamma parent distributions, the D_E and the MD_E charts showed the best detection ability, compared to the rest of the charts. The Q_E chart again showed better performance but only for the small sample size. From the EQL results, it was observed that, for normal processes, most of the charts had better overall performance at either

$\lambda = 0.25$ or $\lambda = 0.50$; while, for the non-normal processes, at $\lambda = 0.05$ or $\lambda = 0.25$. The comparisons of the EWMA charts with the corresponding Shewhart charts indicated the superior performance of the EWMA structures, particularly for the detection of small shifts in σ.

For a particular parent distribution, the performance of the EWMA dispersion charts in Phase II also showed a strong relationship with the relative efficiency of the dispersion estimator used in its construction.

- Chapter 5 showed the impact of two component measurement error on the performance of EWMA control charts for the monitoring of analytical measurements. The two component error model proposed by Rocke and Lorenzato (1995), combined both additive error (that dominates at lower concentrations) and the multiplicative error (that dominates at higher concentrations) in a single model to adequately describe measurement error over the entire range of observations for an analytical process. This chapter evaluated the performance of the EWMA location chart in presence of the two component measurement error.

  The run length results indicated the worst effect of two component error on the EWMA chart performance occurred for low values of CV and the concentration level (μ) of the analyte. It was shown that the adverse effect of two component error model can be reduced by taking extra measurements (k) at each sample point. The use of a cost function approach was made to obtain the optimum choices of n and k. These optimum values indicated that a large number of multiple measurements (k) is usually required when the process variance (σ^2) is small compared to measurement error variances (σ_η^2 and σ_ϵ^2). As the measurement error variances (σ_η^2 and σ_ϵ^2) became smaller compared to σ^2, it was beneficial to take more sample units instead of taking extra measurements. It is also observed that, compared to the case of only additive error, the run length performance of the EWMA chart was more seriously affected by the presence of two component measurement error, particularly at higher concentration levels.

- Chapter 6 proposed the use of run rule schemes with a CUSUM dispersion chart for individual observations. In SPC literature, the investigation of run rules is mostly confined to Shewhart charts and their use with the memory charts (such as the EWMA or the CUSUM charts) is very limited. In this chapter, two run rule schemes for CUSUM dispersion charts were proposed with an aim of quickly detecting small shifts in the process standard deviation (σ). The proposed run rule schemes made use of a warning limit and declared a process to be out-of-control if either a point lies beyond the control limit (h) or if *2-of-2* or *2-of-3* points lie outside the warning limit (w). The run length properties of the proposed schemes were evaluated using Markov chain Monte Carlo methods following the work of Fu et al. (2002). We observed that both of the schemes were efficient and performed best for the detection of small shifts, when the control limit h was set equal to infinity (i.e. $h = \infty$). The run length results were provided for $\text{ARL}_0 = 120$ and 200 but similar behaviours are also expected for other ARL_0 values. Plots of ARL_0 vs w were provided for both the run rules schemes (at $h = \infty$) that can be used to approximate the control limits for the desired ARL_0 values (between 100 to 500).

  The performance of the proposed schemes was compared with the simple dispersion CUSUM and the relevant EWMA dispersion charts (the EWMS chart, the M-EWMS chart and the COMB chart), for individual observations. The comparisons revealed superior run length performance of the proposed schemes as compared to these counterparts, particularly for the detection of small shifts in σ.

- Chapter 7 proposed the use of the progressive mean statistic in nonparametric structures for the efficient detection of shifts in process target or location. As compared to Shewhart, EWMA and CUSUM charting statistics, the quick convergence ability of the PM statistic helped in the early detection of shifts in process parameters. The proposed nonparametric progressive mean ($NPPM$) chart was based on using the transformed sign statistic in the progressive setup. The $NPPM$ chart used the cumulative average of the sample values, observed over time as the monitoring statistic. This can be very useful for processes that have the tendency to go out-of-control at the start of a monitoring cycle or that produce frequent out-of-control signals.

The performance of the $NPPM$ chart was evaluated using different run length characteristics such as the average run length, standard deviation of the run length and the percentile points of the run length distribution. The $NPPM$ chart was equally efficient for the detection of both positive and negative shifts in the in-control process proportion (p_0). The steady state performance of the $NPPM$ chart was shown to be less efficient as compared to than the zero-state performance due to the fact of giving weight to the in-control sample observations. The run length results were provided for $\text{ARL}_0 = 370$ but similar behaviours have been observed for other choices of ARL_0. The values of the control chart multipliers were provided to achieve a specified ARL_0 (between 200 to 500) for some representative choices of sample size n.

The comparisons among the competing charts revealed that the proposed $NPPM$ chart outperformed the recent nonparametric EWMA and nonparametric CUSUM charts, in terms of detecting shifts in process target or location.

8.2 Future Work

We discovered that the investigation of the following issues in SPC also needs attention.

- Distribution fitting of the common cause variation in Phase I.
- Investigating the Phase II performance of Shewhart and EWMA dispersion charts for non-normal and contaminated normal processes when only a limited number of samples are available for the estimation of unknown parameters in Phase I.

  - We already did some work in this direction that includes robust methods of estimating σ in Phase I and further to see how it effects the EWMA chart's performance in Phase II.

- Enhancing the performance of control charts with the use of auxiliary information.

  - A paper in this direction has already been submitted in Journal of Advanced Manufacturing Technology that involves constructing design structure of a Phase II variability chart based on using information of a single auxiliary variable.
  - In another study, we are investigating location estimators that utilize information on one or/and two auxiliary variables for efficient Phase II monitoring.

- Economic-statistical design of memory and memory less dispersion charts.

- Development of distribution free EWMA structures for monitoring process dispersion.

- Investigating the robustness to non-normality of progressive mean charts for monitoring process location and dispersion.

Appendix A

Table A.1: Control chart coefficient t_2 for different dispersion charts under normal and non-normal distributions

Distribution	n	R	S	IQR	D	MD	MAD	Sn	Qn
Normal	3	1.6903	0.8850	1.2530	0.9986	0.5634	0.6713	0.9995	0.9999
	5	2.3260	0.9417	1.2310	1.0016	0.6642	0.8235	1.0034	1.0031
	7	2.7000	0.9574	1.1194	0.9981	0.7022	0.8783	0.9990	0.9998
	10	3.0764	0.9724	1.1009	0.9997	0.7390	0.9128	0.9933	1.0073
	12	3.2576	0.9778	1.0815	1.0005	0.7489	0.9310	0.9957	1.0054
Logistic	3	1.6508	0.8647	1.2237	0.9753	0.5503	0.6525	0.9715	0.9720
	5	2.2989	0.9235	1.1922	0.9776	0.6433	0.7741	0.9543	0.9584
	7	2.7025	0.9453	1.0484	0.9772	0.6798	0.8172	0.9434	0.9528
	10	3.1221	0.9621	1.3794	0.9778	0.7126	0.8433	0.9284	0.9593
	12	3.3289	0.9676	0.9952	0.9767	0.7198	0.8506	0.9230	0.9500
Student's t	3	1.6082	0.8435	1.1922	0.9502	0.5361	0.6253	0.9310	0.9314
	5	2.2457	0.9011	1.1522	0.9490	0.6217	0.7302	0.9036	0.9094
	7	2.6607	0.9268	0.9918	0.9504	0.6573	0.7698	0.8922	0.9038
	10	3.1012	0.9454	0.9617	0.9503	0.6869	0.7883	0.8725	0.9080
	12	3.3308	0.9536	0.9335	0.9505	0.6946	0.7963	0.8680	0.9011
Weibull	3	1.6310	0.8583	1.2091	0.9636	0.5437	0.6067	0.9033	0.9038
	5	2.2496	0.9214	1.1914	0.9685	0.6429	0.7538	0.9085	0.9069
	7	2.6032	0.9419	1.0897	0.9654	0.6803	0.8087	0.9033	0.8928
	10	2.9607	0.9595	1.0698	0.9662	0.7151	0.8470	0.9073	0.9056
	12	3.1321	0.9670	1.0534	0.9670	0.7253	0.8660	0.9090	0.8995
Chi-square	3	1.6091	0.8473	1.1928	0.9507	0.5364	0.5946	0.8853	0.8857
	5	2.2199	0.9078	1.1656	0.9508	0.6289	0.7252	0.8765	0.8768
	7	2.5913	0.9325	1.0526	0.9512	0.6668	0.7808	0.8754	0.8702
	10	2.9607	0.9508	1.0298	0.9507	0.6995	0.8107	0.8705	0.8767
	12	3.1438	0.9579	1.0071	0.9502	0.7075	0.8226	0.8678	0.8680
Gamma	3	1.5891	0.8383	1.1780	0.9389	0.5297	0.5738	0.8543	0.8547
	5	2.1925	0.8991	1.1496	0.9384	0.6203	0.7016	0.8466	0.8479
	7	2.5659	0.9269	1.0358	0.9399	0.6581	0.7522	0.8413	0.8359
	10	2.9374	0.9460	1.0093	0.9387	0.6894	0.7816	0.8388	0.8433
	12	3.1229	0.9546	0.9894	0.9394	0.6981	0.7959	0.8372	0.8361
Exponential	3	1.5004	0.7970	1.1122	0.8864	0.5001	0.4937	0.7351	0.7355
	5	2.0848	0.8668	1.0831	0.8874	0.5844	0.5946	0.7083	0.7155
	7	2.4438	0.8958	0.9498	0.8842	0.6154	0.6298	0.6921	0.6925
	10	2.8252	0.9224	0.9238	0.8849	0.6446	0.6560	0.7005	0.7064
	12	3.0209	0.9347	0.9022	0.8861	0.6530	0.6662	0.6949	0.6931
Lognormal	3	1.1911	0.6399	0.8830	0.7037	0.3970	0.3336	0.4967	0.4969
	5	1.6995	0.7118	0.8385	0.7022	0.4524	0.3807	0.4546	0.4635
	7	2.0654	0.7547	0.6534	0.7033	0.4743	0.3928	0.4332	0.4419
	10	2.4858	0.7953	0.6228	0.7042	0.4928	0.4006	0.4286	0.4466
	12	2.7253	0.8166	0.5931	0.7058	0.4981	0.4019	0.4201	0.4339

Table A.2: Control chart coefficient t_3 for different dispersion charts under normal and non-normal distributions

Distribution	n	R	S	IQR	D	MD	MAD	Sn	Qn
Normal	3	0.8848	0.4615	0.6559	0.5228	0.2949	0.5525	0.8227	0.8231
	5	0.8644	0.3412	0.4606	0.3658	0.2485	0.4807	0.5519	0.5387
	7	0.8293	0.2806	0.4380	0.2952	0.2150	0.4181	0.4259	0.4119
	10	0.7986	0.2327	0.3457	0.2415	0.1869	0.3378	0.3342	0.3027
	12	0.7773	0.2108	0.3223	0.2180	0.1711	0.3143	0.3000	0.2705
Logistic	3	0.9560	0.4997	0.7087	0.5648	0.3187	0.5684	0.8464	0.8468
	5	0.9829	0.3830	0.4924	0.4028	0.2657	0.4720	0.5541	0.5454
	7	0.9929	0.3258	0.4402	0.3318	0.2315	0.4078	0.4297	0.4207
	10	0.9964	0.2750	0.4604	0.2724	0.1998	0.3277	0.3309	0.3161
	12	0.9976	0.2508	0.3142	0.2459	0.1821	0.2999	0.2955	0.2791
Student's t	3	1.0265	0.5413	0.7609	0.6064	0.3422	0.5607	0.8348	0.8352
	5	1.1003	0.4316	0.5230	0.4388	0.2822	0.4548	0.5392	0.5330
	7	1.1442	0.3756	0.4299	0.3621	0.2443	0.3897	0.4171	0.4108
	10	1.1922	0.3226	0.3280	0.2975	0.2089	0.3082	0.3163	0.3083
	12	1.2199	0.2997	0.3019	0.2708	0.1918	0.2844	0.2842	0.2746
Weibull	3	0.9580	0.5082	0.7102	0.5660	0.3193	0.5216	0.7766	0.7770
	5	0.9587	0.3925	0.5010	0.4021	0.2704	0.4602	0.5263	0.5136
	7	0.9384	0.3330	0.4666	0.3280	0.2354	0.4042	0.4132	0.3864
	10	0.9191	0.2816	0.3658	0.2691	0.2041	0.3282	0.3320	0.2887
	12	0.9056	0.2581	0.3414	0.2436	0.1872	0.3067	0.3001	0.2559
Chi-square	3	0.9945	0.5289	0.7372	0.5876	0.3315	0.5224	0.7778	0.7782
	5	1.0177	0.4164	0.5175	0.4206	0.2792	0.4500	0.5177	0.5057
	7	1.0179	0.3591	0.4716	0.3468	0.2444	0.3964	0.4082	0.3860
	10	1.0138	0.3064	0.3672	0.2847	0.2110	0.3223	0.3254	0.2894
	12	1.0093	0.2819	0.3399	0.2578	0.1934	0.2966	0.2922	0.2541
Gamma	3	1.0196	0.5447	0.7559	0.6024	0.3399	0.5143	0.7657	0.7661
	5	1.0504	0.4328	0.5315	0.4333	0.2868	0.4457	0.5130	0.5031
	7	1.0586	0.3752	0.4776	0.3577	0.2508	0.3926	0.4062	0.3818
	10	1.0583	0.3208	0.3691	0.2927	0.2154	0.3164	0.3241	0.2860
	12	1.0565	0.2962	0.3425	0.2662	0.1981	0.2941	0.2925	0.2528
Exponential	3	1.1234	0.6073	0.8328	0.6638	0.3745	0.4924	0.7332	0.7336
	5	1.1942	0.5009	0.5891	0.4867	0.3179	0.4294	0.4950	0.4916
	7	1.2190	0.4397	0.5034	0.4020	0.2764	0.3738	0.3919	0.3720
	10	1.2389	0.3824	0.3912	0.3322	0.2387	0.3057	0.3237	0.2907
	12	1.2451	0.3546	0.3599	0.3010	0.2183	0.2826	0.2912	0.2553
Lognormal	3	1.3956	0.7747	1.0346	0.8246	0.4652	0.3984	0.5931	0.5934
	5	1.5988	0.6864	0.6968	0.6121	0.3760	0.3139	0.3647	0.3687
	7	1.7858	0.6529	0.4583	0.5213	0.3287	0.2629	0.2783	0.2738
	10	1.9611	0.6043	0.3377	0.4337	0.2793	0.2087	0.2244	0.2160
	12	2.1005	0.5927	0.3001	0.4019	0.2595	0.1898	0.1980	0.1856

Table A.3: Lower ($\alpha/2$) quantile points of the distribution of Z for different dispersion charts under normal and non-normal distributions when $\alpha = 0.002$

Distribution	n	R	S	IQR	D	MD	MAD	Sn	Qn
Normal	3	0.0616	0.0326	0.0456	0.0364	0.0205	0.0008	0.0012	0.0012
	5	0.3637	0.1527	0.1958	0.1613	0.1057	0.0219	0.0295	0.0342
	7	0.6946	0.2523	0.1639	0.2617	0.1785	0.0682	0.0855	0.1055
	10	1.0720	0.3537	0.2913	0.3646	0.2650	0.1747	0.2099	0.2546
	12	1.3015	0.4149	0.2967	0.4210	0.3080	0.2066	0.2563	0.3041
Logistic	3	0.0554	0.0296	0.0411	0.0327	0.0185	0.0008	0.0012	0.0012
	5	0.3319	0.1348	0.1751	0.1436	0.0945	0.0204	0.0261	0.0303
	7	0.6292	0.2289	0.1405	0.2378	0.1607	0.0617	0.0811	0.0990
	10	0.9980	0.3350	0.3471	0.3406	0.2485	0.1465	0.1917	0.2427
	12	1.1717	0.3747	0.2667	0.3790	0.2802	0.1844	0.2328	0.2824
Student's t	3	0.0553	0.0290	0.0410	0.0327	0.0184	0.0007	0.0011	0.0011
	5	0.2909	0.1237	0.1549	0.1317	0.0836	0.0200	0.0259	0.0294
	7	0.5894	0.2136	0.1321	0.2185	0.1493	0.0600	0.0731	0.0933
	10	0.9072	0.2996	0.2356	0.3054	0.2210	0.1371	0.1733	0.2132
	12	1.0957	0.3436	0.2439	0.3496	0.2530	0.1740	0.2177	0.2594
Weibull	3	0.0455	0.0241	0.0337	0.0269	0.0152	0.0008	0.0011	0.0011
	5	0.3248	0.1333	0.1684	0.1406	0.0908	0.0218	0.0286	0.0333
	7	0.6191	0.2273	0.1432	0.2345	0.1619	0.0639	0.0814	0.0985
	10	0.9311	0.3136	0.2608	0.3206	0.2285	0.1517	0.1877	0.2198
	12	1.1183	0.3607	0.2646	0.3685	0.2692	0.1796	0.2171	0.2646
Chi-square	3	0.0505	0.0268	0.0374	0.0298	0.0168	0.0008	0.0012	0.0012
	5	0.3133	0.1282	0.1666	0.1375	0.0899	0.0206	0.0269	0.0311
	7	0.5764	0.2111	0.1326	0.2203	0.1491	0.0560	0.0671	0.0867
	10	0.8935	0.3000	0.2445	0.3071	0.2179	0.1372	0.1736	0.2083
	12	1.1015	0.3514	0.2443	0.3579	0.2562	0.1741	0.2149	0.2573
Gamma	3	0.0494	0.0264	0.0367	0.0292	0.0165	0.0007	0.0010	0.0010
	5	0.2733	0.1146	0.1440	0.1197	0.0777	0.0193	0.0260	0.0292
	7	0.5352	0.1947	0.1277	0.2036	0.1406	0.0558	0.0680	0.0862
	10	0.8662	0.2837	0.2322	0.2899	0.2111	0.1338	0.1626	0.1973
	12	1.0556	0.3312	0.2349	0.3337	0.2434	0.1629	0.1998	0.2399
Exponential	3	0.0320	0.0167	0.0237	0.0189	0.0107	0.0005	0.0007	0.0007
	5	0.1890	0.0781	0.0982	0.0809	0.0530	0.0140	0.0174	0.0201
	7	0.3791	0.1402	0.0963	0.1452	0.1003	0.0383	0.0456	0.0572
	10	0.6368	0.2126	0.1793	0.2158	0.1565	0.0895	0.1081	0.1318
	12	0.7745	0.2526	0.1903	0.2552	0.1893	0.1226	0.1382	0.1686
Lognormal	3	0.0202	0.0104	0.0150	0.0119	0.0067	0.0004	0.0006	0.0006
	5	0.1187	0.0484	0.0627	0.0518	0.0338	0.0078	0.0103	0.0116
	7	0.2221	0.0819	0.0581	0.0845	0.0587	0.0235	0.0274	0.0344
	10	0.3637	0.1200	0.1006	0.1234	0.0901	0.0536	0.0657	0.0810
	12	0.4394	0.1411	0.1059	0.1434	0.1047	0.0701	0.0798	0.0943

Table A.4: Upper $(1-\alpha/2)$ quantile points of the distribution of Z for different dispersion charts under normal and non-normal distributions when $\alpha = 0.002$

Distribution	n	R	S	IQR	D	MD	MAD	Sn	Qn
Normal	3	5.0781	2.6336	3.7644	3.0002	1.6927	3.1554	4.6982	4.7004
	5	5.4800	2.1454	2.9096	2.3127	1.5700	2.7535	3.1284	3.1981
	7	5.7617	1.9431	2.7514	2.0399	1.4815	2.5412	2.5681	2.6066
	10	6.0339	1.7497	2.3519	1.8130	1.3976	2.1749	2.2462	2.0895
	12	6.0533	1.6881	2.2293	1.7343	1.3439	2.0810	2.0961	1.9704
Logistic	3	6.0201	3.1611	4.4627	3.5568	2.0067	3.5261	5.2501	5.2527
	5	6.6291	2.5929	3.2389	2.6622	1.7477	2.9255	3.3891	3.4908
	7	7.0971	2.3109	2.8317	2.3066	1.5966	2.5622	2.6496	2.7212
	10	7.5385	2.0834	3.2737	2.0891	1.4848	2.1359	2.2719	2.2251
	12	7.6412	1.9622	2.1889	1.8953	1.4016	2.0237	2.0791	2.0150
Student's t	3	7.6479	4.0606	5.6694	4.5185	2.5493	3.7318	5.5564	5.5591
	5	8.8445	3.4935	3.8829	3.3992	2.0952	2.8208	3.3720	3.4142
	7	9.3920	3.1611	2.9135	2.7993	1.8149	2.5113	2.7258	2.7552
	10	10.4630	2.8866	2.3173	2.4543	1.6569	2.0522	2.1860	2.2001
	12	10.7478	2.7541	2.1320	2.2869	1.5607	1.9289	1.9885	1.9876
Weibull	3	5.8434	3.1282	4.3317	3.4524	1.9478	3.1899	4.7495	4.7518
	5	6.3226	2.5816	3.1947	2.5954	1.7238	2.7920	3.1315	3.2011
	7	6.5423	2.2848	3.0017	2.1934	1.5774	2.5449	2.6048	2.4794
	10	6.8481	2.0662	2.5119	1.9628	1.4827	2.1189	2.3037	2.0122
	12	6.9263	1.9663	2.3748	1.8602	1.4271	2.0443	2.1437	1.8468
Chi-square	3	6.4038	3.4531	4.7471	3.7835	2.1346	3.2357	4.8178	4.8201
	5	6.8253	2.8212	3.3871	2.7541	1.8277	2.8058	3.1928	3.2529
	7	7.4282	2.6012	3.1337	2.4058	1.6632	2.4630	2.5825	2.4927
	10	7.6663	2.2987	2.5376	2.0878	1.5183	2.1404	2.2647	2.0471
	12	7.9404	2.2160	2.3846	1.9777	1.4669	2.0358	2.0848	1.8856
Gamma	3	6.6313	3.6300	4.9158	3.9179	2.2104	3.3087	4.9264	4.9288
	5	7.3437	3.0226	3.5561	2.9458	1.9189	2.8233	3.2150	3.2961
	7	7.5007	2.6402	3.1485	2.4416	1.7032	2.5185	2.6211	2.5309
	10	7.9755	2.4133	2.6271	2.1421	1.5720	2.1215	2.3074	2.0431
	12	8.2333	2.2945	2.3679	2.0237	1.4930	1.9594	2.0808	1.8268
Exponential	3	7.7378	4.3051	5.7361	4.5716	2.5793	3.4219	5.0950	5.0975
	5	8.2139	3.4926	3.8982	3.2668	2.1034	2.8498	3.2589	3.3590
	7	8.6614	3.1324	3.3532	2.7278	1.8455	2.4841	2.5807	2.4814
	10	9.1918	2.8072	2.7316	2.3169	1.6515	2.0598	2.2603	2.0332
	12	9.1887	2.6160	2.4846	2.1323	1.5439	1.9177	2.0122	1.8210
Lognormal	3	13.6859	7.7218	10.1453	8.0858	4.5620	3.6355	5.4130	5.4156
	5	14.9092	6.4870	6.0127	5.5493	3.2444	2.4684	2.8511	2.9129
	7	16.6869	6.1643	3.7764	4.7507	2.9136	1.9804	2.0747	2.0631
	10	18.6468	5.7475	2.5807	3.7692	2.3552	1.4836	1.6497	1.6315
	12	20.3507	5.7654	2.3165	3.6118	2.2258	1.3713	1.4645	1.3670

Table A.5: Relative Efficiency of different dispersion statistics under normal and non-normal distributions

Distribution	n	R	S	IQR	D	MD	MAD	Sn	Qn
Normal	3	99.24	100.00	99.24	99.21	99.25	40.14	40.14	40.13
	5	95.06	100.00	93.77	98.42	93.79	38.53	43.39	45.52
	7	91.05	100.00	56.11	98.20	91.63	37.91	47.26	50.61
	10	84.98	100.00	58.08	98.13	89.53	41.82	50.59	63.42
	12	81.63	100.00	52.33	97.90	89.04	40.78	51.20	64.21
Logistic	3	99.58	100.00	99.57	99.58	99.57	44.01	44.00	44.00
	5	92.87	98.70	99.52	100.00	99.52	45.66	50.36	52.42
	7	85.41	97.06	65.39	100.00	99.41	46.30	55.57	59.13
	10	76.20	94.99	69.67	100.00	98.72	51.40	61.09	71.48
	12	70.58	94.35	63.59	100.00	99.04	50.99	61.84	73.44
Student's t	3	99.97	98.90	99.98	100.00	99.96	50.65	50.66	50.65
	5	85.83	89.81	100.00	96.37	100.00	53.11	57.86	59.98
	7	74.70	84.11	73.52	95.16	100.00	53.90	63.21	66.87
	10	62.58	79.43	79.51	94.37	100.00	60.51	70.38	80.23
	12	56.84	77.19	72.90	93.94	100.00	59.78	71.12	82.11
Weibull	3	99.97	98.38	99.96	99.96	100.00	46.66	46.66	46.66
	5	94.91	94.99	97.48	100.00	97.44	46.25	51.36	53.74
	7	88.83	92.35	62.96	100.00	96.41	46.21	55.17	61.63
	10	80.49	90.06	66.35	100.00	95.22	51.66	57.93	76.33
	12	75.91	89.08	60.42	100.00	95.26	50.60	58.22	78.41
Chi-square	3	99.99	98.02	99.99	99.98	100.00	49.48	49.48	49.47
	5	93.11	93.01	99.27	100.00	99.29	50.82	56.09	58.83
	7	86.15	89.64	66.22	100.00	98.95	51.57	61.13	67.56
	10	76.48	86.36	70.53	100.00	98.56	56.74	64.18	82.30
	12	71.42	84.99	64.62	100.00	98.51	56.62	64.93	85.89
Gamma	3	99.99	97.50	99.98	100.00	99.97	51.24	51.24	51.24
	5	92.89	92.01	99.74	100.00	99.73	52.83	58.07	60.56
	7	85.09	88.39	68.12	100.00	99.72	53.17	62.13	69.42
	10	74.90	84.55	72.70	100.00	99.60	59.33	65.13	84.53
	12	70.16	83.40	67.01	100.00	99.72	58.81	65.78	87.84
Exponential	3	100.00	96.55	99.99	99.96	99.97	56.36	56.35	56.35
	5	90.16	88.59	100.00	98.35	99.97	56.72	60.57	62.67
	7	81.07	83.73	71.81	97.59	100.00	57.26	62.91	69.91
	10	71.31	79.79	76.47	97.30	100.00	63.15	64.22	80.97
	12	65.79	77.65	70.23	96.85	100.00	62.11	63.64	82.37
Lognormal	3	100.00	93.67	100.00	99.98	99.98	96.26	96.28	96.26
	5	71.50	68.05	91.63	83.28	91.60	93.07	98.32	100.00
	7	51.35	51.29	78.03	69.88	79.93	85.70	93.02	100.00
	10	37.58	40.52	79.56	61.67	72.82	86.19	85.34	100.00
	12	30.80	34.73	71.47	56.43	67.41	82.04	82.37	100.00

Appendix B

Table B.1: RL characteristics of the R_E chart for normally distributed quality characteristic when $\text{ARL}_0 = 200$

		n							
		5				10			
		λ				λ			
δ		0.05	0.25	0.50	0.75	0.05	0.25	0.50	0.75
1.00	ARL	200.13	199.55	199.32	199.64	198.04	200.89	198.63	198.89
	MDRL	139.00	140.00	140.00	135.00	137.00	138.00	139.00	138.00
	SDRL	195.72	197.30	196.56	204.32	193.78	199.61	198.43	198.26
1.10	ARL	33.58	42.67	52.66	60.60	22.50	29.57	38.97	47.76
	MDRL	26.00	31.00	37.00	42.00	18.00	21.00	27.00	33.00
	SDRL	27.02	40.24	52.39	60.36	16.02	27.04	38.37	47.04
1.20	ARL	15.79	17.34	20.96	25.47	10.33	10.86	13.30	17.13
	MDRL	13.00	13.00	15.00	18.00	9.00	8.00	10.00	12.00
	SDRL	10.24	14.54	19.61	24.39	5.69	8.41	11.90	16.20
1.30	ARL	10.08	9.75	11.62	13.68	6.66	6.10	6.89	8.46
	MDRL	9.00	8.00	9.00	10.00	6.00	5.00	5.00	6.00
	SDRL	5.64	7.40	10.31	12.72	3.13	4.05	5.59	7.67
1.40	ARL	7.37	6.61	7.25	8.64	5.04	4.29	4.40	5.09
	MDRL	7.00	5.00	5.00	6.00	5.00	4.00	4.00	4.00
	SDRL	3.86	4.62	6.05	7.95	2.18	2.57	3.26	4.28
1.50	ARL	5.86	5.02	5.22	5.87	4.04	3.26	3.22	3.52
	MDRL	5.00	4.00	4.00	4.00	4.00	3.00	3.00	3.00
	SDRL	2.86	3.32	4.10	5.07	1.62	1.76	2.14	2.68
1.60	ARL	4.88	4.08	4.08	4.47	3.38	2.67	2.54	2.70
	MDRL	4.00	3.00	3.00	3.00	3.00	2.00	2.00	2.00
	SDRL	2.31	2.53	3.08	3.75	1.29	1.35	1.57	1.94
1.80	ARL	3.75	2.92	2.84	2.93	2.64	2.02	1.87	1.85
	MDRL	3.00	3.00	2.00	2.00	2.00	2.00	2.00	2.00
	SDRL	1.63	1.68	1.90	2.21	0.97	0.94	1.03	1.12
2.00	ARL	3.06	2.38	2.21	2.24	2.18	1.67	1.52	1.48
	MDRL	3.00	2.00	2.00	2.00	2.00	2.00	1.00	1.00
	SDRL	1.32	1.28	1.38	1.53	0.77	0.74	0.73	0.77
2.50	ARL	2.21	1.69	1.57	1.54	1.60	1.24	1.16	1.14
	MDRL	2.00	2.00	1.00	1.00	2.00	1.00	1.00	1.00
	SDRL	0.92	0.82	0.81	0.85	0.59	0.45	0.39	0.38
3.00	ARL	1.77	1.41	1.29	1.28	1.29	1.09	1.06	1.04
	MDRL	2.00	1.00	1.00	1.00	1.00	1.00	1.00	1.00
	SDRL	0.74	0.62	0.56	0.58	0.47	0.30	0.23	0.20
3.50	ARL	1.52	1.25	1.18	1.16	1.14	1.04	1.02	1.01
	MDRL	1.00	1.00	1.00	1.00	1.00	1.00	1.00	1.00
	SDRL	0.62	0.49	0.42	0.41	0.35	0.19	0.14	0.12
4.00	ARL	1.35	1.16	1.11	1.10	1.06	1.01	1.01	1.01
	MDRL	1.00	1.00	1.00	1.00	1.00	1.00	1.00	1.00
	SDRL	0.53	0.39	0.33	0.32	0.25	0.11	0.09	0.08

Table B.2: RL characteristics of the R_E chart for t-distributed quality characteristic when $\mathrm{ARL}_0 = 200$

		n							
		5				10			
		λ				λ			
δ		0.05	0.25	0.50	0.75	0.05	0.25	0.50	0.75
1.00	ARL	200.06	202.15	193.33	201.64	198.73	199.55	200.58	199.11
	MDRL	139.00	140.00	135.00	141.00	138.00	139.00	141.00	136.00
	SDRL	199.60	201.60	191.70	203.24	196.62	200.09	197.80	200.42
1.10	ARL	48.68	76.79	96.71	111.20	39.44	66.70	90.97	104.02
	MDRL	37.00	55.00	66.00	77.00	30.00	47.00	63.00	73.00
	SDRL	41.48	73.81	97.35	110.86	32.62	64.78	89.62	102.97
1.20	ARL	22.63	35.81	52.59	65.98	17.78	29.11	46.57	59.62
	MDRL	18.00	26.00	37.00	46.00	15.00	22.00	32.00	42.00
	SDRL	16.89	32.84	52.15	65.29	11.72	26.38	45.52	58.95
1.30	ARL	14.35	20.69	30.94	41.02	11.05	15.55	25.62	35.78
	MDRL	12.00	15.00	22.00	29.00	10.00	12.00	18.00	25.00
	SDRL	9.29	17.98	30.02	40.55	6.21	12.78	23.70	35.20
1.40	ARL	10.48	13.31	20.23	27.56	8.11	10.00	16.28	22.87
	MDRL	9.00	10.00	15.00	19.00	7.00	8.00	12.00	16.00
	SDRL	6.21	10.68	18.95	26.65	4.08	7.37	14.86	22.36
1.50	ARL	8.23	9.57	13.85	19.26	6.38	7.22	10.90	15.67
	MDRL	7.00	8.00	10.00	14.00	6.00	6.00	8.00	11.00
	SDRL	4.46	7.34	12.64	18.55	3.01	4.93	9.48	14.74
1.60	ARL	6.77	7.55	10.19	14.28	5.29	5.55	7.71	11.13
	MDRL	6.00	6.00	8.00	10.00	5.00	5.00	6.00	8.00
	SDRL	3.52	5.44	8.96	13.78	2.34	3.49	6.34	10.18
1.80	ARL	5.08	5.03	6.41	8.53	4.04	3.84	4.73	6.42
	MDRL	5.00	4.00	5.00	6.00	4.00	3.00	4.00	5.00
	SDRL	2.45	3.23	5.17	7.85	1.69	2.14	3.47	5.61
2.00	ARL	4.11	3.87	4.60	5.77	3.28	2.98	3.40	4.23
	MDRL	4.00	3.00	4.00	4.00	3.00	3.00	3.00	3.00
	SDRL	1.88	2.32	3.53	4.94	1.32	1.50	2.24	3.38
2.50	ARL	2.87	2.53	2.67	3.02	2.33	1.99	2.02	2.20
	MDRL	3.00	2.00	2.00	2.00	2.00	2.00	2.00	2.00
	SDRL	1.27	1.35	1.70	2.29	0.86	0.88	1.06	1.45
3.00	ARL	2.28	1.96	1.97	2.09	1.85	1.58	1.51	1.56
	MDRL	2.00	2.00	2.00	2.00	2.00	1.00	1.00	1.00
	SDRL	0.96	0.97	1.13	1.37	0.68	0.65	0.69	0.84
3.50	ARL	1.92	1.63	1.60	1.64	1.58	1.33	1.28	1.29
	MDRL	2.00	1.00	1.00	1.00	2.00	1.00	1.00	1.00
	SDRL	0.81	0.76	0.83	0.94	0.58	0.52	0.51	0.56
4.00	ARL	1.70	1.46	1.41	1.43	1.40	1.19	1.16	1.15
	MDRL	2.00	1.00	1.00	1.00	1.00	1.00	1.00	1.00
	SDRL	0.70	0.64	0.66	0.71	0.52	0.41	0.38	0.40

Table B.3: RL characteristics of the R_E chart for Gamma distributed quality characteristic when $\text{ARL}_0 = 200$

		n							
		5				10			
		λ				λ			
δ		0.05	0.25	0.50	0.75	0.05	0.25	0.50	0.75
1.00	ARL	199.05	199.09	201.73	201.65	199.77	199.92	201.94	200.48
	MDRL	137.00	136.00	141.00	139.00	140.00	140.00	143.00	138.00
	SDRL	196.57	195.36	197.85	202.67	197.44	197.35	202.44	202.69
1.10	ARL	46.43	66.42	82.46	91.39	34.82	52.24	71.34	82.33
	MDRL	35.00	48.00	57.00	62.00	27.00	37.00	51.00	57.00
	SDRL	39.70	63.39	82.08	92.58	28.25	49.93	69.23	81.97
1.20	ARL	21.75	29.76	41.96	49.82	15.77	21.75	31.60	41.02
	MDRL	17.00	21.00	30.00	35.00	13.00	16.00	22.00	29.00
	SDRL	16.03	27.30	40.68	49.69	10.25	19.09	30.12	40.52
1.30	ARL	13.89	17.13	24.20	29.48	9.94	12.07	17.06	22.63
	MDRL	12.00	13.00	17.00	21.00	9.00	9.00	12.00	16.00
	SDRL	8.87	14.71	22.94	28.38	5.56	9.57	15.71	21.83
1.40	ARL	10.06	11.54	15.61	19.58	7.43	7.87	10.67	14.12
	MDRL	9.00	9.00	11.00	14.00	7.00	6.00	8.00	10.00
	SDRL	5.97	9.29	14.49	18.78	3.79	5.65	9.53	13.09
1.50	ARL	7.93	8.40	10.89	13.64	5.85	5.79	7.30	9.50
	MDRL	7.00	7.00	8.00	10.00	5.00	5.00	6.00	7.00
	SDRL	4.39	6.38	9.70	13.18	2.71	3.74	5.96	8.63
1.60	ARL	6.55	6.66	8.15	10.15	4.89	4.54	5.50	6.89
	MDRL	6.00	5.00	6.00	7.00	5.00	4.00	4.00	5.00
	SDRL	3.42	4.77	6.96	9.38	2.20	2.77	4.17	6.04
1.80	ARL	4.92	4.58	5.32	6.25	3.75	3.24	3.54	4.18
	MDRL	4.00	4.00	4.00	5.00	4.00	3.00	3.00	3.00
	SDRL	2.42	3.04	4.16	5.44	1.58	1.75	2.44	3.36
2.00	ARL	4.03	3.59	3.87	4.51	3.05	2.58	2.63	2.96
	MDRL	4.00	3.00	3.00	3.00	3.00	2.00	2.00	2.00
	SDRL	1.93	2.21	2.87	3.78	1.20	1.32	1.63	2.19
2.50	ARL	2.80	2.40	2.44	2.58	2.17	1.76	1.70	1.75
	MDRL	3.00	2.00	2.00	2.00	2.00	2.00	2.00	1.00
	SDRL	1.26	1.30	1.58	1.89	0.82	0.79	0.87	1.02
3.00	ARL	2.25	1.88	1.83	1.88	1.74	1.43	1.35	1.34
	MDRL	2.00	2.00	2.00	2.00	2.00	1.00	1.00	1.00
	SDRL	0.99	0.95	1.03	1.21	0.65	0.58	0.57	0.62
3.50	ARL	1.89	1.60	1.54	1.55	1.50	1.25	1.19	1.17
	MDRL	2.00	1.00	1.00	1.00	1.00	1.00	1.00	1.00
	SDRL	0.82	0.75	0.78	0.87	0.57	0.46	0.43	0.42
4.00	ARL	1.67	1.42	1.36	1.36	1.32	1.13	1.09	1.09
	MDRL	2.00	1.00	1.00	1.00	1.00	1.00	1.00	1.00
	SDRL	0.70	0.62	0.63	0.66	0.49	0.35	0.30	0.30

Table B.4: RL characteristics of the S_E chart for normally distributed quality characteristic when $\text{ARL}_0 = 200$

		n							
		5				10			
		λ				λ			
δ		0.05	0.25	0.50	0.75	0.05	0.25	0.50	0.75
1.00	ARL	200.08	200.49	201.25	199.65	199.32	202.96	199.87	199.80
	MDRL	142.00	139.00	140.00	136.00	138.00	142.00	138.00	136.00
	SDRL	197.20	195.53	199.05	201.96	194.62	198.65	198.92	204.47
1.10	ARL	33.18	40.28	50.41	57.95	20.18	24.89	31.82	39.67
	MDRL	26.00	29.00	35.00	40.00	16.00	18.00	23.00	27.00
	SDRL	26.42	37.67	48.83	57.80	13.73	21.66	30.68	39.35
1.20	ARL	15.14	16.17	19.89	23.73	9.32	9.13	10.83	13.35
	MDRL	13.00	12.00	14.00	17.00	8.00	7.00	8.00	10.00
	SDRL	9.76	13.60	18.39	23.17	4.93	6.69	9.26	12.47
1.30	ARL	9.79	9.33	10.54	12.35	6.04	5.27	5.49	6.56
	MDRL	9.00	7.00	8.00	9.00	5.00	4.00	4.00	5.00
	SDRL	5.48	7.17	9.21	11.65	2.74	3.27	4.17	5.72
1.40	ARL	7.15	6.33	6.78	7.87	4.55	3.69	3.62	3.95
	MDRL	6.00	5.00	5.00	6.00	4.00	3.00	3.00	3.00
	SDRL	3.65	4.38	5.59	7.10	1.87	2.08	2.49	3.19
1.50	ARL	5.69	4.82	4.83	5.47	3.68	2.87	2.73	2.84
	MDRL	5.00	4.00	4.00	4.00	3.00	3.00	2.00	2.00
	SDRL	2.75	3.15	3.71	4.68	1.41	1.46	1.72	2.07
1.60	ARL	4.77	3.88	3.85	4.09	3.11	2.36	2.17	2.20
	MDRL	4.00	3.00	3.00	3.00	3.00	2.00	2.00	2.00
	SDRL	2.20	2.39	2.88	3.34	1.13	1.14	1.27	1.47
1.80	ARL	3.65	2.85	2.69	2.82	2.43	1.82	1.64	1.60
	MDRL	3.00	3.00	2.00	2.00	2.00	2.00	1.00	1.00
	SDRL	1.59	1.59	1.77	2.13	0.86	0.82	0.84	0.88
2.00	ARL	3.00	2.31	2.13	2.11	2.02	1.52	1.37	1.33
	MDRL	3.00	2.00	2.00	2.00	2.00	1.00	1.00	1.00
	SDRL	1.28	1.25	1.30	1.42	0.71	0.66	0.60	0.63
2.50	ARL	2.14	1.65	1.51	1.48	1.47	1.16	1.10	1.09
	MDRL	2.00	1.00	1.00	1.00	1.00	1.00	1.00	1.00
	SDRL	0.89	0.81	0.76	0.80	0.55	0.38	0.31	0.30
3.00	ARL	1.72	1.36	1.28	1.25	1.21	1.05	1.03	1.02
	MDRL	2.00	1.00	1.00	1.00	1.00	1.00	1.00	1.00
	SDRL	0.70	0.59	0.54	0.54	0.42	0.22	0.18	0.16
3.50	ARL	1.46	1.23	1.16	1.14	1.08	1.02	1.01	1.01
	MDRL	1.00	1.00	1.00	1.00	1.00	1.00	1.00	1.00
	SDRL	0.59	0.47	0.42	0.40	0.28	0.14	0.10	0.09
4.00	ARL	1.33	1.14	1.10	1.09	1.04	1.01	1.00	1.00
	MDRL	1.00	1.00	1.00	1.00	1.00	1.00	1.00	1.00
	SDRL	0.52	0.37	0.32	0.31	0.19	0.08	0.06	0.05

Table B.5: RL characteristics of the S_E chart for t-distributed quality characteristic when $ARL_0 = 200$

		n							
		5				10			
		λ				λ			
δ		0.05	0.25	0.50	0.75	0.05	0.25	0.50	0.75
1.00	ARL	199.08	198.83	200.58	203.67	201.78	200.43	202.33	198.77
	MDRL	137.00	137.00	140.00	142.00	142.00	141.00	140.00	136.00
	SDRL	200.03	197.99	199.99	202.19	204.81	201.09	204.06	199.70
1.10	ARL	46.76	77.21	102.60	112.71	33.63	61.53	87.04	103.32
	MDRL	35.00	54.00	72.00	78.00	26.00	45.00	60.00	72.00
	SDRL	39.52	75.68	100.88	113.17	26.37	57.93	86.49	102.13
1.20	ARL	22.07	36.59	54.20	68.21	15.09	24.90	41.62	55.59
	MDRL	18.00	26.00	38.00	48.00	13.00	19.00	29.00	39.00
	SDRL	15.89	34.05	53.19	67.00	9.58	21.73	39.92	55.49
1.30	ARL	14.06	20.49	32.28	41.82	9.48	12.85	22.01	31.98
	MDRL	12.00	15.00	23.00	30.00	9.00	10.00	16.00	23.00
	SDRL	8.88	17.68	31.05	40.69	5.03	10.23	21.06	30.88
1.40	ARL	10.19	12.90	20.73	28.19	6.96	8.11	12.93	19.30
	MDRL	9.00	10.00	15.00	20.00	6.00	7.00	9.00	14.00
	SDRL	5.89	10.16	19.29	27.37	3.38	5.67	11.74	18.53
1.50	ARL	7.98	9.38	13.89	19.52	5.55	5.84	8.51	12.40
	MDRL	7.00	7.00	10.00	14.00	5.00	5.00	6.00	9.00
	SDRL	4.36	7.08	12.64	19.11	2.46	3.71	7.09	11.54
1.60	ARL	6.56	7.10	10.11	14.02	4.63	4.55	6.07	8.77
	MDRL	6.00	6.00	8.00	10.00	4.00	4.00	5.00	6.00
	SDRL	3.37	4.95	8.81	13.14	1.94	2.60	4.71	7.86
1.80	ARL	4.95	4.86	6.23	8.31	3.53	3.22	3.78	4.83
	MDRL	5.00	4.00	5.00	6.00	3.00	3.00	3.00	4.00
	SDRL	2.38	3.03	4.93	7.55	1.38	1.65	2.55	3.93
2.00	ARL	4.00	3.76	4.36	5.56	2.87	2.53	2.68	3.20
	MDRL	4.00	3.00	3.00	4.00	3.00	2.00	2.00	3.00
	SDRL	1.82	2.21	3.24	4.72	1.10	1.19	1.60	2.38
2.50	ARL	2.81	2.45	2.55	2.88	2.06	1.74	1.69	1.79
	MDRL	3.00	2.00	2.00	2.00	2.00	2.00	2.00	2.00
	SDRL	1.21	1.26	1.62	2.13	0.73	0.73	0.82	1.01
3.00	ARL	2.22	1.92	1.91	2.00	1.65	1.38	1.33	1.32
	MDRL	2.00	2.00	2.00	2.00	2.00	1.00	1.00	1.00
	SDRL	0.93	0.93	1.05	1.29	0.60	0.54	0.55	0.59
3.50	ARL	1.89	1.61	1.57	1.61	1.42	1.20	1.16	1.15
	MDRL	2.00	1.00	1.00	1.00	1.00	1.00	1.00	1.00
	SDRL	0.78	0.74	0.79	0.91	0.53	0.42	0.39	0.39
4.00	ARL	1.66	1.42	1.37	1.39	1.24	1.10	1.08	1.07
	MDRL	2.00	1.00	1.00	1.00	1.00	1.00	1.00	1.00
	SDRL	0.69	0.61	0.63	0.68	0.43	0.31	0.27	0.27

Table B.6: RL characteristics of the S_E chart for Gamma distributed quality characteristic when $\text{ARL}_0 = 200$

		n							
		5				10			
		λ				λ			
δ		0.05	0.25	0.50	0.75	0.05	0.25	0.50	0.75
1.00	ARL	201.32	198.34	198.74	202.32	199.05	200.52	201.43	200.02
	MDRL	139.00	140.00	137.00	138.00	138.00	140.00	144.00	140.00
	SDRL	199.07	195.98	200.69	205.81	197.17	197.76	199.99	201.55
1.10	ARL	45.87	67.51	85.01	92.86	32.25	48.31	64.76	77.32
	MDRL	34.00	47.00	59.00	65.00	25.00	34.00	45.00	54.00
	SDRL	39.51	65.65	83.96	92.00	24.82	45.85	64.10	76.23
1.20	ARL	21.47	30.87	42.67	51.05	14.45	19.07	27.13	36.00
	MDRL	17.00	22.00	30.00	36.00	12.00	14.00	20.00	25.00
	SDRL	15.66	28.25	41.69	49.81	8.93	16.41	25.39	35.08
1.30	ARL	13.85	17.76	24.10	30.73	9.27	10.50	14.51	19.44
	MDRL	12.00	13.00	17.00	21.00	8.00	8.00	11.00	14.00
	SDRL	8.89	15.30	22.63	30.29	4.99	8.04	13.05	18.68
1.40	ARL	10.21	11.74	15.65	19.64	6.92	6.93	8.90	11.79
	MDRL	9.00	9.00	11.00	14.00	6.00	6.00	7.00	8.00
	SDRL	6.05	9.38	14.41	18.74	3.41	4.76	7.56	11.13
1.50	ARL	7.98	8.65	11.19	14.01	5.42	5.14	6.19	7.88
	MDRL	7.00	7.00	8.00	10.00	5.00	4.00	5.00	6.00
	SDRL	4.47	6.48	9.82	13.13	2.47	3.18	4.97	7.17
1.60	ARL	6.65	6.72	8.36	10.49	4.56	4.08	4.68	5.71
	MDRL	6.00	6.00	6.00	7.00	4.00	4.00	4.00	4.00
	SDRL	3.54	4.78	7.11	9.57	1.98	2.38	3.49	4.89
1.80	ARL	5.01	4.68	5.37	6.54	3.50	2.96	3.06	3.51
	MDRL	5.00	4.00	4.00	5.00	3.00	3.00	3.00	3.00
	SDRL	2.48	3.06	4.30	5.65	1.42	1.57	2.02	2.71
2.00	ARL	4.04	3.61	3.95	4.55	2.85	2.35	2.35	2.53
	MDRL	4.00	3.00	3.00	3.00	3.00	2.00	2.00	2.00
	SDRL	1.96	2.21	2.83	3.81	1.10	1.15	1.39	1.75
2.50	ARL	2.84	2.43	2.41	2.59	2.05	1.67	1.56	1.57
	MDRL	3.00	2.00	2.00	2.00	2.00	2.00	1.00	1.00
	SDRL	1.29	1.33	1.52	1.90	0.77	0.73	0.74	0.86
3.00	ARL	2.26	1.90	1.86	1.90	1.66	1.34	1.27	1.26
	MDRL	2.00	2.00	2.00	2.00	2.00	1.00	1.00	1.00
	SDRL	0.99	0.97	1.06	1.20	0.63	0.52	0.51	0.53
3.50	ARL	1.90	1.61	1.56	1.54	1.41	1.18	1.13	1.12
	MDRL	2.00	1.00	1.00	1.00	1.00	1.00	1.00	1.00
	SDRL	0.81	0.76	0.79	0.86	0.53	0.40	0.36	0.35
4.00	ARL	1.68	1.44	1.38	1.38	1.26	1.09	1.07	1.06
	MDRL	2.00	1.00	1.00	1.00	1.00	1.00	1.00	1.00
	SDRL	0.71	0.62	0.64	0.68	0.45	0.30	0.26	0.25

Table B.7: RL characteristics of the Q_E chart for normally distributed quality characteristic when $\text{ARL}_0 = 200$

		n							
		5				10			
		λ				λ			
δ		0.05	0.25	0.50	0.75	0.05	0.25	0.50	0.75
1.00	ARL	201.31	200.74	200.65	199.90	201.55	200.88	200.16	199.82
	MDRL	142.00	142.00	141.00	139.00	141.00	140.00	139.00	139.00
	SDRL	202.89	203.24	199.05	199.22	197.78	198.20	197.72	197.87
1.10	ARL	33.92	44.25	54.30	63.95	28.20	36.43	46.17	55.76
	MDRL	26.00	32.00	38.00	45.00	22.00	26.00	32.00	39.00
	SDRL	26.83	40.57	53.71	63.94	21.36	33.68	45.04	55.28
1.20	ARL	15.52	17.91	21.83	26.77	12.79	14.05	17.42	21.94
	MDRL	13.00	14.00	15.00	19.00	11.00	11.00	13.00	16.00
	SDRL	10.10	15.16	20.60	25.85	7.67	11.50	16.00	21.03
1.30	ARL	10.12	10.04	11.47	14.08	8.21	8.02	9.21	11.25
	MDRL	9.00	8.00	8.00	10.00	7.00	6.00	7.00	8.00
	SDRL	5.92	7.83	10.38	13.37	4.32	5.85	7.93	10.40
1.40	ARL	7.36	6.75	7.43	8.72	6.06	5.41	5.80	6.82
	MDRL	7.00	5.00	6.00	6.00	6.00	5.00	4.00	5.00
	SDRL	3.83	4.71	6.26	7.97	2.88	3.50	4.57	5.93
1.50	ARL	5.96	5.17	5.27	6.05	4.94	4.14	4.15	4.68
	MDRL	5.00	4.00	4.00	4.00	4.00	4.00	3.00	4.00
	SDRL	2.92	3.39	4.16	5.31	2.23	2.48	3.01	3.89
1.60	ARL	4.89	4.11	4.20	4.63	4.14	3.39	3.27	3.54
	MDRL	4.00	3.00	3.00	3.00	4.00	3.00	3.00	3.00
	SDRL	2.31	2.61	3.22	3.92	1.76	1.93	2.23	2.83
1.80	ARL	3.75	3.01	2.85	3.03	3.18	2.48	2.34	2.40
	MDRL	3.00	3.00	2.00	2.00	3.00	2.00	2.00	2.00
	SDRL	1.63	1.74	1.92	2.28	1.29	1.30	1.44	1.71
2.00	ARL	3.05	2.41	2.24	2.30	2.59	2.01	1.87	1.84
	MDRL	3.00	2.00	2.00	2.00	2.00	2.00	2.00	1.00
	SDRL	1.32	1.31	1.40	1.60	1.01	0.97	1.05	1.13
2.50	ARL	2.20	1.72	1.55	1.57	1.88	1.46	1.35	1.31
	MDRL	2.00	2.00	1.00	1.00	2.00	1.00	1.00	1.00
	SDRL	0.92	0.83	0.79	0.88	0.73	0.63	0.60	0.60
3.00	ARL	1.76	1.41	1.31	1.30	1.51	1.23	1.16	1.14
	MDRL	2.00	1.00	1.00	1.00	1.00	1.00	1.00	1.00
	SDRL	0.73	0.63	0.57	0.59	0.59	0.45	0.40	0.38
3.50	ARL	1.52	1.25	1.18	1.18	1.31	1.12	1.08	1.07
	MDRL	1.00	1.00	1.00	1.00	1.00	1.00	1.00	1.00
	SDRL	0.63	0.49	0.43	0.44	0.49	0.34	0.29	0.26
4.00	ARL	1.36	1.17	1.12	1.11	1.19	1.07	1.04	1.03
	MDRL	1.00	1.00	1.00	1.00	1.00	1.00	1.00	1.00
	SDRL	0.53	0.40	0.35	0.34	0.41	0.26	0.20	0.18

Table B.8: RL characteristics of the Q_E chart for t-distributed quality characteristic when $\mathrm{ARL}_0 = 200$

		n							
		5				10			
		λ				λ			
δ		0.05	0.25	0.50	0.75	0.05	0.25	0.50	0.75
1.00	ARL	199.04	200.30	201.64	199.76	199.73	199.70	201.29	199.41
	MDRL	137.00	141.00	141.00	137.00	137.00	128.00	144.00	141.00
	SDRL	194.77	205.92	206.52	199.85	193.55	184.02	203.22	194.96
1.10	ARL	44.12	66.02	89.60	98.45	31.41	43.29	59.47	69.86
	MDRL	33.00	46.00	62.00	69.00	25.00	31.00	42.00	48.00
	SDRL	37.34	66.00	87.70	97.25	24.59	40.27	58.72	69.41
1.20	ARL	20.34	29.57	43.12	52.08	14.41	17.26	23.88	30.35
	MDRL	17.00	21.00	30.00	36.00	12.00	13.00	17.00	21.00
	SDRL	14.34	27.02	42.29	51.18	9.14	14.75	22.27	29.88
1.30	ARL	12.88	16.37	24.52	32.11	9.27	9.63	12.60	16.32
	MDRL	11.00	12.00	17.00	22.00	8.00	8.00	9.00	12.00
	SDRL	8.19	14.00	23.11	31.97	5.09	7.34	11.39	15.35
1.40	ARL	9.37	10.82	15.60	19.90	6.72	6.50	7.84	9.84
	MDRL	8.00	8.00	11.00	14.00	6.00	5.00	6.00	7.00
	SDRL	5.29	8.40	14.24	18.97	3.37	4.51	6.49	8.93
1.50	ARL	7.38	7.87	10.55	13.73	5.39	4.87	5.50	6.76
	MDRL	7.00	6.00	8.00	10.00	5.00	4.00	4.00	5.00
	SDRL	4.00	5.83	9.38	12.77	2.53	3.11	4.33	6.02
1.60	ARL	6.17	6.09	7.73	9.97	4.53	3.87	4.20	4.75
	MDRL	6.00	5.00	6.00	7.00	4.00	3.00	3.00	4.00
	SDRL	3.11	4.19	6.43	9.10	2.03	2.26	3.09	4.04
1.80	ARL	4.67	4.32	5.04	6.08	3.45	2.86	2.86	3.10
	MDRL	4.00	4.00	4.00	5.00	3.00	3.00	2.00	2.00
	SDRL	2.23	2.70	3.89	5.28	1.44	1.57	1.85	2.35
2.00	ARL	3.80	3.33	3.64	4.14	2.82	2.28	2.18	2.28
	MDRL	4.00	3.00	3.00	3.00	3.00	2.00	2.00	2.00
	SDRL	1.73	1.91	2.60	3.44	1.13	1.14	1.28	1.56
2.50	ARL	2.67	2.24	2.25	2.39	2.03	1.61	1.52	1.50
	MDRL	3.00	2.00	2.00	2.00	2.00	1.00	1.00	1.00
	SDRL	1.14	1.16	1.36	1.66	0.79	0.73	0.75	0.80
3.00	ARL	2.11	1.77	1.70	1.74	1.63	1.34	1.25	1.23
	MDRL	2.00	2.00	1.00	1.00	2.00	1.00	1.00	1.00
	SDRL	0.89	0.85	0.91	1.05	0.63	0.55	0.50	0.50
3.50	ARL	1.79	1.51	1.46	1.46	1.40	1.19	1.14	1.12
	MDRL	2.00	1.00	1.00	1.00	1.00	1.00	1.00	1.00
	SDRL	0.76	0.69	0.70	0.76	0.54	0.42	0.37	0.36
4.00	ARL	1.60	1.35	1.31	1.29	1.26	1.11	1.08	1.07
	MDRL	2.00	1.00	1.00	1.00	1.00	1.00	1.00	1.00
	SDRL	0.66	0.56	0.56	0.58	0.46	0.32	0.27	0.26

Table B.9: RL characteristics of the Q_E chart for Gamma distributed quality characteristic when $\text{ARL}_0 = 200$

		n							
		5				10			
		λ				λ			
δ		0.05	0.25	0.50	0.75	0.05	0.25	0.50	0.75
1.00	ARL	199.52	201.84	200.05	201.24	200.34	201.19	201.61	200.40
	MDRL	137.00	139.00	143.00	142.00	136.00	140.00	143.50	139.00
	SDRL	192.46	202.40	200.43	201.50	200.36	199.28	204.79	199.73
1.10	ARL	43.69	62.11	75.01	85.28	34.74	48.41	63.15	74.44
	MDRL	33.00	44.00	53.00	59.00	27.00	35.00	45.00	51.00
	SDRL	37.61	59.44	74.13	84.71	27.92	44.61	61.25	73.49
1.20	ARL	20.27	27.01	35.85	43.70	15.93	19.85	27.04	33.51
	MDRL	16.00	20.00	25.00	31.00	14.00	15.00	20.00	24.00
	SDRL	14.75	24.24	34.60	42.93	10.19	16.97	25.39	32.56
1.30	ARL	12.99	15.41	20.14	24.72	10.24	11.03	14.26	18.38
	MDRL	11.00	12.00	14.00	17.00	9.00	9.00	10.00	13.00
	SDRL	8.19	12.87	19.07	23.98	5.79	8.59	12.89	17.64
1.40	ARL	9.62	10.32	13.14	16.13	7.46	7.38	8.80	11.46
	MDRL	8.00	8.00	10.00	12.00	7.00	6.00	7.00	8.00
	SDRL	5.70	8.30	11.74	15.32	3.83	5.23	7.52	10.77
1.50	ARL	7.55	7.60	9.03	11.31	5.92	5.43	6.40	7.78
	MDRL	7.00	6.00	7.00	8.00	5.00	5.00	5.00	6.00
	SDRL	4.13	5.66	7.77	10.48	2.84	3.59	5.22	6.94
1.60	ARL	6.26	6.02	6.91	8.37	4.93	4.37	4.81	5.67
	MDRL	6.00	5.00	5.00	6.00	5.00	4.00	4.00	4.00
	SDRL	3.27	4.19	5.73	7.56	2.26	2.70	3.69	4.87
1.80	ARL	4.73	4.27	4.57	5.34	3.79	3.15	3.20	3.58
	MDRL	4.00	4.00	4.00	4.00	4.00	3.00	3.00	3.00
	SDRL	2.35	2.72	3.58	4.59	1.61	1.78	2.17	2.86
2.00	ARL	3.83	3.30	3.43	3.80	3.09	2.49	2.45	2.60
	MDRL	4.00	3.00	3.00	3.00	3.00	2.00	2.00	2.00
	SDRL	1.78	1.97	2.45	3.06	1.27	1.29	1.52	1.88
2.50	ARL	2.67	2.26	2.19	2.29	2.21	1.75	1.64	1.65
	MDRL	2.00	2.00	2.00	2.00	2.00	2.00	1.00	1.00
	SDRL	1.20	1.24	1.33	1.60	0.89	0.82	0.85	0.93
3.00	ARL	2.16	1.77	1.70	1.71	1.77	1.43	1.34	1.31
	MDRL	2.00	2.00	1.00	1.00	2.00	1.00	1.00	1.00
	SDRL	0.95	0.89	0.93	1.04	0.70	0.62	0.59	0.60
3.50	ARL	1.83	1.52	1.45	1.46	1.52	1.23	1.19	1.17
	MDRL	2.00	1.00	1.00	1.00	1.00	1.00	1.00	1.00
	SDRL	0.79	0.71	0.71	0.78	0.60	0.46	0.44	0.42
4.00	ARL	1.61	1.38	1.31	1.31	1.35	1.15	1.11	1.09
	MDRL	1.00	1.00	1.00	1.00	1.00	1.00	1.00	1.00
	SDRL	0.69	0.60	0.57	0.60	0.51	0.38	0.34	0.31

Table B.10: RL characteristics of the D_E chart for normally distributed quality characteristic when $\text{ARL}_0 = 200$

		n							
		5				10			
		λ				λ			
δ		0.05	0.25	0.50	0.75	0.05	0.25	0.50	0.75
1.00	ARL	201.99	200.86	201.21	202.76	195.83	201.49	202.65	201.24
	MDRL	140.00	140.00	138.00	140.50	137.00	144.00	140.00	138.00
	SDRL	198.45	200.95	204.38	205.45	193.83	202.79	203.98	198.55
1.10	ARL	32.48	42.06	50.43	57.91	20.21	25.37	32.19	40.71
	MDRL	25.00	30.00	35.00	41.00	16.00	18.00	23.00	29.00
	SDRL	25.70	39.77	50.73	57.37	14.04	22.81	31.29	39.91
1.20	ARL	15.04	17.18	19.94	24.81	9.34	9.33	11.21	13.91
	MDRL	13.00	13.00	14.00	18.00	8.00	7.00	8.00	10.00
	SDRL	9.72	14.46	18.73	24.04	4.97	7.06	9.72	13.01
1.30	ARL	9.64	9.56	10.87	12.80	6.09	5.38	5.67	6.66
	MDRL	8.00	8.00	8.00	9.00	6.00	4.00	4.00	5.00
	SDRL	5.48	7.28	9.61	12.22	2.78	3.46	4.42	5.71
1.40	ARL	7.16	6.44	6.89	7.99	4.55	3.75	3.69	4.06
	MDRL	6.00	5.00	5.00	6.00	4.00	3.00	3.00	3.00
	SDRL	3.79	4.51	5.61	7.21	1.88	2.10	2.57	3.30
1.50	ARL	5.62	4.91	4.99	5.61	3.70	2.92	2.75	2.92
	MDRL	5.00	4.00	4.00	4.00	3.00	3.00	2.00	2.00
	SDRL	2.73	3.15	3.88	4.83	1.44	1.53	1.74	2.15
1.60	ARL	4.72	3.96	3.89	4.24	3.12	2.42	2.23	2.26
	MDRL	4.00	3.00	3.00	3.00	3.00	2.00	2.00	2.00
	SDRL	2.20	2.46	2.88	3.43	1.14	1.19	1.31	1.53
1.80	ARL	3.65	2.93	2.71	2.83	2.42	1.85	1.65	1.63
	MDRL	3.00	3.00	2.00	2.00	2.00	2.00	1.00	1.00
	SDRL	1.60	1.66	1.78	2.12	0.85	0.85	0.84	0.93
2.00	ARL	2.97	2.33	2.16	2.16	2.02	1.52	1.37	1.35
	MDRL	3.00	2.00	2.00	2.00	2.00	1.00	1.00	1.00
	SDRL	1.28	1.26	1.34	1.47	0.70	0.66	0.61	0.64
2.50	ARL	2.11	1.66	1.53	1.50	1.46	1.18	1.11	1.09
	MDRL	2.00	1.00	1.00	1.00	1.00	1.00	1.00	1.00
	SDRL	0.88	0.81	0.79	0.82	0.55	0.40	0.33	0.31
3.00	ARL	1.71	1.38	1.28	1.25	1.21	1.06	1.03	1.03
	MDRL	2.00	1.00	1.00	1.00	1.00	1.00	1.00	1.00
	SDRL	0.72	0.60	0.54	0.54	0.41	0.23	0.18	0.16
3.50	ARL	1.48	1.23	1.17	1.15	1.09	1.02	1.01	1.01
	MDRL	1.00	1.00	1.00	1.00	1.00	1.00	1.00	1.00
	SDRL	0.61	0.47	0.43	0.41	0.29	0.15	0.11	0.10
4.00	ARL	1.32	1.15	1.11	1.09	1.03	1.01	1.00	1.00
	MDRL	1.00	1.00	1.00	1.00	1.00	1.00	1.00	1.00
	SDRL	0.52	0.38	0.33	0.31	0.18	0.09	0.07	0.06

Table B.11: RL characteristics of the D_E chart for t-distributed quality characteristic when $\mathrm{ARL}_0 = 200$

		n							
		5				10			
		λ				λ			
δ		0.05	0.25	0.50	0.75	0.05	0.25	0.50	0.75
1.00	ARL	201.46	199.79	200.08	200.18	199.57	198.21	201.18	202.78
	MDRL	141.00	138.00	141.00	135.00	135.50	136.00	137.00	139.00
	SDRL	199.82	199.76	196.26	202.64	200.95	196.57	201.99	202.65
1.10	ARL	44.47	71.16	91.83	104.41	29.51	46.86	68.75	83.82
	MDRL	33.00	50.00	63.00	72.00	23.00	34.00	49.00	59.00
	SDRL	38.19	69.20	92.99	104.81	22.78	44.30	67.24	82.40
1.20	ARL	21.06	32.14	47.79	58.45	13.32	17.83	28.28	40.14
	MDRL	17.00	23.00	34.00	40.00	11.00	13.00	20.00	28.00
	SDRL	15.25	29.35	45.61	57.50	8.19	15.21	27.19	38.96
1.30	ARL	13.42	17.95	27.00	35.33	8.43	9.64	14.21	20.42
	MDRL	11.00	13.00	19.00	25.00	8.00	8.00	10.00	14.00
	SDRL	8.43	15.06	26.07	34.39	4.34	7.09	12.72	19.63
1.40	ARL	9.69	11.64	16.92	23.15	6.30	6.32	8.54	12.00
	MDRL	9.00	9.00	12.00	16.00	6.00	5.00	6.00	9.00
	SDRL	5.59	9.28	15.51	22.33	2.98	4.15	7.17	10.94
1.50	ARL	7.63	8.52	11.78	16.06	4.98	4.69	5.74	7.91
	MDRL	7.00	7.00	9.00	11.00	5.00	4.00	4.00	6.00
	SDRL	4.10	6.30	10.50	15.43	2.19	2.82	4.44	6.93
1.60	ARL	6.30	6.61	8.75	11.58	4.16	3.74	4.30	5.56
	MDRL	6.00	5.00	7.00	8.00	4.00	3.00	3.00	4.00
	SDRL	3.20	4.70	7.38	10.83	1.73	2.10	3.05	4.75
1.80	ARL	4.80	4.54	5.38	6.76	3.19	2.72	2.84	3.30
	MDRL	4.00	4.00	4.00	5.00	3.00	2.00	2.00	3.00
	SDRL	2.30	2.84	4.21	5.89	1.24	1.33	1.77	2.50
2.00	ARL	3.85	3.50	3.91	4.71	2.62	2.19	2.17	2.34
	MDRL	4.00	3.00	3.00	4.00	2.00	2.00	2.00	2.00
	SDRL	1.76	2.05	2.80	3.95	0.98	1.01	1.21	1.59
2.50	ARL	2.73	2.32	2.38	2.55	1.90	1.53	1.46	1.46
	MDRL	3.00	2.00	2.00	2.00	2.00	1.00	1.00	1.00
	SDRL	1.17	1.21	1.45	1.85	0.68	0.64	0.67	0.74
3.00	ARL	2.15	1.84	1.76	1.83	1.52	1.25	1.20	1.19
	MDRL	2.00	2.00	2.00	1.00	1.00	1.00	1.00	1.00
	SDRL	0.90	0.90	0.97	1.14	0.56	0.46	0.43	0.44
3.50	ARL	1.83	1.55	1.48	1.51	1.32	1.12	1.09	1.08
	MDRL	2.00	1.00	1.00	1.00	1.00	1.00	1.00	1.00
	SDRL	0.76	0.71	0.72	0.80	0.49	0.34	0.29	0.28
4.00	ARL	1.62	1.38	1.33	1.33	1.17	1.06	1.04	1.04
	MDRL	2.00	1.00	1.00	1.00	1.00	1.00	1.00	1.00
	SDRL	0.67	0.59	0.60	0.61	0.38	0.25	0.21	0.19

Table B.12: RL characteristics of the D_E chart for Gamma distributed quality characteristic when $\text{ARL}_0 = 200$

		n							
		5				10			
		λ				λ			
δ		0.05	0.25	0.50	0.75	0.05	0.25	0.50	0.75
1.00	ARL	198.72	199.21	203.65	199.72	198.84	200.33	198.57	200.90
	MDRL	138.00	138.00	139.50	137.50	138.00	138.00	138.00	137.00
	SDRL	195.13	198.32	208.75	201.34	196.96	200.10	193.20	200.06
1.10	ARL	43.42	60.60	76.31	86.29	28.16	40.60	52.75	65.32
	MDRL	33.00	44.00	53.00	60.50	22.00	29.00	37.00	46.00
	SDRL	36.75	57.87	74.89	84.52	21.42	37.80	52.94	64.45
1.20	ARL	20.66	27.24	36.92	44.14	13.01	15.66	21.30	27.61
	MDRL	17.00	20.00	26.00	31.00	11.00	12.00	16.00	19.00
	SDRL	14.82	24.90	35.33	43.19	7.79	13.09	19.76	26.50
1.30	ARL	13.11	15.62	20.93	25.99	8.37	8.56	10.95	14.25
	MDRL	11.00	12.00	15.00	18.00	7.00	7.00	8.00	10.00
	SDRL	8.18	13.12	19.56	25.19	4.35	6.21	9.58	13.39
1.40	ARL	9.65	10.40	13.34	16.57	6.17	5.77	6.89	8.59
	MDRL	8.00	8.00	10.00	12.00	6.00	5.00	5.00	6.00
	SDRL	5.53	8.11	12.07	15.87	2.93	3.73	5.55	7.72
1.50	ARL	7.60	7.72	9.36	11.53	4.97	4.40	4.74	5.78
	MDRL	7.00	6.00	7.00	8.00	5.00	4.00	4.00	4.00
	SDRL	4.09	5.64	8.05	10.83	2.17	2.64	3.58	4.94
1.60	ARL	6.33	6.06	7.16	8.74	4.12	3.56	3.69	4.28
	MDRL	6.00	5.00	5.00	6.00	4.00	3.00	3.00	3.00
	SDRL	3.26	4.23	6.03	7.98	1.72	2.03	2.55	3.45
1.80	ARL	4.75	4.30	4.69	5.52	3.20	2.57	2.51	2.73
	MDRL	4.00	4.00	4.00	4.00	3.00	2.00	2.00	2.00
	SDRL	2.29	2.74	3.57	4.88	1.24	1.30	1.55	2.05
2.00	ARL	3.89	3.32	3.50	3.86	2.62	2.09	1.97	2.04
	MDRL	4.00	3.00	3.00	3.00	2.00	2.00	2.00	2.00
	SDRL	1.83	1.98	2.52	3.13	1.01	1.00	1.09	1.30
2.50	ARL	2.73	2.24	2.22	2.31	1.89	1.50	1.38	1.37
	MDRL	3.00	2.00	2.00	2.00	2.00	1.00	1.00	1.00
	SDRL	1.21	1.19	1.34	1.65	0.70	0.64	0.62	0.66
3.00	ARL	2.17	1.80	1.71	1.72	1.53	1.24	1.16	1.15
	MDRL	2.00	2.00	1.00	1.00	1.00	1.00	1.00	1.00
	SDRL	0.93	0.90	0.93	1.03	0.59	0.46	0.40	0.40
3.50	ARL	1.85	1.51	1.46	1.45	1.31	1.11	1.08	1.07
	MDRL	2.00	1.00	1.00	1.00	1.00	1.00	1.00	1.00
	SDRL	0.80	0.70	0.72	0.76	0.48	0.33	0.28	0.26
4.00	ARL	1.64	1.37	1.32	1.28	1.19	1.06	1.04	1.03
	MDRL	2.00	1.00	1.00	1.00	1.00	1.00	1.00	1.00
	SDRL	0.70	0.59	0.58	0.58	0.39	0.24	0.19	0.18

Table B.13: RL characteristics of the MAD_E chart for normally distributed quality characteristic when $\text{ARL}_0 = 200$

		n							
		5				10			
		λ				λ			
δ		0.05	0.25	0.50	0.75	0.05	0.25	0.50	0.75
1.00	ARL	198.77	199.92	201.01	200.85	202.57	199.45	199.91	201.75
	MDRL	139.00	138.00	140.00	139.00	139.00	139.00	140.00	141.00
	SDRL	194.50	201.34	198.04	201.87	200.88	200.13	197.03	198.01
1.10	ARL	53.25	65.61	75.09	83.52	33.61	42.69	54.31	62.82
	MDRL	39.00	46.00	52.00	59.00	26.00	30.00	38.00	44.00
	SDRL	46.82	63.14	73.87	82.81	26.46	40.63	53.25	62.17
1.20	ARL	26.11	31.52	37.71	42.45	15.45	17.64	21.68	26.99
	MDRL	20.00	23.00	27.00	30.00	13.00	13.00	15.00	19.00
	SDRL	20.22	28.66	36.35	42.04	10.12	14.76	20.22	26.27
1.30	ARL	16.80	18.92	21.77	25.37	10.01	10.00	11.59	14.32
	MDRL	14.00	14.00	15.00	18.00	9.00	8.00	9.00	10.00
	SDRL	11.68	17.15	21.02	24.63	5.70	7.81	10.22	13.68
1.40	ARL	12.27	12.44	14.59	16.53	7.32	6.72	7.48	8.86
	MDRL	10.00	9.00	11.00	12.00	7.00	5.00	6.00	6.00
	SDRL	7.95	10.41	13.47	15.51	3.86	4.79	6.25	8.14
1.50	ARL	9.62	9.37	10.56	11.88	5.82	5.09	5.44	6.12
	MDRL	8.00	7.00	8.00	8.00	5.00	4.00	4.00	4.00
	SDRL	5.83	7.53	9.37	11.27	2.84	3.33	4.37	5.38
1.60	ARL	8.01	7.53	8.08	9.25	4.86	4.07	4.12	4.60
	MDRL	7.00	6.00	6.00	7.00	4.00	3.00	3.00	3.00
	SDRL	4.73	5.90	7.12	8.54	2.28	2.52	3.05	3.79
1.80	ARL	5.97	5.28	5.56	6.16	3.70	2.98	2.88	3.05
	MDRL	5.00	4.00	4.00	4.00	3.00	3.00	2.00	2.00
	SDRL	3.38	3.78	4.63	5.54	1.64	1.71	1.93	2.34
2.00	ARL	4.86	4.19	4.17	4.50	3.04	2.38	2.25	2.32
	MDRL	4.00	3.00	3.00	3.00	3.00	2.00	2.00	2.00
	SDRL	2.68	2.86	3.24	3.86	1.29	1.27	1.40	1.63
2.50	ARL	3.37	2.78	2.71	2.74	2.17	1.71	1.58	1.58
	MDRL	3.00	2.00	2.00	2.00	2.00	2.00	1.00	1.00
	SDRL	1.76	1.75	1.89	2.10	0.90	0.84	0.82	0.91
3.00	ARL	2.68	2.19	2.08	2.10	1.75	1.40	1.31	1.28
	MDRL	2.00	2.00	2.00	2.00	2.00	1.00	1.00	1.00
	SDRL	1.36	1.29	1.35	1.46	0.73	0.61	0.58	0.58
3.50	ARL	2.27	1.88	1.78	1.76	1.49	1.24	1.18	1.17
	MDRL	2.00	2.00	1.00	1.00	1.00	1.00	1.00	1.00
	SDRL	1.15	1.06	1.06	1.11	0.61	0.48	0.43	0.43
4.00	ARL	2.00	1.68	1.59	1.60	1.33	1.15	1.11	1.10
	MDRL	2.00	1.00	1.00	1.00	1.00	1.00	1.00	1.00
	SDRL	1.01	0.90	0.88	0.93	0.52	0.38	0.33	0.32

Table B.14: RL characteristics of the MAD_E chart for t-distributed quality characteristic when $\text{ARL}_0 = 200$

		n							
		5				10			
		λ				λ			
δ		0.05	0.25	0.50	0.75	0.05	0.25	0.50	0.75
1.00	ARL	199.71	202.90	201.17	198.91	202.61	201.67	198.68	197.59
	MDRL	141.00	141.00	140.00	139.00	138.00	139.00	138.00	137.00
	SDRL	194.97	200.80	200.81	199.09	204.07	199.64	198.71	198.86
1.10	ARL	58.47	76.98	91.49	99.96	36.75	51.61	62.43	72.85
	MDRL	42.00	54.00	64.00	71.00	28.00	37.00	44.00	51.00
	SDRL	53.21	75.20	91.00	97.31	29.97	48.64	61.99	71.49
1.20	ARL	28.96	37.78	49.01	55.84	16.87	21.13	26.73	33.60
	MDRL	23.00	27.00	34.00	39.00	14.00	15.00	19.00	24.00
	SDRL	22.89	36.28	47.67	54.74	11.13	18.64	25.10	32.93
1.30	ARL	18.43	22.64	29.27	34.39	10.83	11.68	14.62	18.42
	MDRL	15.00	17.00	21.00	24.00	9.00	9.00	11.00	13.00
	SDRL	13.32	20.20	28.03	34.05	6.40	9.45	13.27	17.57
1.40	ARL	13.30	15.40	19.63	23.18	7.91	7.87	9.17	11.21
	MDRL	11.00	11.00	14.00	17.00	7.00	6.00	7.00	8.00
	SDRL	8.86	13.18	18.67	22.36	4.24	5.77	7.99	10.45
1.50	ARL	10.63	11.34	13.93	16.71	6.30	5.75	6.47	7.90
	MDRL	9.00	9.00	10.00	12.00	6.00	5.00	5.00	6.00
	SDRL	6.74	9.27	12.92	15.99	3.13	3.90	5.34	7.14
1.60	ARL	8.92	9.06	10.82	12.86	5.25	4.63	4.94	5.78
	MDRL	8.00	7.00	8.00	9.00	5.00	4.00	4.00	4.00
	SDRL	5.45	7.00	9.67	12.33	2.51	2.98	3.85	5.00
1.80	ARL	6.57	6.20	7.18	8.11	3.96	3.34	3.40	3.67
	MDRL	6.00	5.00	5.00	6.00	4.00	3.00	3.00	3.00
	SDRL	3.72	4.58	6.04	7.36	1.79	1.92	2.43	2.91
2.00	ARL	5.32	4.92	5.26	5.92	3.28	2.67	2.57	2.75
	MDRL	5.00	4.00	4.00	4.00	3.00	2.00	2.00	2.00
	SDRL	2.95	3.51	4.24	5.35	1.43	1.48	1.66	2.01
2.50	ARL	3.70	3.16	3.21	3.44	2.32	1.86	1.73	1.74
	MDRL	3.00	3.00	3.00	3.00	2.00	2.00	1.00	1.00
	SDRL	1.93	2.08	2.34	2.76	0.96	0.92	0.94	1.05
3.00	ARL	2.89	2.46	2.40	2.49	1.86	1.50	1.40	1.39
	MDRL	3.00	2.00	2.00	2.00	2.00	1.00	1.00	1.00
	SDRL	1.50	1.47	1.62	1.85	0.77	0.68	0.66	0.69
3.50	ARL	2.45	2.08	2.02	2.02	1.59	1.31	1.23	1.22
	MDRL	2.00	2.00	2.00	2.00	2.00	1.00	1.00	1.00
	SDRL	1.25	1.20	1.28	1.34	0.65	0.53	0.49	0.49
4.00	ARL	2.16	1.81	1.76	1.78	1.41	1.20	1.15	1.13
	MDRL	2.00	2.00	1.00	1.00	1.00	1.00	1.00	1.00
	SDRL	1.09	1.01	1.03	1.13	0.56	0.44	0.39	0.38

Table B.15: RL characteristics of the MAD_E chart for Gamma distributed quality characteristic when $\text{ARL}_0 = 200$

		n							
		5				10			
		λ				λ			
δ		0.05	0.25	0.50	0.75	0.05	0.25	0.50	0.75
1.00	ARL	198.94	198.42	198.90	198.41	200.25	199.58	198.98	201.79
	MDRL	139.50	138.00	140.00	140.00	139.00	139.50	138.50	137.00
	SDRL	195.48	196.08	196.63	197.47	200.37	195.83	198.88	203.21
1.10	ARL	59.71	76.70	90.77	99.50	37.84	51.31	64.28	74.45
	MDRL	44.00	55.00	65.00	69.00	29.00	36.00	46.00	52.00
	SDRL	53.42	74.22	87.83	99.48	30.56	48.19	61.43	74.28
1.20	ARL	28.92	38.69	48.21	54.83	17.44	21.61	28.47	35.13
	MDRL	22.00	27.00	34.00	38.00	14.00	16.00	20.00	25.00
	SDRL	23.24	36.07	46.89	54.60	11.82	19.02	27.23	34.46
1.30	ARL	18.53	22.96	28.87	34.91	11.17	12.38	15.45	19.35
	MDRL	15.00	17.00	20.00	25.00	10.00	10.00	11.00	14.00
	SDRL	13.47	20.90	28.12	33.28	6.68	9.93	14.13	18.60
1.40	ARL	13.69	15.67	19.94	23.14	8.12	8.10	9.69	12.09
	MDRL	11.00	12.00	14.00	16.00	7.00	6.00	7.00	9.00
	SDRL	9.32	13.43	18.97	22.71	4.35	6.03	8.52	11.35
1.50	ARL	10.64	11.77	14.34	16.85	6.48	6.08	6.86	8.26
	MDRL	9.00	9.00	10.00	12.00	6.00	5.00	5.00	6.00
	SDRL	6.83	9.87	13.28	16.18	3.31	4.26	5.79	7.37
1.60	ARL	8.81	9.28	10.99	12.95	5.41	4.85	5.33	6.23
	MDRL	8.00	7.00	8.00	9.00	5.00	4.00	4.00	5.00
	SDRL	5.39	7.42	9.95	12.11	2.68	3.17	4.17	5.47
1.80	ARL	6.65	6.39	7.31	8.36	4.07	3.47	3.56	3.96
	MDRL	6.00	5.00	5.00	6.00	4.00	3.00	3.00	3.00
	SDRL	3.90	4.76	6.35	7.68	1.86	2.07	2.55	3.19
2.00	ARL	5.38	4.98	5.31	5.95	3.35	2.78	2.72	2.90
	MDRL	5.00	4.00	4.00	4.00	3.00	2.00	2.00	2.00
	SDRL	3.03	3.62	4.36	5.22	1.48	1.53	1.77	2.17
2.50	ARL	3.70	3.26	3.30	3.50	2.40	1.90	1.81	1.82
	MDRL	3.00	3.00	3.00	3.00	2.00	2.00	2.00	1.00
	SDRL	1.97	2.12	2.46	2.79	1.01	0.95	1.03	1.13
3.00	ARL	2.94	2.51	2.48	2.56	1.91	1.55	1.46	1.45
	MDRL	3.00	2.00	2.00	2.00	2.00	1.00	1.00	1.00
	SDRL	1.54	1.53	1.72	1.91	0.81	0.73	0.72	0.76
3.50	ARL	2.44	2.10	2.04	2.08	1.63	1.35	1.27	1.26
	MDRL	2.00	2.00	2.00	2.00	2.00	1.00	1.00	1.00
	SDRL	1.25	1.23	1.30	1.41	0.68	0.57	0.53	0.54
4.00	ARL	2.17	1.85	1.79	1.82	1.45	1.23	1.17	1.16
	MDRL	2.00	2.00	1.00	1.00	1.00	1.00	1.00	1.00
	SDRL	1.10	1.03	1.07	1.17	0.59	0.46	0.42	0.43

Table B.16: RL characteristics of the SN_E chart for normally distributed quality characteristic when $\mathrm{ARL}_0 = 200$

		n							
		5				10			
		λ				λ			
δ		0.05	0.25	0.50	0.75	0.05	0.25	0.50	0.75
1.00	ARL	199.34	202.81	201.56	201.04	198.67	201.18	198.08	202.60
	MDRL	137.00	141.00	140.00	139.00	137.00	142.00	139.00	141.00
	SDRL	198.25	200.79	201.44	200.26	194.83	197.35	193.44	199.34
1.10	ARL	50.30	61.94	71.82	79.93	30.11	39.57	52.47	60.85
	MDRL	37.00	44.00	51.00	56.00	23.00	29.00	37.00	43.00
	SDRL	44.16	58.50	69.90	78.41	23.45	36.54	51.06	59.36
1.20	ARL	23.90	28.70	33.16	38.39	13.74	15.37	19.80	24.87
	MDRL	19.00	21.00	24.00	27.00	12.00	12.00	14.00	18.00
	SDRL	18.06	26.11	31.58	37.41	8.60	13.02	18.24	24.08
1.30	ARL	15.38	16.52	18.80	22.23	8.69	8.75	10.39	12.55
	MDRL	13.00	13.00	13.00	16.00	8.00	7.00	8.00	9.00
	SDRL	10.37	14.01	17.46	21.24	4.74	6.56	8.89	11.65
1.40	ARL	11.37	11.33	12.57	14.25	6.49	5.94	6.50	7.81
	MDRL	10.00	9.00	9.00	10.00	6.00	5.00	5.00	6.00
	SDRL	7.17	9.18	11.36	13.52	3.21	4.07	5.32	7.03
1.50	ARL	9.11	8.39	9.05	10.08	5.16	4.43	4.71	5.29
	MDRL	8.00	7.00	7.00	7.00	5.00	4.00	4.00	4.00
	SDRL	5.47	6.56	7.88	9.42	2.42	2.80	3.62	4.59
1.60	ARL	7.48	6.67	6.99	7.73	4.34	3.61	3.66	3.98
	MDRL	7.00	5.00	5.00	6.00	4.00	3.00	3.00	3.00
	SDRL	4.28	5.02	5.98	7.16	1.93	2.11	2.60	3.15
1.80	ARL	5.63	4.74	4.73	5.06	3.34	2.67	2.56	2.64
	MDRL	5.00	4.00	4.00	4.00	3.00	2.00	2.00	2.00
	SDRL	3.05	3.31	3.76	4.38	1.40	1.42	1.65	1.91
2.00	ARL	4.58	3.75	3.60	3.80	2.74	2.14	1.99	1.99
	MDRL	4.00	3.00	3.00	3.00	3.00	2.00	2.00	2.00
	SDRL	2.42	2.47	2.75	3.15	1.11	1.09	1.16	1.31
2.50	ARL	3.17	2.58	2.43	2.42	1.98	1.55	1.42	1.40
	MDRL	3.00	2.00	2.00	2.00	2.00	1.00	1.00	1.00
	SDRL	1.63	1.56	1.62	1.78	0.79	0.71	0.67	0.69
3.00	ARL	2.53	2.03	1.90	1.89	1.59	1.28	1.22	1.20
	MDRL	2.00	2.00	2.00	1.00	2.00	1.00	1.00	1.00
	SDRL	1.27	1.19	1.18	1.25	0.63	0.51	0.47	0.46
3.50	ARL	2.14	1.75	1.63	1.60	1.37	1.16	1.12	1.10
	MDRL	2.00	1.00	1.00	1.00	1.00	1.00	1.00	1.00
	SDRL	1.07	0.97	0.93	0.95	0.53	0.39	0.34	0.32
4.00	ARL	1.89	1.55	1.47	1.45	1.24	1.09	1.07	1.06
	MDRL	2.00	1.00	1.00	1.00	1.00	1.00	1.00	1.00
	SDRL	0.93	0.81	0.78	0.80	0.45	0.30	0.27	0.24

Table B.17: RL characteristics of the SN_E chart for t-distributed quality characteristic when $\text{ARL}_0 = 200$

		n							
		5				10			
		λ				λ			
δ		0.05	0.25	0.50	0.75	0.05	0.25	0.50	0.75
1.00	ARL	202.11	200.34	200.56	199.90	200.38	200.12	201.57	200.03
	MDRL	139.00	139.00	138.00	138.00	138.00	139.00	143.00	136.00
	SDRL	203.21	199.25	202.78	199.98	198.13	197.52	199.62	203.57
1.10	ARL	54.92	72.45	90.27	96.44	33.83	46.34	60.31	71.72
	MDRL	40.00	51.00	63.00	67.00	26.00	33.00	42.00	50.00
	SDRL	49.33	70.55	90.10	95.28	26.76	43.73	59.24	71.21
1.20	ARL	27.44	35.10	46.20	52.48	15.51	18.98	25.11	31.52
	MDRL	22.00	25.00	33.00	36.00	13.00	14.00	18.00	22.00
	SDRL	21.35	32.95	44.79	51.78	9.84	16.32	23.52	31.12
1.30	ARL	17.64	21.20	27.26	32.26	9.86	10.40	13.33	17.01
	MDRL	14.00	15.00	19.00	23.00	9.00	8.00	10.00	12.00
	SDRL	12.51	18.78	25.83	31.20	5.42	8.02	12.01	16.29
1.40	ARL	12.59	14.36	17.86	21.74	7.23	6.96	8.31	10.29
	MDRL	11.00	11.00	13.00	15.00	7.00	6.00	6.00	7.00
	SDRL	8.26	12.56	16.70	21.26	3.66	4.92	7.08	9.45
1.50	ARL	9.93	10.59	12.94	15.44	5.75	5.21	5.93	7.13
	MDRL	8.00	8.00	9.00	11.00	5.00	4.00	5.00	5.00
	SDRL	6.21	8.66	11.75	14.47	2.74	3.35	4.77	6.27
1.60	ARL	8.30	8.35	9.94	11.61	4.84	4.16	4.48	5.14
	MDRL	7.00	7.00	7.00	8.00	4.00	4.00	4.00	4.00
	SDRL	4.95	6.58	8.86	10.95	2.20	2.53	3.36	4.38
1.80	ARL	6.19	5.79	6.47	7.35	3.69	3.04	3.04	3.26
	MDRL	5.00	5.00	5.00	5.00	3.00	3.00	2.00	3.00
	SDRL	3.49	4.19	5.49	6.55	1.57	1.70	2.09	2.46
2.00	ARL	5.02	4.51	4.82	5.20	3.05	2.44	2.34	2.43
	MDRL	4.00	4.00	4.00	4.00	3.00	2.00	2.00	2.00
	SDRL	2.75	3.11	3.83	4.50	1.26	1.28	1.44	1.69
2.50	ARL	3.48	2.95	3.00	3.14	2.15	1.70	1.60	1.58
	MDRL	3.00	3.00	2.00	2.00	2.00	2.00	1.00	1.00
	SDRL	1.84	1.85	2.19	2.43	0.85	0.80	0.83	0.88
3.00	ARL	2.75	2.33	2.23	2.27	1.74	1.39	1.30	1.29
	MDRL	2.00	2.00	2.00	2.00	2.00	1.00	1.00	1.00
	SDRL	1.40	1.38	1.46	1.62	0.69	0.59	0.55	0.58
3.50	ARL	2.30	1.96	1.89	1.89	1.50	1.23	1.18	1.17
	MDRL	2.00	2.00	2.00	1.00	1.00	1.00	1.00	1.00
	SDRL	1.16	1.12	1.16	1.24	0.60	0.46	0.42	0.42
4.00	ARL	2.04	1.73	1.66	1.65	1.32	1.14	1.10	1.09
	MDRL	2.00	1.00	1.00	1.00	1.00	1.00	1.00	1.00
	SDRL	1.02	0.91	0.95	1.00	0.50	0.36	0.32	0.31

Table B.18: RL characteristics of the SN_E chart for Gamma distributed quality characteristic when $\text{ARL}_0 = 200$

		n							
		5				10			
		λ				λ			
δ		0.05	0.25	0.50	0.75	0.05	0.25	0.50	0.75
1.00	ARL	199.44	201.15	198.60	199.03	201.82	199.72	200.52	198.83
	MDRL	137.00	140.00	139.00	138.00	141.00	142.00	140.00	138.00
	SDRL	198.31	197.49	197.66	197.46	196.36	199.05	197.93	198.43
1.10	ARL	56.36	73.71	86.87	96.68	36.13	51.95	67.13	79.54
	MDRL	41.00	53.00	60.00	67.00	27.00	37.00	48.00	55.00
	SDRL	49.77	70.40	86.15	96.24	29.20	49.65	65.64	78.13
1.20	ARL	27.85	35.94	45.54	52.87	16.91	21.65	29.45	37.44
	MDRL	22.00	25.00	32.00	37.00	14.00	16.00	21.00	26.00
	SDRL	21.61	33.77	44.60	52.49	11.27	18.92	28.02	36.55
1.30	ARL	18.07	21.56	27.03	32.51	10.63	11.84	15.93	20.78
	MDRL	15.00	16.00	19.00	22.00	9.00	9.00	12.00	15.00
	SDRL	13.06	19.35	25.23	31.83	6.12	9.60	14.70	19.83
1.40	ARL	12.97	14.24	18.05	21.53	7.83	8.00	9.88	12.70
	MDRL	11.00	11.00	13.00	15.00	7.00	6.00	7.00	9.00
	SDRL	8.64	12.15	16.74	20.75	4.12	5.84	8.62	12.00
1.50	ARL	10.30	10.74	12.89	15.63	6.22	5.89	6.89	8.61
	MDRL	9.00	8.00	10.00	11.00	6.00	5.00	5.00	6.00
	SDRL	6.39	8.78	11.50	14.90	3.05	3.96	5.68	7.71
1.60	ARL	8.47	8.47	9.89	11.58	5.18	4.72	5.22	6.28
	MDRL	7.00	7.00	7.00	8.00	5.00	4.00	4.00	5.00
	SDRL	5.08	6.62	8.88	10.88	2.43	2.98	4.09	5.43
1.80	ARL	6.36	5.98	6.53	7.54	3.90	3.40	3.47	3.94
	MDRL	6.00	5.00	5.00	5.00	4.00	3.00	3.00	3.00
	SDRL	3.55	4.39	5.45	6.89	1.69	1.98	2.42	3.18
2.00	ARL	5.10	4.58	4.86	5.37	3.21	2.66	2.64	2.91
	MDRL	5.00	4.00	4.00	4.00	3.00	2.00	2.00	2.00
	SDRL	2.77	3.16	3.94	4.70	1.37	1.44	1.69	2.21
2.50	ARL	3.59	3.04	3.05	3.19	2.29	1.83	1.75	1.77
	MDRL	3.00	3.00	2.00	2.00	2.00	2.00	2.00	1.00
	SDRL	1.88	1.93	2.21	2.56	0.93	0.89	0.96	1.06
3.00	ARL	2.81	2.35	2.34	2.37	1.84	1.50	1.41	1.38
	MDRL	3.00	2.00	2.00	2.00	2.00	1.00	1.00	1.00
	SDRL	1.44	1.41	1.55	1.70	0.75	0.66	0.66	0.68
3.50	ARL	2.39	1.98	1.92	1.93	1.57	1.30	1.24	1.23
	MDRL	2.00	2.00	2.00	2.00	2.00	1.00	1.00	1.00
	SDRL	1.21	1.12	1.17	1.26	0.62	0.52	0.49	0.49
4.00	ARL	2.07	1.75	1.69	1.69	1.39	1.19	1.14	1.14
	MDRL	2.00	2.00	1.00	1.00	1.00	1.00	1.00	1.00
	SDRL	1.03	0.94	0.98	1.03	0.54	0.42	0.37	0.38

Table B.19: RL characteristics of the QN_E chart for normally distributed quality characteristic when $\text{ARL}_0 = 200$

		n							
		5				10			
		λ				λ			
δ		0.05	0.25	0.50	0.75	0.05	0.25	0.50	0.75
1.00	ARL	198.93	203.55	196.97	198.36	200.62	201.97	199.67	200.09
	MDRL	137.00	143.00	136.00	138.00	136.00	141.00	137.00	137.00
	SDRL	195.57	201.22	198.33	198.92	202.24	200.79	199.60	200.76
1.10	ARL	49.02	63.44	74.51	83.92	26.60	34.82	43.86	51.52
	MDRL	36.00	45.00	52.00	59.00	21.00	25.00	31.00	35.00
	SDRL	42.48	61.83	72.27	81.53	20.13	31.66	42.26	51.64
1.20	ARL	23.99	28.96	35.93	41.58	12.07	13.13	15.98	20.04
	MDRL	19.00	21.00	25.00	29.00	10.00	10.00	12.00	14.00
	SDRL	18.20	27.04	34.70	40.94	7.16	10.66	14.43	19.12
1.30	ARL	15.02	16.97	20.84	24.76	7.77	7.33	8.24	10.00
	MDRL	12.00	13.00	15.00	17.00	7.00	6.00	6.00	7.00
	SDRL	10.16	14.65	19.77	24.12	3.93	5.21	6.85	9.22
1.40	ARL	11.19	11.43	13.25	15.83	5.75	5.06	5.35	6.25
	MDRL	10.00	9.00	9.00	11.00	5.00	4.00	4.00	5.00
	SDRL	7.09	9.39	12.14	15.12	2.71	3.23	4.18	5.40
1.50	ARL	8.83	8.51	9.68	10.95	4.61	3.89	3.82	4.21
	MDRL	8.00	7.00	7.00	8.00	4.00	3.00	3.00	3.00
	SDRL	5.30	6.61	8.61	10.19	1.99	2.26	2.72	3.42
1.60	ARL	7.25	6.73	7.27	8.37	3.87	3.12	3.03	3.15
	MDRL	6.00	5.00	5.00	6.00	4.00	3.00	3.00	2.00
	SDRL	4.13	5.00	6.19	7.63	1.62	1.73	2.00	2.40
1.80	ARL	5.43	4.70	4.97	5.43	2.98	2.34	2.13	2.17
	MDRL	5.00	4.00	4.00	4.00	3.00	2.00	2.00	2.00
	SDRL	2.88	3.20	4.00	4.70	1.17	1.20	1.28	1.47
2.00	ARL	4.45	3.75	3.73	3.96	2.48	1.92	1.74	1.70
	MDRL	4.00	3.00	3.00	3.00	2.00	2.00	1.00	1.00
	SDRL	2.32	2.45	2.78	3.27	0.96	0.92	0.95	1.01
2.50	ARL	3.09	2.52	2.43	2.47	1.78	1.40	1.28	1.25
	MDRL	3.00	2.00	2.00	2.00	2.00	1.00	1.00	1.00
	SDRL	1.55	1.51	1.65	1.83	0.69	0.59	0.55	0.53
3.00	ARL	2.46	2.00	1.91	1.88	1.45	1.19	1.13	1.10
	MDRL	2.00	2.00	2.00	1.00	1.00	1.00	1.00	1.00
	SDRL	1.22	1.11	1.17	1.22	0.56	0.42	0.35	0.33
3.50	ARL	2.08	1.72	1.62	1.62	1.26	1.09	1.06	1.05
	MDRL	2.00	1.00	1.00	1.00	1.00	1.00	1.00	1.00
	SDRL	1.00	0.92	0.91	0.96	0.46	0.29	0.25	0.23
4.00	ARL	1.85	1.52	1.46	1.44	1.15	1.05	1.03	1.03
	MDRL	2.00	1.00	1.00	1.00	1.00	1.00	1.00	1.00
	SDRL	0.90	0.76	0.76	0.75	0.37	0.22	0.18	0.16

Table B.20: RL characteristics of the QN_E chart for t-distributed quality characteristic when $\text{ARL}_0 = 200$

		n							
		5				10			
		λ				λ			
δ		0.05	0.25	0.50	0.75	0.05	0.25	0.50	0.75
1.00	ARL	200.58	198.10	198.68	200.95	199.96	203.90	199.53	198.06
	MDRL	138.00	138.00	137.00	139.00	137.00	143.00	138.00	138.00
	SDRL	200.48	196.40	199.86	198.82	200.14	199.80	199.37	196.35
1.10	ARL	55.48	75.75	92.17	102.09	31.15	44.37	58.74	68.64
	MDRL	41.00	54.00	64.00	71.00	24.00	32.00	41.00	47.00
	SDRL	49.16	73.47	90.92	100.93	24.08	40.82	57.37	68.38
1.20	ARL	27.06	37.33	48.23	56.55	14.40	17.03	23.81	30.22
	MDRL	21.00	26.00	34.00	40.00	12.00	13.00	17.00	21.00
	SDRL	21.27	35.01	47.63	55.37	9.02	14.48	22.56	29.53
1.30	ARL	17.31	22.09	28.45	34.67	9.23	9.35	12.53	15.88
	MDRL	14.00	16.00	20.00	25.00	8.00	7.00	9.00	11.00
	SDRL	12.12	19.88	26.84	33.58	5.03	7.09	11.08	14.92
1.40	ARL	12.53	14.48	18.47	23.02	6.76	6.45	7.80	9.68
	MDRL	11.00	11.00	13.00	16.00	6.00	5.00	6.00	7.00
	SDRL	7.98	12.46	17.59	22.46	3.35	4.37	6.42	8.79
1.50	ARL	9.86	10.70	13.43	16.40	5.44	4.79	5.37	6.58
	MDRL	8.00	8.00	10.00	12.00	5.00	4.00	4.00	5.00
	SDRL	6.06	8.72	12.10	15.47	2.46	3.03	4.17	5.79
1.60	ARL	8.27	8.45	9.97	12.64	4.54	3.88	4.15	4.75
	MDRL	7.00	7.00	7.00	9.00	4.00	3.00	3.00	4.00
	SDRL	4.90	6.52	8.79	11.96	2.01	2.33	3.04	3.99
1.80	ARL	6.13	5.88	6.68	7.73	3.44	2.84	2.80	3.00
	MDRL	5.00	5.00	5.00	6.00	3.00	3.00	2.00	2.00
	SDRL	3.38	4.27	5.48	7.05	1.43	1.52	1.84	2.26
2.00	ARL	4.98	4.56	4.90	5.63	2.85	2.26	2.18	2.24
	MDRL	4.00	4.00	4.00	4.00	3.00	2.00	2.00	2.00
	SDRL	2.63	3.05	3.88	4.94	1.14	1.13	1.29	1.53
2.50	ARL	3.49	2.95	2.92	3.25	2.03	1.60	1.49	1.47
	MDRL	3.00	3.00	2.00	2.00	2.00	1.00	1.00	1.00
	SDRL	1.78	1.80	2.05	2.59	0.78	0.73	0.72	0.77
3.00	ARL	2.72	2.29	2.26	2.36	1.63	1.32	1.24	1.22
	MDRL	2.00	2.00	2.00	2.00	2.00	1.00	1.00	1.00
	SDRL	1.36	1.31	1.48	1.67	0.64	0.53	0.49	0.48
3.50	ARL	2.31	1.95	1.87	1.89	1.41	1.18	1.12	1.11
	MDRL	2.00	2.00	2.00	1.00	1.00	1.00	1.00	1.00
	SDRL	1.13	1.08	1.12	1.22	0.54	0.41	0.35	0.33
4.00	ARL	2.01	1.71	1.64	1.65	1.26	1.10	1.07	1.06
	MDRL	2.00	1.00	1.00	1.00	1.00	1.00	1.00	1.00
	SDRL	0.97	0.91	0.92	1.00	0.46	0.31	0.27	0.25

Table B.21: RL characteristics of the QN_E chart for Gamma distributed quality characteristic when $\text{ARL}_0 = 200$

		n							
		5				10			
		λ				λ			
δ		0.05	0.25	0.50	0.75	0.05	0.25	0.50	0.75
1.00	ARL	199.71	201.41	200.79	198.00	200.89	201.45	202.50	201.80
	MDRL	137.00	139.00	138.00	138.00	138.00	139.00	142.00	142.00
	SDRL	197.64	200.83	199.13	196.50	204.05	201.54	200.56	201.30
1.10	ARL	55.62	75.13	92.29	97.63	31.41	43.94	57.71	69.64
	MDRL	41.00	53.00	63.00	68.00	24.00	31.00	41.00	48.00
	SDRL	49.72	72.73	92.60	97.44	24.78	41.47	55.39	70.20
1.20	ARL	26.92	36.80	48.97	56.21	14.40	17.03	23.30	30.23
	MDRL	21.00	27.00	34.00	40.00	12.00	13.00	17.00	21.00
	SDRL	21.19	34.03	47.72	55.28	9.09	14.12	21.92	29.22
1.30	ARL	17.32	22.23	28.85	34.15	9.07	9.46	12.24	15.87
	MDRL	14.00	17.00	20.00	24.00	8.00	7.00	9.00	11.00
	SDRL	12.36	19.68	27.85	33.22	4.90	7.18	10.97	14.92
1.40	ARL	12.68	14.93	19.12	23.22	6.73	6.42	7.61	9.57
	MDRL	11.00	11.00	14.00	16.00	6.00	5.00	6.00	7.00
	SDRL	8.10	12.69	17.58	22.68	3.30	4.32	6.32	8.74
1.50	ARL	9.95	10.97	13.47	16.92	5.38	4.82	5.27	6.56
	MDRL	9.00	8.00	10.00	12.00	5.00	4.00	4.00	5.00
	SDRL	6.07	9.04	12.27	16.47	2.52	3.00	4.08	5.70
1.60	ARL	8.23	8.52	10.35	12.65	4.50	3.86	4.05	4.79
	MDRL	7.00	7.00	8.00	9.00	4.00	3.00	3.00	4.00
	SDRL	4.84	6.53	9.19	11.86	2.00	2.27	3.01	4.00
1.80	ARL	6.15	5.94	6.82	7.88	3.44	2.84	2.80	3.02
	MDRL	5.00	5.00	5.00	6.00	3.00	3.00	2.00	2.00
	SDRL	3.46	4.35	5.76	7.14	1.41	1.52	1.80	2.28
2.00	ARL	4.94	4.51	4.95	5.67	2.81	2.26	2.16	2.22
	MDRL	4.00	4.00	4.00	4.00	3.00	2.00	2.00	2.00
	SDRL	2.64	3.12	4.01	5.00	1.12	1.14	1.27	1.49
2.50	ARL	3.46	2.99	3.03	3.30	2.03	1.60	1.51	1.48
	MDRL	3.00	3.00	2.00	3.00	2.00	1.00	1.00	1.00
	SDRL	1.77	1.84	2.18	2.63	0.79	0.71	0.74	0.78
3.00	ARL	2.73	2.34	2.27	2.37	1.64	1.33	1.24	1.23
	MDRL	2.00	2.00	2.00	2.00	2.00	1.00	1.00	1.00
	SDRL	1.37	1.37	1.48	1.67	0.64	0.54	0.49	0.49
3.50	ARL	2.31	1.97	1.90	1.93	1.40	1.17	1.13	1.11
	MDRL	2.00	2.00	2.00	2.00	1.00	1.00	1.00	1.00
	SDRL	1.15	1.10	1.17	1.26	0.54	0.40	0.36	0.34
4.00	ARL	2.02	1.74	1.66	1.67	1.26	1.10	1.07	1.07
	MDRL	2.00	2.00	1.00	1.00	1.00	1.00	1.00	1.00
	SDRL	0.99	0.93	0.92	0.99	0.46	0.30	0.27	0.26

Appendix C

Markov Chain Approach

In Chapter 6, we used Fu et al. (2003)'s approach, with necessary adjustments, to approximate the run length distribution of the proposed CUSUM schemes.

The different rules that have been investigated in this study are denoted as ϕ_i.

- ϕ_1 : Any point of either S^+ or S^- falls outside h
- ϕ_2: Any two consecutive points of either S^+ or S^- fall between w and h.
- ϕ_3: Two out of three consecutive points of either S^+ or S^- fall between w and h.

Here we will only describe the procedure for using the Markov chain for the upper CUSUM (S^+) with Scheme II as the procedure for the lower CUSUM (S^-) is very similar. Note that the proposed run rule Scheme II requires combining rules ϕ_1 and ϕ_3 for making any decision regarding the state of the process.

The continuous space of the CUSUM statistic S^+ can be discretized by partitioning the interval $[0, h)$ in to m sub-intervals of width Δ and the interval $[h, \infty)$ as the $(m+1)^{\text{th}}$ region, where Δ is defined as $\Delta = h/(m+1)$. These sub-intervals are used to define the states of the Markov chain. For the proposed Scheme II, the second rule (ϕ_3) further divides the space of S^+

in to three regions; $(r_1, r_2 \,\text{and}\, r_3)$:

$$R(S_t^+) = \begin{cases} r_1 & 0 \leq S_t^+ < w, \\ r_2 & w \leq S_t^+ < h, \\ r_3 & S_t^+ \geq h \end{cases} \tag{C.1}$$

$R(S_t^+)$ indicates whether at time t, the value of S^+ lies below the warning limit, between warning and action limit or above the action limit. Any point in the region r_3 or two out of three consecutive points in the region r_2 indicates the process is out-of-control. Let m^* be the number of states in the interval $[0, w)$ thus $m^* = w/\Delta$ (rounded to the nearest integer). Also let $S_t(q) = [S_{t-q+1}, \ldots, S_t]$ be the monitoring statistic, where q is the number of consecutive points to be kept in history. The 2^{nd} rule of Scheme II i.e. ϕ_3 requires to keep history of the three observations i.e. for ϕ_3 we have $q = 3$. The state of the Markov chain at time t, Y_t, for Scheme II (using rules ϕ_1 and ϕ_3) is defined by the region occupied by S^+ at time $(t-1)$ and the value of S^+ at time t: $Y_t = [R(S_{t-1}^+), S_t^+]$ – for details see Fu et al. (2003). The state space Ω is then defined as the possible realizations of $[R(S_{t-1}^+), S_t^+]$:

$$\Omega = \{(\Psi, \Psi), (\Psi, 0), \ldots, (\Psi, m), (r_1, 0), \ldots, (r_1, m), (r_2, 0), \ldots, (r_2, m^*-1), \alpha\} \tag{C.2}$$

Here Ψ represents the dummy initial state (no observations) and α represents the absorbing state (out-of-control) for the Markov chain Y_t respectively. Let n_Ω represents the number of elements in the state space Ω. To compute the run length distribution, we require the initial distribution (π_0) of the Markov chain and the transition probability matrix $(\mathbf{M})$, which has the form.

$$\mathbf{M} = \left[\begin{array}{c|c} \mathbf{N} & \mathbf{C} \\ \hline \mathbf{0} & 1 \end{array}\right]. \tag{C.3}$$

where $\mathbf{N}$ and $\mathbf{C}$ are matrices of transition probabilities (described below) of order $(n_\Omega - 1) \times (n_\Omega - 1)$ and $(n_\Omega - 1) \times 1$ respectively and $\mathbf{0}$ is $1 \times (n_\Omega - 1)$ matrix of zeros. $\mathbf{N}$ represents transition probabilities from one in-control state to another in-control state whereas **C** represents probabilities from an in-control state to an out-of-control state. A sample transition matrix is presented below for the highly simplified case when $m = 2, h = 3, w = 1$ and $m^* = 1$.

	(Ψ,Ψ)	$(\Psi,0)$	$(\Psi,1)$	$(\Psi,2)$	$(r_1,0)$	$(r_1,1)$	$(r_1,2)$	$(r_2,0)$	α
(Ψ,Ψ)		$F(0)$	p_1	p_2					$1-F(2)$
$(\Psi,0)$					$F(0)$	p_1	p_2		$1-F(2)$
$(\Psi,1)$								$F(-1)$	$1-F(-1)$
$(\Psi,2)$								$F(-2)$	$1-F(-2)$
$(r_1,0)$					$F(0)$	p_1	p_2		$1-F(2)$
$(r_1,1)$								$F(-1)$	$1-F(-1)$
$(r_1,2)$								$F(-2)$	$1-F(-2)$
$(r_2,0)$					$F(0)$				$1-F(0)$
α									1

The probabilities in each row should add up to 1, hence the probability for the absorbing state is given as 1 minus the sum of transition probabilities between the in-control states.
The entries in the above matrix can be read as:

- the row for (Ψ, Ψ) represents the dummy initial state when no observations have been observed.

- the row for $(r_1, 0)$ indicates that $R(S^+_{t-1}) = r_1$ and $S^+_t = 0$, i.e. both the points lie in region r_1, hence we will get in-control probabilities for $S^+_{t+1} = 0, 1, 2$. For $S^+_{t+1} = 3$, the monitoring statistic gets out-of-control with probability $1 - F(2)$.

- the row for $(r_1, 2)$ indicates that $R(S^+_{t-1}) = r_1$ and $S^+_t = 2$, i.e. S^+_{t-1} is in region r_1 whereas S^+_t lies in region r_2, hence we will get in-control probability for only $S^+_{t+1} = 0$. For $S^+_{t+1} = 1, 2$ the monitoring statistic gets out-of-control with probability $1 - F(-2)$.

Similarly the other entries can be defined, for details – see Fu et al. (2003). For the transition matrix **M**, many of the entries must be 0 since the corresponding transition is impossible. These entries are omitted for simplicity.

For an in-control process (i.e. $X_t \sim N(0,1)$), the random variable V_t (defined previously) approximately follows a standard normal distribution (Hawkins (1981)), i.e. $V_t \approx N(0,1) \implies V_t' = V_t - k \approx N(-k,1)$. For an out-of-control process (i.e. $X_t \sim N(0,\lambda)) \implies V_t \approx N(\mu_v, \sigma_v)$, where μ_V and σ_V depend upon the magnitude of shift in the in-control process standard deviation σ_0, defined as (see Yeh et al. (2005)):

$$\mu_V = 2.355(\lambda^{1/2} - 1) \qquad \text{and} \qquad \sigma_V = \lambda^{1/2} \tag{C.4}$$

The required probabilities that constitute the transition matrix $\mathbf{M}$ are defined as (Fu et al. (2003))

$$p_i = \int_{(i-0.5)\Delta}^{(i+0.5)\Delta} \frac{1}{\sqrt{2\pi\sigma_v}}\, e^{-\frac{1}{2}\left[\frac{v'-\mu_{v'}}{\sigma_v}\right]^2} dv \qquad p_{m+1} = \int_{((m+1)-0.5)\Delta}^{\infty} \frac{1}{\sqrt{2\pi\sigma_v}}\, e^{-\frac{1}{2}\left[\frac{v'-\mu_{v'}}{\sigma_v}\right]^2} dv$$

$$p_{-(m+1)} = \int_{-\infty}^{(-(m+1)+0.5)\Delta} \frac{1}{\sqrt{2\pi\sigma_v}}\, e^{-\frac{1}{2}\left[\frac{v'-\mu_{v'}}{\sigma_v}\right]^2} dv \qquad F(i) = \sum_{j=-(m+1)}^{i} p_j$$

where $\mu_{v\prime} = \mu_v - k$. Using these probabilities, the transition matrix $\mathbf{M}$ is computed and the mean and standard deviation of the run length distribution are obtained by matrix multiplications using the following results (Fu et al. (2002)).

$$\text{ARL} = E(\text{RL}) = \pi_0(\mathbf{I} - \mathbf{N})^{-1}\mathbf{1}' \tag{C.5}$$

and

$$\text{SDRL} = \sqrt{E(\text{RL}^2) - [E(\text{RL})]^2} \qquad \text{where} \qquad E(\text{RL}^2) = \pi_0(\mathbf{I} + \mathbf{N})(\mathbf{I} - \mathbf{N})^{-2}\mathbf{1}' \tag{C.6}$$

where $\pi_0 = (1, 0, \ldots, 0)$ and $\mathbf{1} = (1, 1, \ldots, 1)$.

The accuracy of the Markov chain estimate of the run length characteristics increases with an increase in the number of states (m), used to discritize the continuous state of the CUSUM statistics. Following the recommendations of Fu et al. (2002, 2003), we have used $m = 500$ in this study.

References

Abbas, N., M. Riaz, and R. J. M. M. Does (2011). Enhancing the performance of EWMA charts. *Quality and Reliability Engineering International 27*(6), 821–833.

Abbasi, S. A. (2010). On the performance of EWMA chart in presence of two component measurement error. *Quality Engineering 22*(3), 199–213.

Abbasi, S. A. (2012). Letter to editor: A new nonparametric EWMA sign control chart. *Expert Systems with Applications 39*(9), 8503.

Abbasi, S. A. and A. Miller (2011a). D chart: An efficient alternative to monitor process dispersion. *Proceedings of the World Congress on Engineering and Computer Science (WCECS) 2011, San Francisco, USA 2*, 933–938.

Abbasi, S. A. and A. Miller (2011b). Increasing the sensitivity of variability EWMA control charts. *Electrical Engineering and Applied Computing 1*, 431–443.

Abbasi, S. A. and A. Miller (2011c). MDEWMA chart: An efficient and robust alternative to monitor process dispersion. *Journal of Statistical Computation and Simulation, ifirst*(1), 1–22.

Abbasi, S. A. and A. Miller (2012). On proper choice of variability control chart for normal and non-normal processes. *Quality and Reliability Engineering International 28*(3), 279–296.

Abbasi, S. A., A. Miller, and M. Riaz (2012a). Monitoring process dispersion using EWMA control charts. *To be submitted*.

Abbasi, S. A., A. Miller, and M. Riaz (2012b). Nonparametric progressive mean control chart for monitoring process target. *Quality and Reliability Engineering International - DOI: 10.1002/qre.1458*.

Abbasi, S. A., M. Riaz, and A. Miller (2012a). Enhancing the performance of CUSUM scale charts. *Computers & Industrial Engineering, doi.org/10.1016/j.cie.2012.03.013 63*(2), 400–409.

Abbasi, S. A., M. Riaz, and A. Miller (2012b). On proper choice of Phase I dispersion control chart. *To be submitted*.

Abraham, B. (1977). Control charts and measurement error. *Proceedings of 31st Annual Technical Conference, American Society for Quality Control (ASQC)*, 370–374.

Abu-Shawiesh, M. O. and M. B. Abdullah (2000). Estimating the process standard deviation based on downton's estimator. *Quality Engineering 12*(3), 357–363.

Abu-Shawiesh, M. O. A. (2008). A simple robust control chart based on MAD. *Journal of Mathematics and Statistics 4*(2), 102–107.

Acosta-Mejia, C. A. and J. Pignatiello, J.J. (2008). Modified R charts for improved performance. *Quality Engineering 20*(3), 361–369.

Acosta-Mejia, C. A. and J. Pignatiello, J.J. (2009). ARL-design of S charts with k-of-k runs rules. *Communications in Statistics-Simulation and Computation 38*, 1625–1639.

Alloway, J. A. and M. Raghavachari (1991). Control chart based on the hodges-lehmann estimator. *Journal of Quality Technology 23*(4), 336–347.

Alwan, L. C. (1999). *Statistical Process Analysis* (2nd ed.). New York: McGraw-Hill.

Alwan, L. C. (2000). Statistical Process Analysis, McGraw-Hill International Editions: Singapore.

Alwan, L. C. and H. V. Roberts (1995). The problem of misplaced control limits. *Applied Statistics 44*, 269–278.

Amin, R. W. and A. J. Searcy (1991). A nonparametric exponentially weighted moving average control scheme. *Communications in Statistics-Simulation and Computation 20*(4), 1049–1072.

Amin, R. W. and O. Widmaier (1999). Sign control charts with variable sampling intervals. *Communications in Statistics - Theory and Methods 28*(8), 1961–1985.

Antzoulakos, D. and A. Rakitzis (2008). The modified r out of m control chart. *Communication in Statistics-Simulations and Computations 37*(2), 396–408.

Antzoulakos, D. L. and A. C. Rakitzis (2010). Runs rules schemes for monitoring process variability. *Journal of Applied Statistics 37*(7), 1231–1247.

Aryal, S., D. K. Bhaumik, S. Santra, and R. D. Gibbons (2009). Confidence interval for random-effects calibration curves with left-censored data. *Environmetrics 20*(2), 181–189.

Bakir, S. (2006). Distribution-free quality control charts based on signed-rank-like statistics. *Communications in Statistics - Theory and Methods 35*(4), 743–757.

Bakir, S. T. and M. R. Reynolds (1979). Nonparametric procedure for process control based on within-group ranking. *Technometrics 21*(2), 175–183.

Balakrishnana, N., I. S. Triantafylloub, and M. V. Koutrasb (2009). Nonparametric control charts based on runs and wilcoxon-type rank-sum statistics. *Journal ofStatisticalPlanningandInference 139*(2), 3177–3192.

Barnard, G. A. (1959). Control charts and stochastic processes. *Journal of the Royal Statistical Society (B) 21*(2), 239–271.

Bartram, J. and R. Ballance (1996). *Water Quality Monitoring - A Practical Guide to the Design and Implementation of Freshwater Quality Studies and Monitoring Programmes* (1st ed.). London: Spon Press.

Bennett, C. A. (1954). Effect of measurement error on chemical process control. *Industrial Quality Control 10*, 17–20.

Bickel, P. J. and E. L. Lehmann (1976). Descriptive statistics for nonparametric models III: Dispersion. *The Annals of Statistics 4*, 1139–1158.

Bissell, D. (1994). *Statistical methods for SPC and TQM* (1st ed.). New York: Chapman & Hall.

Bohm, W. and P. Hackl (1996). The effect of serial correction on the in-control average run length of cumulative score charts. *Journal of Statistical Planning and Inference 54*, 15–30.

Bonet-Domingo, E., L. Escuder-Gilabert, M. J. Medina-Hernandez, and S. Sagrado (2006). Uncertainty-based internal quality control. harmonization considerations. *Analytical Chemistry 78*(23), 8113–8120.

Bonetti, P. O., A. Waeckerlin, G. Schuepfer, and A. Frutiger (2000). Improving time-sensitive processes in the intensive care unit: the example of Door-to-Needle Time in acute myocardial infarction. *International Journal for Quality in Health Care 12*(4), 311–317.

Borror, C. M., D. C. Montgomery, and G. C. Runger (1999). Robustness of the ewma control chart to non-normality. *Journal of Quality Technology 31*(3), 309–316.

Braun, W. J. and D. Park (2008). Estimation of σ for individuals charts. *Journal of Quality Technology 40*(3), 332–344.

Brook, D. and D. Evans (1972). An approach to the probability distribution of CUSUM run length. *Biometrika 59*, 539 – 549.

Burr, I. W. (1967). The effect of non-normality on the constants for $\overline{X}$ and R charts. *Industrial Quality Control 23*, 566–569.

Carson, P. K. and A. B. Yeh (2008). Exponentially Weighted Moving Average (EWMA) control charts for monitoring an analytical process. *Industrial and Engineering Chemistry Research 47*(2), 405–411.

Chakraborti, S. and S. Eryilmaz (2007). A nonparametric shewhart-type signed-rank control chart based on runs. *Communications in Statistics: Simulation and Computation 36*(2), 335–356.

Chakraborti, S., S. Eryilmaz, and S. W. Human (2009). A Phase II nonparametric control chart based on precedence statistics with runs-type signaling rules. *Computational Statistics and Data Analysis 53*, 1054–1065.

Chakraborti, S., S. W. Human, and M. Graham (2009). Phase I statistical process control charts: An overview and some results. *Quality Engineering 21*(1), 52 62.

Chakraborti, S., P. Van Der Laan, and S. Bakir (2001). Nonparametric control charts: An overview and some results. *Journal of Quality Technology 33*(3), 304–315.

Champ, C. and W. H. Woodall (1987). Exact results for shewhart control charts with supplementary runs rules. *Technometrics 29*(4), 393–399.

Champ, C. W. and W. H. Woodall (1997). Signal probabilities of runs rules supplementing a shewheart control chart. *Communications in Statistics Part B: Simulation and Computation 26*(4), 1347–1360.

Chan, L. K. and J. Zhang (2000). Some issues in the design of EWMA charts. *Communications in Statistics Part B: Simulation and Computation 29*(1), 207–217.

Chang, Y. M. and T. L. Wu (2011). On average run lengths of control charts for autocorrelated processes. *Methodology and Computing in Applied Probability 13*(2), 419–431.

Chatterjee, S. and P. Qiu (2009). Distribution-free cumulative sum control charts using bootstrap-based control limits. *Annals of Applied Statistics 3*, 349–369.

Chen, G. (1998). The run length distributions of the R, S and S^2 control charts when σ is estimated. *Canadian Journal of Statistics 26*(2), 311–322.

Chen, G. M., S. W. Cheng, and H. S. Xie (2001). Monitoring process mean and variability with one EWMA chart. *Journal of Quality Technology 33*, 223–233.

CITAC/EURACHEM-GUIDE (2002). Guide to quality in analytical chemistry: An aid to accreditation. *http://www.eurachem.org/guides/CITAC%20EURACHEM%20GUIDE.pdf*.

Cocchi, D. and M. Scagliarini (2007). Control charts and the effect of the two-component measurement error model. *Working Paper. Dipartimento di Scienze Statistiche "Paolo Fortunati", Alma Mater Studiorum Universit di Bologna, Bologna, IT.*.

Crosby, N. T., J. A. Day, W. A. Hardcastle, D. G. Holcombe, and R. D. Treble (1995). *Quality in Analytical Chemistry Laboratory*. Chichester: Wiley.

Crowder, S. V. and M. Hamilton (1992). Average run lengths of EWMA controls for monitoring a process standard deviation. *Journal of Quality Technology 24*, 44–50.

Cruthis, E. N. and S. E. Rigdon (1992). Comparing two estimates of variance to determine the stability of a process. *Qual. Eng. 5*(1), 67–74.

Cryer, J. D. and T. P. Ryan (1990). The estimation of sigma for an X chart: $\overline{MR}/d_2$ or $\overline{S}/c_4$. *Journal of Quality Technology 22*(3), 187–192.

Currie, L. A. (1968). Limits for qualitative detection and quantitative determination: Application to radiochemistry. *Analytical Chemistry 40*(3), 586–593.

Das, N. (2009). A comparison study of three non-parametric control charts to detect shift in location parameters. *International Journal of Advanced Manufacturing Technology 41*(7-8), 799–807.

Das, N. and A. Bhattacharya (2008). A new non-parametric control chart for controlling variability. *Quality Technology & Quantitative Management 5*(4), 351–361.

Derman, C. and S. Ross (1995). An improved estimator of σ in quality control. *Probability in the Engineering and Informational Sciences 9*, 411–415.

Domangue, R. and S. C. Patch (1991). Some omnibus exponentially weighted moving average statistical process monitoring schemes. *Technometrics 33*, 299–313.

Downton, F. (1966). Linear estimates with polynomial coefficients. *Biometrika 53*(1), 129–141.

Duncan, A. J. (1951). Operating characteristics of R charts. *Industrial Quality Control 7*, 40–41.

EURACHEM-GUIDE (1998). The fitness for purpose of analytical methods: A laboratory guide to method validation and related topics. *http://www.eurachem.org/guides/mval.htm*.

Ewan, W. and K. Kemp (1960). Sampling inspection of continuous process with no autocorrelation between successive results. *Biometrika 47*, 363380.

Fu, J. C., G. Shmueli, and Y. M. Chang (2003). A unified markov chain approach for computing the run length distribution in control charts with simple or compound rules. *Statistics & Probability Letters 65*, 457–466.

Fu, J. C., F. A. Spiring, and H. Xie (2002). On the average run lengths of quality control schemes using a markov chain approach. *Statistics & Probability Letters 56*, 369–380.

Funk, W., V. Damman, and G. Donnevert (1995). *Quality Assurance in Analytical Chemistry.* New York: VCH.

Gan, F. F. (1993). An optimal design of EWMA control charts based on median run length. *Journal of Statistical Computation and Simulation 45*, 169184.

Gan, F. F. (1994). An optimal design of cumulative sum control chart based on median run length. *Communications in Statistics - Simulation and Computation 23*, 485503.

Garfield, F. M. (1984). *Quality Assurance Principles for Analytical Laboratories*. Virginia: AOAC.

Gibbons, R. D. and D. K. Bhaumik (2001). Weighted random-effects regression models with application to interlaboratory calibration. *Technometrics 43*(2), 192–198.

Gibbons, R. D., D. E. Coleman, and R. F. Maddalone (1997). An alternative minimum level definition for analytical quantification. *Environmental Science and Technology 31*(7), 2071–2077.

Gorard, S. (2005). Revisiting a 90-year-old debate: The advantages of the mean deviation. *British Journal of Educational Studies 53*(4), 417–430.

Graham, M. A., S. Chakraborti, and S. W. Human (2011). A nonparametric ewma sign chart for location based on individual measurements. *Quality Engineering 23*(3), 227–241.

Gunter, B. H. (1989). The use and abuse of C_{pk}, part 2. *Quality Progress 22*, 108–109.

H, W. W. and N. M. M. (1985). Multivariate CUSUM quality control process. *Technometrics 27*(3), 285–292.

Hare, L. B. (1993). Youden memorial address. *ASQC statistics division newsletter 13*(4), 4–8.

Hawkins, D. (1981). A CUSUM for scale parameter. *Journal of Quality Technology 13*(4), 226–231.

Hawkins, D. (1993). Cumulative sum control charting: An underutilized spc tool. *Quality Engineering 5*(3), 463–477.

Hawkins, D. and D. Olwell (1998). *Cumulative Sum Charts and Charting Improvement*. Springer, New York.

Hibbert, D. B. (2007). *Quality Assurance for the Analytical Chemistry Laboratory*. Oxford, New York.

Hubaux, A. (1970). Decision and detection limits for linear calibration curves. *Analytical Chemistry 42*(8), 849–855.

Human, S. W., S. Chakraborti, and C. F. Smit (2010). Nonparametric shewhart-type sign control charts based on runs. *Communications in Statistics - Theory and Methods 39*(11), 2046–2062.

Huwang, L., Y. T. Wang, Y. A. B., and Z. J. Chen (2009). On the exponentially weighted moving variance. *Naval Research Logistics 56*(7), 659–668.

Hwang, S. L., J. T. Lin, G. F. Liang, Y. J. Yau, T. C. Yenn, and C. C. Hsu (2008). Application control chart concepts of designing a pre-alarm system in the nuclear power plant control room. *Nuclear Engineering and Design 238*(12), 3522–3527.

Hyndman, R. J. and Y. Fan (1996). Sample quantiles in statistical packages. *American Statistician 50*(4), 361–365.

Ihaka, R. and R. Gentleman (1996). R: A language for data analysis and graphics. *Journal of Computational and Graphical Statistics 5*(3), 299–314.

ISO7870 (1993). Control charts-general guide and introduction.

ISO7873 (1993). Control charts for arithematic means with warning limits.

ISO7966 (1993). Acceptance control charts.

ISO8258 (1991). Shewhart control charts.

James, P. C. (1989). C_pk equivalencies. *Quality 28*(9), 75.

Jensen, W. A., L. A. Jones-Farmer, C. W. Champ, and W. H. Woodall (2006). Effects of parameter estimation on control chart properties: A literature review. *Journal of Quality Technology 38*(4), 349–364.

Jones, G. (2004). Markov chain Monte Carlo estimation for the two-component model. *Technometrics 46*(1), 99–107.

Jones, L. A., C. W. Champ, and S. E. Rigdon (2001). The performance of exponentially weighted moving average charts with estimated parameters. *Technometrics 43*(2), 156–167.

Jones, L. A., C. W. Champ, and S. E. Rigdon (2004). The run length distribution of the CUSUM with estimated parameters. *Journal of Quality Technology 36*(1), 95–108.

Jones-Farmer, L. A. and C. W. Champ (2010). A distribution free Phase I control chart for subgroup scale. *Journal of Quality Technology 42*(4), 373–387.

Kanazuka, T. (1986). The effect of measurement error on the power of charts. *Journal of Quality Technology 18*(2), 91–95.

Kao, S. C. and C. Ho (2007). Robustness of R-chart to non normality. *Communications in Statistics: Simulation and Computation 36*(5), 1089–1098.

Kateman, G. and L. Buydens (1993). *Quality control in analytical chemistry* (2 ed.), Volume 60. Wiley-Interscience.

Khilare, S. K. and D. T. Shirke (2010). A nonparametric synthetic control chart using sign statistic. *Communications in Statistics - Theory and Methods 39*(18), 3282–3293.

Khoo, M. B. C. (2003). Design of runs rules schemes. *Quality Engineering 16*, 2743.

Khoo, M. B. C. (2004). Some control charts for the process mean and variance based on downtons estimator. *IEEE International Engineering Management Conference 3*, 1071–1074.

Kim, M. (2005). *Number of replications required in control chart Monte Carlo simulation studies*. Ph.d. diss, University of Northern Colorado.

Klein, M. (2000). Two alternatives to the shewhart X control chart. *Journal of Quality Technology 32*, 427431.

Koutras, M. V., S. Bersimis, and P. E. Maravelakis (2007). Statistical process control using shewhart control charts with supplementary runs rules. *Methodology and Computing in Applied Probability 9*, 207–224.

Levinson, W. A. and A. Polny (June, 1999). SPC for tool particle counts. *Semiconductor International 22*(6), 117–121.

Li, S., L. Tang, and S. Ng (2010). Nonparametric CUSUM and EWMA control charts for detecting mean shifts. *Journal of Quality Technology 42*(2), 209–226.

Li, Z. and Z. Wang (2010). Adaptive CUSUM of the Q chart. *International Journal of Production Research 48*(5), 1287–1301.

Lim, T. and M. Cho (2009). Design of control charts with m-of-m runs rules. *Quality and Reliability Engineering International*, 10851101.

Linna, K. W. and W. H. Woodall (2001). Effect of measurement error on Shewhart control charts. *Journal of Quality Technology 33*(2), 213–222.

Linna, K. W., W. H. Woodall, and K. L. Busby (2001). The performance of multivariate control charts in the presence of measurement error. *Journal of Quality Technology 33*(3), 349–355.

Lucas, J. M. and R. B. Crosier (1982). Fast initial response for CUSUM quality-control schemes: Give your CUSUM a head start. *Technometrics 24*(3), 199205.

Lucas, J. M. and M. S. Saccucci (1990). Exponentially Weighted Moving Average control schemes. properties and enhancements. *Technometrics 32*(1), 1–12.

MacGregor, J. F. and T. J. Harris (1993). The exponentially weighted moving variance. *Journal of Quality Technology 25*(2), 106–118.

Mahoney, J. F. (1998). The influence of parent population distribution on d_2 values. *IIE Transactions (Institute of Industrial Engineers) 30*(6), 563–569.

Maravelakis, P., J. Panaretos, and S. Psarakis (2005). An examination of the robustness to non normality of the EWMA control charts for the dispersion. *Communications in Statistics: Simulation and Computation 34*(4), 1069–1079.

Maravelakis, P. E. (2007). The effect of measurement error on the performance of the CUSUM control chart. In *IEEM 2007: 2007 IEEE International Conference on Industrial Engineering and Engineering Management*, pp. 1399–1402.

Maravelakis, P. E., J. Panaretos, and S. Psarakis (2004). EWMA chart and measurement error. *Journal of Applied Statistics 31*(4), 445–455.

Masson, P. (2007). Quality control techniques for routine analysis with liquid chromatography in laboratories. *Journal of Chromatography A 1158*(1-2), 168–173.

McDonald, D. (1990). Cusum procedure based on sequential ranks. *Naval Research Logistics 37*(5), 627–646.

Miller, I. and M. Miller (1995). *Statistical methods for quality with applications to engineering & management*. Prentice-Hall, Inc.

Mittag, H. and D. Stemann (1998a). Gauge imprecision effect on the performance of the x-s control chart. *Journal of Applied Statistics 25*(3), 307–317.

Mittag, H. J. (1995). Measurement error effects on control chart performance. *ASQC 49th Annual Quality Congress Proceedings*, 66–73.

Mittag, H. J. and D. Stemann (1998b). Gauge imprecision effect on the performance of the $\bar{X}-S$ control chart. *Journal of Applied Statistics 25*(3), 307–317.

Montgomery, D. C. (2009). *Introduction to statistical quality control* (6th ed.). New York: Wiley.

Montgomery, D. C., J. C. C. Torng, J. K. Cochran, and F. P. Lawrence (1995). Statistically constrained economic design of the EWMA control chart. *Journal of Quality Technology 27*(3), 250–256.

Mukherjee, A. and S. Chakraborti (2012). A distribution-free control chart for the joint monitoring of location and scale. *Quality and Reliability Engineering International 28*(3), 335–352.

Mullins, E. (2003). *Statistics for the Quality Control Chemistry Laboratory*. Cambridge: The Royal Society of Chemsitry.

Nelson, P. R. (1985). Power curves for the analysis of means. *Technometrics 27*, 6573.

Neubauer, A. S. (1997). The EWMA control chart: Properties and comparison with other quality control procedures by computer simulation. *Clinical Chemistry 43*(4), 594–601.

Ng, C. H. and K. E. Case (1989). Development and evaluation of control charts using Exponentially Weighted Moving Averages. *Journal of Quality Technology 21*(4), 242–250.

Noble, C. E. (1951). Variations in conventional control charts. *Industrial quality control 8*, 17–22.

North, W. R. S. (1982). The quangle-a modification of the CUSUM chart. *Journal of the Royal Statistical Society, Series C (Applied Statistics) 31*(2), 155–158.

Ou, Y., D. Wen, Z. Wu, and M. Khoo (2012). A comparison study on effectiveness and robustness of control charts for monitoring process mean and variance. *Quality and Reliability Engineering International 28*(1), 3–17.

Page, E. S. (1954). Continuous inspection schemes. *Biometrika 41*, 100–115.

Palm, A. C. (1990). Tables of run length percentiles for determining the sensitivity of shewhart control charts for averages with supplementary runs rules. *Journal of Quality Technology 22*(4), 289–298.

Pappanastos, E. A. and B. M. Adams (1996). Alternative designs of the hodges-lehmann control chart. *Journal of Quality Technology 28*(2), 213–223.

Park, C. and M. R. Reynolds (1987). Nonparametric procedures for monitoring a location parameter based on linear placement statistics. *Sequential Anal. 6*(4), 303–323.

Pawar, V. Y. and D. T. Shirke (2010). A nonparametric shewhart-type synthetic control chart. *Communications in Statistics: Simulation and Computation 39*(8), 1493–1505.

Qiu, P., C. Zou, and Z. Wang (2010). Nonparametric profile monitoring by mixed effects modeling. *TECHNOMETRICS 52*(3), 265–277.

Quesenberry, C. P. (1993). The effect of sample size on estimated limits for X and $\overline{X}$ control charts. *Journal of Quality Technology 25*(4), 237–247.

Reynolds, M. and J. Arnold (1990). CUSUM charts with variable sampling intervals. *Technometrics 32*, 371–384.

Reynolds Jr., M. and Z. Stoumbos (2004a). Control charts and the efficient allocation of sampling resources. *Technometrics 46*(2), 200–214.

Reynolds Jr., M. and Z. Stoumbos (2004b). Should observations be grouped for effective process monitoring? *Journal of Quality Technology 36*(4), 343–366.

Rhoads, T., D. Montgomery, and C. Mastrangelo (1996). A fast initial response scheme for the Exponentially Weighted Moving Average control chart. *Quality Engineering 9*(2), 317–327.

Riaz, M. (2008). A dispersion control chart. *Communications in Statistics-Simulation and Computation 37*, 1239–1261.

Riaz, M., N. Abbas, and R. J. M. M. Does (2011). Improving the performance of CUSUM charts. *Quality and Reliability Engineering International 27*(4), 415–424.

Riaz, M. and A. Saghir (2008). A mean deviation-based approach to monitor process variability. *Journal of Statistical Computation and Simulation 79*(10), 1173–1193.

Riaz, M. and A. Saghir (2009). A mean deviation-based approach to monitor process variability. *Journal of Statistical Computation and Simulation 79*(10), 1173–1193.

Rigdon, S., E. Cruthis, and C. Champ (1994). Design strategies for individuals and moving range control charts. *Journal of Quality Technology 26*, 274–287.

Roberts, S. W. (1959). Control chart tests based on geometric moving averages. *Technometrics 42*(1), 239–250.

Rocke, D. M. (1989). Robust control charts. *Technometrics 31*(2), 173–184.

Rocke, D. M. (1992). $\overline{X}_Q$ and R_Q charts: Robust control charts. *The Statistician 41*, 97–104.

Rocke, D. M. and B. Durbin (2001). A model for measurement error for gene expression arrays. *Journal of Computational Biology 8*(6), 557–569.

Rocke, D. M., B. Durbin, M. Wilson, and H. D. Kahn (2003). Modeling uncertainty in the measurement of low-level analytes in environmental analysis. *Ecotoxicology and Environmental Safety 56*(1), 78–92.

Rocke, D. M. and S. Lorenzato (1995). A two component model for measurement error in analytical chemistry. *Technometrics 37*(2), 176–184.

Roes, K., R. Does, and Y. Schurink (1993). Shewhart-type control charts for individual observations. *Journal of Quality Technology 25*(3), 188–198.

Rousseeuw, P. J. and C. Croux (1993). Alternatives to the median absolute deviation. *Journal of the American Statistical Association 88*(424), 1273–1283.

Ryan, P. R. (2000). *Statistical methods for quality improvement* (2nd ed.). New York: Wiley.

Schaffer, J. R. and M. J. Kim (2007). Number of replications required in control chart Monte Carlo simulation studies. *Communications in Statistics: Simulation and Computation 36*(5), 1075–1087.

Schoonhoven, M. and R. J. M. M. Does (2010). The $\overline{X}$ control chart under non-normality. *Quality and Reliability Engineering International 26*(2), 167–176.

Schoonhoven, M. and R. J. M. M. Does (2012). A robust standard deviation control chart. *Technometrics 54*(1), 73–82.

Schoonhoven, M., M. Riaz, and R. J. M. M. Does (2008). Design schemes for the $\overline{X}$ control chart. *Quality and Reliability Engineering International 25*, 581–594.

Schoonhoven, M., M. Riaz, and R. J. M. M. Does (2011). Design and analysis of control charts for standard deviation with estimated parameters. *Journal of Quality Technology 43*(4), 307–333.

Shiau, J. and J. Sun (2010). A new strategy for Phase I analysis in SPC. *Quality and Reliability Engineering International 26*, 475–486.

Shmueli, G. and A. Cohen (2003). Run-length distribution for control charts with runs and scans rules. *Communications in Statistics - Theory and Methods 32*(2), 475–495.

Shu, L. and W. Jiang (2008). A new EWMA chart for monitoring process dispersion. *Journal of Quality Technology 40*(3), 319–331.

Siegmund, D. (1985). *Sequential Analysis: Tests and Con?dence Intervals*. Springer-Verlag, New York.

Sim, C. H. and W. K. Wong (2003). R-charts for the exponential, laplace and logistic processes. *Statistical Papers 44*(4), 535–554.

Steiner, S. H. (1999). EWMA control charts with time-varying control limits and fast initial response. *Journal of Quality Technology 31*(1), 75–86.

Stoumbos, Z. G. and M. R. J. Reynolds (2000). Robustness to non normality and autocorrelation of individual control charts. *Journal of Statistical Computation and Simulation 66*, 145–187.

Tatum, L. G. (1997). Robust estimation of the process standard deviation for control charts. *Technometrics 39*(2), 127–141.

Taverniers, I., M. De Loose, and E. Van Bockstaele (2004). Trends in quality in the analytical laboratory. ii. analytical method validation and quality assurance. *TrAC - Trends in Analytical Chemistry 23*(8), 535–552.

Thompson, M. and R. Wood (1995). Harmonized guidelines for internal quality control in analytical chemistry laboratories. *Pure and Appl. Chemistry 67*(4), 649–666.

Vardeman, S. B. (1999). A brief tutorial on the estimation of the process standard deviation. *IIE Transactions 31*, 503–507.

Vining, G. (2009). Technical advice: Phase I and phase II control charts. *Quality Engineering 21*, 478–479.

Walker, E., J. W. Philpot, and J. Clement (1991). False signal rates for the shewhart control chart with supplementary runs tests. *Journal of Quality Technology 23*(3), 247–252.

Wang, Z. and R. Liang (2008). Discuss on applying SPC to quality management in university education. In *Proceedings of the 9th International Conference for Young Computer Scientists, ICYCS 2008*, pp. 2372–2375.

Western-Electric (1956). *Statistical Quality Control Handbook*. Western Electric Corporation.

Westgard, J. O., T. Groth, T. Aronsson, and D. V. C. H. (1977). Combined shewhart-CUSUM control chart for improved quality control in clinical chemistry. *Clinical Chemistry 23*(10), 1881–1887.

Woodall, W. H. (1983). The distribution of the run length of one-sided cusum procedures for continuous random variables. *Technometrics 25*, 295301.

Woodall, W. H. (2000). Controversies and contradictions in statistical process control. *Journal of Quality Technology 32*(4), 341–350.

Woodall, W. H. (2006). The use of control charts in health-care and public-health surveillance. *Journal of Quality Technology 38*(2), 89–104.

Wortham, A. W. and L. J. Ringer (1971). Control via exponential smoothing. *Transportation and Logistic Rev 7*, 33–39.

Wu, C., Y. Zhao, and Z. Wang (2002). The median absolute deviations and their application to Shewhart $\overline{X}$ control charts. *Communications in Statistics - Simulation and Computation 31*, 425–442.

Wu, Z., J. Jiao, M. Yang, Y. Liu, and Z. Wang (2009). An enhanced adaptive cusum control chart. *IIE Transactions (Institute of Industrial Engineers) 41*(7), 642–653.

Yang, S. F. and S. W. Cheng (2011). A new nonparametric cusum sign control chart. *Quality and Reliability Engineering International Early View*, 1–9.

Yang, S. F., J. S. Lin, and S. W. Cheng (2011). A new nonparametric ewma sign control chart. *Expert Systems with Applications 38*(5), 6239–6243.

Yeh, A. B., L. Huwang, R. N. McGrath, and Z. Zhang (2010). On monitoring process variance with individual observations. *Quality and Reliability Engineering International 26*(6), 631–641.

Yeh, A. B., L. Huwang, and C. Wu (2005). A multivariate EWMA control chart for the monitoring of process variability with individual onservations. *IIE Transaction 37*(11), 1023–1035.

Zhang, L. and G. Chen (2004). EWMA charts for monitoring the mean of censored Weibull lifetimes. *Journal of Quality Technology 36*(3), 321–328.

Zhang, S. and Z. Wu (2005). Designs of control charts with supplementary runs rules. *Computers and Industrial Engineering 49*(1), 76–97.

Zhang, W. and Y. Tian (2005). Weighted-loss-function cusum chart for monitoring mean and variance of a production process. *International Journal of Production Research 43*(14), 3027–3044.

Zorn, M. E., R. D. Gibbons, and W. C. Sonzogni (1999). Evaluation of approximate methods for calculating the limit of detection and limit of quantification. *Environmental Science and Technology 33*(13), 2291–2295.

Zou, C. and F. Tsung (2011). A multivariate sign ewma control chart. *TECHNOMETRICS 53*(1), 84–97.